THE SURFACE PRESSURE FEATURES AND PRECIPITATION STRUCTURE OF PRE-STORM MESOSCALE CONVECTIVE SYSTEMS

Scot M. Loehrer

Colorado State University

DEPARTMENT OF ATMOSPHERIC SCIENCE

PAPER NO. 518

THE SURFACE PRESSURE FEATURES AND PRECIPITATION STRUCTURE OF PRE-STORM MESOSCALE CONVECTIVE SYSTEMS

by

Scot M. Loehrer

Department of Atmospheric Science
Colorado State University
Fort Collins, CO 80523

Fall 1992

Atmospheric Science Paper No. 518

[redacted] cR

ABSTRACT

THE SURFACE PRESSURE FEATURES AND PRECIPITATION STRUCTURE OF PRE-STORM MESOSCALE CONVECTIVE SYSTEMS

The surface pressure features accompanying 16 mesoscale convective systems (MCSs) have been documented using data from the May-June 1985 Oklahoma-Kansas Preliminary Regional Experiment for STORM-Central (OK PRE-STORM). The general synoptic-scale environmental conditions as well as the detailed mesoscale aspects of the systems are examined. Radar data are examined to show the reflectivity structure of each MCS. Also, the upper-air data are examined to show the system-relative airflow structure associated with these systems.

The general synoptic-scale conditions were very similar to those shown by Maddox (1983) found in conjunction with the genesis region of mesoscale convective complexes (MCCs). There was a generally weak surface front, most often quasi-stationary in nature, and low-level warm advection by a low-level southerly jet which also advected in very moist air. Also, a weak 500 mb short wave feature was often found in conjunction with these systems.

In the mature-to-dissipating stages of 12 of the 16 cases, the radar reflectivity and surface pressure structures were found to be very similar. Composite depictions of the pressure features are developed based on these similarites. At some time during the mature-to-dissipating stage for each case, the radar reflectivity structure became asymmetric (Houze et al. 1990) in nature with a leading bow-shaped convective line with a region of enhanced stratiform precipitation found to the rear of the far northern portion of the convective line. This structure is quite similar to that shown by Pedgley (1962) for

MCS cases in England. Two of the four other MCSs that did not develop these particular structures were cold-frontal systems positioned directly along a cold front. Atmospheric conditions in these regions did not allow the development of these common structures. One system was too short-lived to have developed into the common structure of the 12 systems.

There were four paths that the 12 systems took to the development of this asymmetric structure. First, there were systems which initially had a disorganized pattern of convection, but towards the end of their existence developed a small convective line on their southern end. Any convection on the northern end became stratiform, leading to the asymmetric structure (2 cases). Second, there were convective lines which were initially symmetric in nature but slowly developed a region of enhanced stratiform precipitation on their northern ends (4 cases). Third, there were cases where a back-building convective line led to a region at the southern end of the system lacking stratiform precipitation (3 cases). Finally, there were cases consisting initially of intersecting convective lines, one oriented east-west and the other oriented northeast-southwest extending to its south. An enhanced stratiform area developed to the northwest of the apex of the two lines and then the east-west line dissipated (3 cases).

The surface pressure structure shows a fairly weak pre-squall low ahead of the convective line. A mesohigh was typically associated with the convective line as well as much of the stratiform precipitation region. A wake low was found at the back edge of the enhanced stratiform precipitation region. An intense pressure gradient was typically found along the back edge of and extending into the enhanced stratiform precipitation region. For the cases containing special soundings, the system-relative upper-air flow structure showed a rapidly descending, strong rear inflow jet in the region of the wake low.

In summary, a remarkable and unexpected result from this study is that although MCSs observed over the mesonetwork during PRE-STORM originated in a variety of ways, they tended to develop a common cloud and precipitation structure during their mature-to-dissipating stages, a pattern characterized here by the term "asymmetric" after Houze et al. (1990). This repeatable structure also had a repeatable surface pressure pattern associated with it (as described above). These findings have led to the development of an updated model for the surface pressure pattern accompanying squall lines, one containing both symmetric and asymmetric structures. This model is consistent with but extends past models based on a small number of cases (Fujita 1955, Pedgley 1962, Johnson and Hamilton 1988).

ACKNOWLEDGEMENTS

I would like to express my sincere appreciation to my advisor, Dr. Richard Johnson, for his guidance and advice throughout the completion of this paper. I would also like to thank the other committee members, Dr. Thomas McKee and Dr. Jack Cermak.

I would also like to thank Jim Bresch, Bill Gallus and Xin Lin for their help with the use of the computer systems at the Atmospheric Science Department.

Thanks are also extended to José Meitín for providing the mesonetwork and upper-air data, as well as his help in aquiring, in conjunction with Robert Hueftle, the radar data. For the National Weather Service surface station data, thanks go to the National Climatic Data Center. Much of the computer time was provided by the National Center for Atmospheric Research.

Finally, thanks to Gail Cordova for help in the final preperation of the manuscript and Judy Sorbie-Dunn who drafted several of the figures.

This research was supported by the National Oceanic and Atmospheric Administration through the Cooperative Institute for Research in the Atmosphere under grant NA 90 RAH 00077-9-01.

TABLE OF CONTENTS

LIST OF FIGURES

LIST OF TABLES

Chapter 1

INTRODUCTION

During the months of May and June 1985, a field experiment was conducted to investigate the structure, evolution, and dynamics of mesoscale convective systems (MCSs): the Oklahoma-Kansas Preliminary Regional Experiment for STORM-Central (OK PRE-STORM). Very high resolution data sets were collected using mesonet stations, soundings, conventional and Doppler radars, satellites and wind profilers (Cunning 1986).

It is well known that distinct surface pressure features are associated with MCSs; however, previous studies have drawn inferences regarding their structure and properties from the examination of only a limited number of cases (Fujita 1955, Pedgley 1962, Johnson and Hamilton 1988). The generality of these previous results is not well understood nor is the precise relationship between the surface pressure features and the precipitation features for all classifications of MCSs. In order to improve our understanding of this aspect of MCSs, each of the PRE-STORM MCSs that were sufficiently observed by the high resolution data array is examined to document its surface pressure features and to determine the relationship between these features and the convective and stratiform precipitation regions of the MCS.

In this thesis surface pressure and air flow, radar reflectivity patterns and the system-relative upper air flow are examined for each PRE-STORM MCS adequately sampled by the network. The May-June 1985 period was a very active one for MCSs in the PRE-STORM area (Augustine and Howard 1988). A total of 16 systems were judged to have sufficiently crossed the high resolution data array to be examined. Several others were only partially within the network and were judged to have been insufficiently obsevered to be included in this thesis. Based on these 16 cases, similarities in the patterns were explored and the results were then synthesized into two basic classifications. A schematic has been developed to summarize these features.

Chapter 2 details some of the background research on the subjects of surface pressure fields, radar reflectivity patterns and the features in the upper air flow for MCSs. Chapter 3 describes the data sets used as well as the analysis procedures. Chapter 4 details the synoptic situation, surface pressure and flow features, radar reflectivity features as well as the upper-air flow features associated with each of the May 1985 cases. Chapter 5 does the same for the June 1985 cases. Chapter 6 then relates each of the cases and leads to the development of the schematic and compares it to those previously developed. Lastly, Chapter 7 gives a summary of the study and recommendations for future research.

Chapter 2

BACKGROUND RESEARCH

2.1 Observations and Mechanisms of Surface Pressure Features

The typical surface pressure field associated with an MCS with a leading convective line and a trailing stratiform precipitation region consists of a pre-squall low, a mesohigh and a wake low (Fujita 1955, Pedgley 1962). The best documented and understood of these features is the mesohigh. It is typically positioned just to the rear of the leading edge of the convective line. It was identified in the studies which arose from the Thunderstorm Project (Byers and Braham 1949), such as Williams (1948, 1953). It was, at first, suggested by Tepper (1950) that the strong gradient at the leading edge of the mesohigh (or the "pressure jump line" as he termed it) was actually the cause of the convection. Through later work, this hypothesis was shown not to be the case since the mesohigh forms after the convective development. Fujita (1955, 1959) then proposed what has become the accepted major cause of the mesohigh. He suggests that it is largely due to air aloft being cooled by rainfall evaporation and brought down to the surface by downdrafts and spreading over the ground.

The formation of the pre-squall low was first discussed by Hoxit et al. (1976). They propose that its formation was due to upper tropospheric subsidence warming downwind of the system. They show that a surface pressure fall of 2-4 mb h^{-1} can be hydrostatically produced by sinking of the order of tens of centimeters per second in the 100-500 mb layer. Fritsch and Chappell (1980) performed a modeling study to show the development of convectively driven mesoscale pressure systems and they found that this "local compensating subsidence" (Fritsch 1975) actually occurred not just downwind of the convective system, but all around them. They suggest that mesolows may or may not form depending on how the individual thunderstorms are positioned and on what their interactions are with each other and their enviroment. In other words, the subsidence warming must be focused, continue over a long enough time period and extend through a deep enough layer to lead to the development of a mesolow.

The wake low, while having been identified as being associated with MCSs, did not recieve the same attention as to its dynamical causes as the mesohigh until quite recently. It was first observed by Williams (1953, 1954), where he termed it a "depression-type wave". He observed that the low appeared along the rear edge of the surface precipitation, and this has been confirmed by Pedgley (1962), Zipser (1977) as well as Johnson and Hamilton (1988). In contrast to the mesohigh and pre-squall low, both of which develop soon after the initial convection begins, the wake low has the tendency to develop in the mature-to-dissipating stage of the MCS (Fujita 1955, Pedgley 1962, Johnson and Hamilton 1988).

The first to hypothesize the dynamical cause of the wake low was Williams (1963). He demonstrated that the hydrostatic pressure falls associated with subsidence warming can account for the wake low. He did not, however, establish why this feature was present. Johnson and Hamilton (1988) hypothesized a cause related to the upper-air flow regimes associated with the MCS, and this will be discussed in section 2.3.

2.2 Schematics of Surface MCS Structure

The first detailed description of the surface pressure field accompanying a squall line was prepared by Fujita (1955) and is shown in Fig. 2.1. He shows two of the major pressure features, the mesohigh ("thunderstorm high") and the wake low ("wake depression"). He leaves out the pre-squall low, as it did not appear in his analyses of the cases he examined. It also depicts an accentuated pressure gradient ahead of the mesohigh, indicative of the gust front ("pressure surge line"), which is the leading edge of the cold downdraft air which spreads out upon reaching the ground. In this schematic, although different levels of precipitation are not delineated, it is apparent that there is not any preferential positioning of the stratiform precipitation behind the convective line. This precipitation

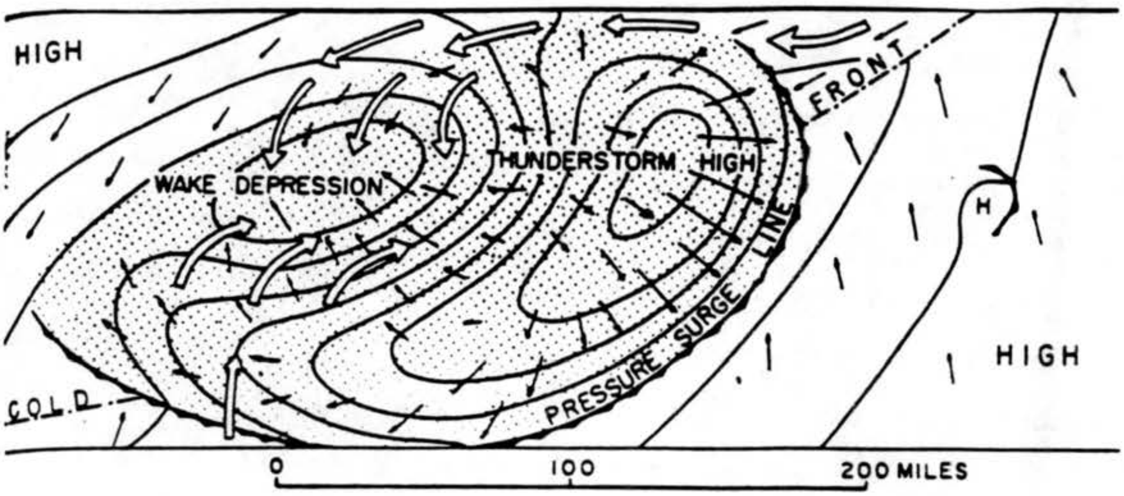

Figure 2.1: Schematic of surface pressure field in a squall line thunderstorm. Small arrows indicate surface wind; large arrows relative flow into the wake. Stippling indicates extent of precipitation cooled air (from Fujita 1955).

pattern has been defined by Houze et al. (1990) as a symmetric-type structure (Fig. 2.2a). In Fujita's (1955) schematic, the wake low is positioned along the back-central portion of the system ahead of the rain termination line. The ground-relative surface airflow features depicted include a weak south to southeast flow ahead of the system. Very strong outflow exists along the leading edge of the system. The flow is then strongly divergent to the rear of the mesohigh. Finally, the flow is shown to be strongly convergent along the axis of the wake low.

Several adjustments were made to this basic schematic by Johnson and Hamilton (1988) based on their study of the 10-11 June 1985 PRE-STORM case (Fig. 2.3). First, they added a pre-squall low. Second, they separate out different precipitation levels. They show a convective line, followed by a transition zone, which is an area of weaker precipitation to the rear of the convective line, and then an enhanced area of stratiform precipitation. They show the enhanced and weaker stratiform precipitation to be centered symmetrically behind the convective line. Hence it still is a symmetric-type system. They also explicitly place the wake low at the back edge of the precipitation. Lastly, they place the maximum convergence to the rear of the wake low, rather than along its axis.

The occurrence of the main convergence (divergence) to the rear of the wake low (mesohigh) has been studied by Garratt and Physick (1983) and Vescio (1990). They found that due to the highly transient nature of the pressure gradient features, the air does not have the time, due to its short residence within these gradients, to come into geostrophic balance. The results of this are shown in the schematic, with the flow passing forward through the mesohigh, a divergence maximum to the rear of the mesohigh, flow passing backward through the wake low, and a convergence maximum to the rear of the wake low. It takes the wind time to adjust to the change in direction of the gradient, hence the shift of the wind direction occurs to the rear of the shift of the gradient direction.

A different schematic structure was developed by Pedgley (1962) based on his examination of several convective systems which passed through southeastern England on 28 August 1958 (Fig. 2.4). It is quite similar to the Fujita schematic in many respects. It shows a pressure surge line ahead of the mesohigh, which is along the convective line.

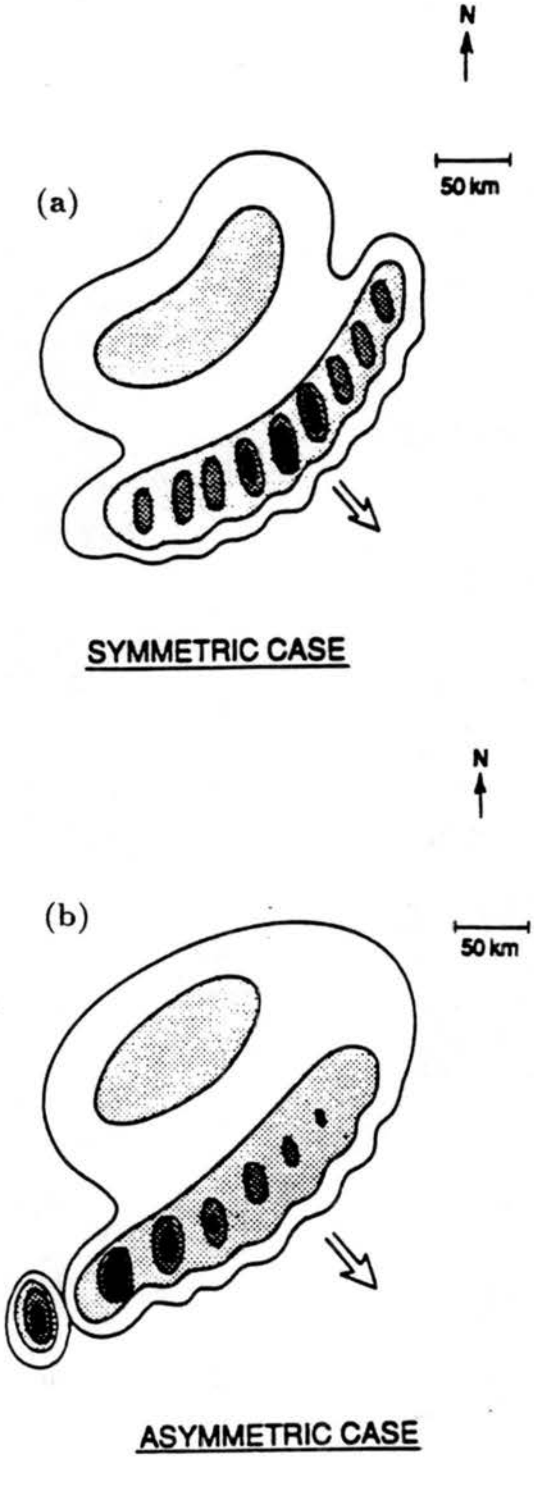

Figure 2.2: Schematic of a) symmetric and b) asymmetric leading-line/trailing stratiform mesoscale precipitation system organization. Large vector indicates direction of system motion. Levels of shading denote increasing radar reflectivity, with most intense values corresponding to convective cell cores (from Houze et al 1990).

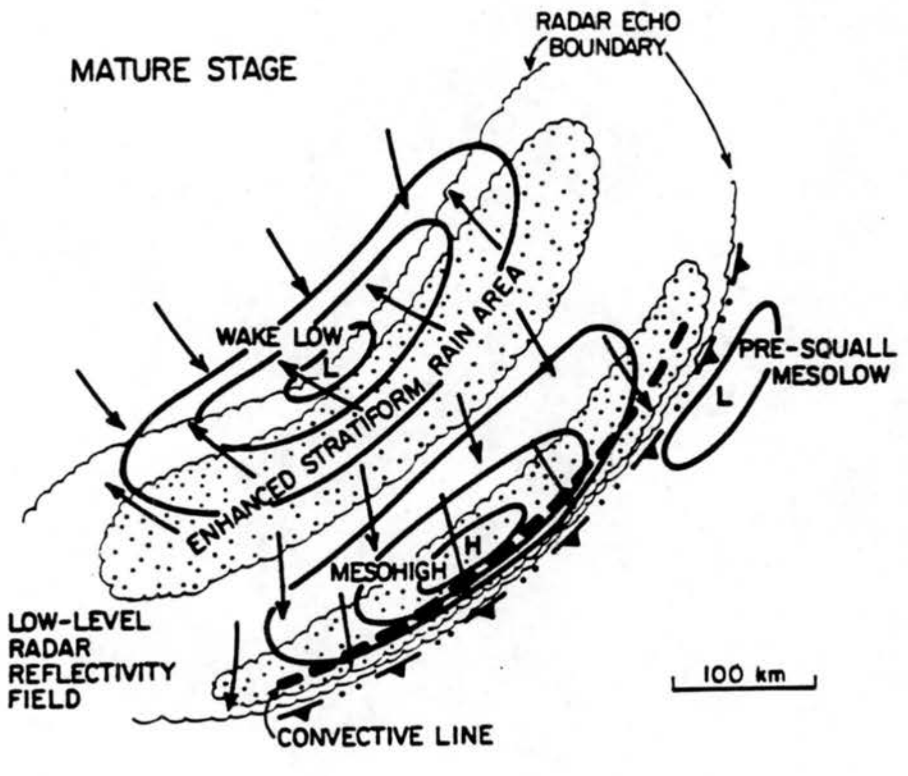

Figure 2.3: Schematic of surface pressure, wind field and precipitation during the mature stage of a squall line with a trailing stratiform rain region. Arrows show ground-relative wind streamlines (from Johnson and Hamilton 1988).

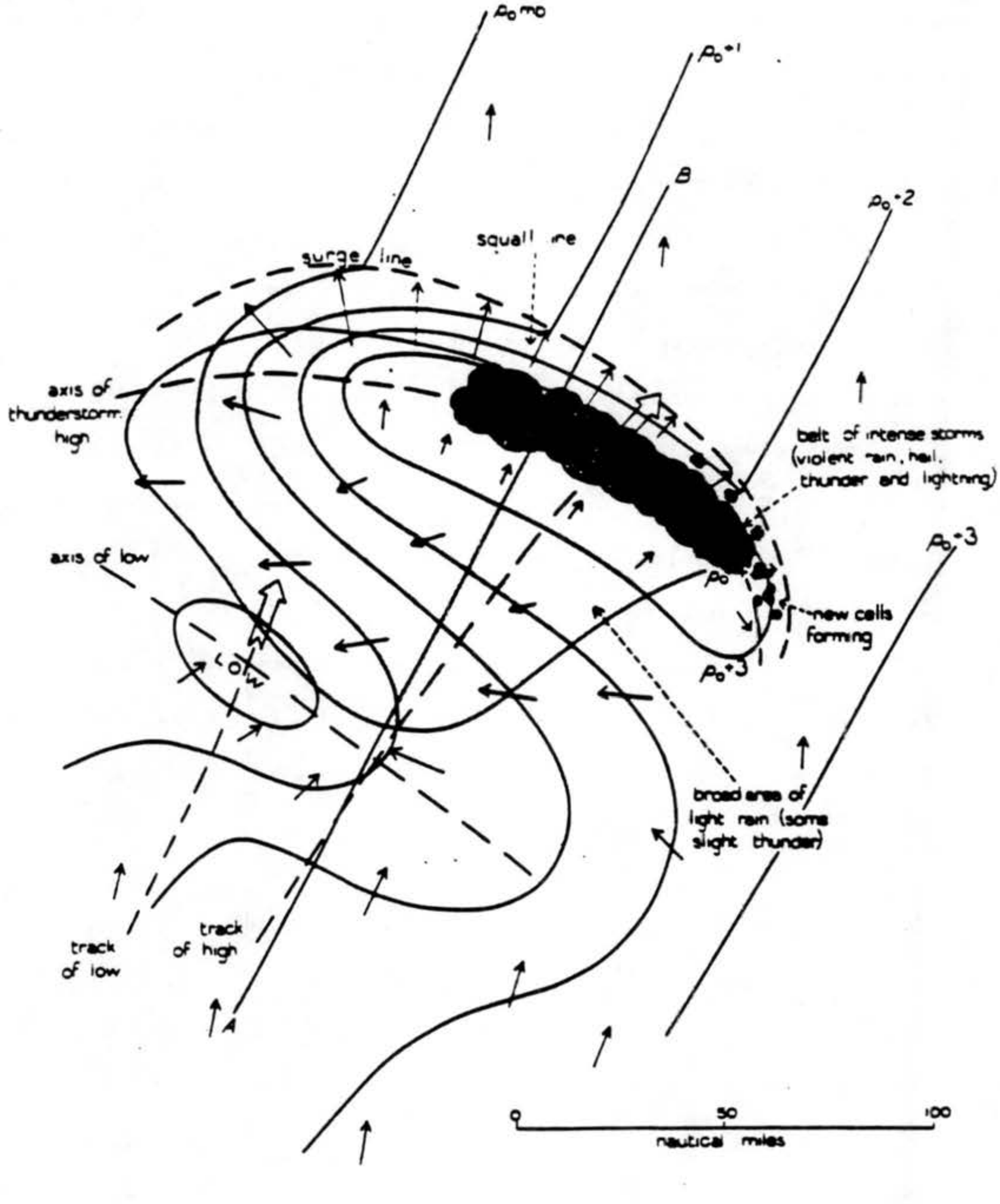

Figure 2.4: Schematic of surface pressure, wind field and precipitation during the mature stage of a squall line with a trailing stratiform rain region. Arrows show ground-relative wind direction (from Pedgley 1962).

Strong outflow is present ahead of the convective line. The flow is strongly divergent to the rear of the mesohigh and strongly convergent along the axis of the wake low. Significant differences do exist between this and Fujita's schematics. Pedgley shows a preferential positioning of the stratiform precipitation along the convective line with the wake low positioned to the rear of the stratiform precipitation area. This structure resembles the asymmetric type MCS (Fig. 2.2b) as defined by Houze et al. (1990).

In these previous attempts at schematics of MCSs, only a limited number of cases were examined. One of the main motivations of this thesis is to expand on those previous attempts at schematics of MCSs by examining the features associated with a larger sample of cases, leading to a more generally applicable schematic of these systems.

In his study of the PRE-STORM MCSs, Blanchard (1990) attempted to develop a classification scheme for MCSs based on the radar data. His study has come under question (Doswell 1991) for the problems involved in the terminolgy used. The distinction between his "linear" and "occluding" systems is not clear due to the changeable nature of several of the systems during their existence both inside and outside of the PRE-STORM area. In this study, the changeable nature of the systems has been taken into account through the extensive study of each system throughout its life cycle.

2.3 Observations of MCS Upper-air Features

A schematic of the mature stage of a midlatitude squall line with a trailing stratiform precipitation region from Houze et al. (1989) is shown in Fig. 2.5. It shows three general system-relative flow features. First, there is a system-relative front-to-rear (FTR) flow which originates at low levels ahead of the system and rapidly ascends in the region of convective updrafts. It then ascends more gently through the stratiform precipitation region. It has been suggested that this ascending FTR flow is partially responsible for the development of the stratiform precipitation region by transporting hydrometeors from the convective line rearward [Smull and Houze (1985, 1987a), Rutledge and Houze 1987]. Then there is a system-relative rear-to-front (RTF) flow which originates to the rear of the system and descends towards the convective line. Lastly, there is FTR flow at the lower levels. This is a representation of the surface outflow from the system.

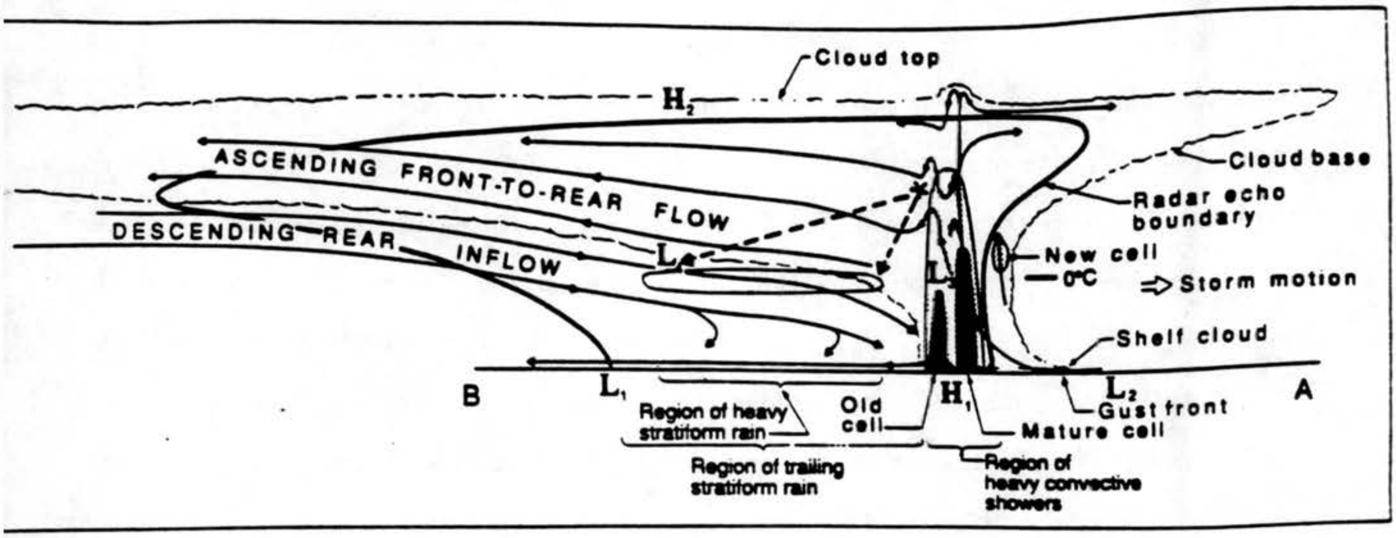

Figure 2.5: Schematic of a squall line with a trailing stratiform rain area viewed in a vertical cross section oriented perpendicular to the convective line (from Houze et al. 1989).

Johnson and Hamilton (1988) developed a schematic which focuses more on the rear portion of the system (Fig. 2.6). They suggest a physical link between the positioning of the wake low at the back edge of the stratiform precipitation area and the existence of the descending rear inflow jet (maximum of the RTF flow) crossing this line. They found that the maximum warming and drying associated with the rear inflow jet appeared about 1 km above ground level just to the rear of the light precipitation. This is where the minimum pressure occurs, and they suggest that this can be explained hydrostatically as a direct result of subsidence warming. The warming is maximized along the back edge of the precipitation due to the fact that in the rain area there is strong evaporative cooling and moistening offsetting a large portion of the subsidence warming.

The first observation of the rear inflow in an MCS was reported by Newton (1950); however, it was only qualitatively determined and its strength and temporal and spatial variation were not examined. The first attempt at a quantitative examination of the rear inflow was by Smull and Houze (1987b). They summarized the results of previous studies with respect to the relative airflow measured to the rear of the convective systems. Of the 18 cases they examined, ten were found to have rear inflow of less than 5 m s^{-1} and were termed "Stagnation Zone" cases. Five were "Weak Rear Inflow" cases (5-10 m s^{-1}) and three were "Strong Rear Inflow" cases with rear inflow greater than 10 m s^{-1}. One of the goals of this thesis is the documentation of the relationship of the rear inflow jet to the position and intensity of the wake low. There are problems with comparing the results of this thesis with those from the papers summarized by Smull and Houze (1987b). First, in many of those studies the rear inflow was not the primary concern. Second, little or no information is available on the temporal and spatial variability of the rear inflow in those cases. Lastly, the positioning of the rear inflow relative to the position of a wake low, or even the existence of a wake low, was not known in many of the cases.

Another upper-air feature present in many, but not all, MCSs is a midlevel cyclonic vortex or mesovortex. These features are often too small to be observed by the typical synoptic-scale sounding network, and hence were not observed until recently through the use of satellite data (Johnston 1982, Bartels and Maddox 1991) and numerical modeling

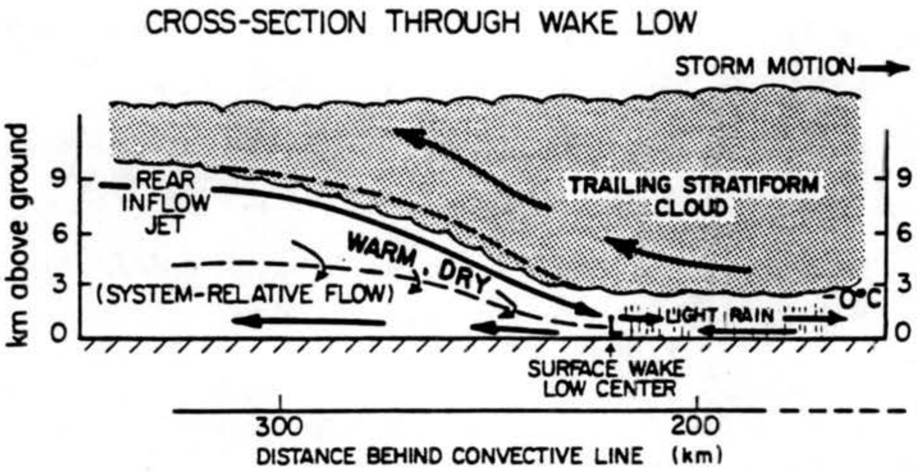

Figure 2.6: Schematic cross section through wake low (from Johnson and Hamilton 1988). Arrows indicate system-relative winds.

(Zhang and Fritsch (1987, 1988a,b). Bartels and Maddox found that mesovortices typically form in large scale enviroments charactized by weak flow, weak vertical shear and weak background relative vorticity. In some cases these features are seen to deform the stratiform precipitation region into a hook-like pattern (Leary and Rappaport 1987, Houze et al. 1989, Brandes 1990, Johnson and Bartels 1992).

The fact that midlevel cyclonic vortices are present in some cases and not others led Houze et al. (1989) to develop two conceptual models of the low-level reflectivity and midlevel flow. In Fig. 2.7a they show a typical symmetric-type system with a non-rotational midlevel flow structure, indicative of the ascending FTR and descending RTF flow regimes. In Fig. 2.7b they show a typical asymmetric-type system with a midlevel cyclonic vortex in the northern portion of the system.

This thesis attempts to expand upon the findings of Smull and Houze (1987b) by examing the system-relative flow structure, not just at the back edge of the system as they did, but also examine it throughout the remainder of the MCS focusing on the wake low region.

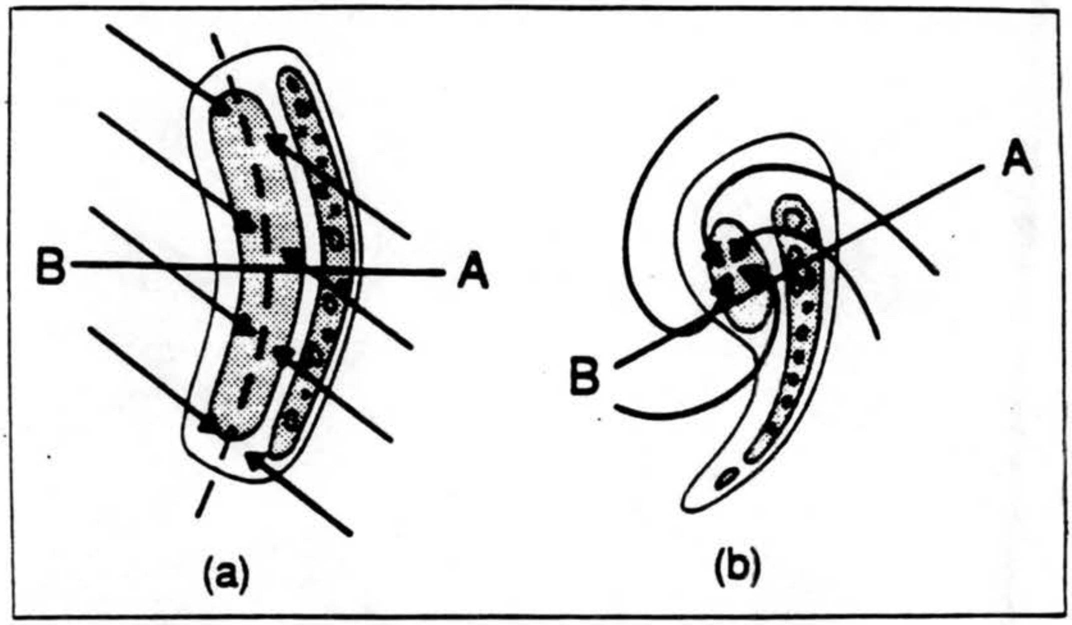

Figure 2.7: Schematic mid-level horizontal cross section through a) a symmetric MCS, and b) an asymmetric MCS with a mesovortex. Arrows represent the mid-level system-relative flow and are superimposed on low-level radar reflectivity. Stipling indicates regions of higher reflectivity (from Houze et al. 1989).

Chapter 3

DATA AND ANALYSIS PROCEDURES

3.1 Surface Data

In the construction of the surface analyses, data from the 84 automated stations of the PRE-STORM mesonetwork were used. The northern portion of the network consisted of 40 National Center for Atmospheric Research (NCAR)/Field Observing Facility (FOF) Portable Automated Mesonetwork II (PAM) sites. In the southern portion, 40 National Severe Storms Laboratory (NSSL) Surface Automated Mesonetwork (SAM) stations were used. Additionally, two PAM sites were collocated with two SAM sites. The stations were located in an 8 by 10 rectangular array with an approximate station spacing of 50 km (Fig. 3.1). Each of the stations measured the dry and wet bulb temperatures, station pressure, wind direction and wind speed as five-minute averages. Additionally, accumulated rainfall was measured at five minute inteverals and the maximum wind gust in the five-minute period was recorded.

In order to reduce the effects of the elevation differences across the network on the station pressure, the pressures were adjusted hydrostatically to 480 m (the average elevation for all the stations in the network). To accomplish this, it was assumed that the surface virtual temperature was approximately equal to the mean virtual temperature of the column from the station elevation to 480 m. Using this assumption, the following equation can be applied:

$$P_{480} = P_s exp\left[\frac{g(z_s - 480)}{R_d\overline{T}_v}\right]$$

where g is the gravitational acceleration (=9.8 m s^{-2}), R_d is the gas constant for dry air (=287 J kg^{-1} K^{-1}), z_s is the station elevation (m), p_s is the surface pressure (mb), $\overline{T}_v$ is

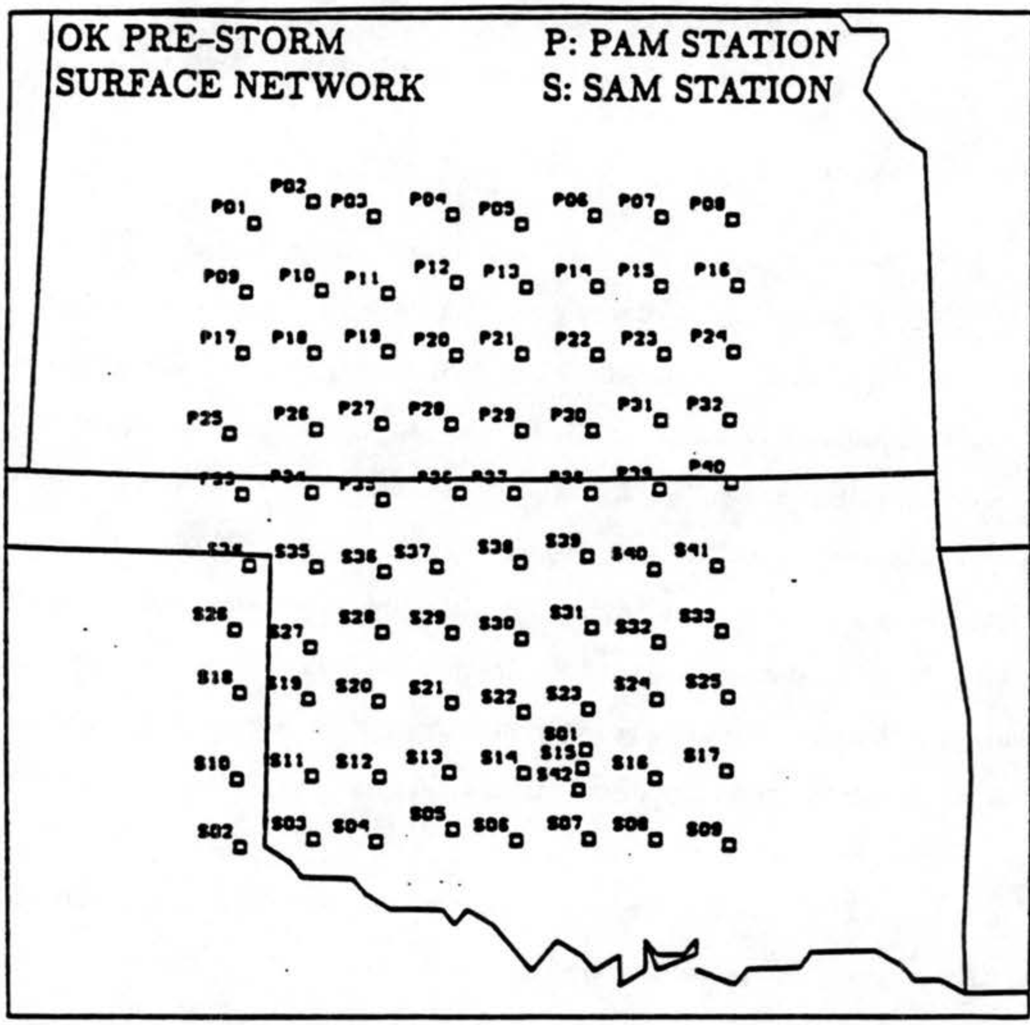

Figure 3.1: The PRE-STORM PAM and SAM surface array (from Stumpf 1988).

the mean virtual temperture of the column from the station elevation to 480m, and P_{480} is the pressure at 480m.

An additional adjustment was then conducted to remove the effects of the diurnal tide. The adjustments from this diurnal solar tide oscillation were taken from Stumpf (1988) and are shown in Fig. 3.2.

The final adjustment was to remove the errors resulting from individual station bias. This was done following procedures described by Fujita (1963) and Johnson and Toth (1986) and is described in Appendix A. It was done for several time periods throughout the experiment due to the changeable nature of the biases for several stations. These corrections can be found for each case also in Appendix A.

Due to the sheer number of pressure analyses needed for this study, it was necessary to use an objective analysis scheme to complete the analyses in a reasonable amount of time. It was decided to use a Barnes-type scheme (Barnes 1964, 1973). In order to accurately depict the strong pressure gradients present in many MCS cases, it was decided to apply a time-to-space transformation procedure to the five-minute data. To do an analysis for some specific time, the five-minute data from 15 minutes before to 15 minutes after this time were used. The assumption was made that the systems are relatively steady-state over the half-hour period. To properly position each of these data points, the velocity of each system was calculated from the average velocity of the leading edge of the convective line over the lifetime of the system within the PRE-STORM area. Each data point was then placed on a string either side of the station, as shown in Fig. 3.3. This was done every 15 minutes throughout the lifetime of the system, while it was within the PRE-STORM area.

3.2 Radar Data

Base-scan reflectivity data from the National Weather Service (NWS) WSR-57 radars at Amarillo, Texas, Oklahoma City and Norman, Oklahoma, Wichita and Garden City, Kansas and Monett, Missouri were used (Fig. 3.4).

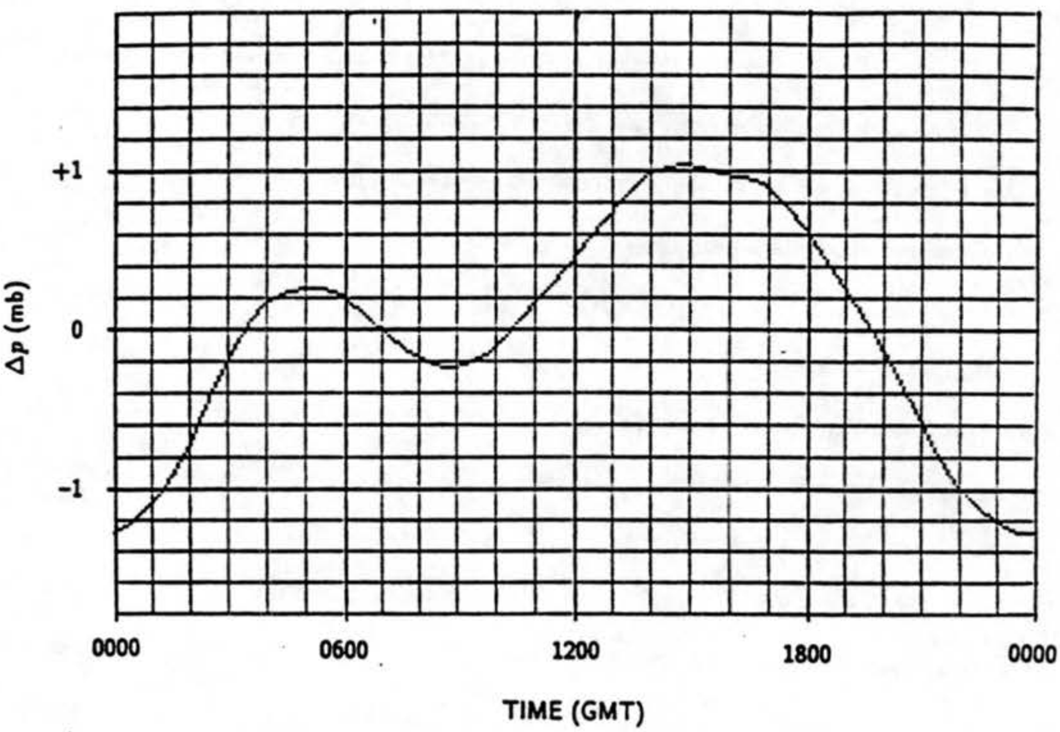

Figure 3.2: The diurnal tide curve. Units are in mb. Time is UTC. Values shown on the curve were subtracted from the pressure data as a function of time (from Stumpf 1988).

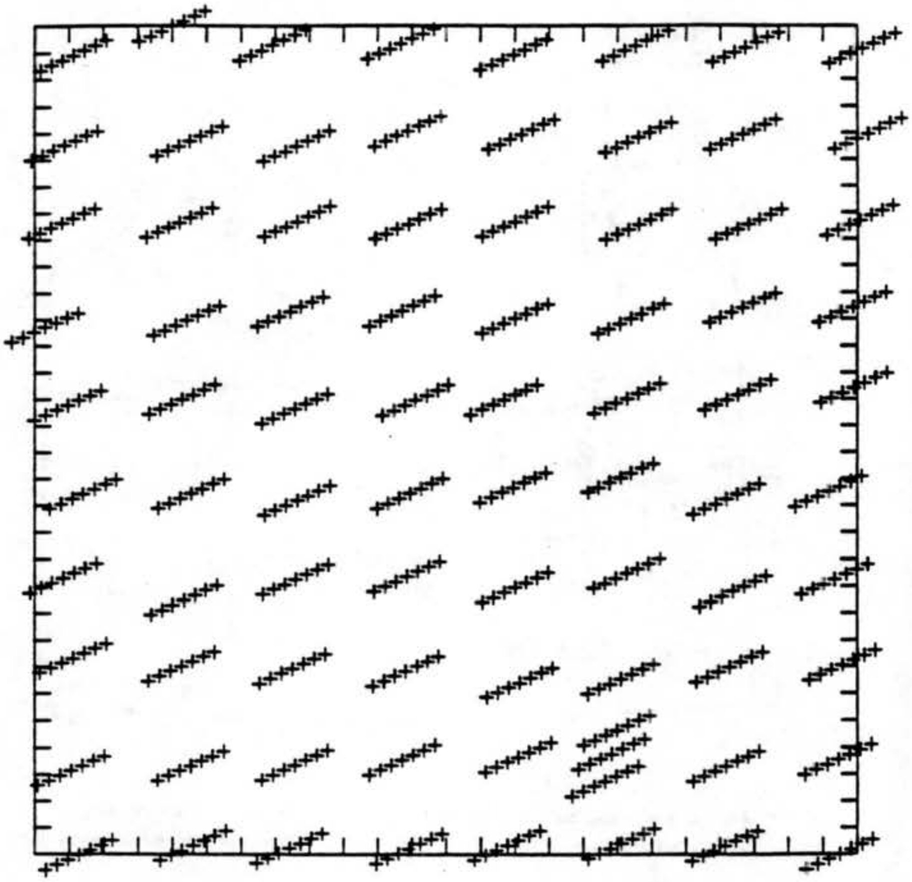

Figure 3.3: Example of placement of data points (+) using the five-minute data and system velocity. Here using velocity of the 3-4 June 1985 case (from 240° at 18 m s^{-1}). Each tick mark represents about 16 km.

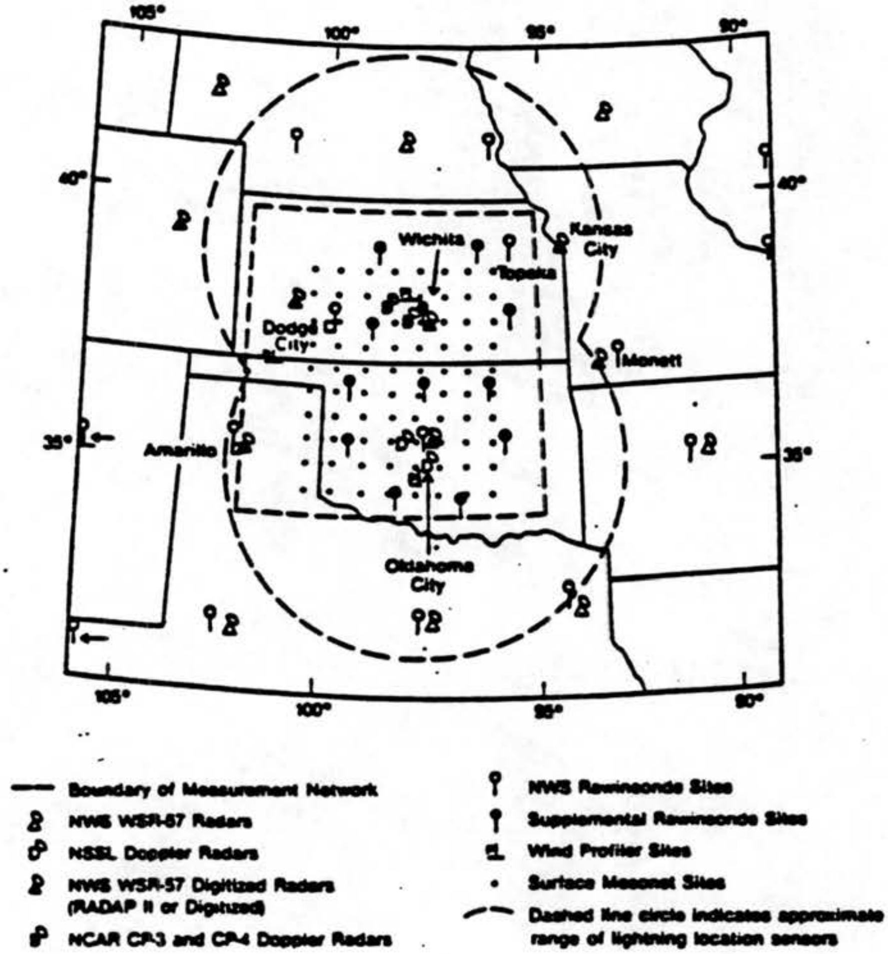

Figure 3.4: The OK PRE-STORM observational mesonetwork (from Cunning 1986).

Except for the Norman and the majority of the Wichita radar data, the volume scan radars were digitized by the NWS second generation Radar Data Processor (RADAP-II). These data were recorded at each 2° radial at a 2 km gate spacing.

For the majority of the Wichita radar data, the Hurricane Research Division NOAA/ERL/AOML research radar digitizer was used. This digitizer had higher resolution data then was available with the RADAP-II data, recording at each 1° radial at a gate spacing of 1 km. Data from Wichita were also available for a larger portion of the needed times than from RADAP-II.

Additionally, for one case, the NOAA/ERL/NSSL Norman radar was used, this used a digitizer which recorded data at each 2° radial at a 1 km gate spacing (Meitín 1987).

The low-level base scan (0.5° elevation angle) reflectivity data were used to construct the composite radar images which consist of digitized data from several radar sites. These were compiled every 30 minutes throughout the lifespan of each system while they were within the limits of the radars.

3.3 Upper-air Data

The PRE-STORM upper-air network included the 15 surrounding NWS sounding sites as well as 12 supplemental sites within the PRE-STORM area (Fig. 3.5). The soundings measured temperature, moisture, wind, pressure and height. The data were interpolated to 25 mb levels, with the surface kept as an additional level. If spurious data existed, the levels which were affected were dropped from the analysis.

The availablity of supplemental soundings was highly variable (Meitín and Cunning 1985). During most of the examined cases, soundings were taken at at least three-hour intervals, and as often as every 90 minutes. For several cases, however, few, if any, supplemental soundings were taken.

The main use of this data for this study is the examination of the system-relative wind field. This is found by subtracting the velocity of the system (as calculated from the radar data) from the actual wind field over the time period of the analysis.

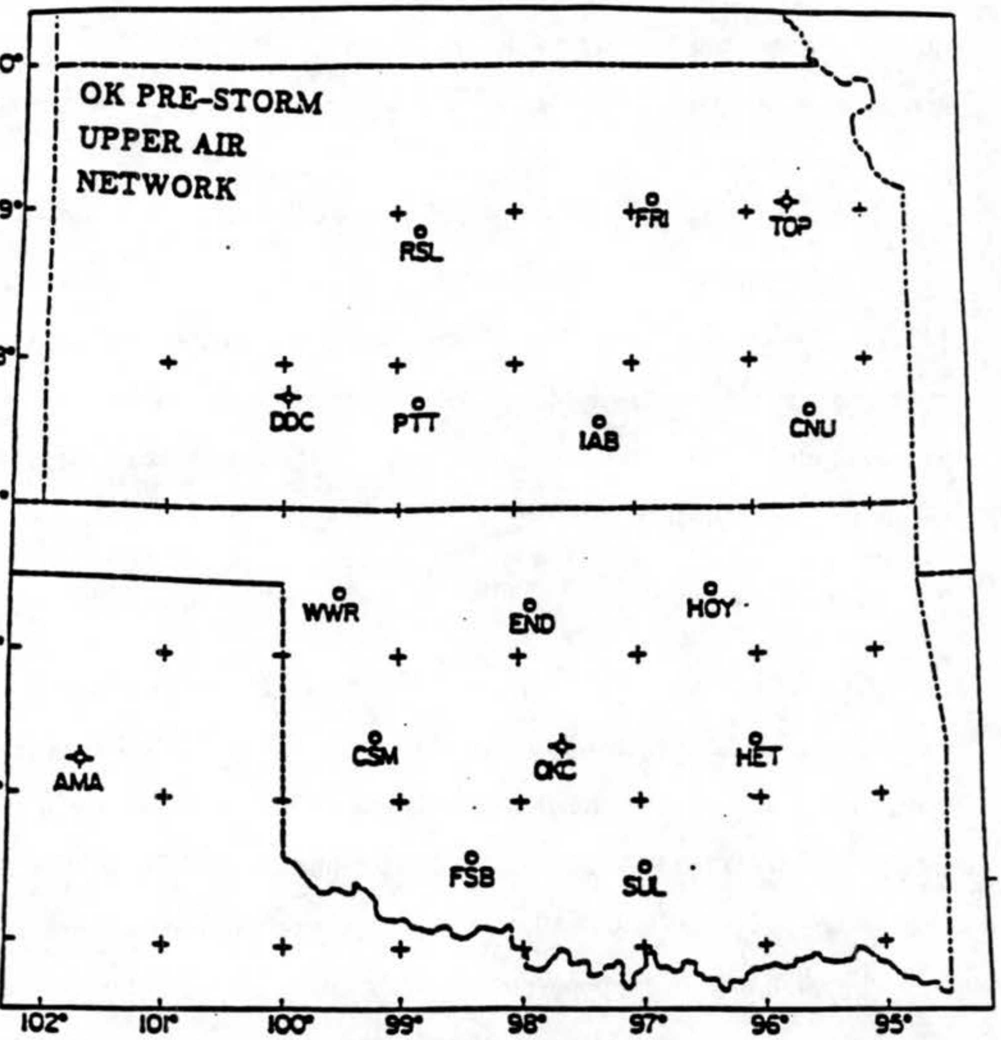

Figure 3.5: The PRE-STORM upper-air mesonetwork. Crossed circles indicate NWS sites. Plain circles indicate supplemental sites (from Stumpf 1988).

Chapter 4

MCS CASES: MAY 1985

4.1 Introduction

During the month of May 1985, seven separate MCSs passed through the PRE-STORM network. These cases occurred on 7, 13(2), 21, 27, 28, and 29 May. Several other systems occurred during this period, but were not adequately sampled by the intensive PRE-STORM network: 10-11, 12-13, 21, and 27 May. Each of the latter MCSs developed along the periphery of the mesonet and it could not be determined if the features of interest here, particularly the wake low, existed with these systems.

The purpose of this chapter is to give a detailed overview of each of the seven major systems in May. Much of the information in this chapter as well as in Chapter 5 (June MCSs) is quite repetitive due to the many similarities that are to be found in these MCSs. Despite this, there are very significant differences in the way each system evolved into these similar patterns. For that reason as well as just the need to show in detail the similarities in these systems, it was decided to give each system a detailed overview. The section of the most general interest is the System Overview section of each case, and in particular, the Mature Stage subsections since this is where much of the information is drawn for the purposes of creating a schematic. Many of the findings from this and the June MCS chapter are summarized in Chapter 6. Chapter 4 examines the general synoptic situation leading to the development of each MCS, the radar reflectivity structure, the surface pressure and ground-relative flow features, the system-relative upper-air flow, as well as time series of the mesonet data.

4.2 May 7 case

4.2.1 Synoptic situation

The conditions at 0000 UTC (all times UTC) 7 May are discussed to show the environment at the time of the initial convective development associated with this case. At the surface (Fig. 4.1a) a weak stationary front extended across the northern portion of the Texas panhandle into northern Oklahoma. The conditions north of the front were characterized by temperatures in the 15-22°C range, dewpoints in the 12-18°C range, and an easterly flow. South of the front temperatures were near 27°C, dewpoints around 15°C, and there was a southeast flow.

At 850 mb (Fig. 4.1b) a trough extended across southern Colorado, eastern New Mexico, into western Texas. Weak warm advection was occurring across the Texas panhandle and Oklahoma. Very moist air was across central Texas, Oklahoma, and western Kansas. A moderate low-level (850 mb) jet was evident within the PRE-STORM network at this time (Fig. 4.2) with 10-15 m s^{-1} flow out of the south to southeast. At 700 mb (not shown) the winds veered from 850 mb to a west to southwest flow across Oklahoma and southern Kansas, indicative of the low-level warm advection which was evident at 850 mb. At 500 mb (Fig. 4.1c) a weak ridge was over Kansas and Oklahoma, with a weak short-wave feature in eastern Colorado. The flow was weak and out of the west over Kansas, Oklahoma and Texas (5-15 m s^{-1}).

4.2.2 Radar overview

The initial development of convection associated with this system occurred in northeastern New Mexico at 2200 6 May (not shown). Additionally, very intense multi-cellular convection developed in the northeastern Texas panhandle and northwestern Oklahoma. Convection lasted for eight hours in this location, until the MCS passed by, and caused extensive hail and flood damage (Storm Data, May 1985). By 0300 (not shown) the convection in New Mexico developed into a small convective line in western Texas. Then by 0600 (Fig. 4.3a) the convective line met up with the northwestern Oklahoma convection. A large area of light stratiform precipitation developed on its northern end. Largely random convection was in northern Oklahoma and southern Kansas, although a fairly linear

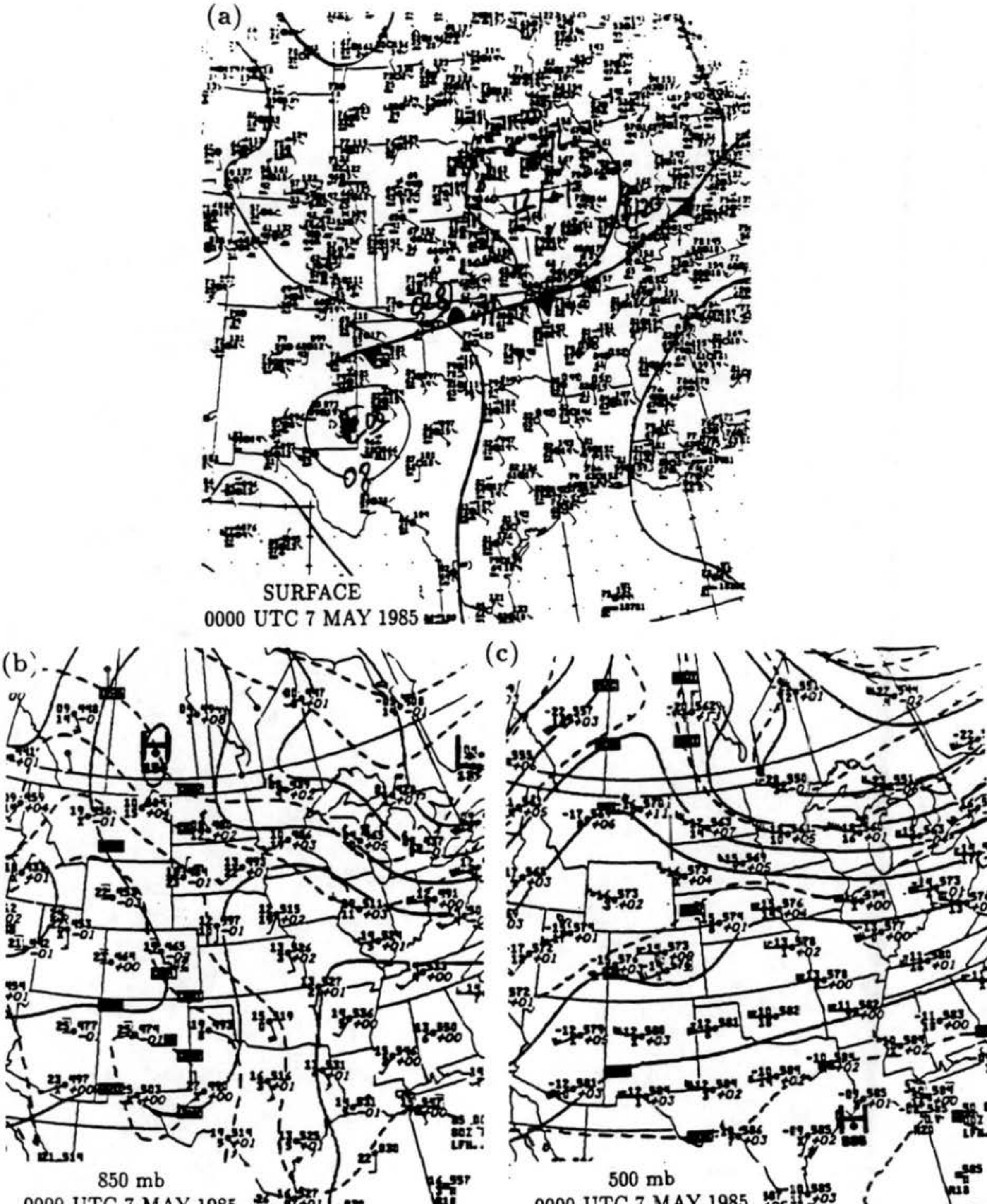

Figure 4.1: 0000 UTC 7 May 1985 NMC analyses: a) surface; b) 850 mb; c) 500 mb. Solid contours represent in a. sea-level pressure and in b. and c. geopotential height. Dashed contours in b. and c. represent temperature in °C.

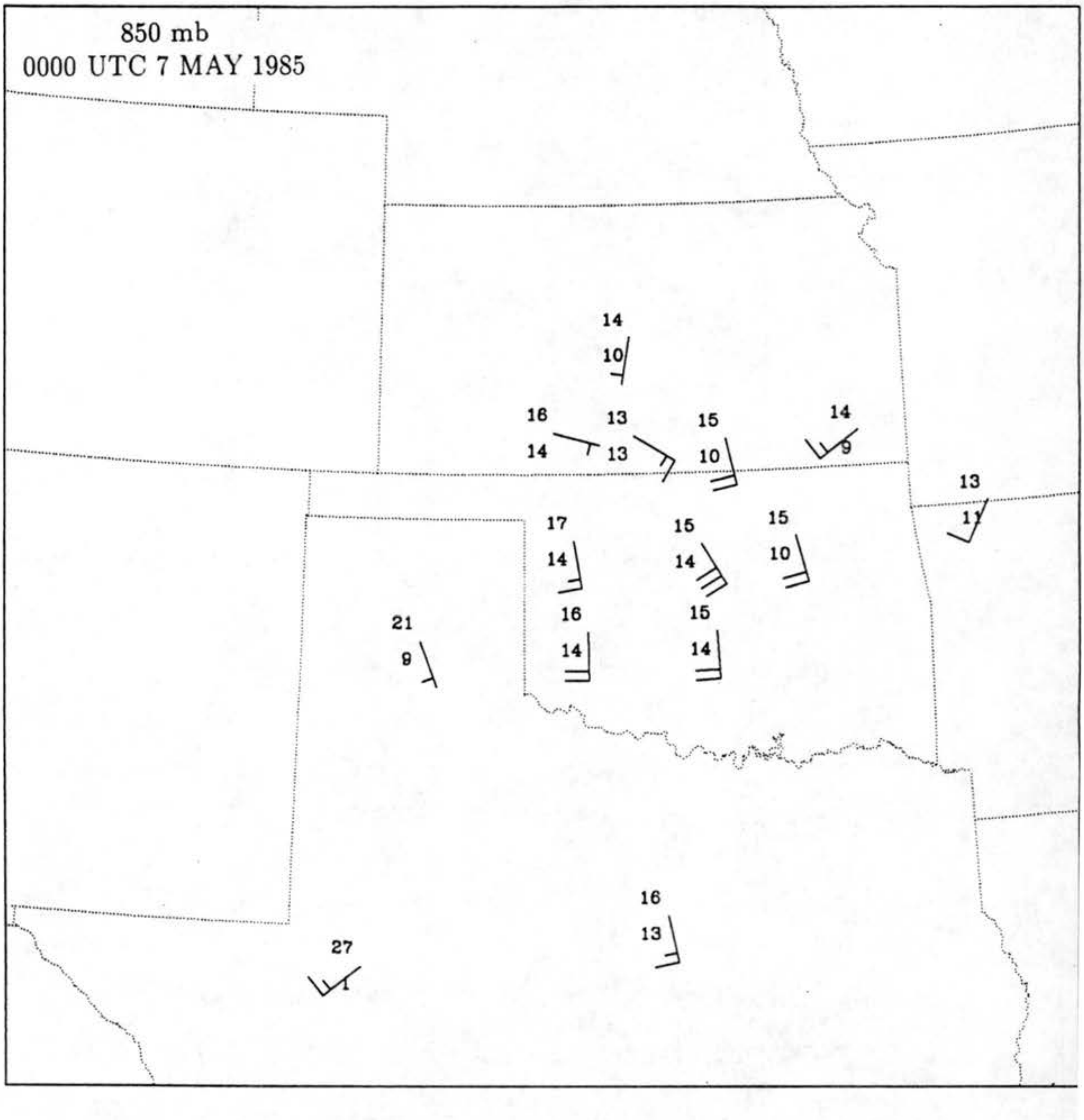

Figure 4.2: 0000 UTC 7 May 1985 PRE-STORM 850 mb data. One full barb represents 5 m s^{-1}. Temperature and dewpoint in °C.

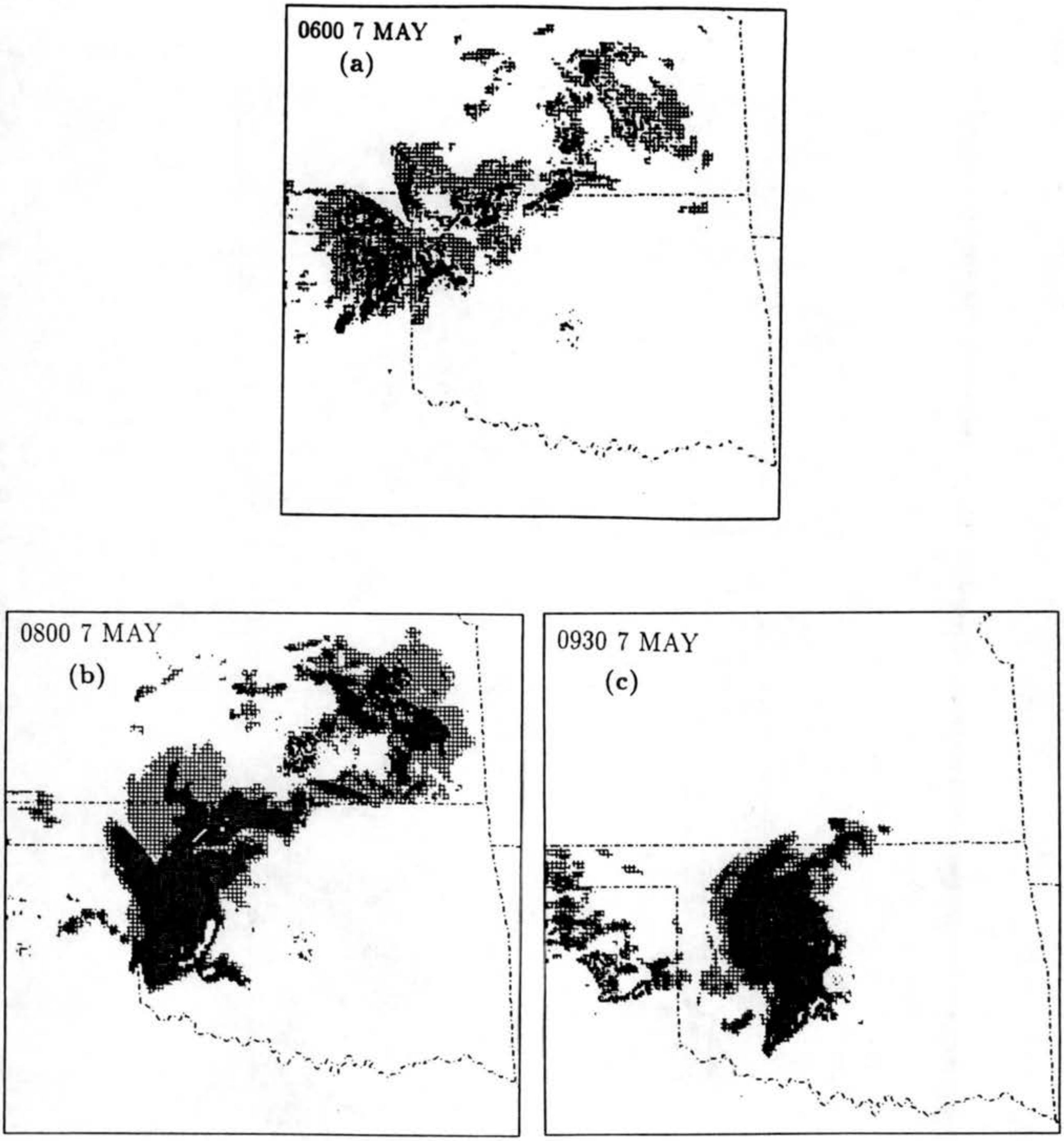

Figure 4.3: Radar composites for 7 May. Reflectivity thresholds are 15, 25, 40 and 49 dBZ. Figures include: a) 0600 UTC Amarillo TX, Oklahoma City OK and Wichita KS; b) 0800 UTC Amarillo TX, Oklahoma City OK, and Wichita KS; c) 0930 UTC Amarillo TX and Oklahoma City OK; d) 1100 UTC Oklahoma City OK and Wichita KS; e) 1300 Amarillo TX; Oklahoma City OK and Wichita KS.

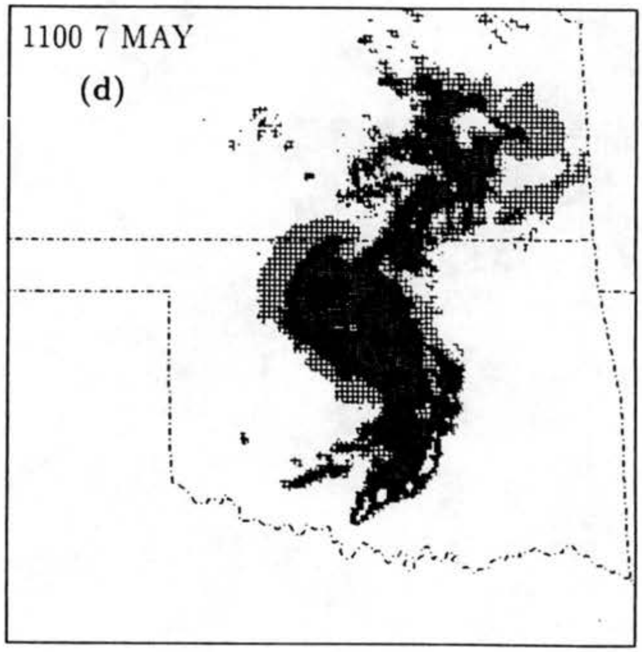

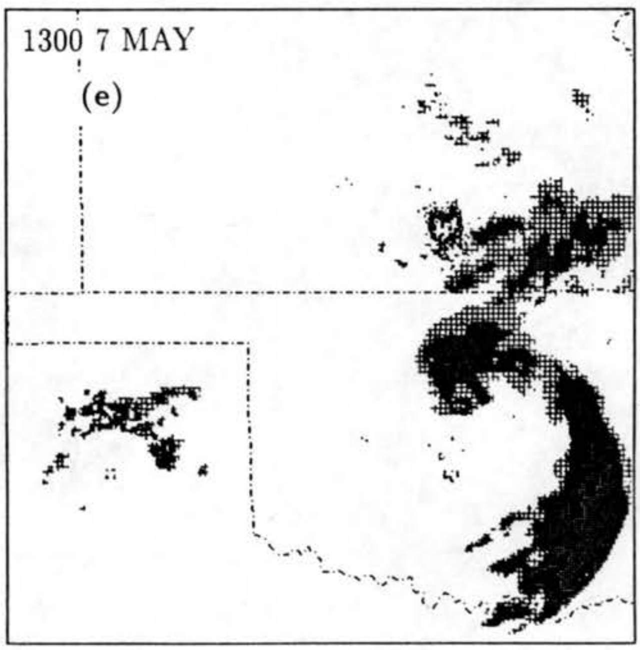

Figure 4.3: Continued.

(east-west) structure was evident in northern Oklahoma, with a small area of trailing stratiform precipitation to the rear of its western portion.

The system became well developed by 0800 (Fig. 4.3b). Two distinct convective lines were found, and they gave the appearance of an occluded-type wave cyclone but, as has been noted by Smull and Augustine (1992) in their study of the second MCS on 3-4 June 1985, this was due to the chance, short-lived superposition of two convective modes. The only reports of severe weather with this MCS occurred on the southern end of the convective line and they were mostly large hail.

Several important changes in the reflectivity structure occurred by 0930 (Fig. 4.3c). First, the east-west convective line dissipated. Second, an extensive area of moderate stratiform precipitation developed, mostly to the rear of the northern portion of the convective line. This placed the system at this time into the asymmetric category of MCSs as defined by Houze et al. (1990). A core of mixed heavy stratiform and convective precipitation was present to the rear of the far northern end of the convective line. The convective portion was from the remainder of the east-west convective line. Finally, a "comma"-type structure developed as the stratiform precipitation on the southern end of the system dissipated. These changes continued such that by 1100 (Fig. 4.3d) a more distinct "comma"-type structure developed. There was further erosion of the stratiform precipitation in the southern and central portions of the system. Further erosion was also occurring within the stratiform echo itself just south of the circular core of heavy stratiform precipitation. A second distinct core of heavy stratiform precipitation developed to the rear of the north side of the convective line. Finally, by 1300 (Fig. 4.3e) the convective line dissipated, and the stratiform cores started to weaken, especially in the mesovortex region. Also, the erosion of stratiform precipitation led to a cutoff of the "comma head" from the rest of the system.

4.2.3 System overview

This section and similar sections for all subsequent cases contain surface and upper-air mesoanalyses for each of the cases. At the surface, the adjusted pressure (referred to as pressure) contours as well as plots of temperature, dewpoint, and the ground-relative winds are examined. In order to facilitate the comparison of these features with the MCS, the radar reflectivity plots are overlaid on these plots. These plots are examined to show how the surface pressure features (mesohighs, wake lows, etc.) are positioned relative to the radar reflectivity features (convective lines, stratiform precipitation regions, etc.). Also they are used to show how the surface flow field is affected by the MCS and its associated pressure field and what changes occurred in these structures over the lifetime of the system within the mesonet. The upper-air maps examine the temperature, dewpoint, and ground-relative winds at constant pressure levels. These upper-air maps are used to examine the existence of, and conditions associated with, midlevel mesovorticies. The single-station graphs show the system-relative flow features. These are examined to give a view of the rear inflow structure associated with these MCSs since, as mentioned in Chapter 2, a proposed cause of wake lows is a descending rear inflow jet. Finally, there are mesonet time series plots of temperature, dewpoint, pressure, wind speed, direction, and gusts (winds ground-relative). These are examined to show more clearly the changes in these fields with the passage of specific pressure features.

Initial conditions (0600)

The environment at the time the MCS began to move into the PRE-STORM network is shown in the 850 mb and 500 mb maps at 0600 (Fig. 4.4a, b). The most striking feature was the considerable warming at 850 mb (0.7-1.4°C) as well as the cooling at 500 mb (1.2-3.2°C) that occurred in Oklahoma since 0000. This was especially evident in western Oklahoma, just ahead of the system at CSM (see Fig. 3.5 for location), where the 850 mb (500 mb) temperature increased (decreased) by 1.4°C (3.2°C). There was also a tongue of very moist air in this area at 850 mb. This was indicative of the destabilization of the atmosphere ahead of the MCS.

MCS enters mesonet (0730)

By 0730 the MCS had nearly completely entered the PRE-STORM area (Fig. 4.5). The flow around the MCS was characterized by weak (5 m s^{-1}) south-southeast flow ahead of the system and easterly flow to its north. This placed the weak front somewhere

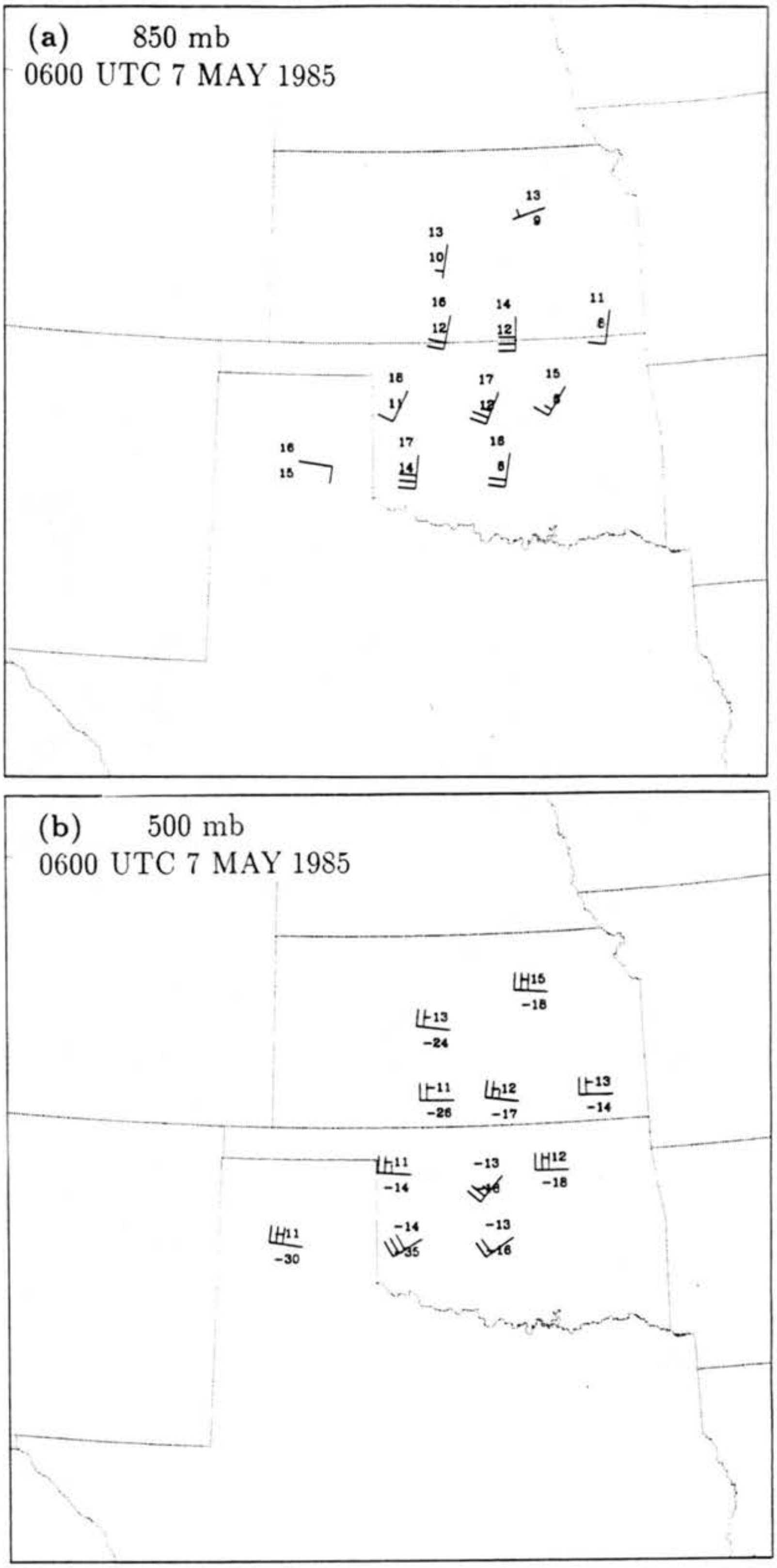

Figure 4.4: Same as Fig. 4.2 except for 0600 UTC 7 May at a) 850 mb and b) 500 mb.

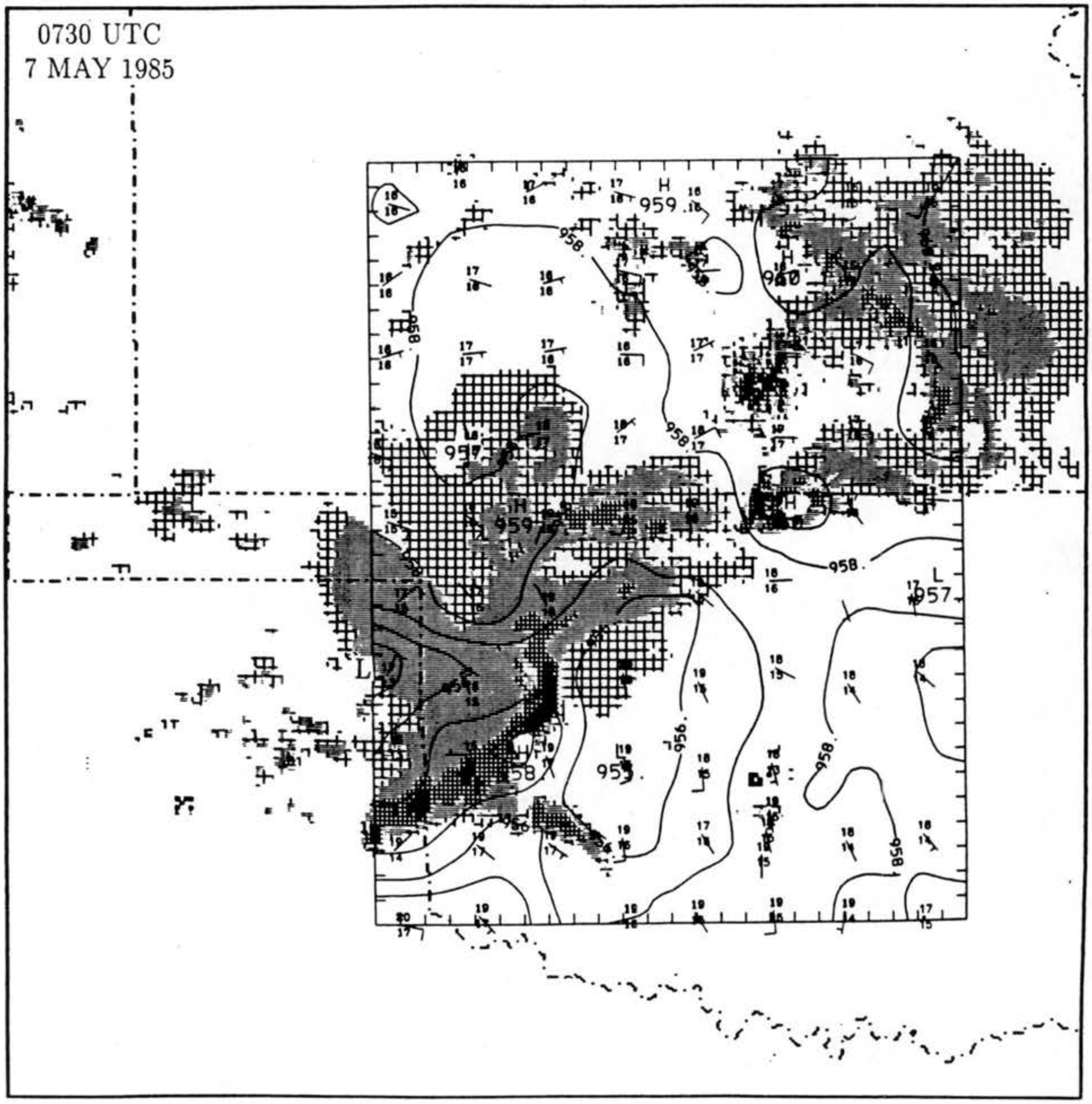

Figure 4.5: Pressure at 480 m, in millibars, at 0730 UTC 7 May 1985. Reflectivity thresholds are 15, 25, 40, and 49 dBZ. Temperature and dewpoint (°C) are plotted at individual stations. Winds are in m s^{-1}, with one full barb equivalent to 5 m s^{-1}.

along extreme northern Oklahoma or southern Kansas. The east-west convective line appeared to have formed along this front. A tongue of moist air existed just ahead of the northeast-southwest convective line (17°C dewpoint).

An extensive and relatively deep pre-squall low existed ahead of the system. Each convective line had its own distinct, although weak, mesohigh, with the northern one (in northwestern Oklahoma) being more diffuse. Each line also developed its own wake low, both being along the back edge of an enhanced stratiform precipitation region. Again, the northern one (in southern Kansas) was more diffuse and not as deep as the southern one (in northeast Texas, centered to the west of the mesonet). The northern features were more diffuse because of the relative weakness of the east-west convective line and its associated stratiform area. The surface flow field within the system itself was not well defined at this time.

Mesovortex development stage (0900)

By 0900 (Fig. 4.6) the pre-squall low weakened considerably, filling by 2 mb. This may have been partially due to the decrease in the intensity of the convective line, i.e., weaker compensating subsidence ahead of the line. The mesohighs strengthened by 1-2 mb, and there were now two separate centers along the northeast-southwest line, as well as another near the apex of the two convective lines in an area of leading stratiform precipitation. Strong outflow existed along the southern end of the line (15 m s^{-1}) and strong divergence was occurring to the rear of the mesohigh features. The two wake lows were still present, with their shape tending to conform to the shape of the back edge of the stratiform region, although there were no strong gradients associated with either wake low. A cyclonic vortex at the surface appeared to be trying to develop around the northern wake low (in extreme southern Kansas), although it was not a closed vortex at this time.

The first look at the rear inflow structure occurred at this time. At CSM (Fig. 4.7a), which was on the southern edge of the stratiform region just south of the southern wake low (point A in Fig. 4.6), three upper-air flow features were evident. At low levels the strong FTR outflow from the system was found. In the mid-levels there was a 400 mb deep layer of moderate-to-strong rear inflow, peaking at 650 mb (7 m s^{-1}) and 450 mb

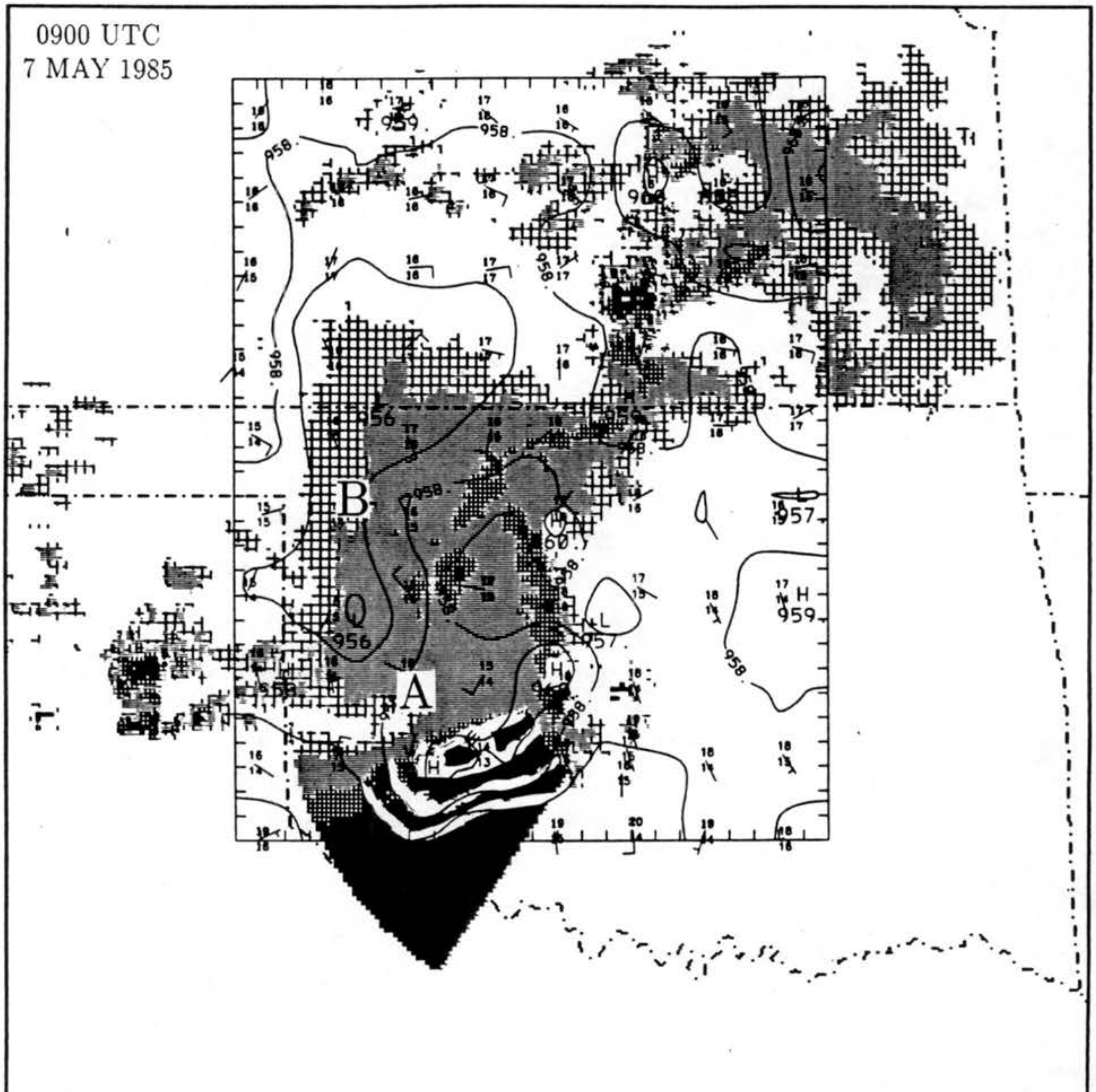

Figure 4.6: Same as Fig. 4.5 except for 0900 UTC 7 May.

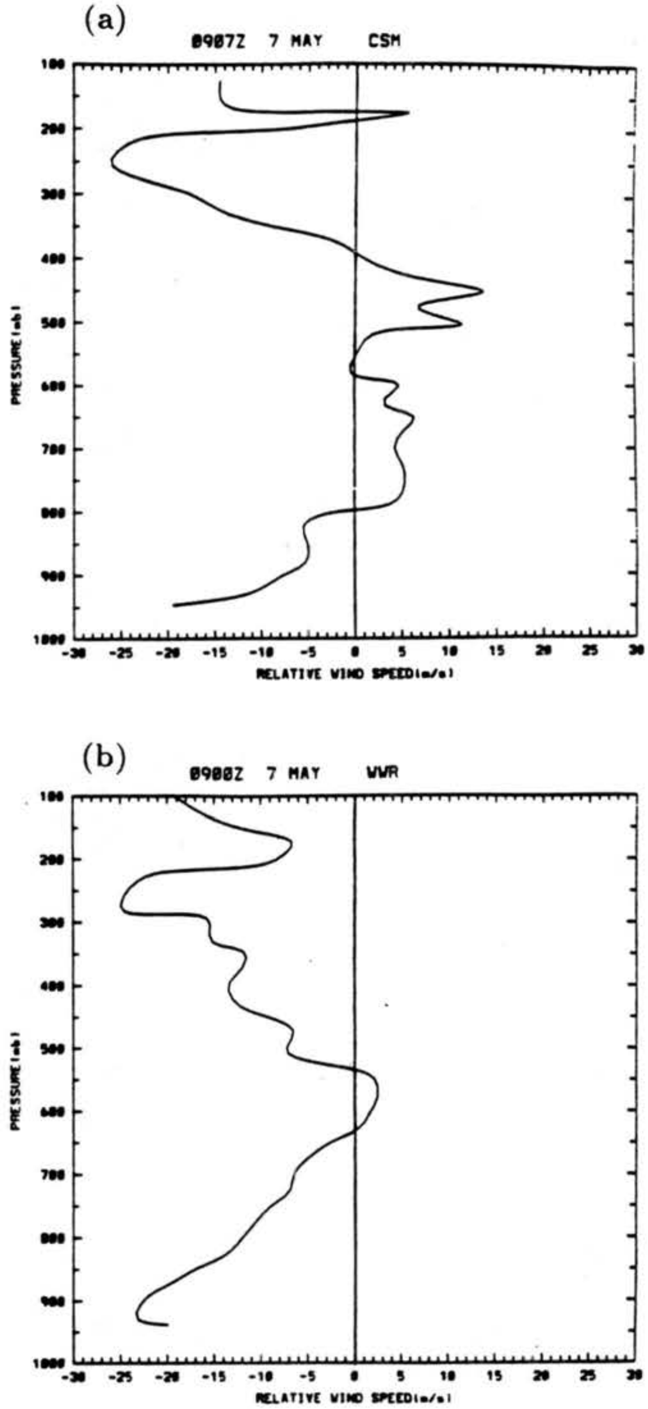

Figure 4.7: System-relative upper-air winds, in m s^{-1}, for: a) CSM at 0907 UTC; b) WWR at 0900 UTC. The 0 m s^{-1} line is highlighted. Positive (negative) values imply RTF (FTR) flow.

(15 m s^{-1}). At upper levels another FTR flow maximum occurred at 250 mb (26 m s^{-1}) and this was due to the outflow aloft at or near cloud top. At WWR (Fig. 4.7b), which was located at the back edge of the enhanced stratiform region between the two wake lows (point B in Fig. 4.6), only a shallow and weak RTF flow occurred, with a maximum at 575 mb (3 m s^{-1}). This weaker and shallower rear inflow may have been part of the reason for the relative weakness of the wake low in this region, as less warming and drying can occur when such a shallow layer descends.

The 850 mb map (Fig. 4.8) shows the existence of a mesovortex. In this ground-relative reference frame, the mesovortex appeared clearly only at this level. It appeared more clearly in the mesovortex-relative reference frame presented by Brandes (1990) and Brandes and Ziegler (1992). Brandes (1990) placed the center of circulation in the northern stratiform precipitation region based on Doppler radar data. Brandes and Ziegler (1992) placed it 100 km farther south based on the sounding data. Both studies showed that in the mesovortex-relative reference frame the mesovortex extended from near the surface to about 5-6 km. In the ground-relative reference frame shown here, however, the mesovortex was clearly shown only at 850 mb and there was not a closed surface vortex at this time.

Mature stage (0930-1030)

During this time period, several very important changes occurred in the stratiform precipitation structure as well as in the pressure patterns. At 0930 (Fig. 4.9) there was still a double wake low structure. Now, however, a closed circulation at the surface developed around the northern wake low. While this low was in a position expected for wake lows, the mechanism for its formation may have been complicated by the existence of a mesovortex that was shown to be present in this region of the MCS at 0900 (Fig. 4.8). Also at this time the circular core of mixed stratiform and convective precipitation had a distinct mesohigh (958 mb) associated with it. By 1030 (Fig. 4.10) there was a distinct decrease in the strength, as well as the areal coverage of the heavy stratiform precipitation core. Coinciding with this, the mesohigh (958 mb) which was present in this region only an hour earlier was replaced by a low (955 mb). Examination of analyses at intermediate times indicated that the mesolow actually developed within this region and

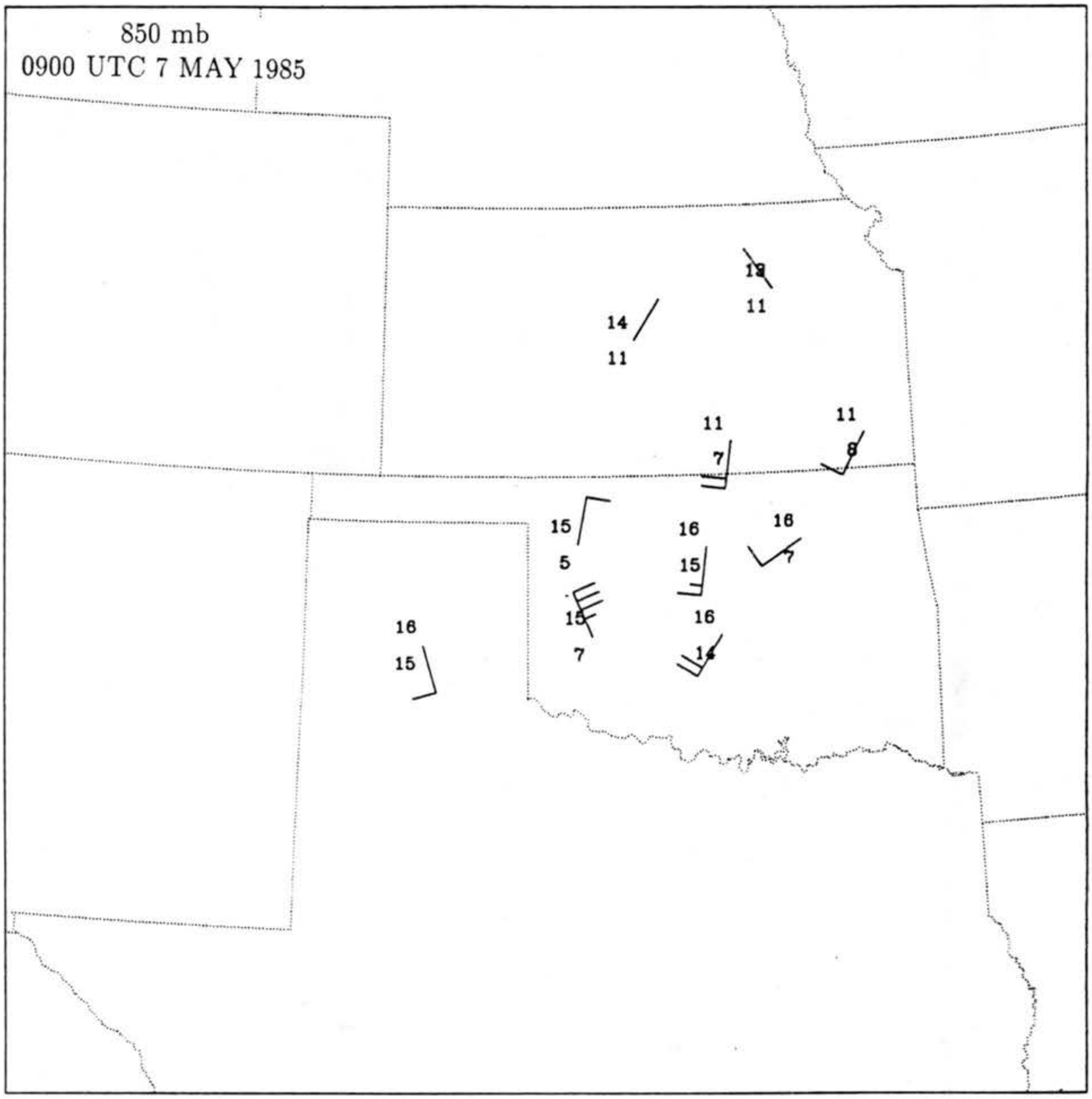

Figure 4.8: Same as Fig. 4.2 except for 0900 UTC 7 May at 850 mb.

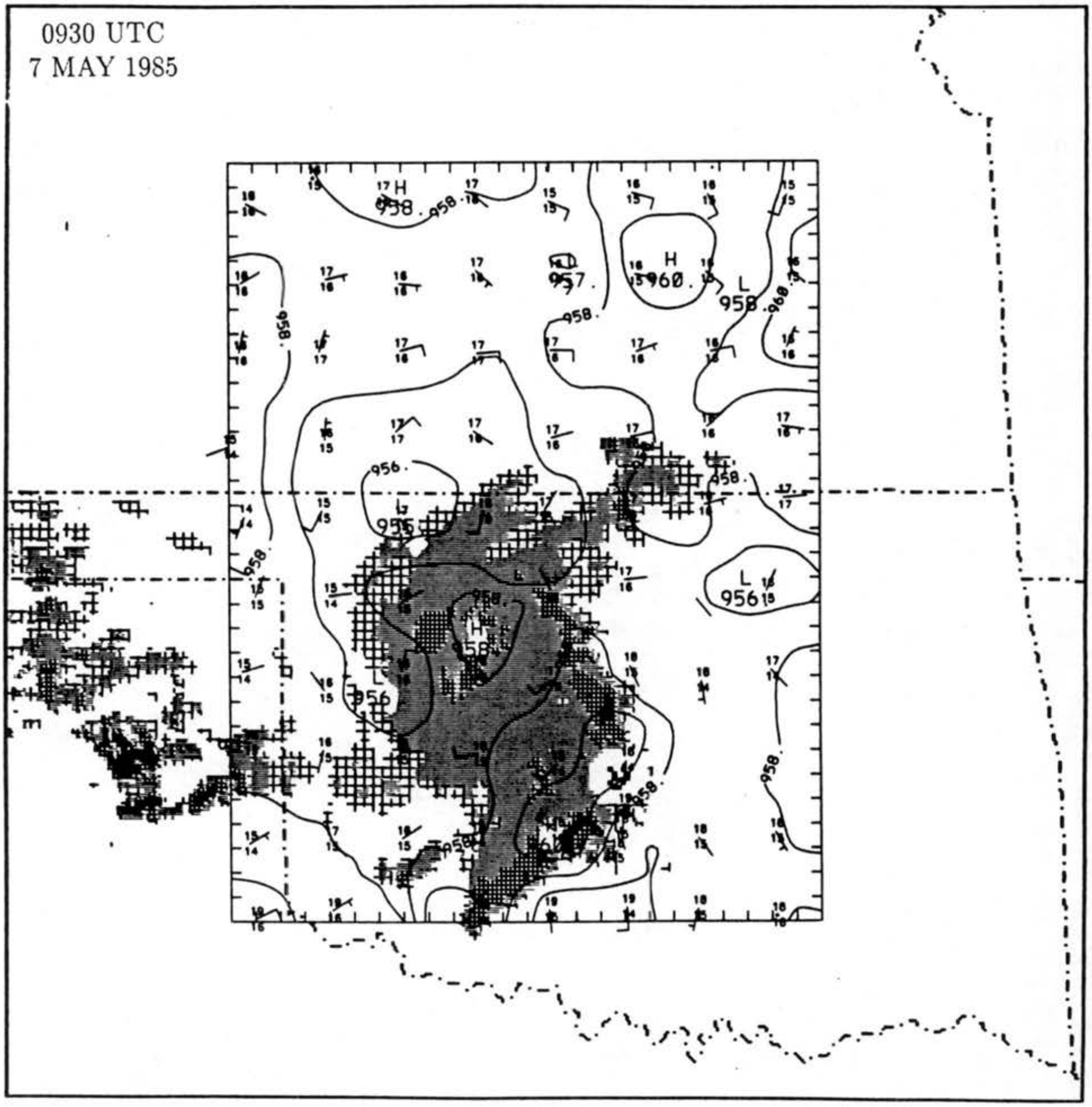

Figure 4.9: Same as Fig. 4.5 except for 0930 UTC 7 May.

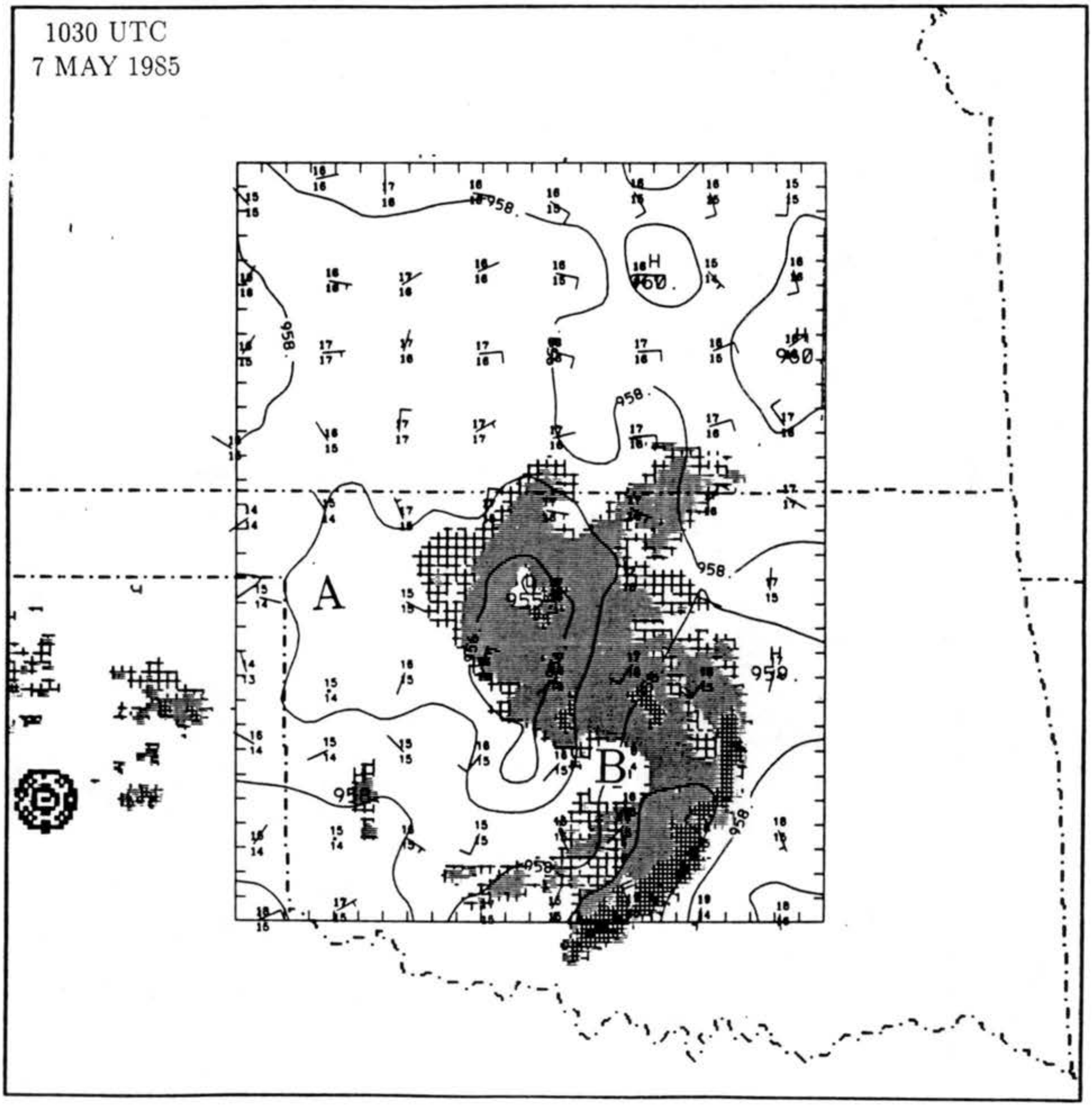

Figure 4.10: Same as Fig. 4.5 except for 1030 UTC 7 May.

was not associated with either of the previous wake lows, the northern one of which had completely filled (although its vortex was still present on the northwest side of the MCS) and the southern one of which was present only as a lobe of lower pressure extending to the south of this new low. In particular, the analysis at 1000 (not shown due to lack of OKC radar data) indicated three distinct low pressure centers, the two previous as well as this new one.

Why was there such a dramatic change in these features? One possible explanation for the decrease in strength of the stratiform precipitation as well as the development of a low where a high had been present can be postulated based on the trajectory analysis performed by Brandes and Ziegler (1992) for this case. They found (their Fig. 4) that at the 4.5 km level, the air that entered the mesovortex underwent marked descent. This would tend to imply a strong warming and drying in this area leading to the observed decrease in precipitation intensity as well as a warming of the column which could have led to the observed lowering of the pressure. Such a mechanism has also been postulated by Johnson et al. (1989) for the 23-24 June case. Due to a lack of data in Oklahoma at 1030 the upper-air maps are not shown here, but Brandes (1990) has shown that the mesovortex was still present, now near END, and that it expanded in the vertical, so that it now extended from the surface to above 6 km.

The rear inflow at WWR (Fig. 4.11a), which was about 50 km to the rear of the "comma head" (point A in Fig. 4.10), was still shallow (150 mb deep) and had a peak at 475 mb (8 m s^{-1}) which is about 100 mb higher than it was 90 minutes earlier. At OKC (Fig. 4.11b), which was located just behind the convective line (point B in Fig. 4.10), there was a relatively deep and strong rear inflow jet which had its maximum at 850 mb (11 m s^{-1}). The positions of both of these layers were consistent with a rear inflow jet that sloped upward toward the rear of the system.

Dissipating stage (1130-1300)

By 1130 (Fig. 4.12) the accentuated erosion of the stratiform precipitation on the south side of the comma head was obvious. The wake low positioned itself in the center of a region where there must have been a very strong descent in the rear inflow, because in

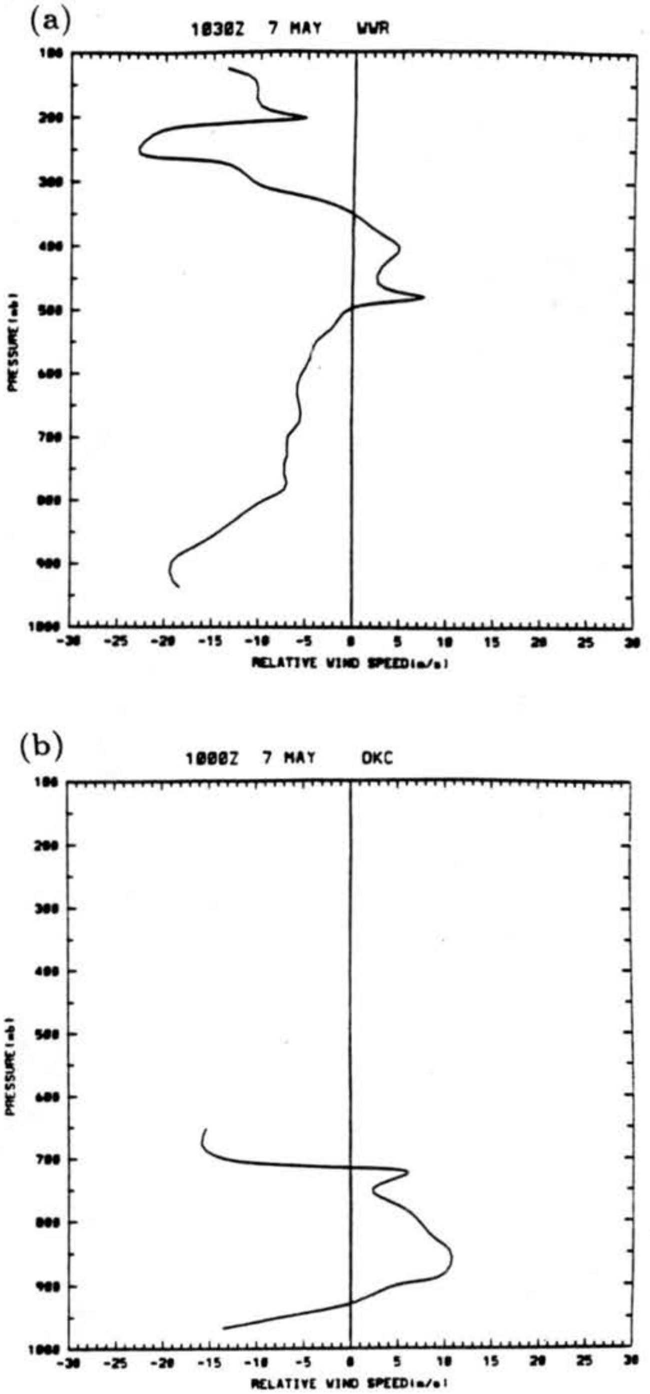

Figure 4.11: Same as Fig. 4.7 except for: a) 1030 UTC at WWR and b) 1000 UTC at OKC.

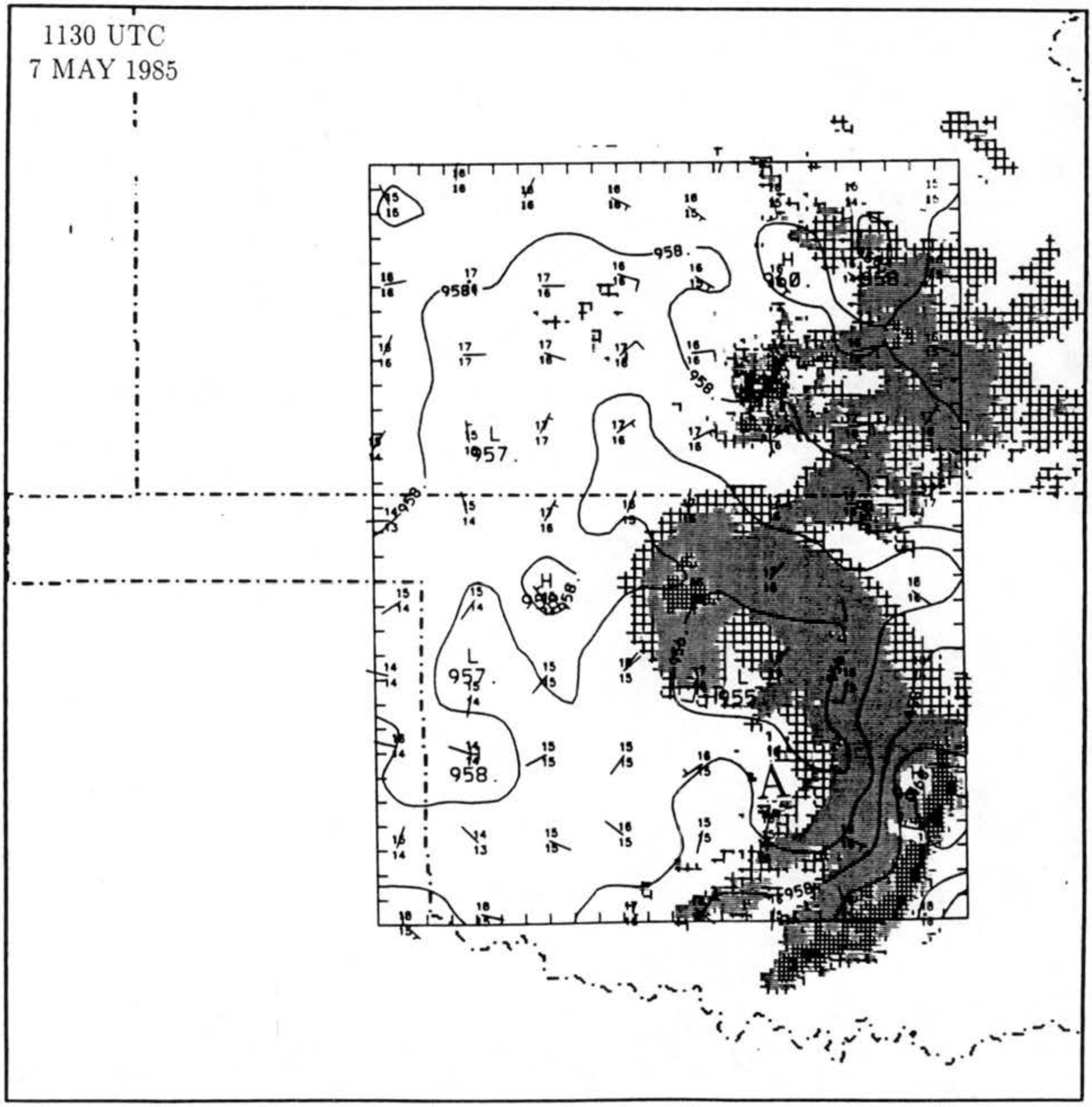

Figure 4.12: Same as Fig. 4.5 except for 1130 UTC 7 May.

this region the stratiform precipitation eroded from within as can be seen by the "hole" in the reflectivity field around the low. This seems to lend credence to the idea that there was accentuated descending flow associated with the rear inflow jet coming in around the south side of the mesovortex as shown by Brandes and Ziegler. By 1200 (Fig. 4.13) the low moved to the back side of the enhanced area of stratiform precipitation which was to the rear of the north side of the convective line. This was in a position that is more in compliance with the accepted position of a wake low (Pedgley 1962, Johnson and Hamilton 1988). The low seems to now have become a true wake low feature again. It is conjectured that it has moved back into this position because all of the stratiform precipitation in the rest of the system had now dissipated and there was no longer strong localized warming and drying effects within those regions. The unusual behavior of the mesolows in this case was likely due to the complex upper-air flow and mesovortex that was seen here.

The analysis at 1200 marked the first time that a strong surface pressure gradient developed. The tightening of the gradient, in this case, was not related to either a deepening of the low or a strengthening of the mesohigh since both features were nearly constant for several hours. Rather, it was simply due to the low actually moving to a position closer to the mesohigh. Just after this time, at 1215 (not shown), the wake low deepened rapidly by 2 mb leading to an intensified gradient, but just as quickly filled again. The cause of this rapid change is unknown.

Also of interest at 1200 (Fig. 4.13) was the formation of a lobe of low pressure on the northwest side of the MCS. There was a closed surface vortex around this feature, and as such, it is presumed to be a regeneration of a surface low associated with the mesovortex. This feature was present for the remainder of the lifetime of the MCS within the mesonet.

The rear inflow structure is shown in Fig. 4.14 at 1105 at OKC, which was at the rear edge of a newly developed area of enhanced stratiform precipitation behind the central portion of the convective line (point A in Fig. 4.12). It shows that there was a deep (400 mb) and strong RTF flow that was a maximum at 525 mb (13 m s^{-1}). Comparing this to the OKC sounding about 1 h earlier (Fig. 4.11) it can be seen that the rear inflow was 325 mb higher at the back edge of the stratiform region than it was just behind the convective line. This is again consistent with a downward-sloping rear inflow jet.

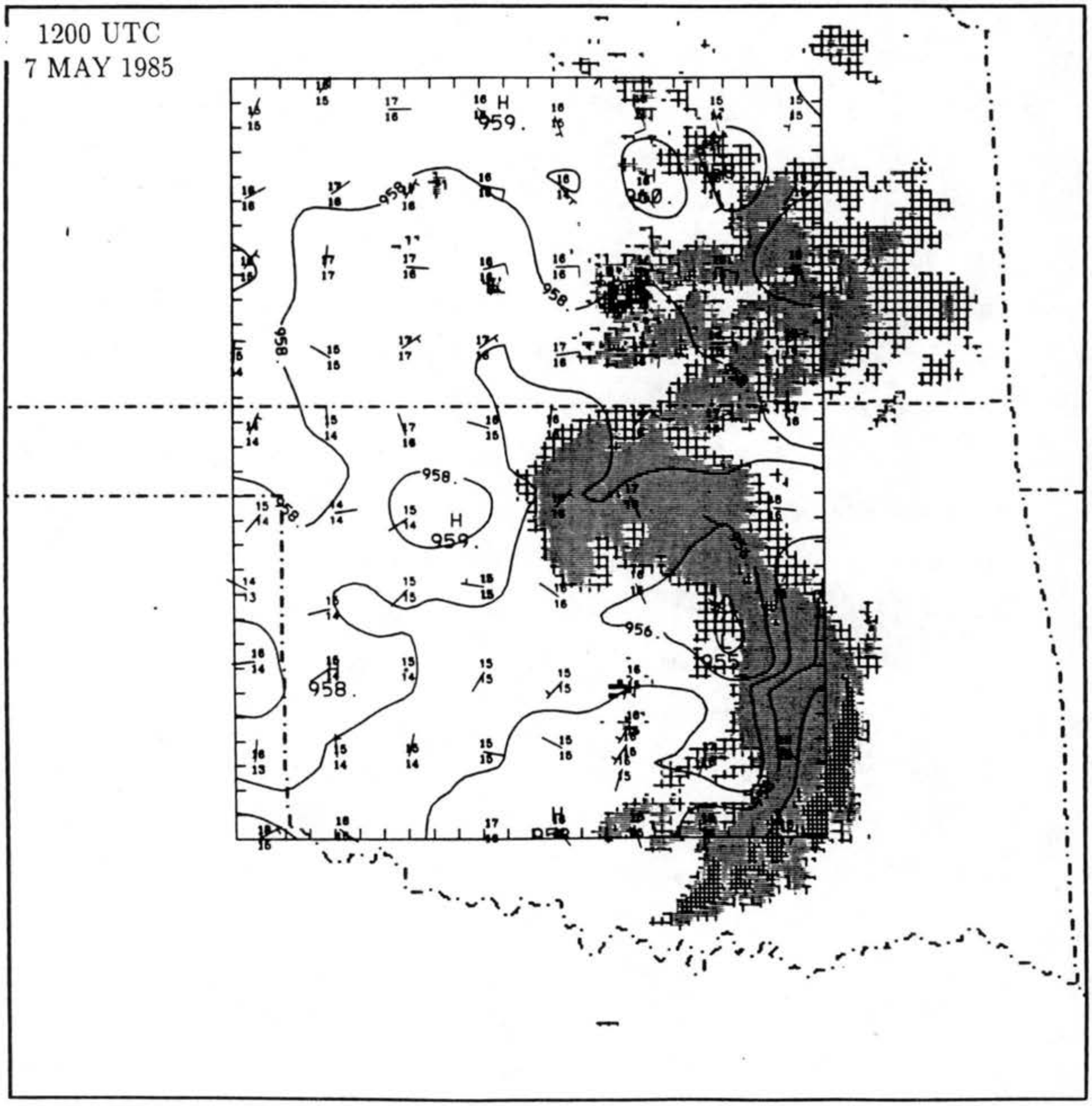

Figure 4.13: Same as Fig. 4.5 except for 1200 UTC 7 May.

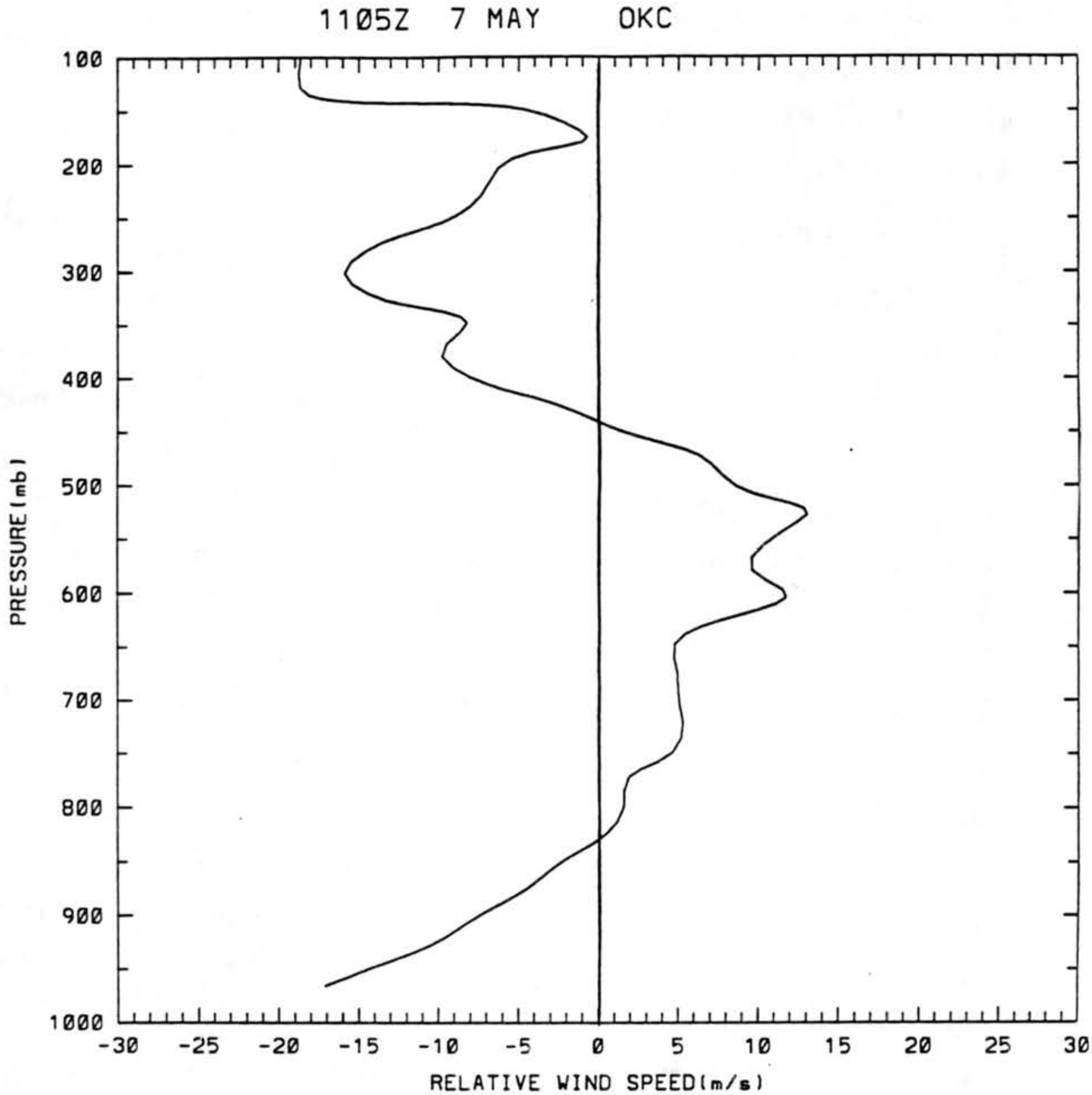

Figure 4.14: Same as Fig. 4.7 except for 1105 UTC 7 May at OKC.

The mesovortex was still present and was still located within the northern area of stratiform precipitation at 1200 as shown by the 850 mb and 700 mb maps (Fig. 4.15a,b). It is still apparent that the inflow into this mesovortex along its southern flank (for example at OKC) was very warm and dry and this was continuing to lead to the erosion of the stratiform precipitation region between the mesovortex and the rest of the system. Eventually, by 1300 (see Fig. 4.3e) this led to an almost complete cutoff of the precipitation associated with the mesovortex from that in the rest of the system.

4.2.4 Mesonet time series

The conditions associated with the northern wake low are summarized by station P35 (Fig. 4.16a; for station locations please see Fig. 3.1). Just prior to the mesohigh there was a 1°C temperature increase and a 2°C dewpoint decrease (0710) which almost appeared to be a heat burst event, but the cause of this feature is beyond the scope of this thesis. A weak mesohigh (0745), with a 1.5 mb increase in 30 minutes, was present and was accompanied by a sharp 1°C temperature rise and 2°C dewpoint fall, then there was a gentle shift to cooling and moistening. Only moderate winds occurred with the mesohigh passage and there was a windshift from southeast to northwest. Then the northern wake low approached (0945) and it can be seen that a very weak gradient (by the standards of the other wake lows, but strong relative to synoptic-scale pressure gradients) was associated with these features, with only a 4 mb drop over 90 minutes. There was a dewpoint drop of 2°C that occurred with this low. The wind shifted to the southeast as the low moved over, then back to northwest after it passed, but due to the weak gradient present in this area there were generally light winds with its passage.

The station which showed the greatest effect from the main wake low which developed within the stratiform precipitation core was S32 (Fig. 4.16b). The mesohigh (1030) at this station was quite weak with only a 1 mb increase in 30 minutes. But it was accompanied by a strong cooling and moistening as well as a 16 m s^{-1} wind gust. The wind shifted gently from the east-southeast to the southwest as the mesohigh passed. The wake low (1200) here was quite sharp, with a 3.5 mb drop in 30 minutes. The low was also accompanied by a dewpoint drop of 0.5°C. The wind associated with the low was still quite light, probably

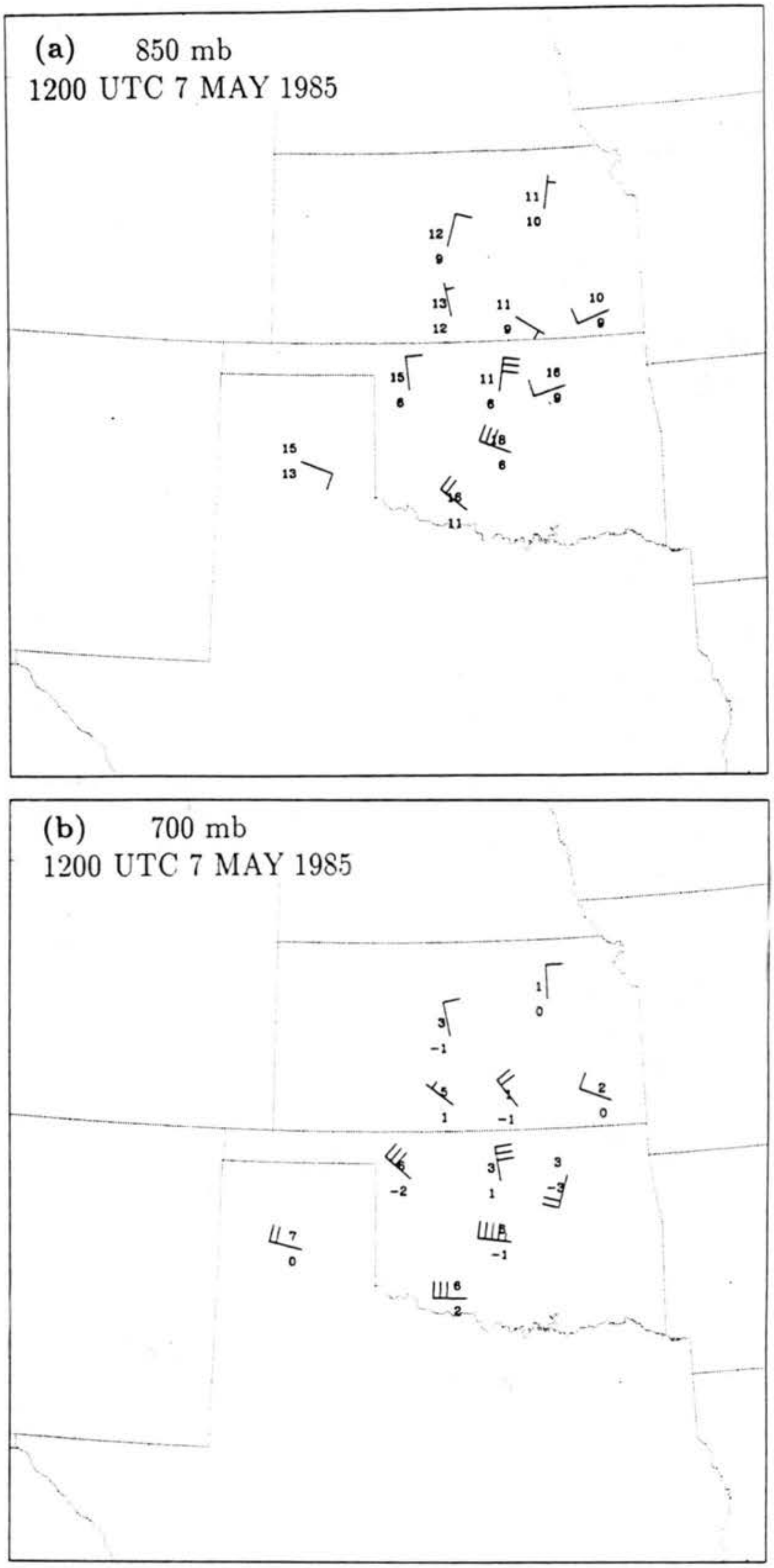

Figure 4.15: Same as Fig. 4.2 except for 1200 UTC 7 May at: a) 850 mb; b) 700 mb.

(a)

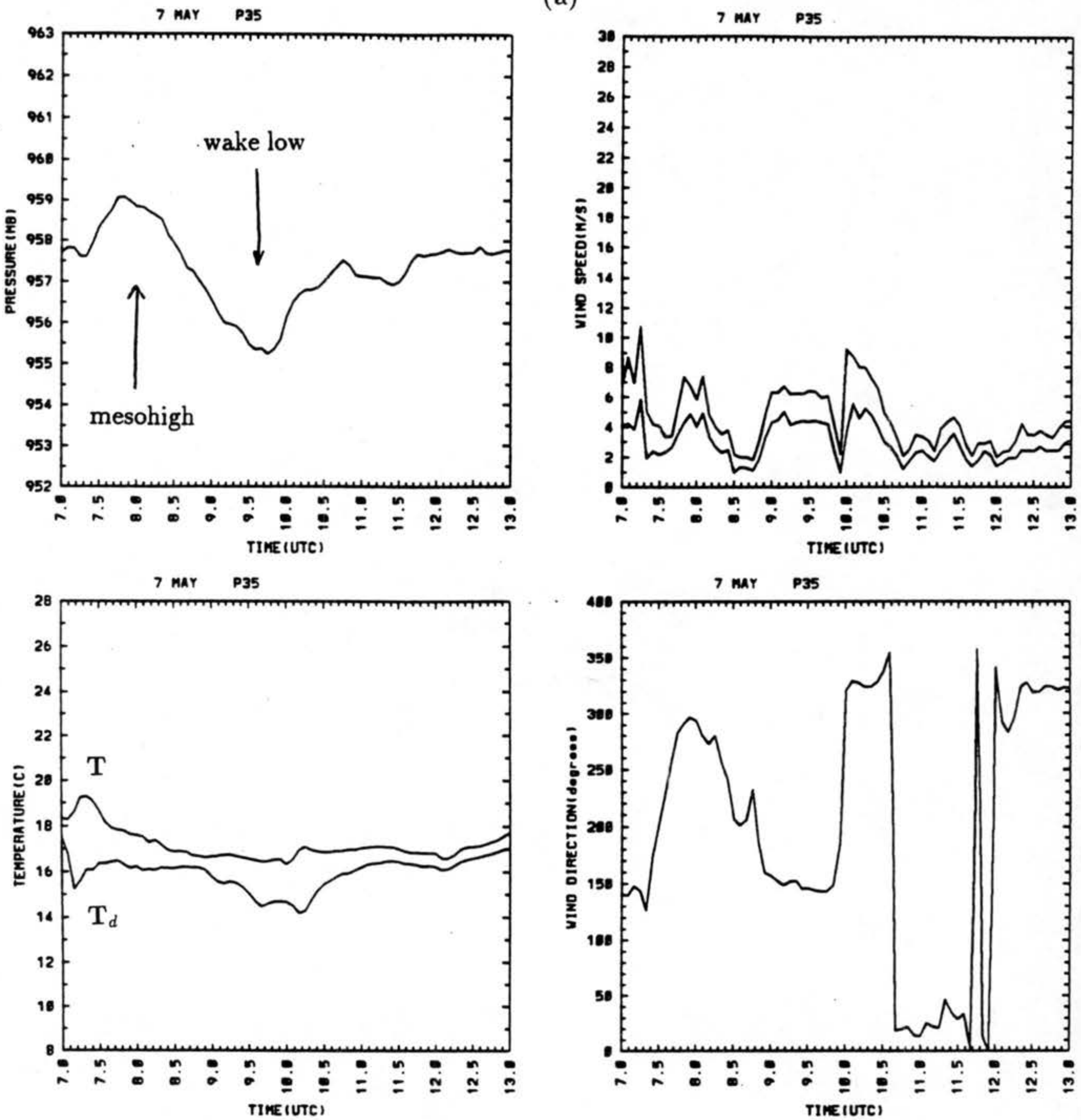

Figure 4.16: Time series of: In upper-left, 480 m pressure with mesohighs and wake lows highlighted; in upper-right, 5-minute average winds (lower curve) and 5-minute maximum wind gust (upper curve); in lower-left, 5-minute average temperature (upper curve) and dewpoint (lower curve) and; in lower-right, 5-minute average wind direction. Data from station: a) P35 and b) S32. Time is UTC and 7.5 = 0730 UTC and each tick mark is 6 minutes.

(b)

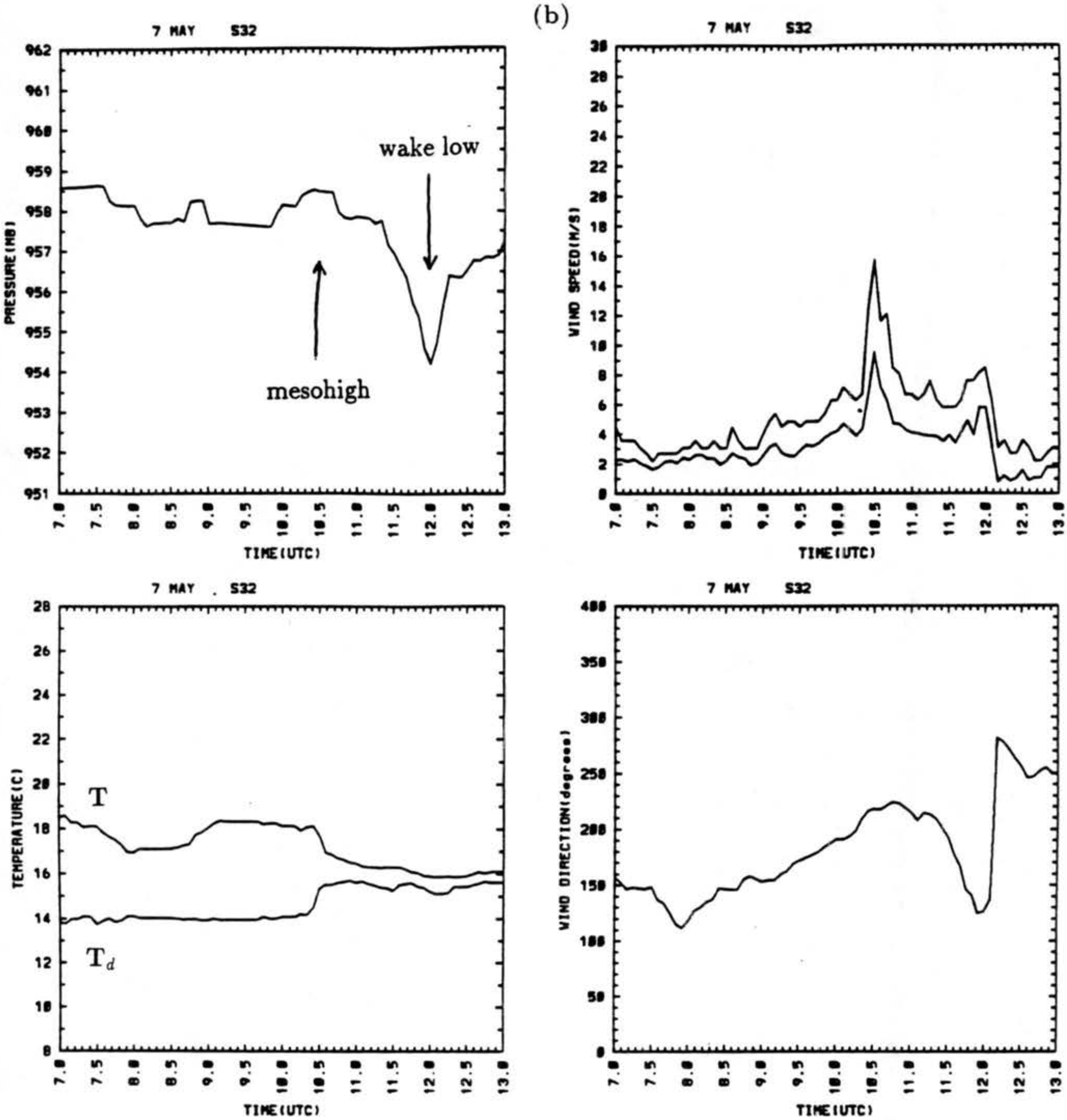

Figure 4.16: Continued.

an indication that the deepness of the low at this time was short-lived, as described in the previous section, and was not able to greatly effect the wind speeds (Vescio and Johnson 1992). The wind direction shifted quite drastically from the southwest to the southeast as the low moved over, then back to the northwest after it passed.

4.3 May 13 cases

4.3.1 Synoptic overview

The 1200 13 May maps summarize the environment at the time of initial development of these MCSs. At the surface (Fig. 4.17a) a strong frontal system was present. A 998 mb low was over the Texas panhandle, with a cold front extending to its south through western Texas, and a stationary front extended to its east across the Oklahoma-Kansas border. The warm sector was characterized by warm, humid air and a south-southeasterly flow. To the west of the cold front there was slightly cooler and much drier air with a northwest flow. To the north of the stationary front it was slightly cooler than in the warm sector but still moist with an easterly flow.

At 850 mb (Fig. 4.17b) a closed low was centered along the Texas and Oklahoma panhandles. Very strong southerly flow was over eastern Texas and Oklahoma, with a more southeasterly flow in Kansas. A tongue of very moist air was over eastern Texas, Oklahoma, and southern Kansas. At 500 mb (Fig. 4.17c) the closed low was over extreme south-central Canada with a trough extending south into central Colorado and New Mexico. Generally weak flow was present in Oklahoma with 10-15 m s^{-1} southwesterly flow. The 300 mb flow (Fig. 4.17d) was characterized by a 35 m s^{-1} jet core extending from northwestern Kansas to central Wisconsin. The flow was diffluent over western Oklahoma.

4.3.2 Radar overview

The initial development with this system occurred over extreme southwestern Oklahoma into northern Texas just prior to 1200 (not shown). By 1325 (Fig. 4.18a) a line of scattered, intense cells developed. The cell along the Oklahoma-Texas border produced a weak (F0) tornado at this time. There was no trailing stratiform precipitation at this

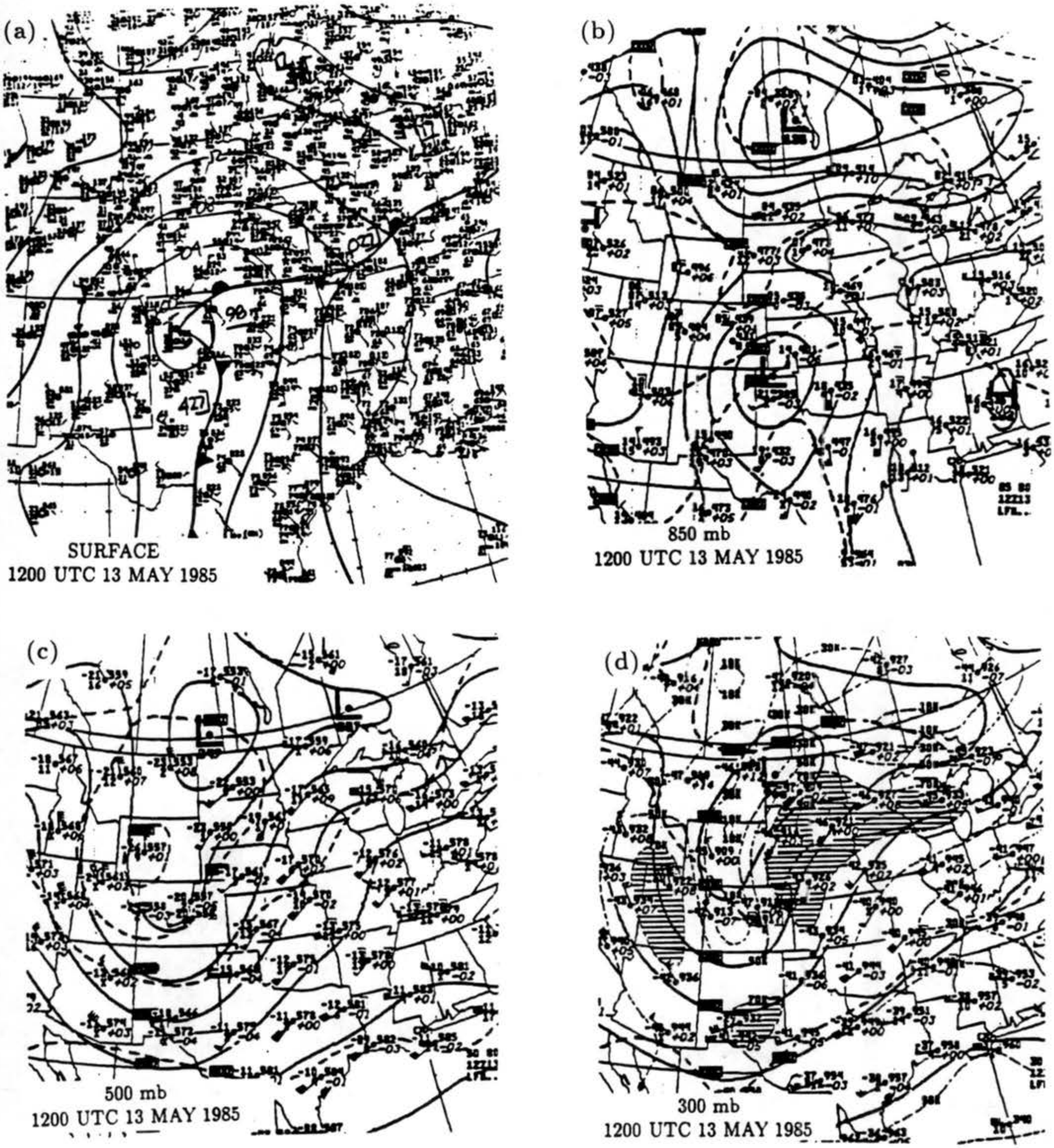

Figure 4.17: Same as Fig. 4.1 except for 1200 UTC 13 May at: a) Surface, b) 850 mb, c) 500 mb and, d) 300 mb. In d. solid contours represent geopotential height, dashed contours wind speed in knots (2 kt = 1 m s^{-1}).

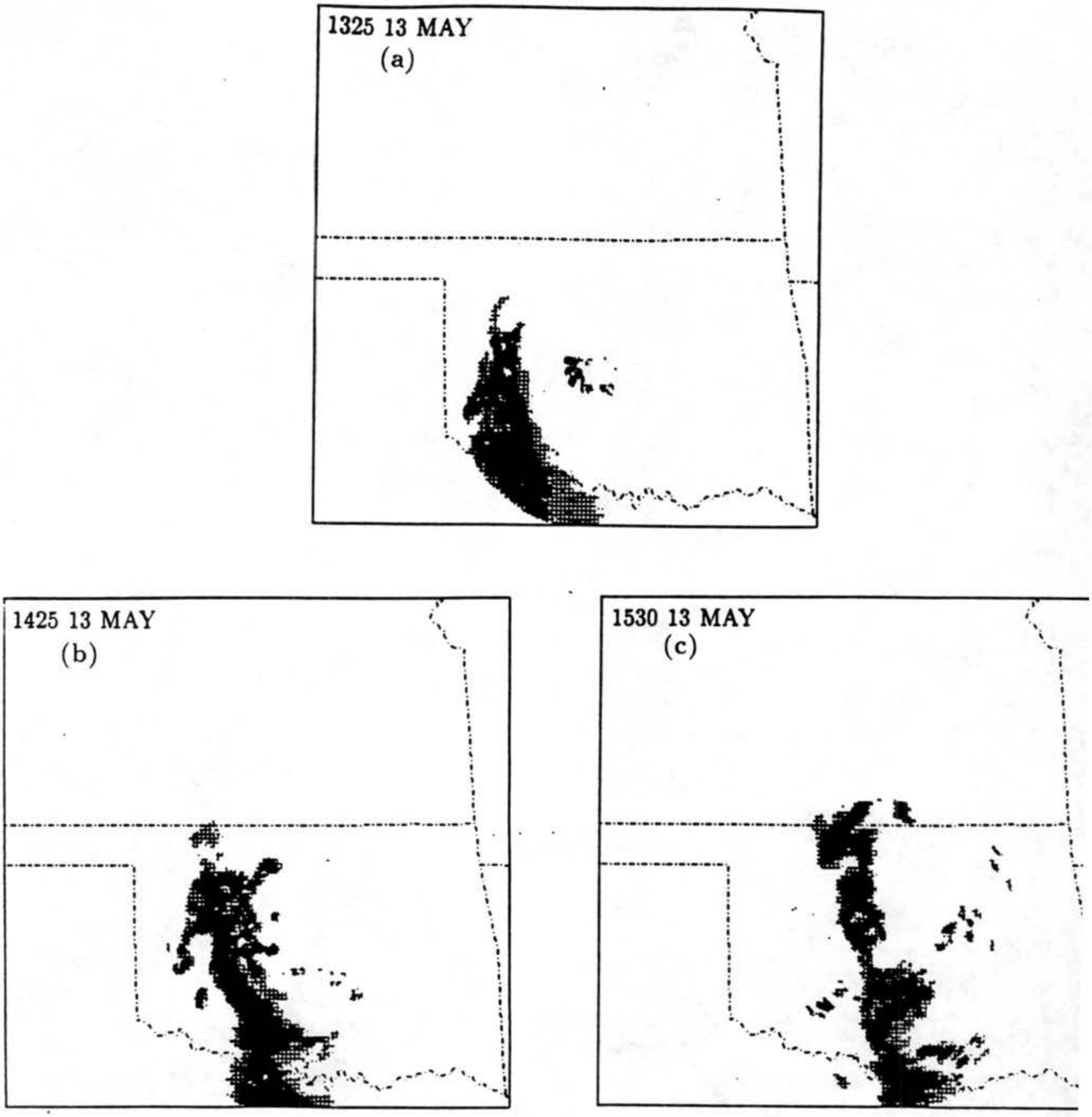

Figure 4.18: Same as Fig. 4.3 except for 13 May 1985 at: a) 1325 UTC Oklahoma City OK; b) 1425 UTC Oklahoma City OK; c) 1530 UTC Oklahoma City OK; d) 1630 UTC Oklahoma City OK; e) 1700 UTC Oklahoma City OK and Wichita KS; f) 1735 UTC Oklahoma City OK and Wichita KS.

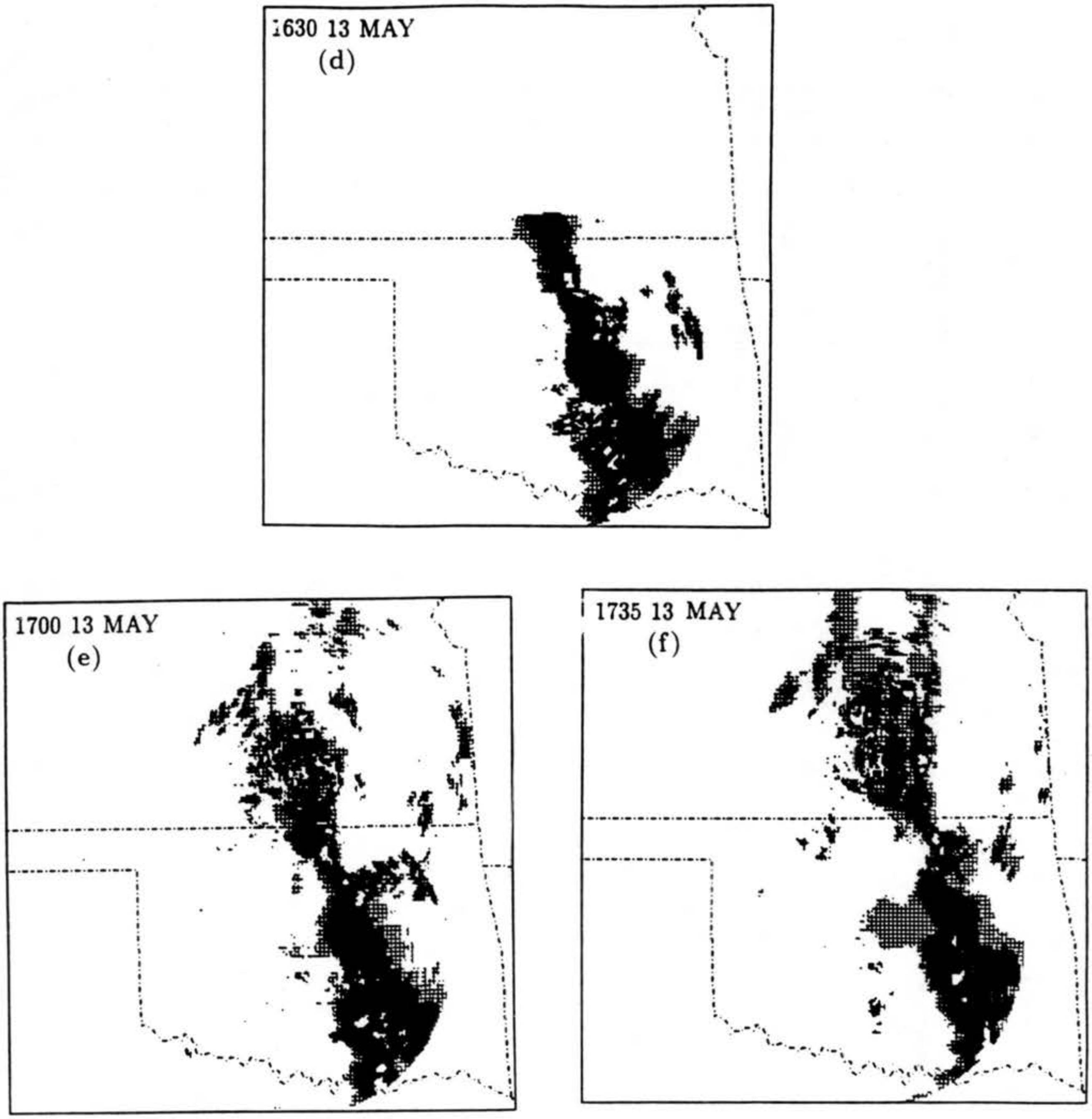

Figure 4.18: Continued.

time. A small area of stratiform precipitation developed to the rear of the northern portion of this line by 1425 (Fig. 4.18b). By 1530 (Fig. 4.18c) the stratiform precipitation area dissipated. The convective line itself was quite weak at this time (peak reflectivities of 40-46 dBZ). There were numerous reports of severe winds over the next several hours, many originating from behind the convective line. By 1630 (Fig. 4.18d) it was becoming evident that there were two separate areas of convection. The northern area (in northern Oklahoma) was taking more of a northeast turn and the southern area (in southern Oklahoma) was moving toward the east. Further distinctions between these areas are discussed later.

At 1700 (Fig. 4.18e) data from the Wichita radar were finally available. The convection in Kansas and extreme northern Oklahoma was felt to be a separate convective system since it developed its own distinct stratiform precipitation pattern. Due to ground clutter from Wichita it was difficult to discern the structure of the northern system at this time. The northern part of the southern MCS was beginning to lose its convective structure and becoming more stratiform in nature. Concurrently, the convection in the southern portion of the system appeared to be moving at a more rapid pace than the northern (stratiform) part of the system, tending to give the impression of an asymmetric system. At 1735 (Fig. 4.18f) the structure of both systems became clear. The southern MCS had a definite asymmetric structure with the stratiform precipitation confined to the northern portion of the system while the northern system was more symmetric. By 1900 (not shown) both systems had started to dissipate and move out of the network and new convection had developed in western Kansas, which did not develop further.

4.3.3 System overview

Developing stage (1430-1500)

The first appearance of the wake low (in extreme south-central Oklahoma) occurred at 1430 (Fig. 4.19). It appears to have formed *in situ* rather than advecting in from outside the mesonet, this will be further discussed in reference to the mesonet timeseries. The low associated with the frontal systems mentioned in the synoptic section was located

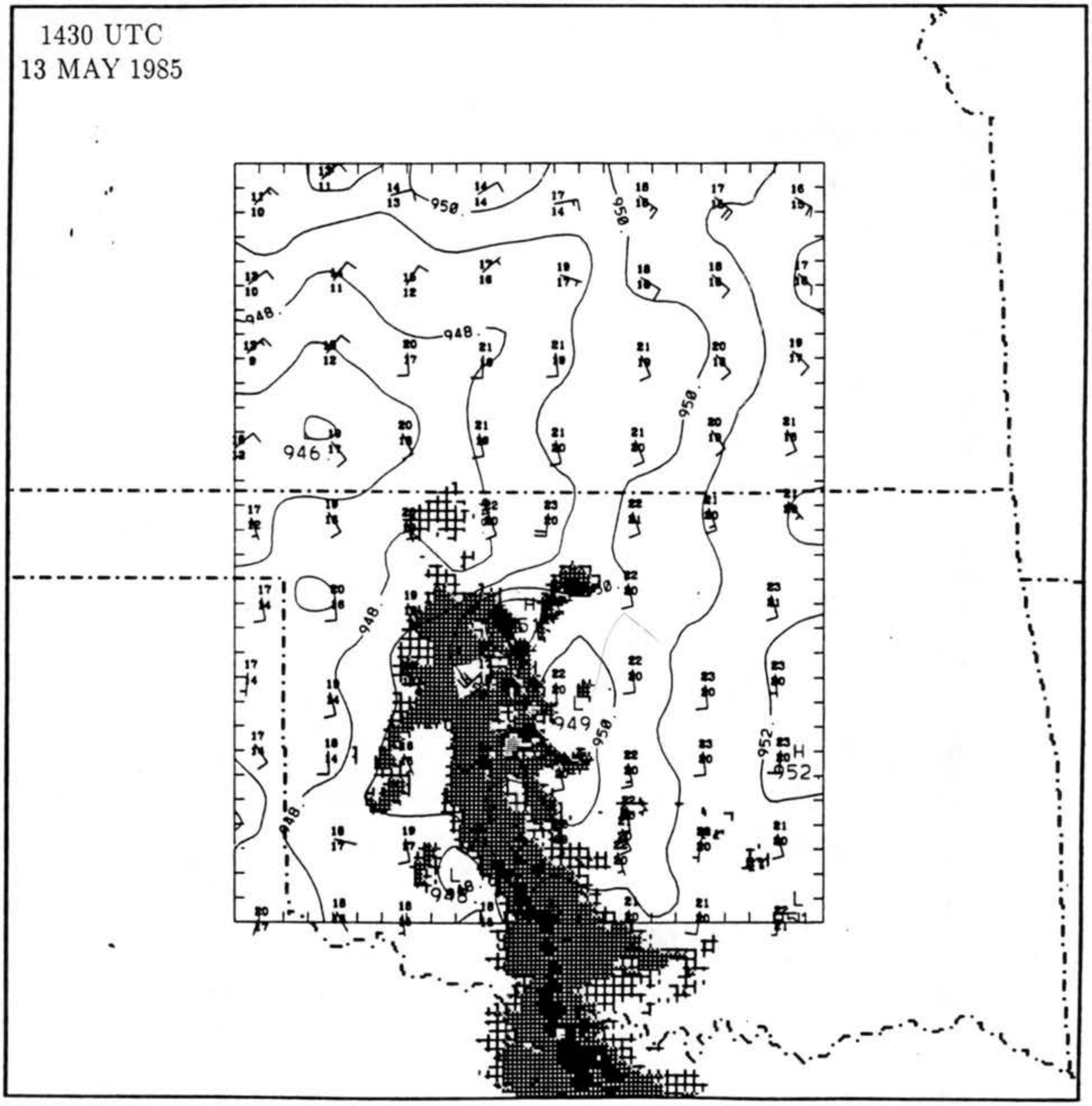

Figure 4.19: Same as Fig. 4.5 except for 1430 UTC 13 May.

in extreme south-central Kansas, the stationary front was in central Kansas, as indicated by the wind shift from southerly to easterly as well as the temperature contrast. The undisturbed flow in Oklahoma was southerly, but there were distinct changes within the MCS. A weak pre-squall low was ahead of the northern area of convection. A distinct mesohigh was in the northern portion of this convection. The flow was strongly divergent to the rear of this high. The wake low forming at this time may have been due to the initial development of the stratiform precipitation area (as mentioned in the radar discussion). With the development of the stratiform area, it possibly may have helped to force a stronger localized heating and drying at its rear edge leading to the lowering of the surface pressure. However, any effects due to the rear inflow structure cannot be discerened due to the lack of upper-air soundings taken for this case.

By 1500 (Fig. 4.20) the wake low deepened considerably (2 mb) and moved farther to the north along the rear edge of the enhanced stratiform precipitation region. The moderate gradient between this wake low and the mesohigh started to greatly effect the flow field as there was now strong flow (10 m s^{-1}) through the wake low. The flow features in this case were quite similar to those described by Garratt and Physick (1983) and Vescio and Johnson (1992) with strong divergence to the rear of the mesohigh, flow through the wake low, and convergence to the rear of the wake low. For the next two hours (not shown) these features continued to move to the northeast with this area of convection and remained nearly constant in strength and the wake low filled 1 mb. This may be due to the loss of significant stratiform precipitation over this period as mentioned in the radar summary.

Development of intense pressure gradient (1700-1830)

By 1700 (Fig. 4.21) the accentuated gradient reappeared all along the back edge of the southern system (in southern Oklahoma). A new diffuse wake low was found at the back edge of the enhanced area of stratiform precipitation. The precipitation area which had the wake low earlier had broken off from the southern system due to its more northerly movement and was a part of the northern system (in Kansas and extreme northern Oklahoma). It still had a strong gradient associated with it, but it was

Figure 4.20: Same as Fig. 4.5 except for 1500 UTC 13 May.

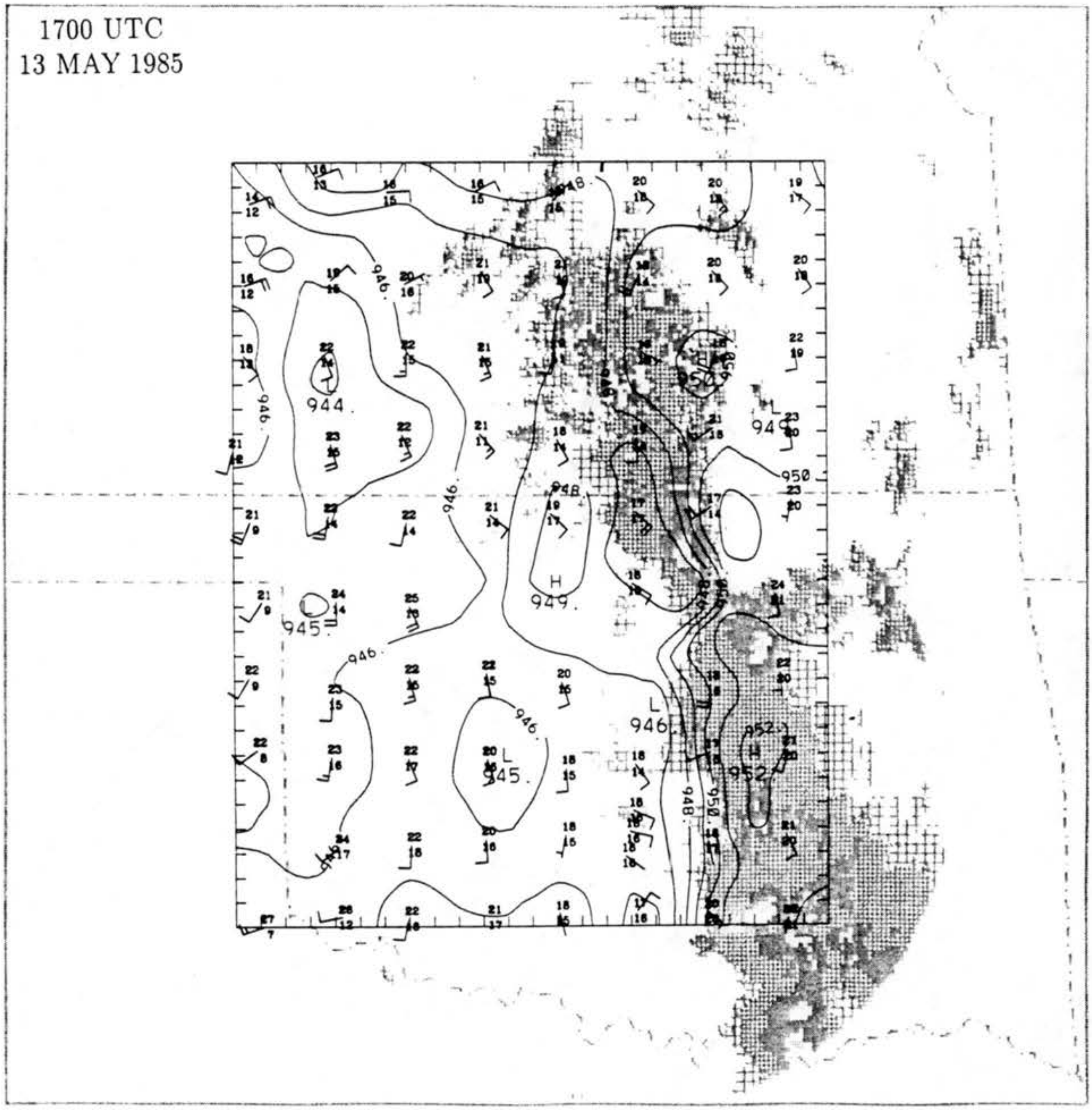

Figure 4.21: Same as Fig. 4.5 except for 1700 UTC 13 May.

actually along the convective line. This feature rapidly dissipated by 1730 and the gradient weakend. Why this odd positioning of the gradient occurred, behind the convective line in the north and behind the stratiform region in the south, is unknown.

Despite having a well developed symmetric-type structure with an enhanced stratiform region, the northern system (over Kansas) did not have a wake low associated with it at 1730 (Fig. 4.22). Again, the reasons for this are highly speculative, but it could have been due to the differences in the environment over Kansas versus those found in Oklahoma as discussed in the synoptic section.

The southern system now developed an extremely intense gradient along its back edge with two wake lows, one on the north side and the other just behind the stratiform area associated with the convective line. This was a phase of rapid deepening of the wake low with a 1-2 mb decrease in its central pressure since 1700. Intense divergence occurred to the rear of the mesohigh due to the development of this intense gradient. Also, this gradient caused the severe winds mentioned in the radar section, as will be shown in the time series section. This was the only case for which severe winds (winds in excess of 25 m s^{-1}) were actually reported in association with the wake low (although winds as strong were seen with the passage of other wake lows during PRE-STORM).

A further deepening of 1 mb occurred within the wake lows leading to an even more intense gradient by 1800 (Fig. 4.23). This was the most intense gradient to have occurred in any of the PRE-STORM cases studied. The lows were found on either side of a westward bulge in the stratiform precipitation region. The northern system still had no wake low and virtually no accentuated gradient along its back edge.

The southern system was mostly outside of the mesonet by 1830 (Fig. 4.24). A wake low finally appeared in association with the northern system. It appeared on the south side of a region that experienced a strengthening of the stratiform precipitation region. Unfortunately, the PAM network had an outage for the remainder of the lifetime of this system so little else can be determined about this feature.

Also notice that the cold front was now evident in the western portion of the mesonet with a windshift from southerly to northwesterly and a sharp temperature drop. A line of

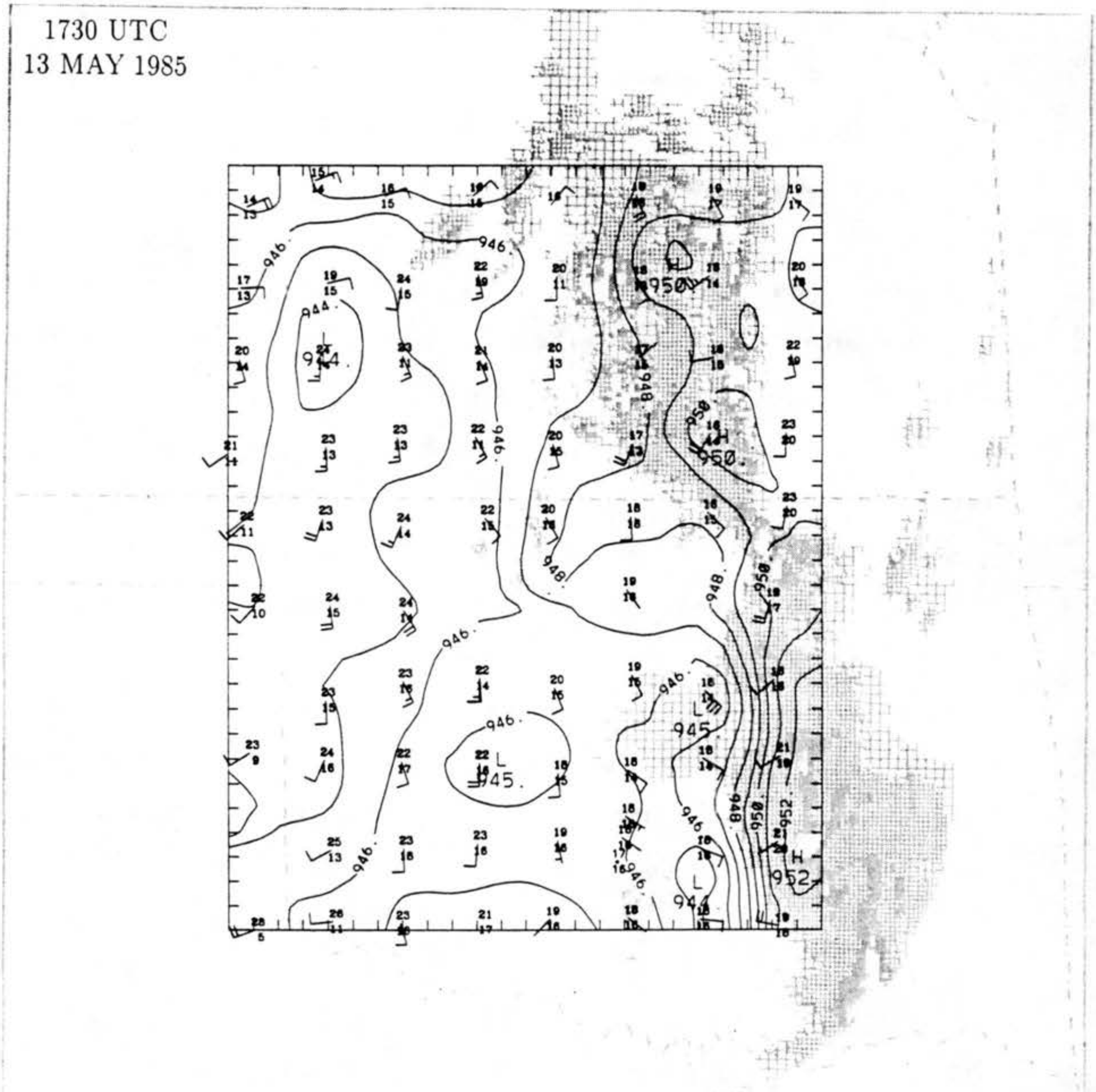

Figure 4.22: Same as Fig. 4.5 except for 1730 UTC 13 May.

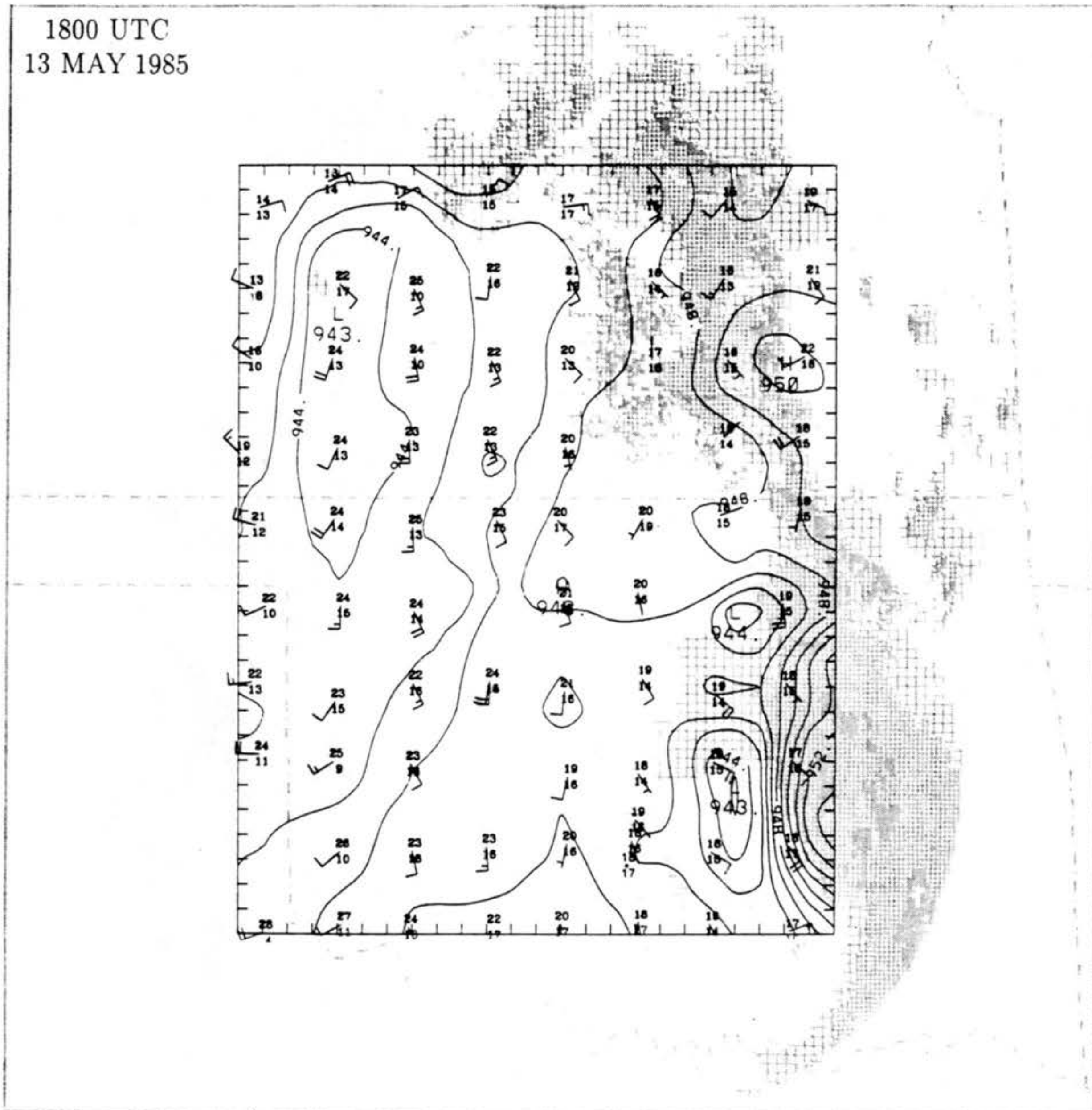

Figure 4.23: Same as Fig. 4.5 except for 1800 UTC 13 May.

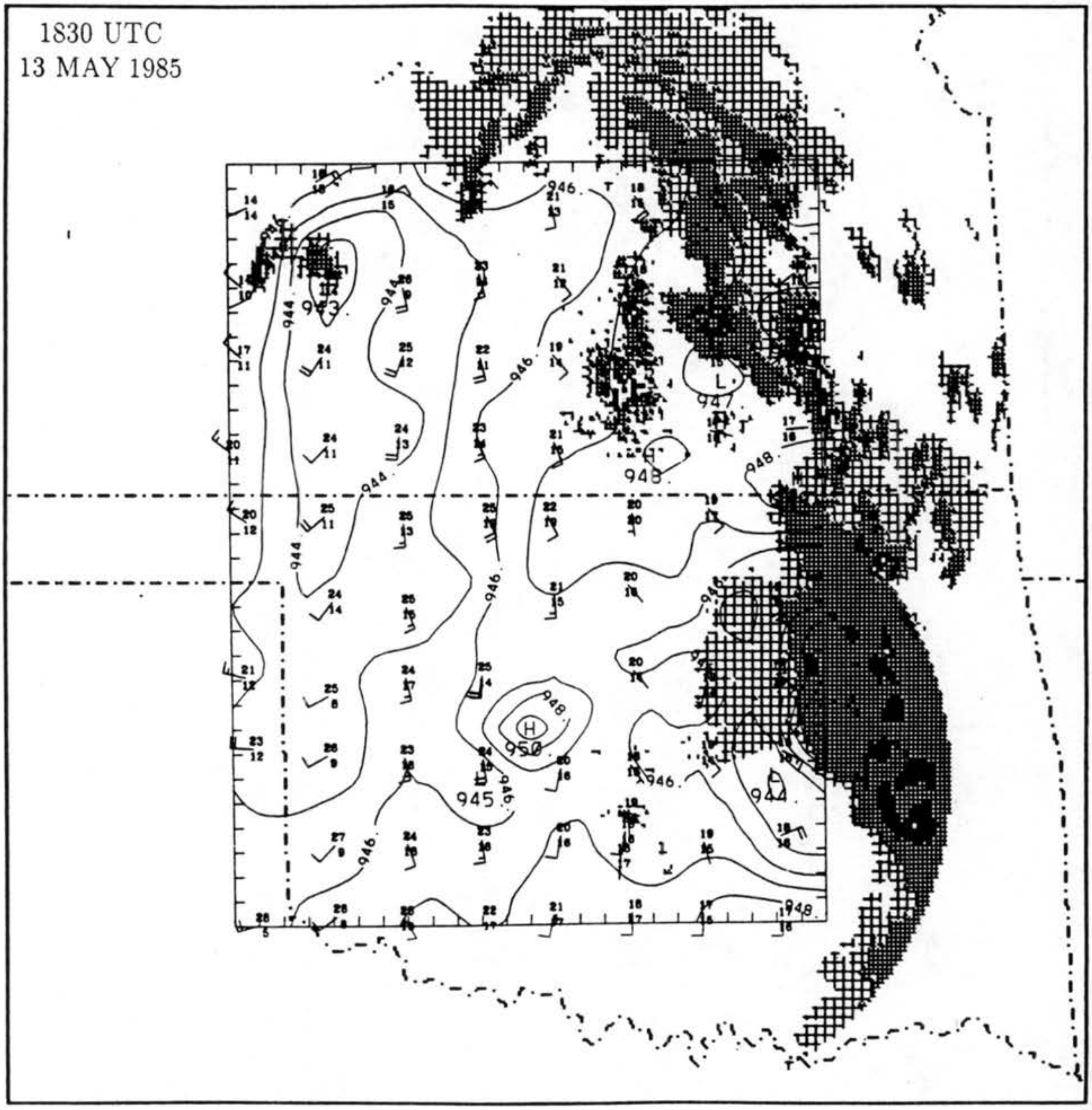

Figure 4.24: Same as Fig. 4.5 except for 1830 UTC 13 May.

convection developed along this front but did not develop into an organized system within the PRE-STORM area.

4.3.4 Mesonet time series

For this case, several time series are examined in a west-to-east line through the axis of the main wake low features. The first is at S13 (Fig. 4.25a, see Fig. 3.1), where the initial wake low apparently formed. Here, when the mesohigh (1430) reached its peak pressure, the pressure plummeted 5.5 mb in 5 minutes (1435). The suddeness of this drop lends credence to the idea that the low did, in fact, form near this station and did not advect into the mesonet. Due to the sudden shift from mesohigh to wake low, it was impossible to discern distinct features associated with each separately. So the feature as a whole was accompanied by a sharp drop (4°C) in both temperature and dewpoint, and a 21 m s^{-1} wind gust. As the pressure rose, the wind shifted from the south-southeast to the south-southwest. Then as the pressure decreased, the wind shifted from the southwest to the southeast. By the time the system reached S16 (Fig. 4.25b) the wake low started to deepen. The mesohigh (1600) was very weak here with just a 1 mb increase and it had no strong winds with it, but it did lead to a shift from southerly to westerly flow. Then the wake low approached (1745), with a 9 mb drop in 40 minutes, a 2°C drying, a 15 m s^{-1} wind gust, as well as a shift to southeast flow. Then at S17 (Fig. 4.25c), which was the station most affected by the wake low in its deepening phase, the time series looks much like the S13 time series with the steep pressure drop occuring right after the mesohigh (1800) reached its peak pressure. This was probably due to the rapid deepening of the wake low (1820) which was occuring as it moved over this station. Here there was a 10 mb drop in 15 minutes, which was concentrated in a 6 mb drop in 5 minutes. The winds were sustained at 14 m s^{-1} and gusted to 23 m s^{-1}. Overall, wind gusts exceeded 20 m s^{-1} at eight mesonet sites and reached a maximum of 26 m s^{-1}.

4.4 May 21 Case

(a)

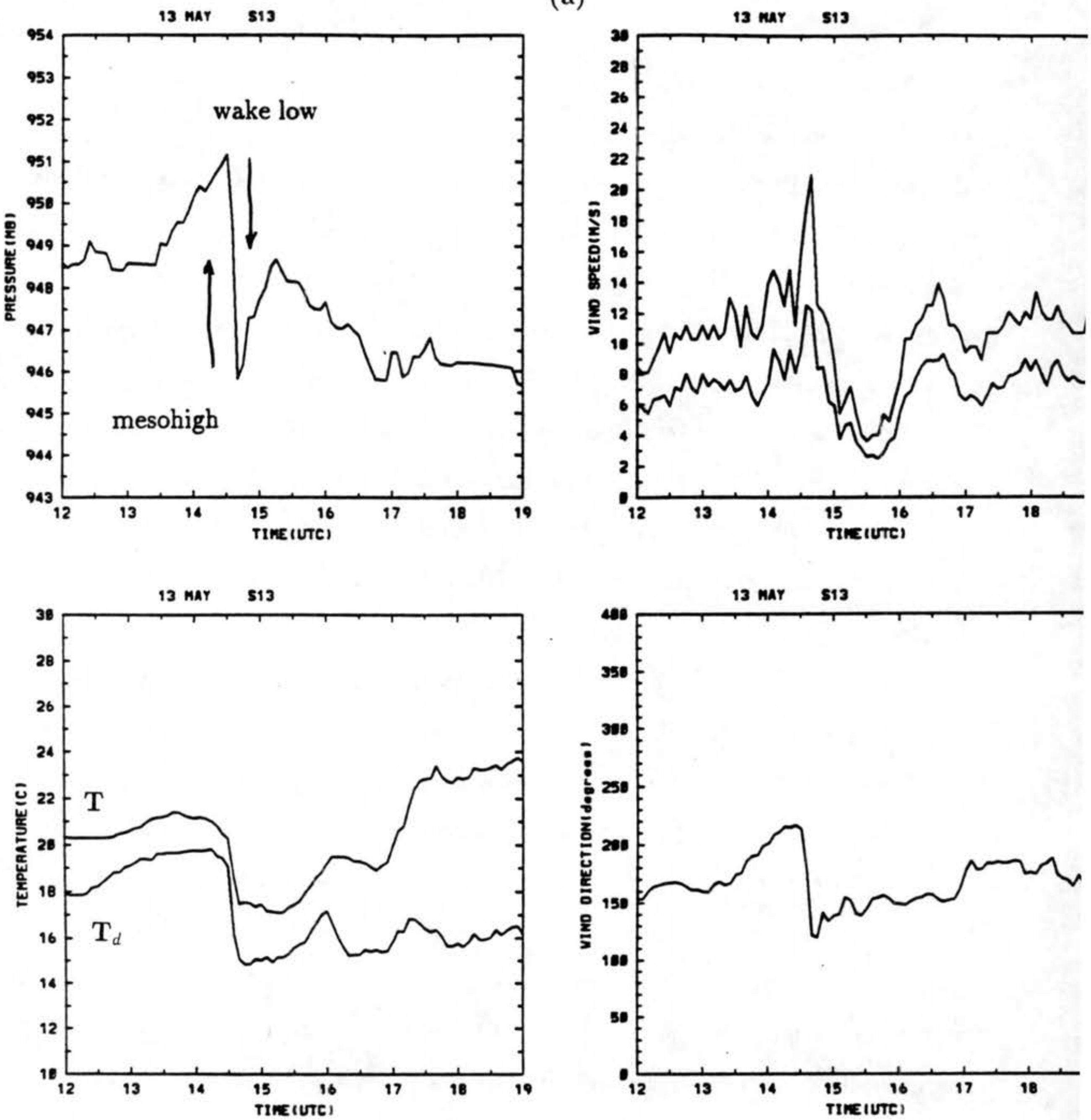

Figure 4.25: Same as Fig. 4.16 except for 13 May at station: a) S13; b) S16; c) S17. Note different time scale as each tick mark represents 30 minutes.

(b)

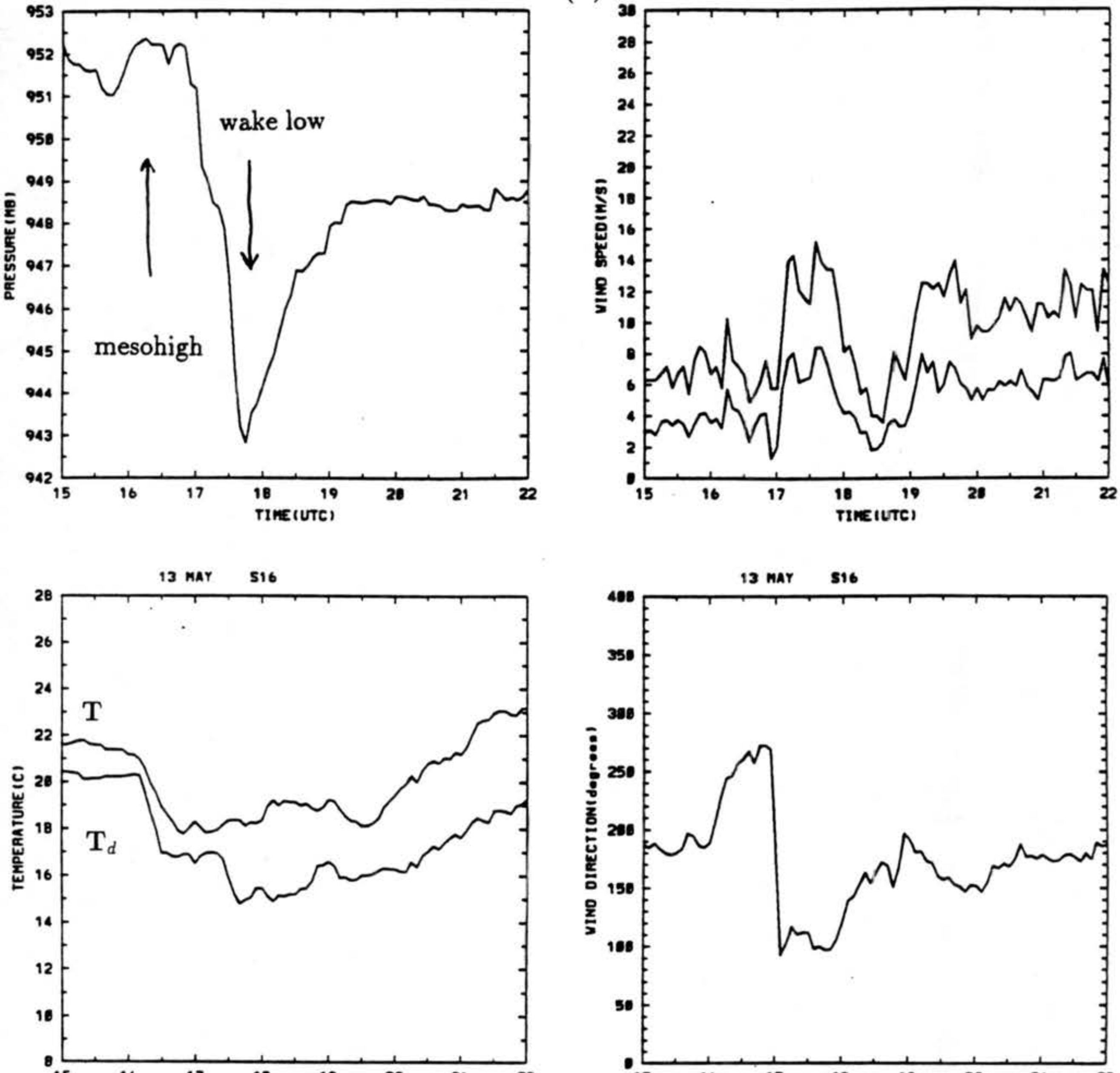

Figure 4.25: Continued.

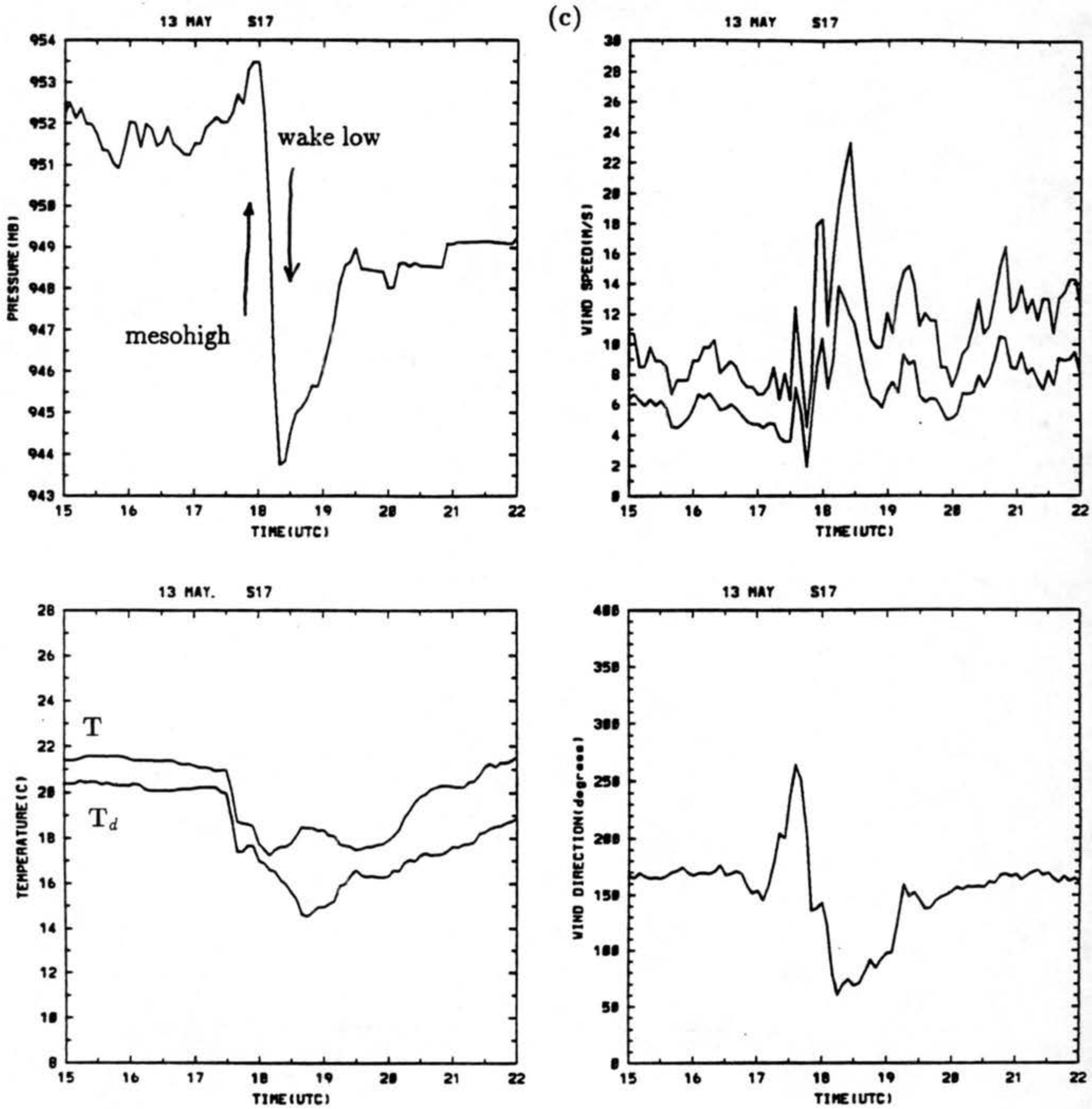

Figure 4.25: Continued.

4.4.1 Synoptic overview

The 0000 21 May maps are used to summarize the conditions associated with the development of this MCS. At the surface (Fig. 4.26a), there was a cold front extending southeast from central Indiana to central and southern Colorado. There was no temperature contrast across the front, with 20°C temperatures on either side. It was much drier to the north of the front with dewpoints in the lower 10's just north to around 0°C well north of the front, versus the upper 10's south of the front. Flow was mostly easterly in Kansas, north of the front and southerly in Oklahoma, south of the front.

At 850 mb (Fig. 4.26b) there was a low centered in southeast New Mexico with a nearly closed vortex around it. There was northerly flow in Kansas and southeasterly flow in Oklahoma and Texas. The flow was very weak over Kansas and Oklahoma, and around 10 m s^{-1} in Texas. Very moist air extended from eastern Texas into Kansas. At 500 mb (Fig. 4.26c) a weak short wave trough was evident over eastern New Mexico and western Texas, although there was no hint of a closed vortex, as there was at 850 mb. The flow was quite weak with 5-8 m s^{-1} westerly flow over Oklahoma and Texas.

4.4.2 Radar overview

This case was barely covered by the PRE-STORM radar network, so for this discussion the NMC facsimile radar summary maps are used. For this case they gave a good overview of the features associated with this system. The initial development associated with this system occurred in west-central Texas as two very intense cells around 2030 20 May (Fig. 4.27a). By 0130 (Fig. 4.27b) the convection developed into a northeast-southwest line to the south of several areas of convection in the Texas panhandle and Oklahoma. By 0330 (Fig. 4.27c) the system over Texas became a well developed MCS with an apparently asymmetric structure. The majority of the stratiform precipitation was at the northern end of the system. There was apparently not a region of enhanced stratiform precipitation at this time. A separate, distinct east-west convective line formed from the earlier, more random convection along the Oklahoma-Texas border. By 0630 (Fig. 4.27d) the system developed a structure very similar to that of the mature stage of the 7 May

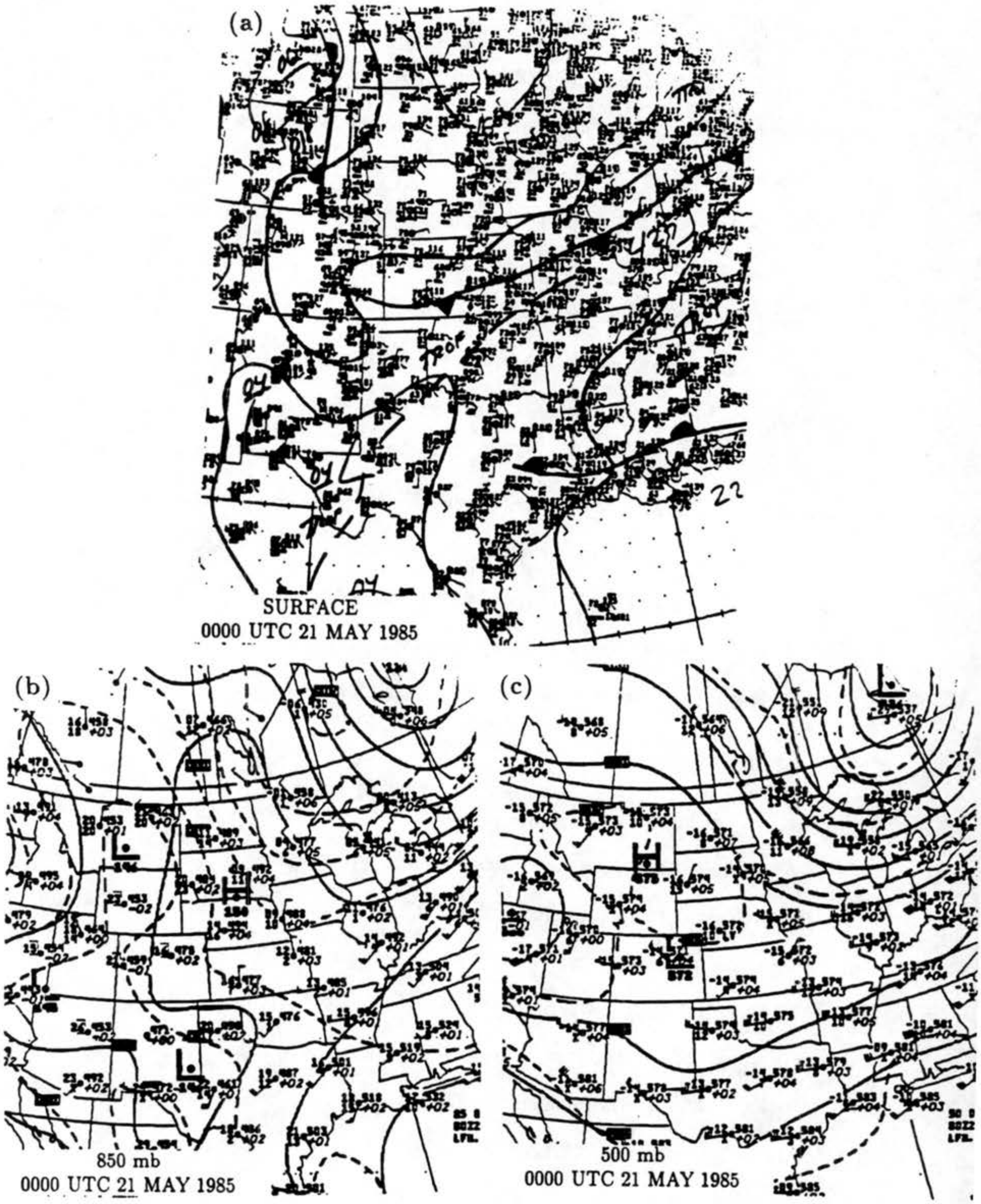

Figure 4.26: Same as Fig. 4.1 except for 0000 UTC 21 May.

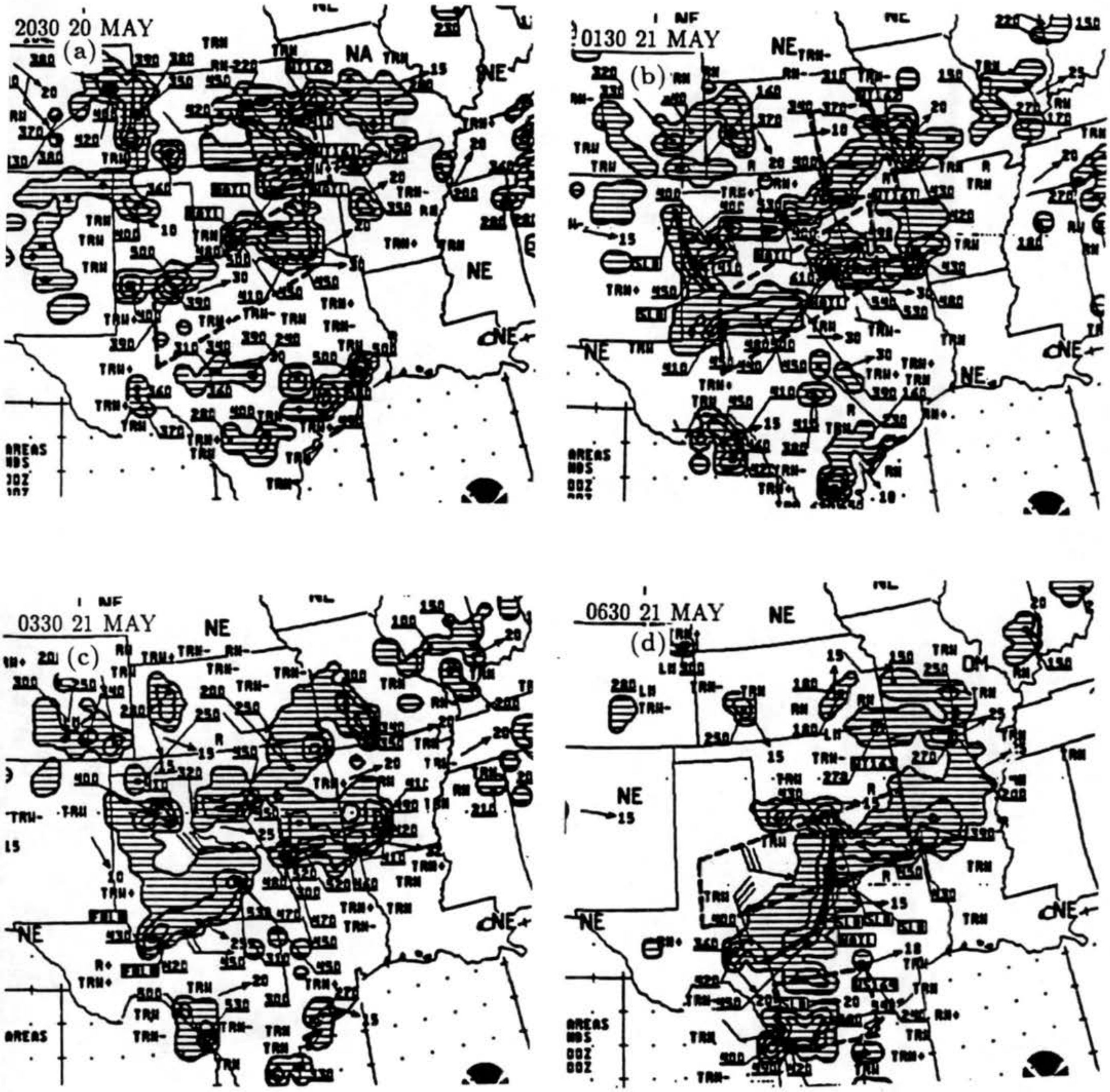

Figure 4.27: NMC radar summary charts for: a) 2030 UTC 20 May; b) 0130 UTC 21 May; c) 0330 UTC 21 May; d) 0630 UTC 21 May; e) 0730 UTC 21 May; f) 1030 UTC 21 May; g) 1830 UTC 21 May.

Figure 4.27: Continued.

case, with the two separate convective lines, one east-west the other northeast-southwest. Also a region of enhanced stratiform precipitation developed on the northwest side of the system, to the rear of where the two lines met, also much like 7 May. By 0730 (Fig. 4.27e) the enhanced stratiform core became more prominent. Also the central portion of the northeast-southwest convective line bowed ahead considerably. By 1030 (Fig. 4.27f) a hook-like structure developed in the northern stratiform precipitation area. Also, the east-west convective line dissipated. Finally, by 1830 (Fig. 4.27g) the convective line moved to eastern Louisiana but a very distinct "comma"-type reflectivity structure developed, much like that which developed on 7 May.

4.4.3 System overview

As previously mentioned, this system was poorly covered by both the mesonet and radar data. Only the extreme northern portion of the MCS was sampled. Fortunately, this was the area of a portion of the enhanced stratiform precipitation, as well as a portion of the wake low structure, so it was decided to include it within this summary.

Initial appearance in mesonet (0700-0730)

At 0700 most of the stratiform precipitation was to the south of the mesonet, but there was a visible enhanced stratiform region (Fig. 4.28). Only a hint of the mesohigh was evident. Also the wake low was visible, with the lowering pressure along the back edge of the stratiform area. By 0730 (Fig. 4.29) there was a more prominent mesohigh along the leading portion of the stratiform region. Also, the wake low was more evident right along the back edge of the stratiform precipitation region. The flow in the wake low was out of the east in response to the pressure gradient. The wake low then weakened over a two hour period as the stratiform area also weakened.

Regeneration of wake lows (0930-1130)

By 0930 (Fig. 4.30) the stratiform precipitation regenerated and the wake low reap-

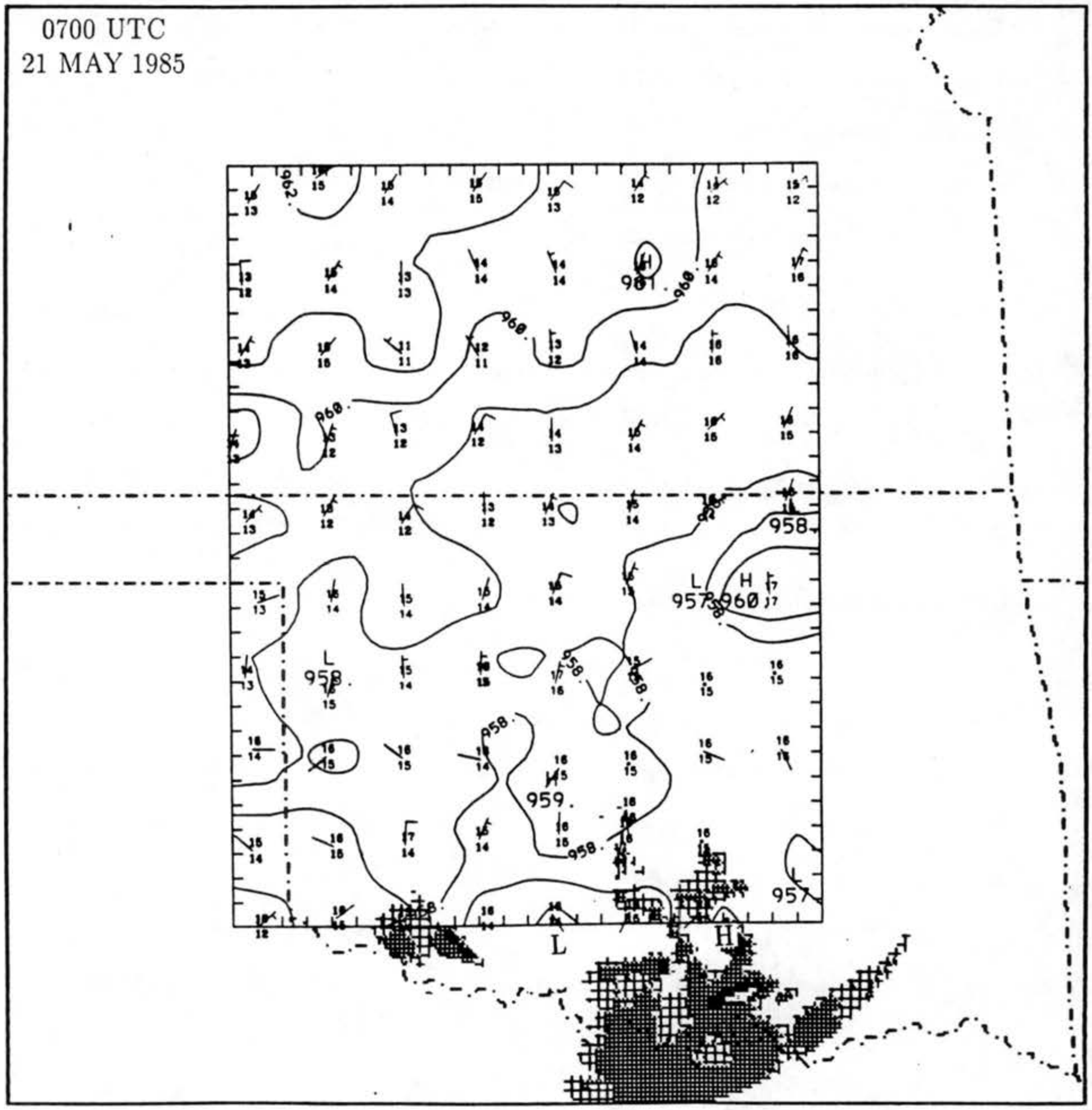

Figure 4.28: Same as Fig. 4.5 except for 0700 UTC 21 May.

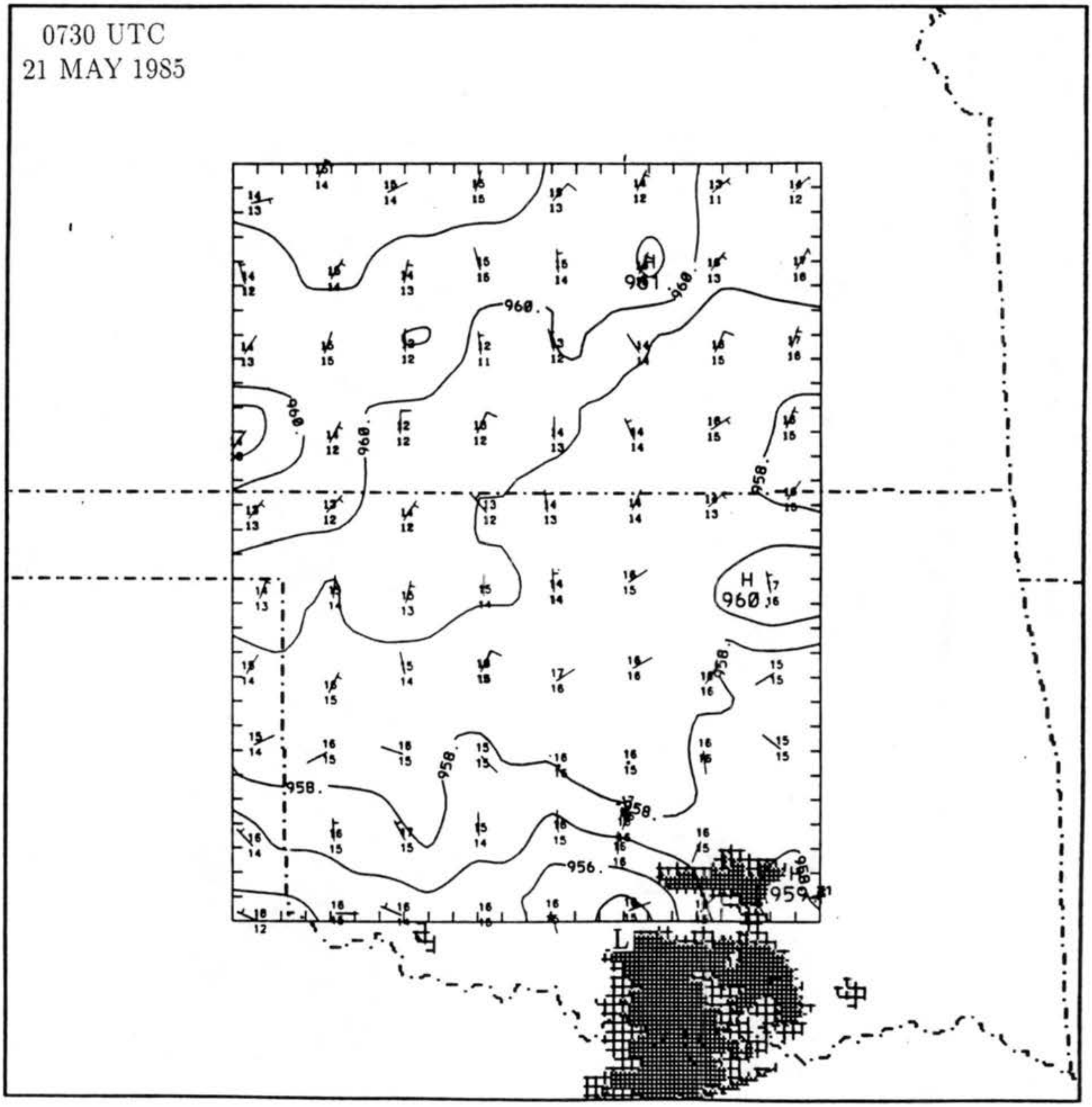

Figure 4.29: Same as Fig. 4.5 except for 0730 UTC 21 May.

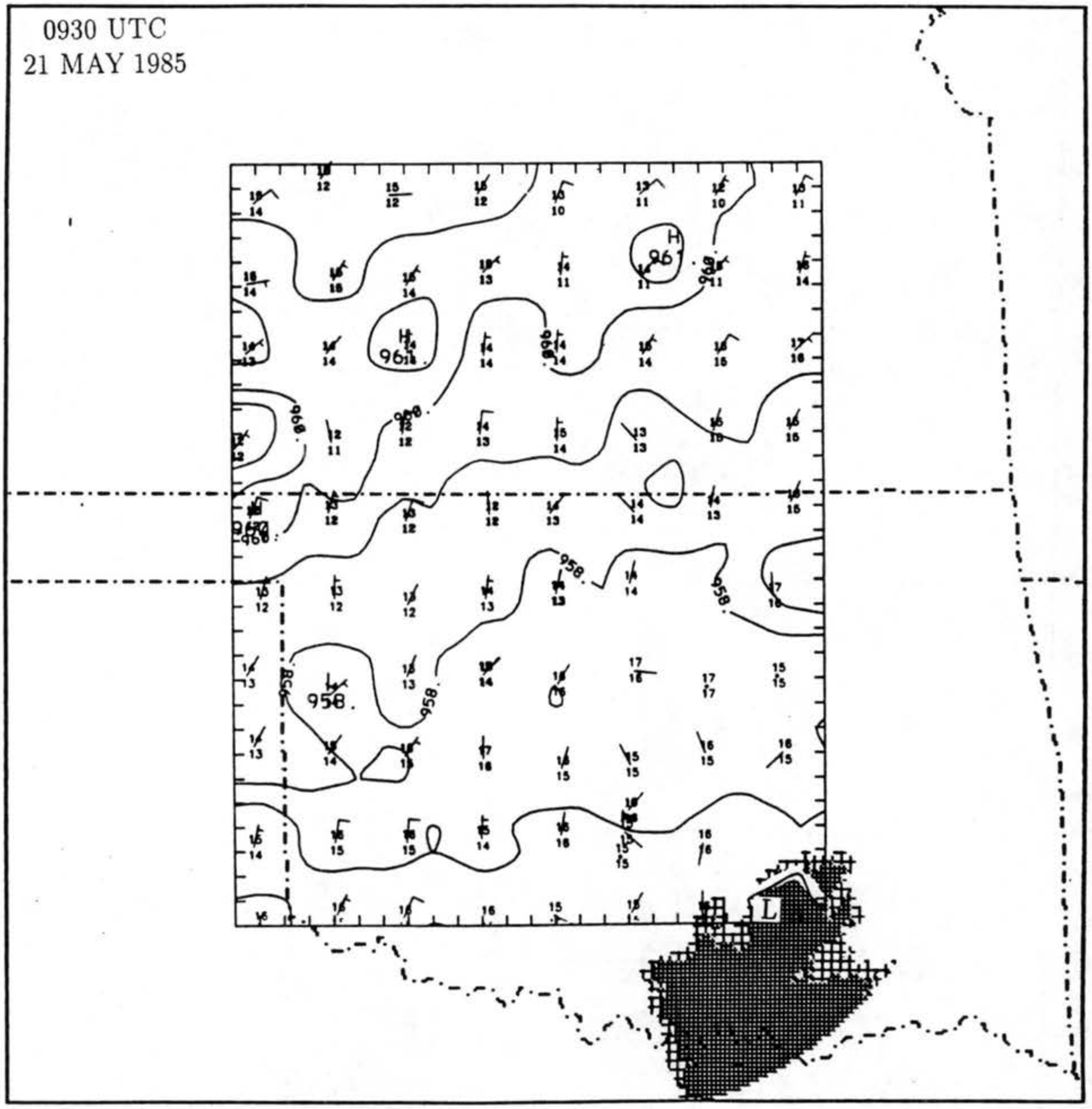

Figure 4.30: Same as Fig. 4.5 except for 0930 UTC 21 May.

peared along the back edge of the region of enhanced precipitation [1] By 1000 (Fig. 4.31) there was a regeneration of enhanced stratiform precipitation on the western side, leading to the development of another wake low on its back edge. By 1100 (Fig. 4.32) the enhanced stratiform precipitation diminished in intensity somewhat, but it was more within the mesonet, so the wake low was viewed more clearly as being on the northwest corner of the system, along the back edge of the slightly enhanced stratiform region.

Mesovortex (1200)

At this time the upper-air maps give the idea that this MCS helped to develop a mesovortex. Remember that at 0000 there was a nearly closed vortex at 850 mb, but it did not extend any farther in the vertical. By 1200, at 850 mb (Fig. 4.33a) there was a distinctly closed vortex centered along the Texas-Oklahoma border, although it appeared to be slightly to the east of the NMC placement of the low. This would place the low within the northern stratiform region of this MCS, which was where the vortex was on the 7 May case (Brandes, 1990). At 700 mb (Fig. 4.33b) there was a nearly closed cyclonic circulation, but its positioning is suspect due to a missing report out of Stephenville, Texas. The nearly closed circulation was also present at 500 mb (Fig. 4.33c) also positioned along the Texas-Oklahoma border. There was, apparently, a rear inflow jet coming around the southern end of this vortex, which is what would be suspected given that the reflectivity structure here so resembles the 7 May case which had a strong rear inflow jet around the southern portion of that vortex. It cannot be determined if the vortex reached the surface in this case due to the positioning of the system relative to the mesonet.

4.5 May 27 case

4.5.1 Synoptic overview

The 0000 27 May maps are examined to determine the environment for the development of this MCS. At the surface (Fig. 4.34a) a 1000 mb low was in southern Wisconsin

---

[1] The reflectivity scheme used here was selected for ease of viewing the pressure features and does not clearly show the finer gradations neccessary to show this regeneration of the enhanced stratiform precipitation.

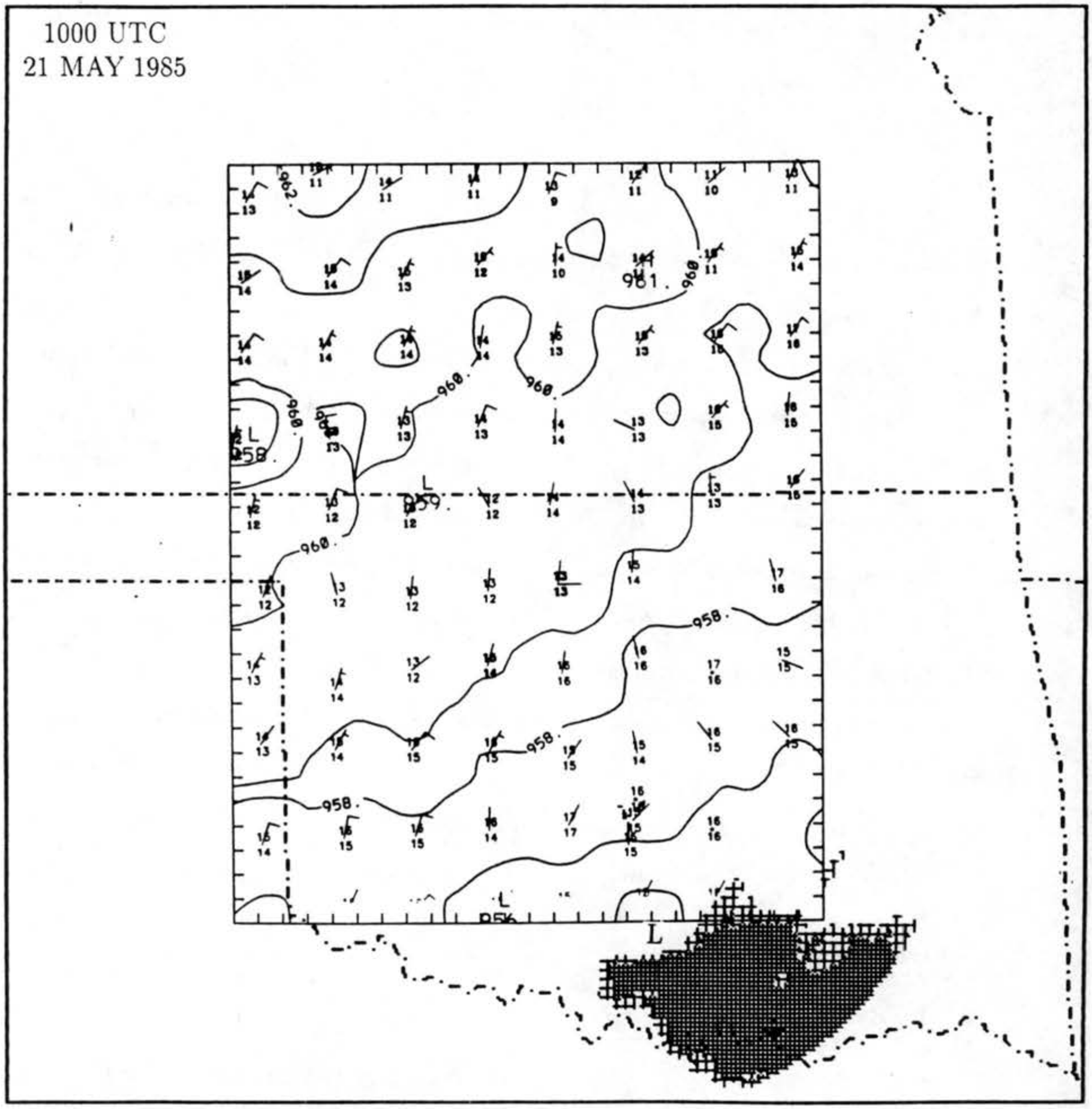

Figure 4.31: Same as Fig. 4.5 except for 1000 UTC 21 May.

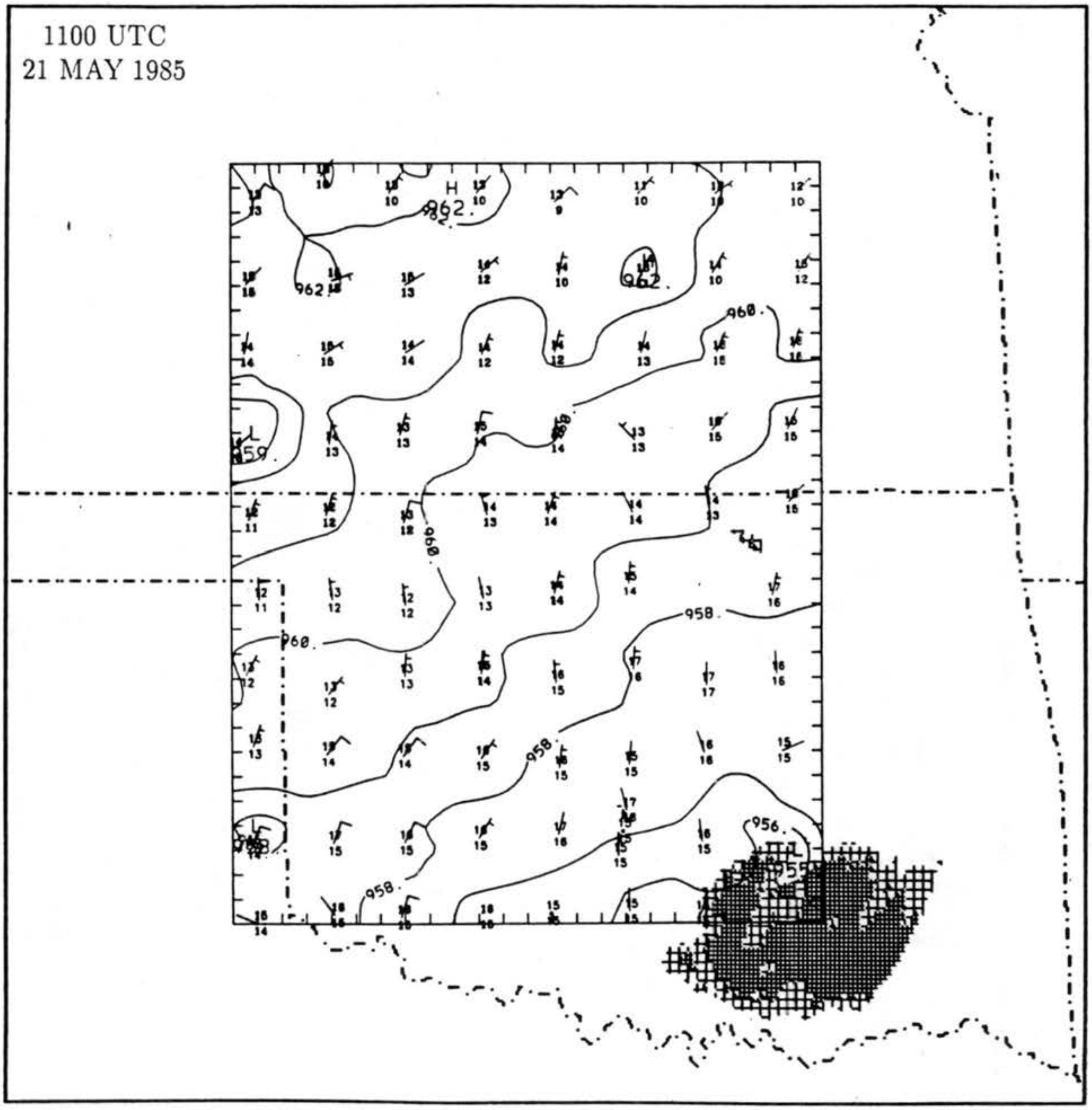

Figure 4.32: Same as Fig. 4.5 except for 1100 UTC 21 May.

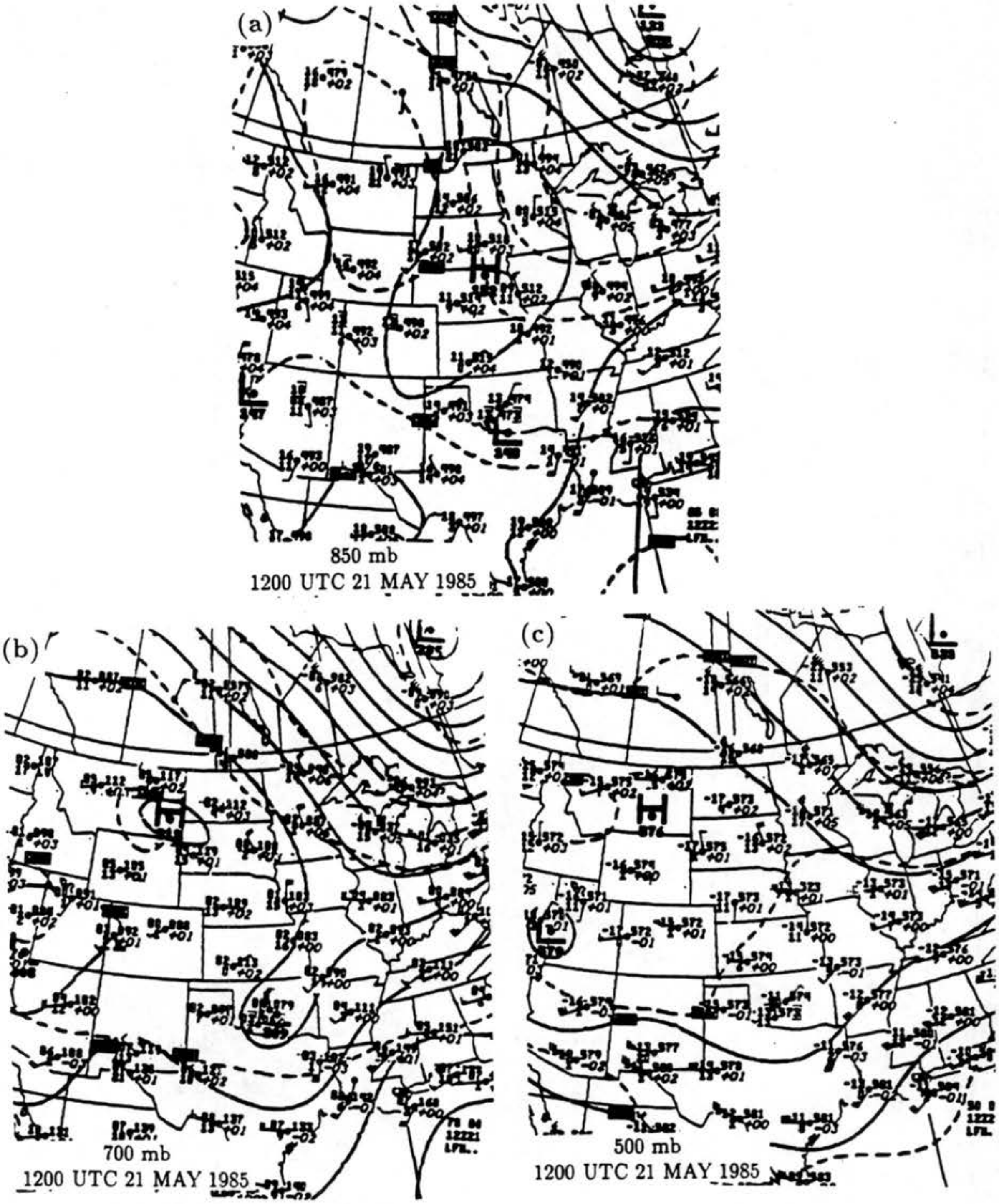

Figure 4.33: Same as Fig. 4.1 except for 1200 UTC 21 May at: a) 850 mb; b) 700 mb; c) 500 mb. Solid contours in b. represent geopotential height. Dashed contours in b. represent temperature in °C.

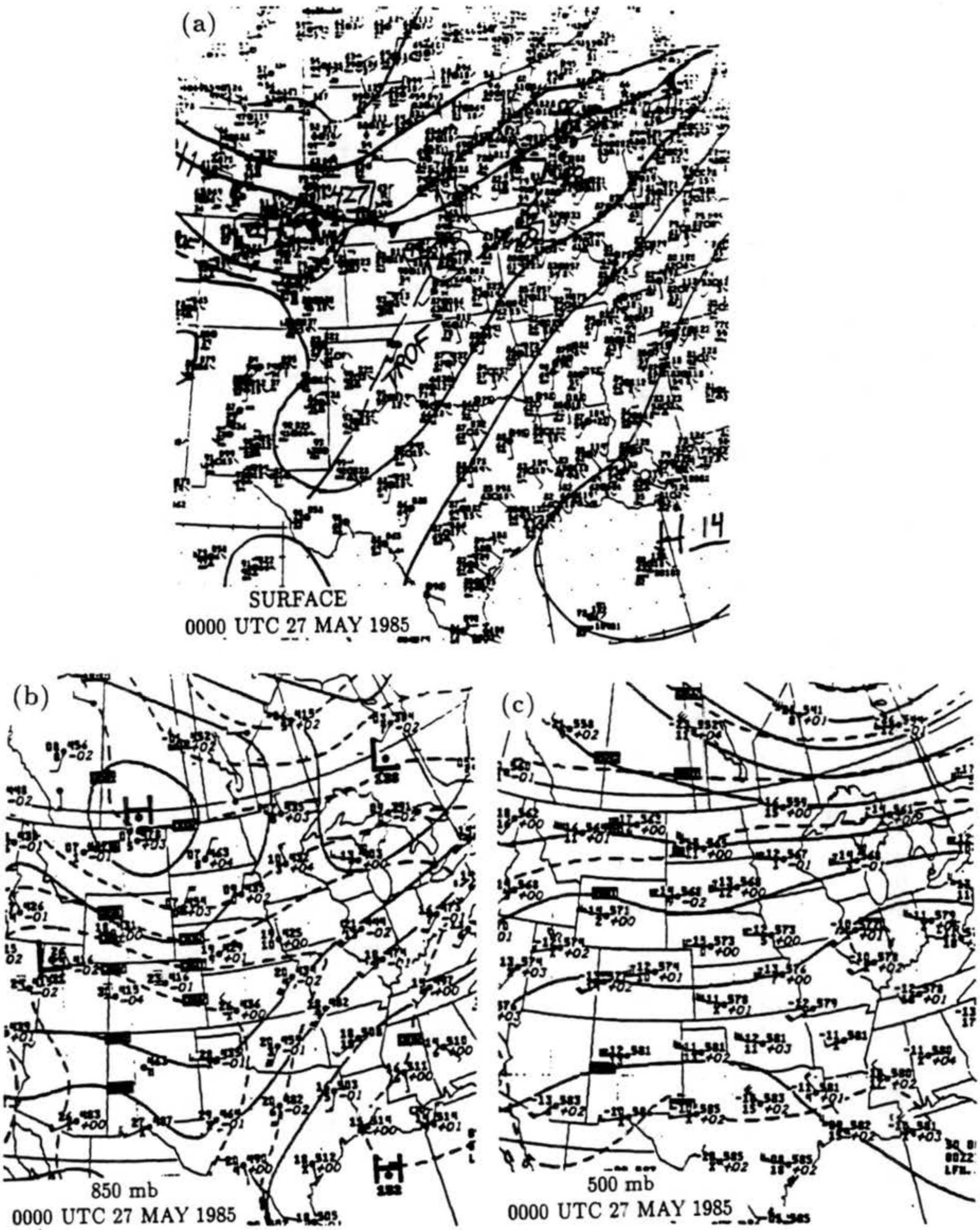

Figure 4.34: Same as Fig. 4.1 except for 0000 UTC 27 May.

with a cold front extending to the southwest through central Iowa, southern Nebraska and southeastern Wyoming. It was very warm to the south of the front (25-33°C) with a southerly flow, and to the north it was cool (12-22°C) with a northerly flow.

At 850 mb (Fig. 4.34b) a large trough extended from the Great Lakes southwest to the Great Basin. Another north-south oriented trough extended across western Texas. Strong (15 m s^{-1}) flow out of the southwest was evident over central Oklahoma and eastern Kansas. Very moist air with dewpoints over 15°C extended over the same region. There was a weak trough at 500 mb over Nebraska and Kansas (Fig. 4.34c). Very weak westerly flow was present extending from western Nebraska south to western Texas (8-10 m s^{-1}).

4.5.2 Radar overview

As discussed by Carbone et al. (1990) the initial development associated with this MCS occurred in the lee of the Rockies in eastern Wyoming and northern Colorado on the afternoon of 26 May (not shown). By 0500 (Fig. 4.35a) the system moved to north-central Kansas and was in a highly decayed state. There were also two other systems present. The one in eastern Kansas stayed just outside of the mesonet. The one in Oklahoma started as very intense convective cells in northern Oklahoma around 0000. These storms produced 40 severe weather reports, mostly large hail. While the Oklahoma system was interesting, it was not adequately covered by the PRE-STORM radar network (OKC radar data was not collected) nor by the NMC radar summaries, so it is not included in this survey.

As for the north-central Kansas system, by 0600 (Fig. 4.35b) several areas of new convection were developing along a line to the south of the east side of the decaying system. So, by 0700 (Fig. 4.35c) the system regenerated with a line of convection now evident. At this time the system had an asymmetric structure. A couple of reports of severe hail occurred in conjunction with the far southern end of this convective line. At 0800 (Fig. 4.35d) the southern end of the MCS merged with the system in eastern Kansas, leading to an enhancement of the convection in this area. This enhanced area of convection lasted for several hours as it moved to the south, a movement contrary to that of the system under study which moved from 290° at 17 m s^{-1}.

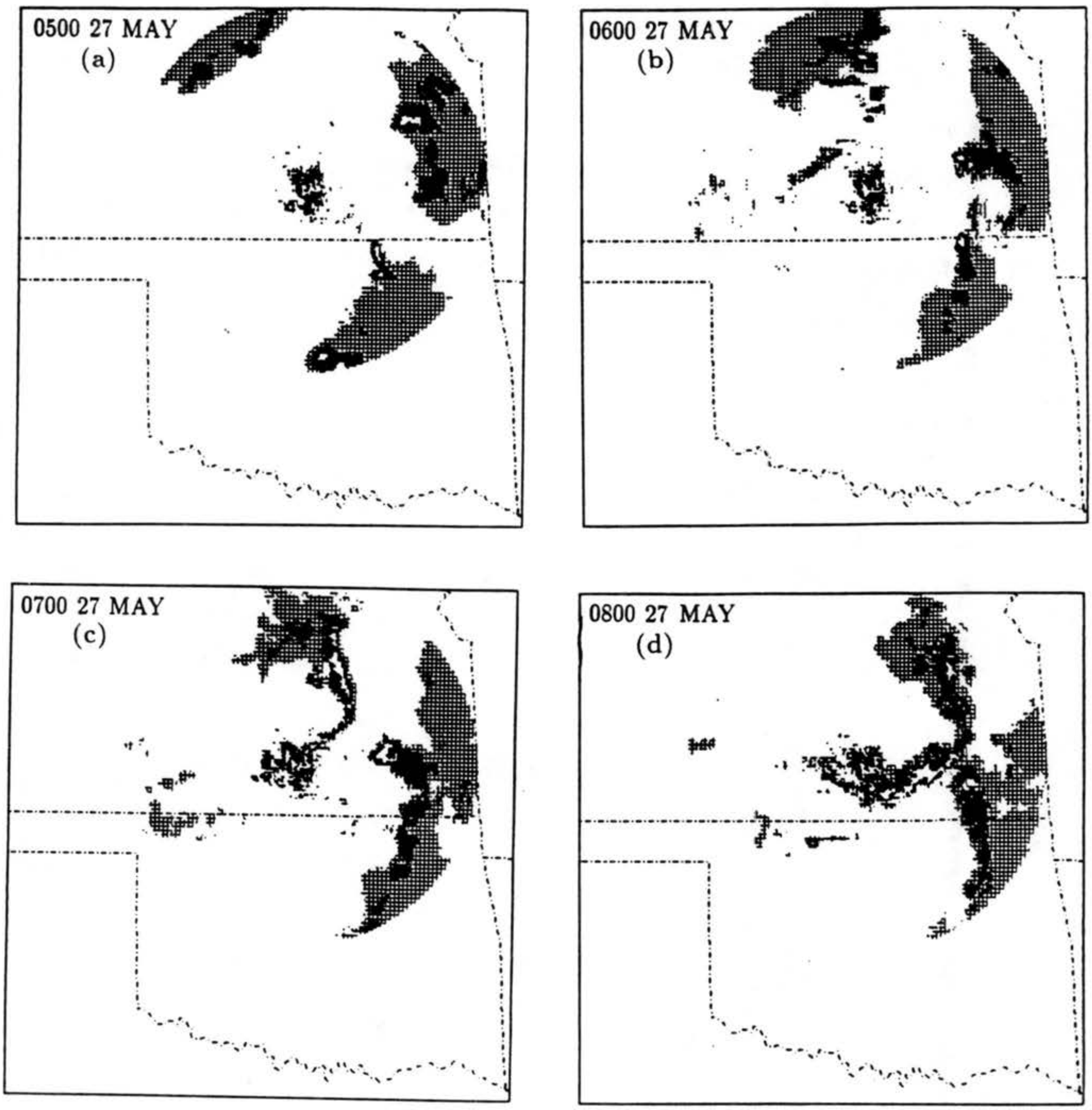

Figure 4.35: Same as Fig. 4.3 except for 27 May at: a) 0500 UTC; b) 0600 UTC; c) 0700 UTC; d) 0800 UTC. All using Wichita KS.

4.5.3 System overview

Gust front appearance (0500)

A very intense gust front can be seen emanating from the central Kansas MCS, with 15 m s^{-1} northerly flow and an enhanced pressure gradient along its leading edge (Fig. 4.36). The air in western Kansas and the Oklahoma panhandle into western Texas was very dry, whereas to the east of this area it was quite moist. Oklahoma was dominated by a southerly flow of 5 m s^{-1}, leading to convergence along the leading edge of the gust front in central Kansas. The central Oklahoma system can be seen to have a very intense mesohigh and gust front associated with it but its precipitation structure was not clearly discernable.

Convective line formation (0600)

At this time the convection in Kansas was seen to be forming along the leading edge of the gust front (Fig. 4.37). This has been confirmed by Carbone et al. (1990). One reason why the convection developed in this area, rather than in western Kansas was the existence of the dry line feature mentioned earlier. Carbone et al. found that the lack of moisture to the west of the dryline feature greatly limited the susceptibility of the area to deep convection so that even the strong convergence along the gust front was not enough to start convection in this dry air. Crook et al. (1990) show through a modeling study that other forcing mechanisms for this convective line were increased low-level shear as well as a mesoscale oscillation forced by the earlier convection associated with this system.

There was also the initial appearance of a lowering of the pressure along the back edge of the stratiform region, indicative of the formation of a wake low. Its intensity cannot be determined due to its placement in the far northwestern corner of the mesonet.

The rear inflow structure at this time near the wake low is provided by RSL (Fig. 4.38), which was located within the stratiform region (point A in Fig. 4.37). It indicated a 350 mb deep layer of generally weak rear inflow with a maximum at 600 mb (6 m s^{-1}). This was a weaker rear inflow than that found in other wake low regions, but the intensity of the wake low itself was unknown at this time due to its position at the edge of the mesonet and it may have been just developing.

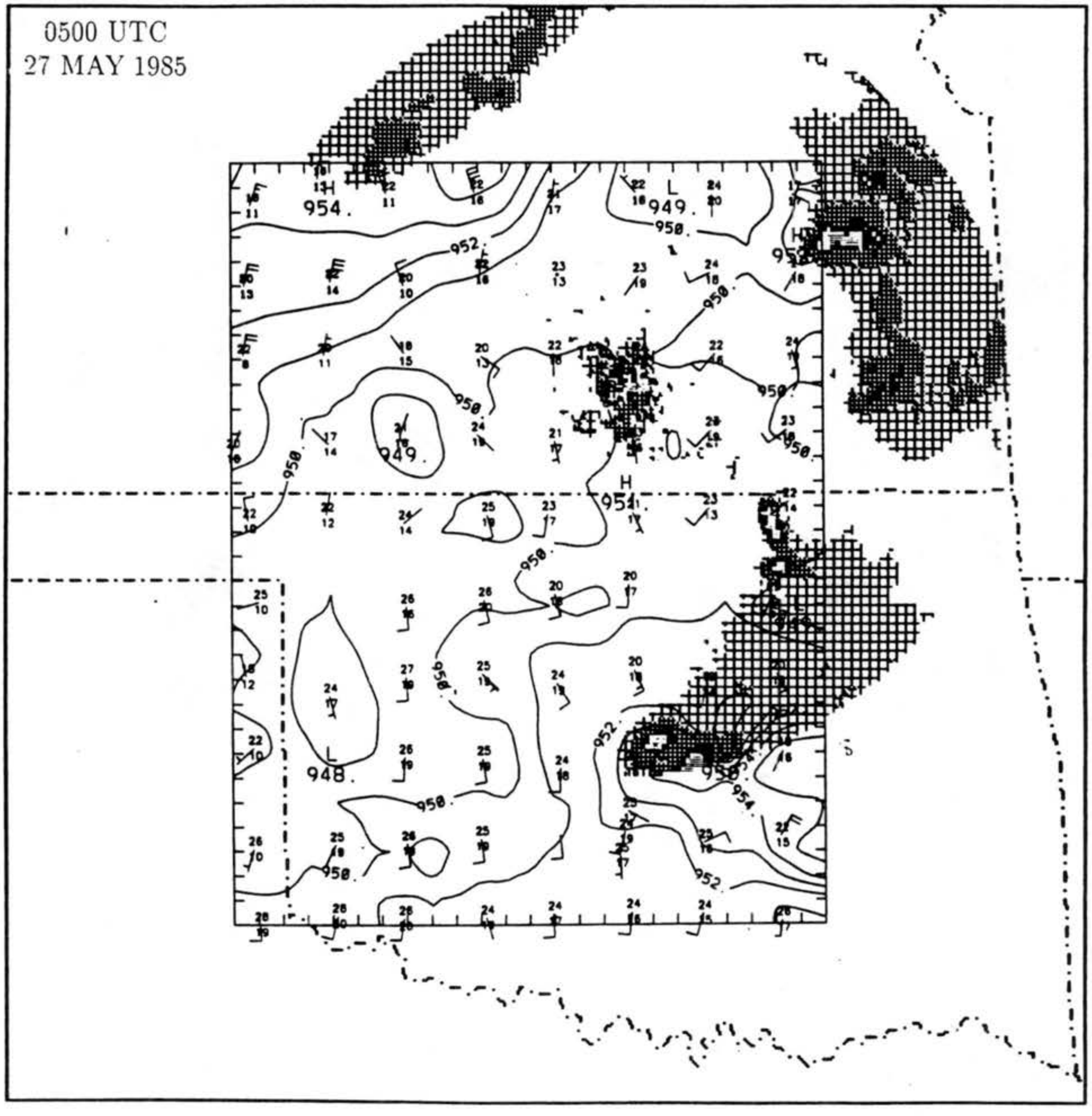

Figure 4.36: Same as Fig. 4.5 except for 0500 UTC 27 May.

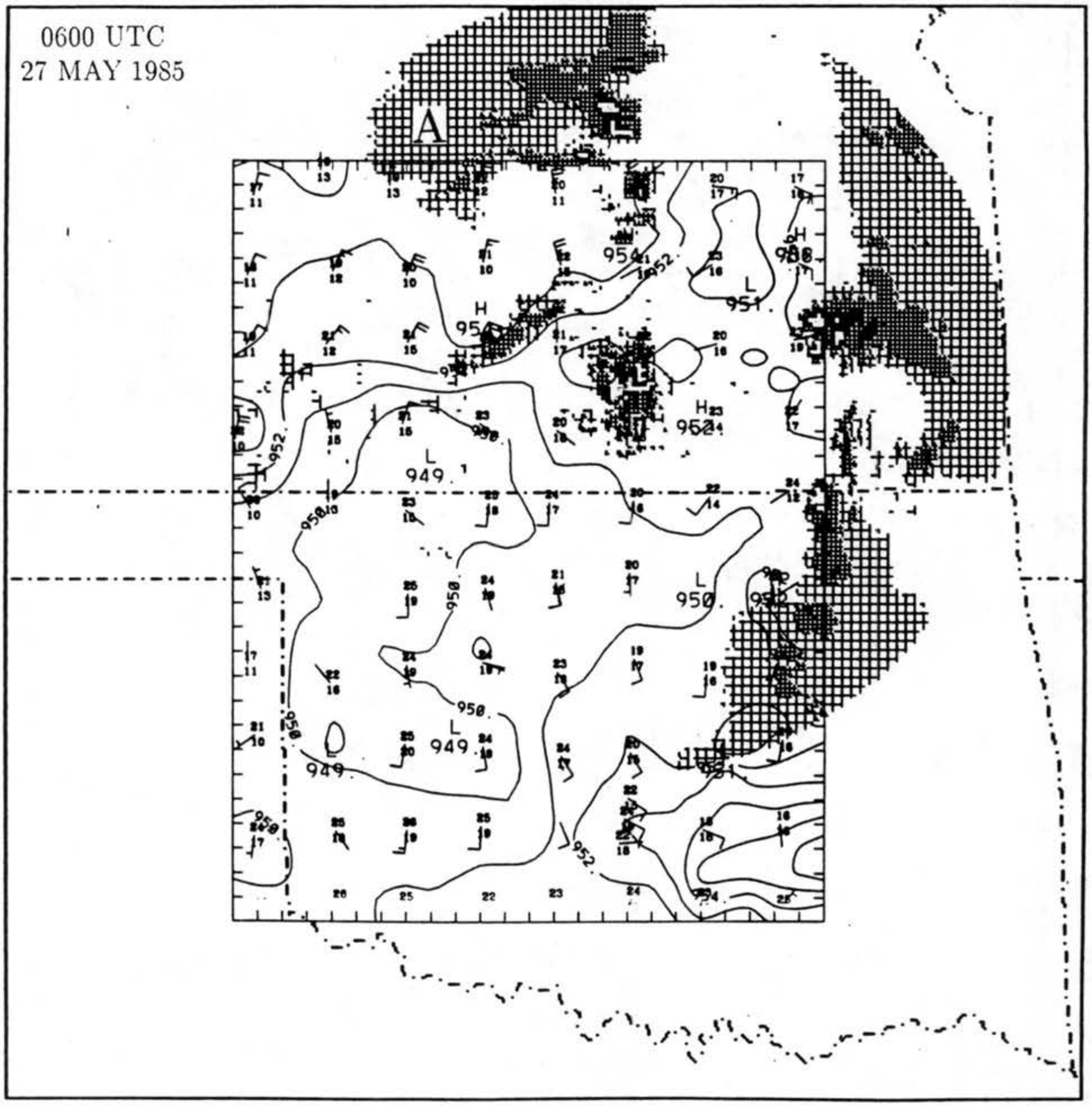

Figure 4.37: Same as Fig. 4.5 except for 0600 UTC 27 May.

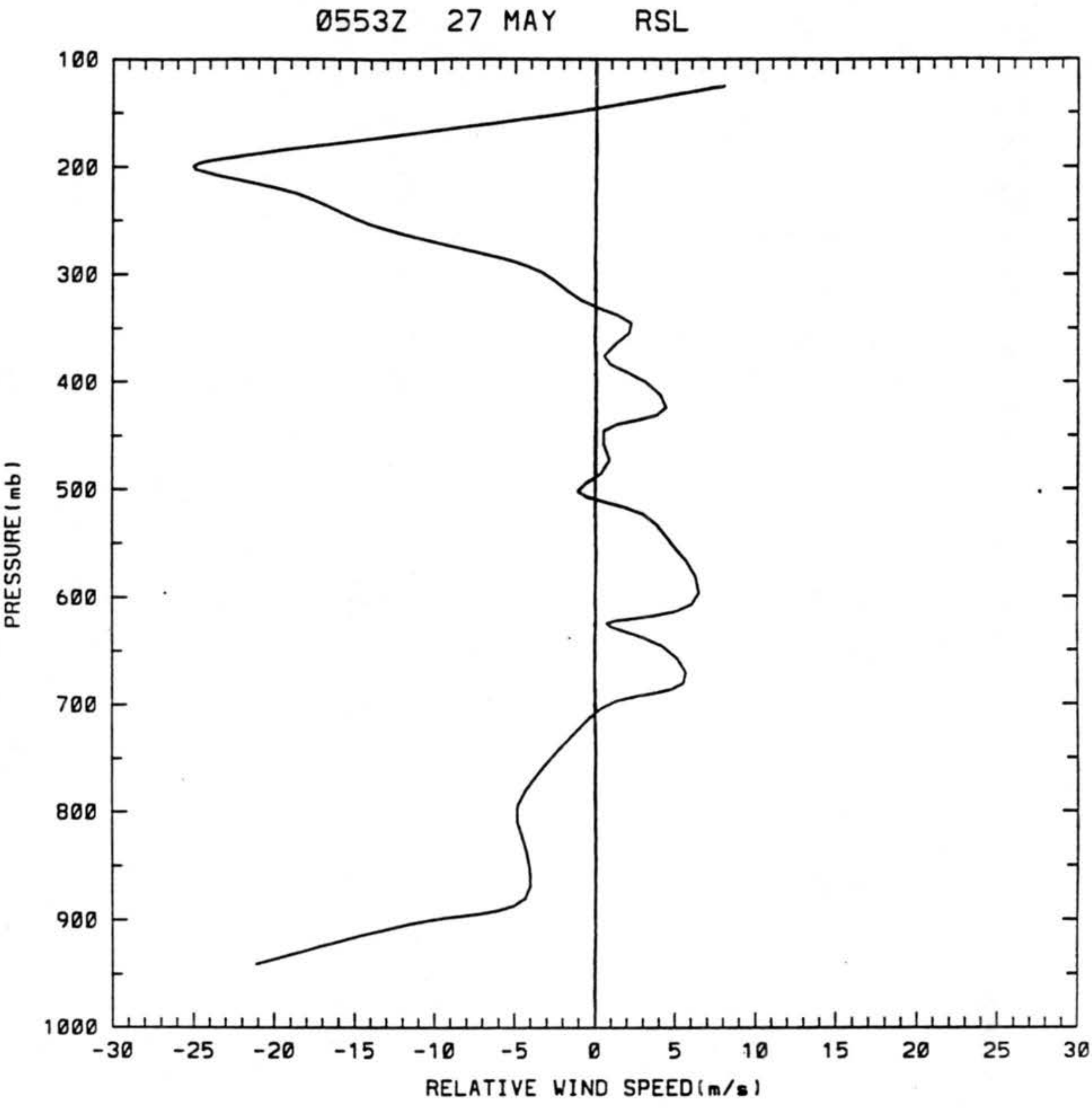

Figure 4.38: Same as Fig. 4.7 except for 0553 UTC 27 May at RSL.

Mature stage (0730)

The mesohighs associated with the squall line over Kansas, at this time, were still the same strength as they were earlier (Fig. 4.39). But now a deep wake low formed within the mesonet to the rear of the enhanced stratiform precipitation core. The exact placement of the wake low was questionable since the stratiform area straddles the far northern portion of the mesonet. The typical MCS flow features were evident in the northern portion of the system, with divergence to the rear of the mesohigh, accentuated easterly flow (10 m s^{-1}) through the wake low, and weak convergence to the rear of the wake low.

The rear inflow along and to the rear of the wake low region is shown by the RSL and FRI soundings (Figs. 4.40a,b). RSL was about 100 km to the rear of the stratiform area (point A in Fig. 4.39) and indicated a 325 mb deep rear inflow layer with a maximum at 525 mb (9 m s^{-1}). At FRI, which was just behind the northern portion of the convective line within the stratiform area (point B in Fig. 4.39) there was a 425 mb deep rear inflow layer in the lower troposphere maximized at 775 mb (10 m s^{-1}). These two soundings show the tendency of the rear inflow to descend as it approached the convective line.

The rear inflow behind the central portion of the line is indicated by the PTT sounding (Fig. 4.40c). It was located about 100 km to the rear of the convective line (point C in Fig. 4.39), and shows only a 200 mb deep layer of rear inflow without a true maximum level (generally 6 m s^{-1}).

Dissipating stage (0900)

A large mesohigh formed along the convective development which occurred when the southern portion of this MCS merged with the eastern Kansas MCS; this high was now 3 mb stronger than earlier (Fig. 4.41). The wake low filled 2 mb, probably partially due to the dissipation of the enhanced stratiform region. The easterly flow through the wake low also noticeably weakened to 5 m s^{-1} due to the loss of the stronger gradient.

The rear inflow near the wake low is shown by the FRI sounding (Fig. 4.42a), which was located at the back edge of the stratiform area just to the north of the wake low (point A in Fig. 4.41). It indicated a 375 mb deep rear inflow with a peak at 600 mb (12

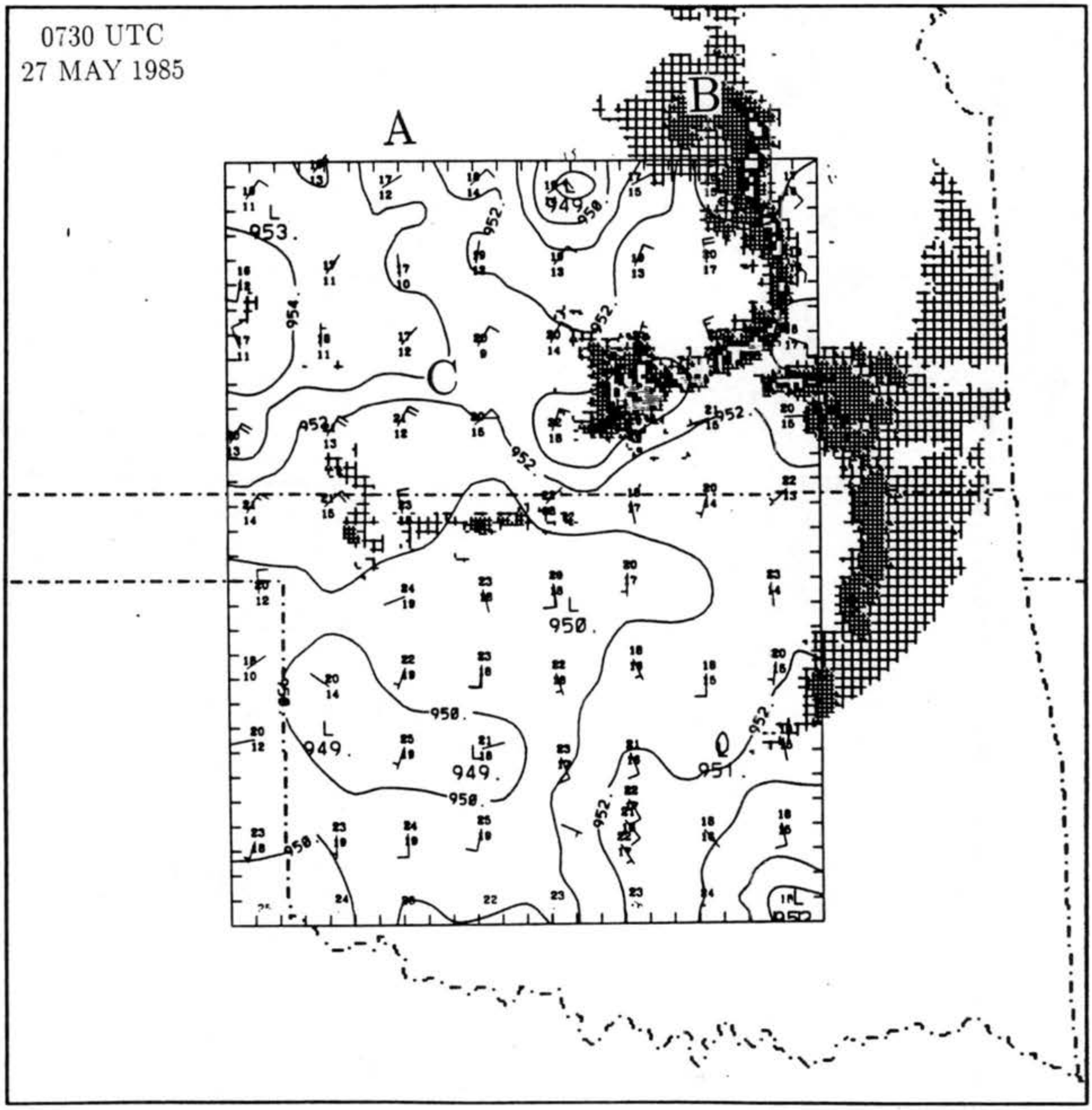

Figure 4.39: Same as Fig. 4.5 except for 0730 UTC 27 May.

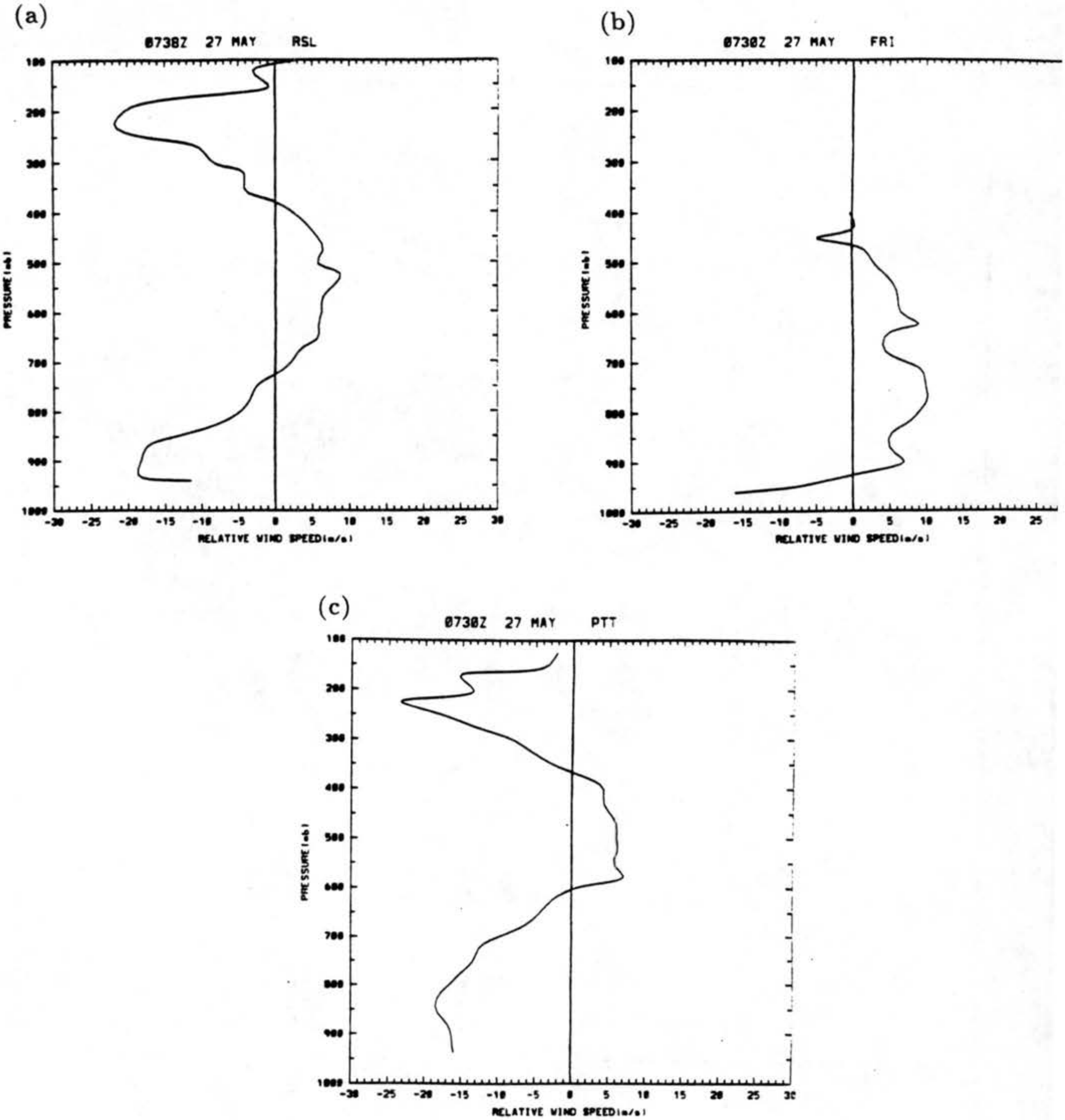

Figure 4.40: Same as Fig. 4.7 except for 27 May at: a) 0738 UTC at RSL; b) 0730 UTC at FRI; c) 0730 UTC PTT.

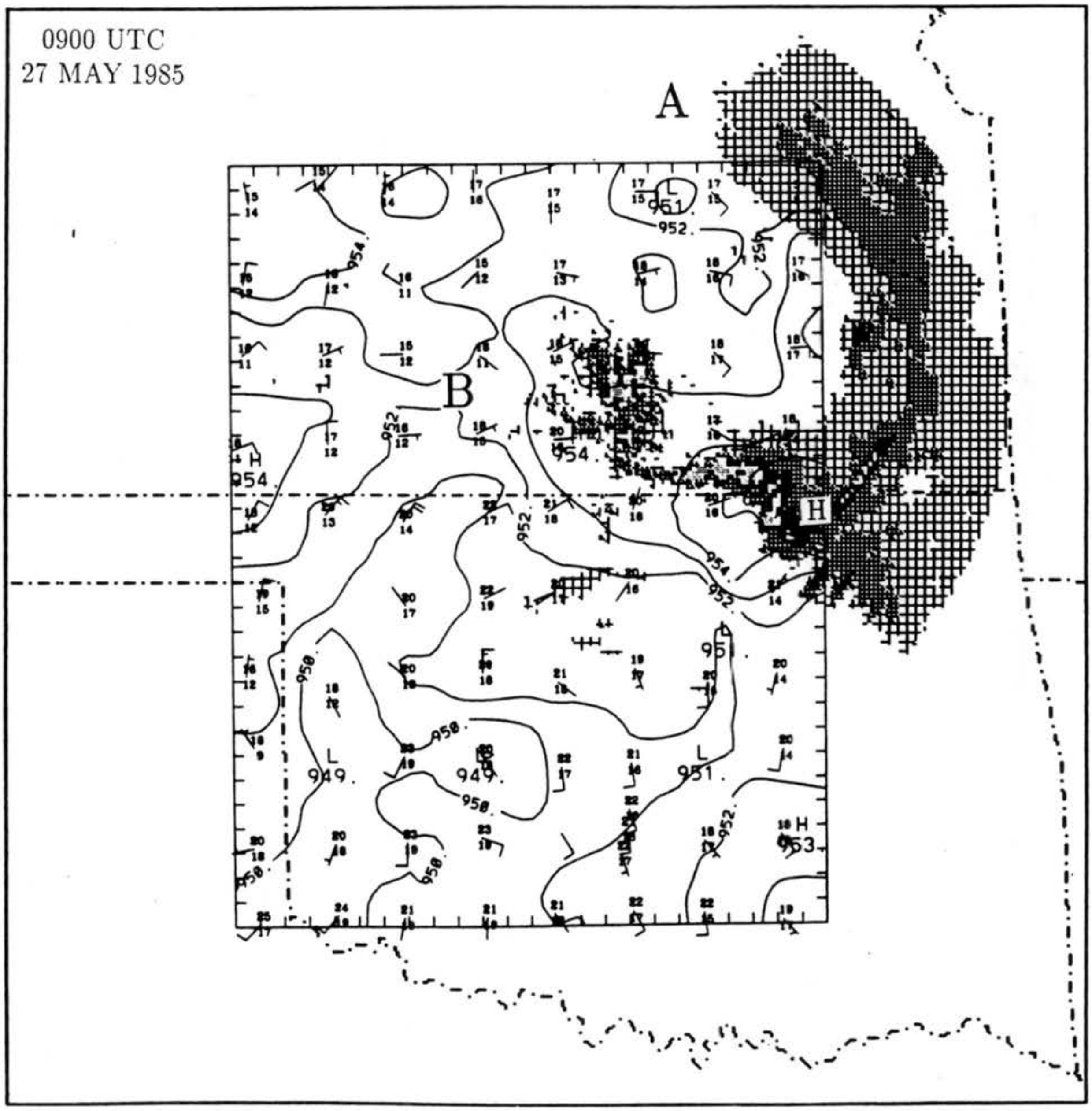

Figure 4.41: Same as Fig. 4.5 except for 0900 UTC 7 May.

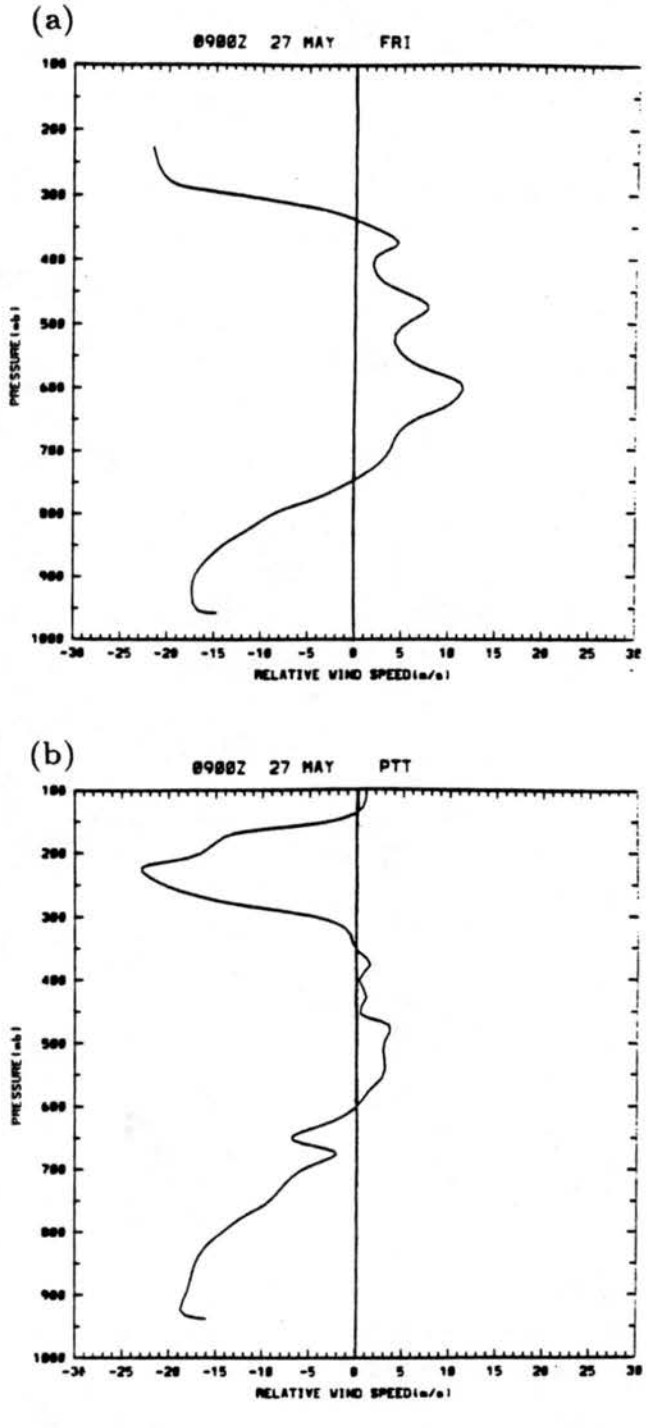

Figure 4.42: Same as Fig. 4.7 except for 27 May at: a) 0900 UTC at FRI; b) 0900 UTC at PTT.

m s^{-1}). This was 175 mb higher than it was at FRI 90 minutes earlier, again indicating a descending rear inflow jet.

At PTT (Fig. 4.42b), which was 200 km to the rear of the southern portion of the system which was without stratiform precipitation (point B in Fig. 4.41), there was only a 250 mb deep rear inflow layer, having a weak amplitude (4 m s^{-1}). Comparison with the sounding taken here 1 h earlier shows that the rear inflow in this section of the system was not descending, but was remaining at a constant height. This may have been due to the lack of stratiform precipitation and its associated downdrafts within this portion of the system. Carbone et al. (1990) also found that the rear inflow in the region to the south of the wake low did not descend. In fact, they found, based on data from the wind profiler at McPherson, Kansas that the inflow actually ascended in this region.

4.5.4 Mesonet time series

The conditions in the area of the initial development of the convective line are shown from P20 (Fig. 4.43, see Fig. 3.1). There was a sharp pressure rise of 4.5 mb over 3 hrs, concentrated in a 3 mb rise in 20 minutes, associated with the mesohigh. The highest pressure occurred at 0600, the time of the development of the convective line. Note also that there was a 3°C temperature and a 2°C dewpoint increase, as well as a 19 m s^{-1} wind gust all associated with the gust front from the dissipated system. This would be indicative of a rapid destabilization in this area with such a rapid low-level warming and moistening, helping to lead to the development of the convective line in this region. Also, there was a sharp shift from east to northwest flow as the high passed over.

The wake low conditions are summarized with stations P04 (Fig. 4.44) and P05 (Fig. 4.45). At P04 the wake low was not very deep. The mesohigh (0520) was quite sharp with a 4 mb increase in 30 minutes. Associated with it was a sharp dewpoint decrease of 7°C, which was associated with the passage of the dry line feature, a shift from weak northeast to strong northwest flow (24 m s^{-1} gusts). There was a double drop in the pressure, the first (0640) was the wake low passing over the station and the second (0740) was due to the rapid deepening the low underwent in the next 30 minutes. The gradient was not sharp enough (4 mb in 70 minutes) to produce a wind speed signature, but the wind shifted

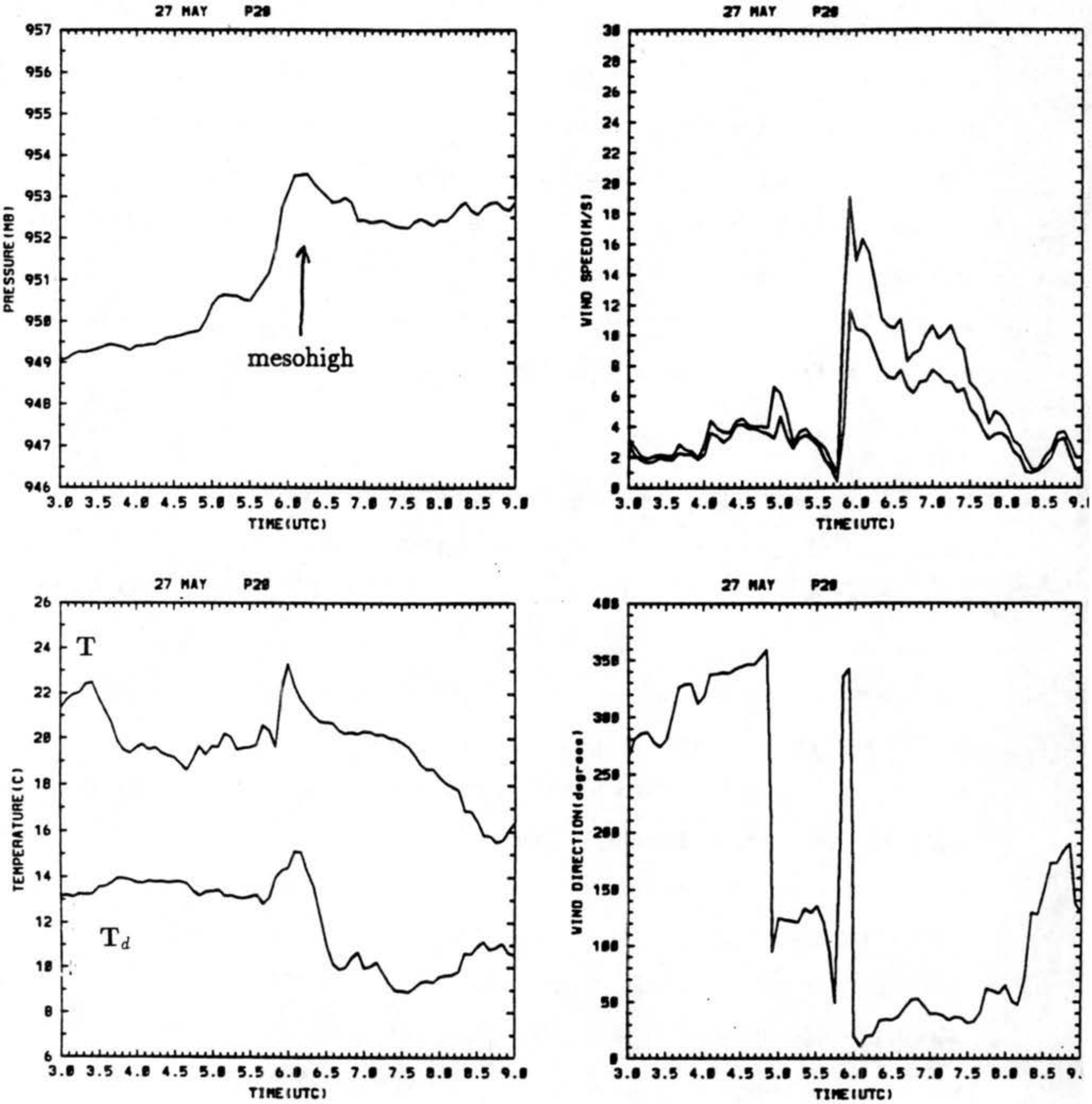

Figure 4.43: Same as Fig. 4.16 except for 27 May at station P20.

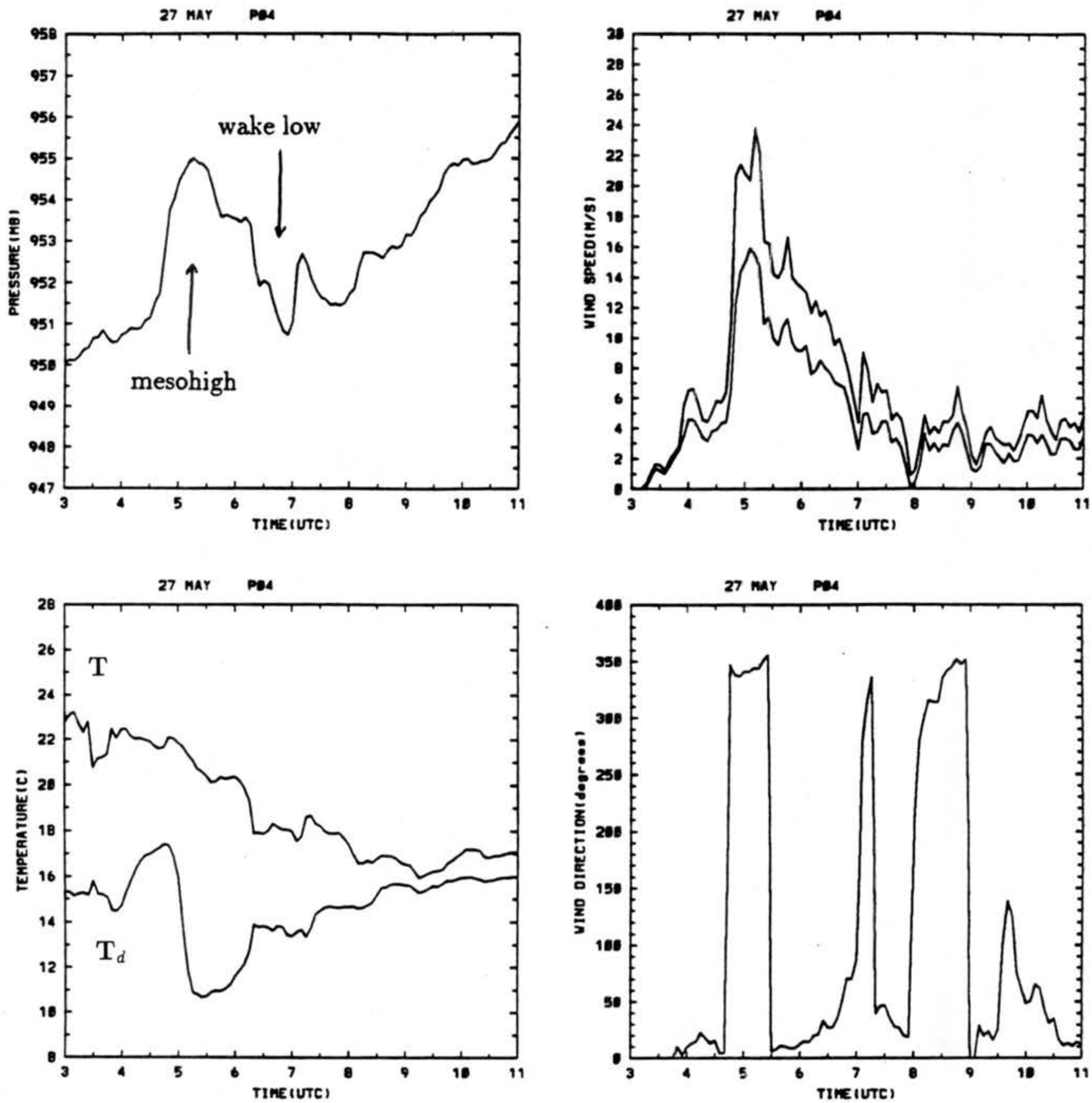

Figure 4.44: Same as Fig. 4.16 except for 27 May at station P04. Note different time scale as each tick mark represents 30 minutes.

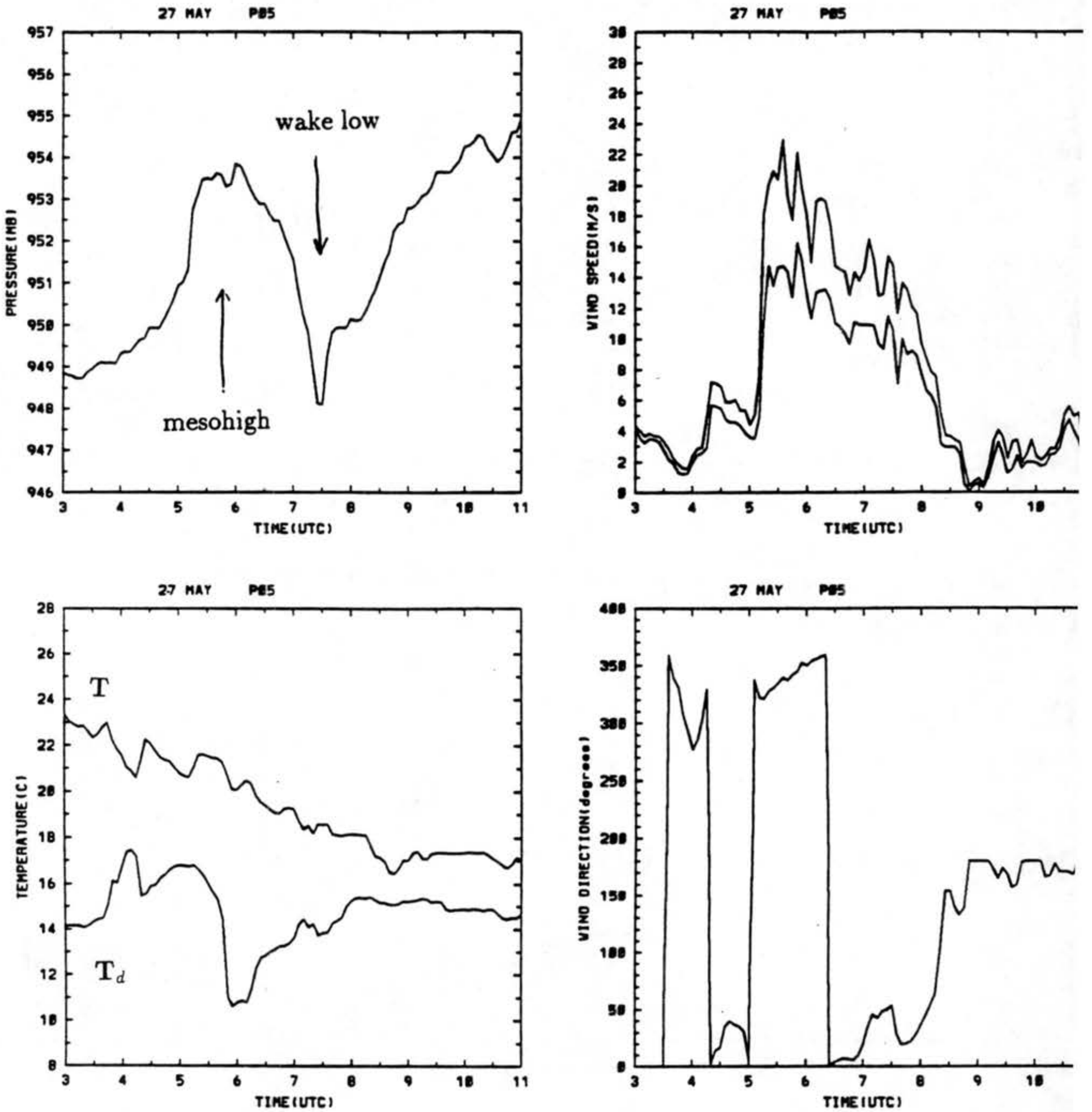

Figure 4.45: Same as Fig. 4.16 except for 27 May at station P05. Note different time scales as each tick mark represents 30 minutes.

from the northwest in the mesohigh to northeast druing the pressure fall, then back to the northwest in the pressure rise, and again back to the northeast with the second pressure decrease. At P05 the mesohigh (0510) was still sharp (5 mb increase in 2 hrs) with a 23 m s^{-1} wind gust and a shift to northwest flow. But here the wake low (0730) deepened considerably with a 5.5 mb drop in 25 minutes along with a shift to northeasterly flow and continued strong winds (16 m s^{-1}). Also at the time of lowest pressure there was a 0.5°C temperature (dewpoint) increase (decrease). This may be a weak "heat burst" feature. Johnson (1983) and Johnson et al. (1989) associate heat bursts with downbursts (Fujita 1985) initiated from the trailing stratiform cloud which penetrate through a shallow stable layer near the ground. A full examination of these features is beyond the scope of this study.

4.6 May 28 case

4.6.1 Synoptic conditions

The environmental situation associated with the initial development of this MCS is examined using the 0000 28 May maps. At the surface (Fig. 4.46a), a 1006 mb low was over the Ohio Valley with a cold front extending to the southwest to the Kansas-Oklahoma border, then a stationary front extended from the Oklahoma panhandle to the northwest along the Colorado Front Range. It was very warm and quite humid along both sides of the front, a southeast flow existed across Oklahoma, while north of the front in Kansas the flow was out of the east.

At 850 mb (Fig. 4.46b) there was a sharp trough extending southeastward from central Colorado into northwestern Texas. There was a moist tongue of air from central Texas north to western Nebraska. There was attendant weak flow from the southeast in western Nebraska and Oklahoma to a southwest flow in Texas. Extensive warm advection was occurring over western Nebraska. The winds at 700 mb (Fig. 4.46c) veered sharply over western Nebraska to westerly, and very dry air was here as well. A weak trough extended from eastern Montana south to eastern New Mexico. At 500 mb (Fig. 4.46d) a weak ridge was evident over Nebraska south to Oklahoma. A weak trough extended from

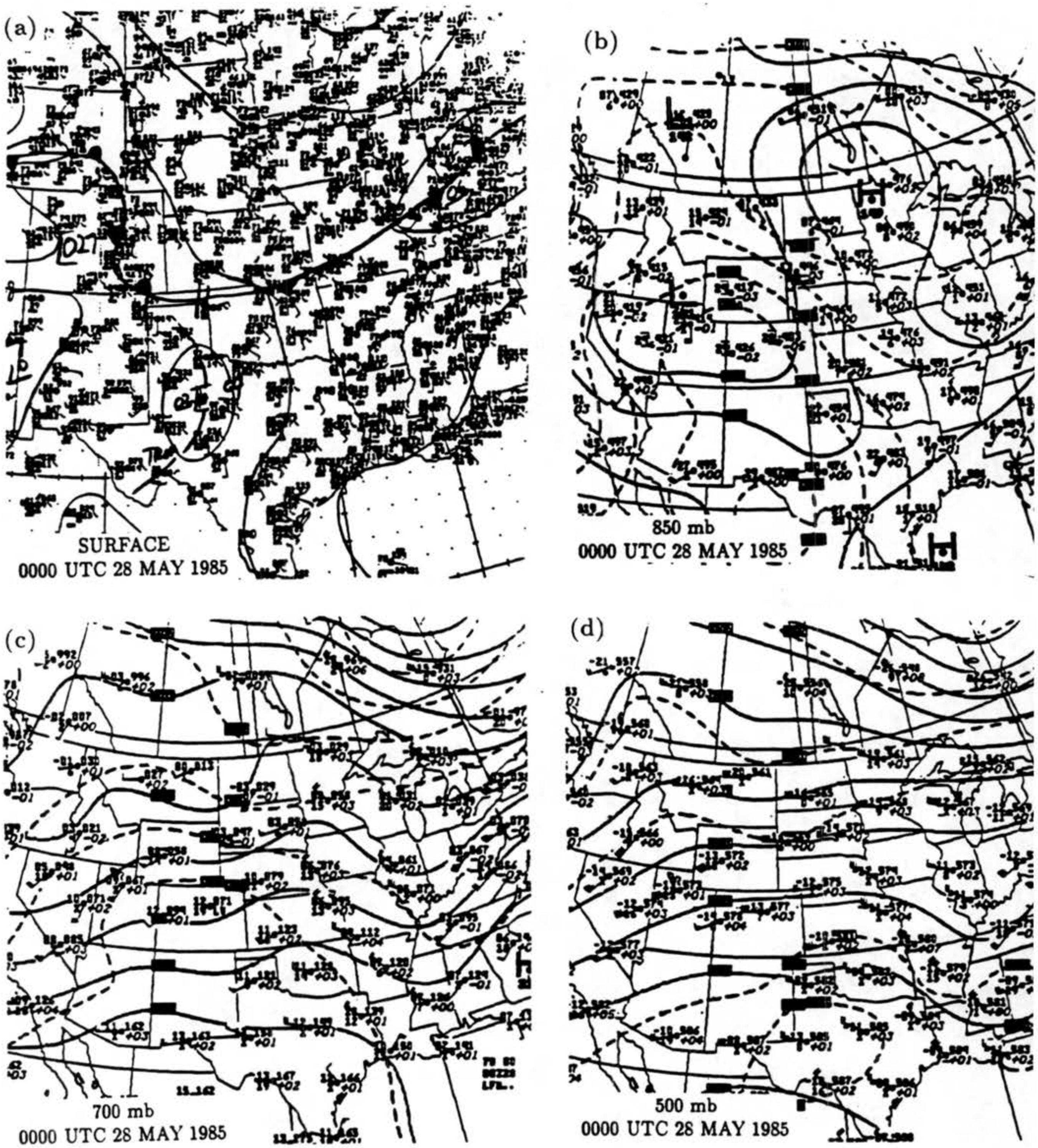

Figure 4.46: Same as Fig. 4.1 except for 0000 UTC 28 May at: a) Surface; b) 850 mb; c) 700 mb; d) 500 mb. Solid contours in c. represent geopotential height. Dashed contours in c. represent temperature in °C.

eastern Montana to eastern New Mexico. The flow was weak (10-15 m s^{-1}) and out of the west in western Nebraska and Kansas.

4.6.2 Radar overview

The initial development associated with this system occurred in the southwestern Nebraska panhandle as scattered intense cells around 2300 27 May (not shown). It took until 0930 (Fig. 4.47a) for the system to reach the PRE-STORM area. The system appeared to have a symmetric structure, with an enhanced area of stratiform precipitation behind the central portion of the system. By 1030 (Fig. 4.47b) the MCS began to take on more of a mixed symmetric/asymmetric structure. This was occurring partially due to the development of new convection along the southern flank of the MCS. Also there had been further development of weak stratiform rain on the north end of the MCS. The MCS became clearly asymmetric by 1150 (Fig. 4.47c) as the enhanced stratiform precipitation region was now confined to the northern portion of the system. By 1400 (Fig. 4.47d) the MCS developed more intense convection on its southern flank. Also within the stratiform precipitation region a hook-like feature appeared. By 1500 (Fig. 4.47e) the convective line started to dissipate, as had the hook-like feature in the stratiform precipitation region.

4.6.3 System overview

For this MCS there were no special soundings taken, hence the information given here leans heavily on the study of Houze et al. (1989) and their study of the Doppler data for this case.

Initial appearance in mesonet (0930)

All three pressure features were evident for the first time at 0930 (Fig. 4.48). A pre-squall low was found ahead of the system, and was deepest along the central portion of the system, where the strongest convection was at this time. A moderate outflow (5-10 m s^{-1}) and a very strong leading edge gradient indicate that a strong gust front was emanating from the system on its southern flank. A strong mesohigh was located behind the convective line, and a strong wake low was in the extreme northwest portion

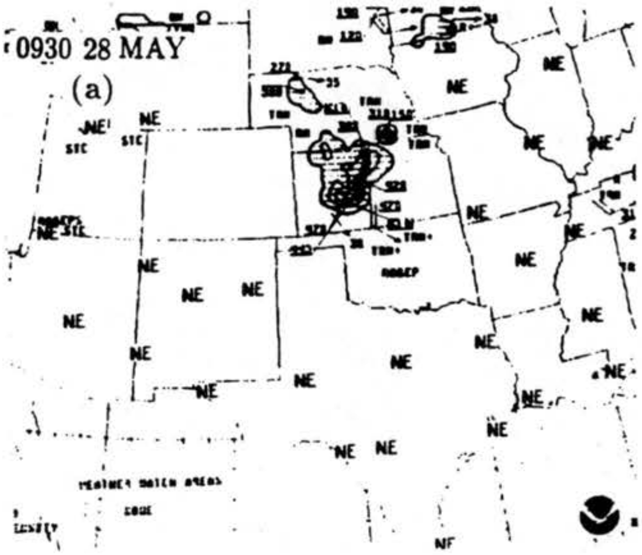

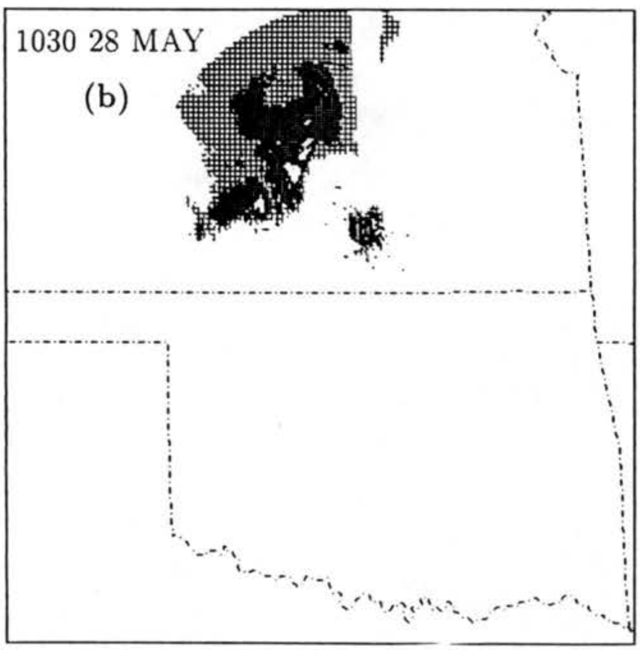

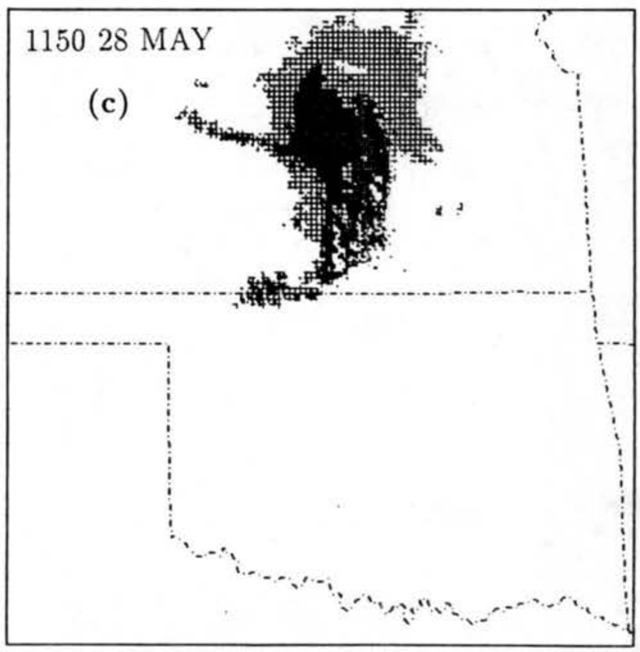

Figure 4.47: In a: NMC radar summary chart for 0930 UTC 28 May. In b-e: Same as Fig. 4.3 except for 28 May at: b) 1030 UTC; c) 1150 UTC; d) 1400 UTC; e) 1500 UTC. All using Wichita KS.

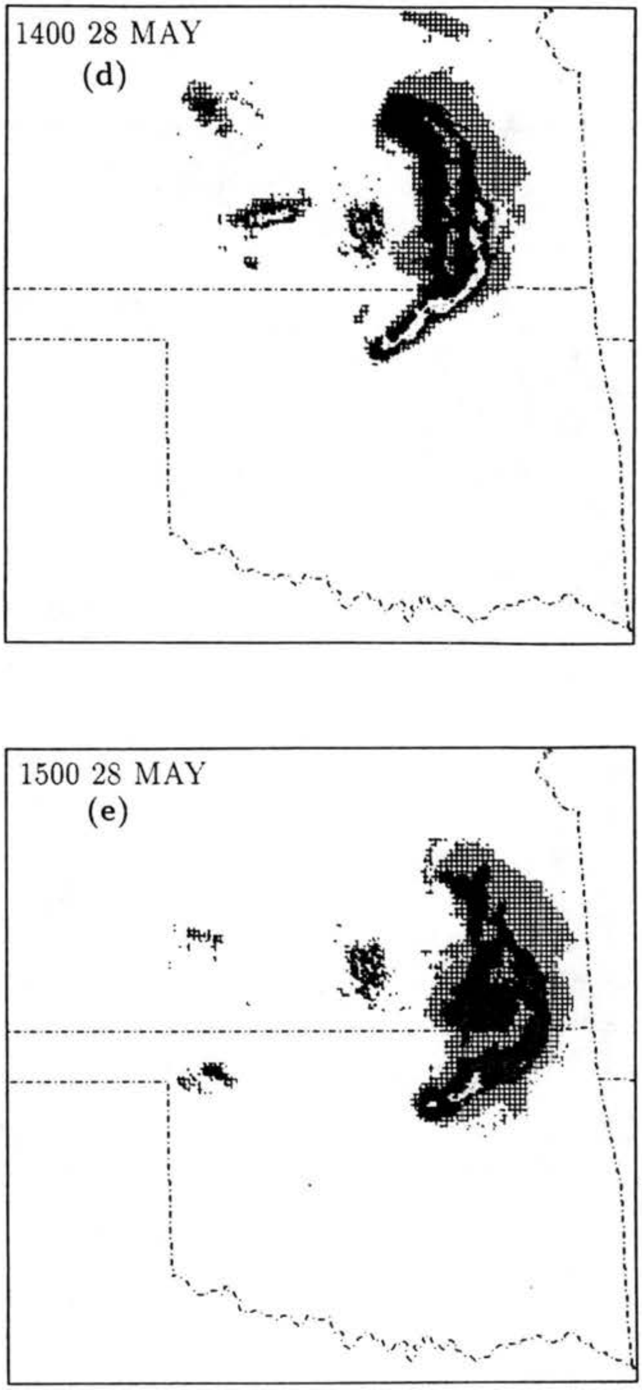

Figure 4.47: Continued.

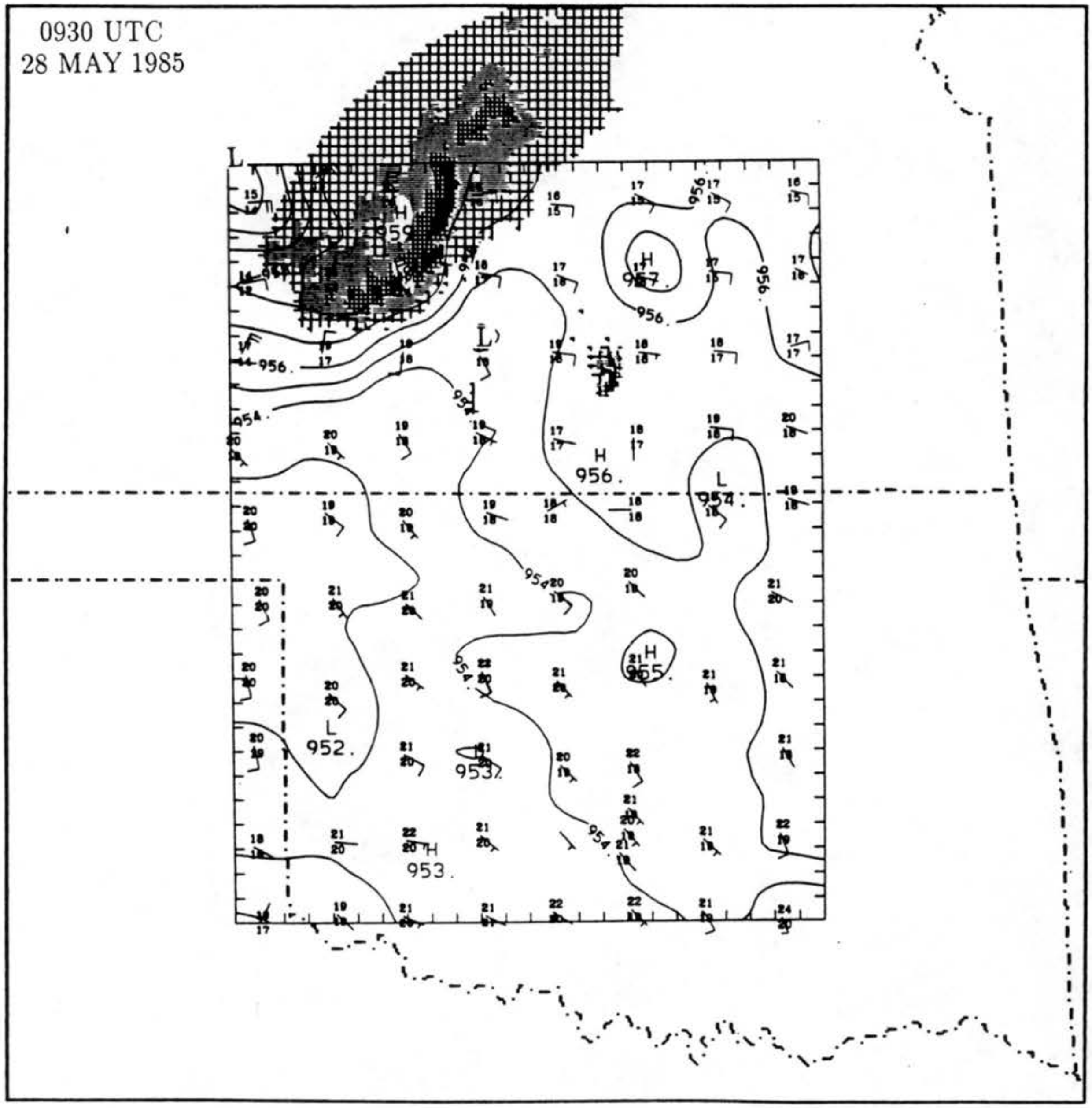

Figure 4.48: Same as Fig. 4.5 except for 0930 UTC 28 May.

of the network. The exact position of the wake low relative to the rest of the system is undetermined at this and most other times for this case due to the system being along the northern edge of the mesonet. At this time, however, it was felt to be positioned along the back edge of the stratiform precipitation region to the rear of the central portion of the system, due to the symmetric nature of the system (as shown with the NMC radar summary map in the radar section).

Development of accentuated pressure gradient (1030)

The strong gradient along the leading edge of the southern portion of the system was still evident, as was the strong outflow from the system (Fig. 4.49). The mesohigh split and maintained constant intensity, with two southern centers over the intense convective cells and the northern one within the stratiform region. The wake low deepened by 1 mb and an accentuated gradient developed along the trailing edge of the enhanced stratiform region. The wake low itself was along the back edge of the weak stratiform precipitation.

Additional convective development (1200)

The radar plot here is 10 minutes prior to the surface data (Fig. 4.50). The mesohigh in the central portion of the system strengthened by 2 mb. Also notice that new convection developed along the leading edge of the outflow from the system, much like that occurring with the 27 May case. There was quite strong convergence here with 5-7.5 m s^{-1} southerly flow to the south and 5-10 m s^{-1} northerly outflow from the system. There was divergence occurring to the rear of the mesohigh in the northern part of the system. At this time the wake low had either weakened considerably, moved between stations [2] or moved slightly north of the mesonet. But there was still 10 m s^{-1} easterly flow through the low.

Mesovortex appearance (1300)

At this time (Fig. 4.51), the wake low returned to the mesonet and deepened by 1

---

[2]When these pressure features are in between reporting stations for a 10-20 minute period, even with the use of the five-minute data at the stations, the features will not be captured fully by this method. Hence, they may appear to "dissappear" for a time.

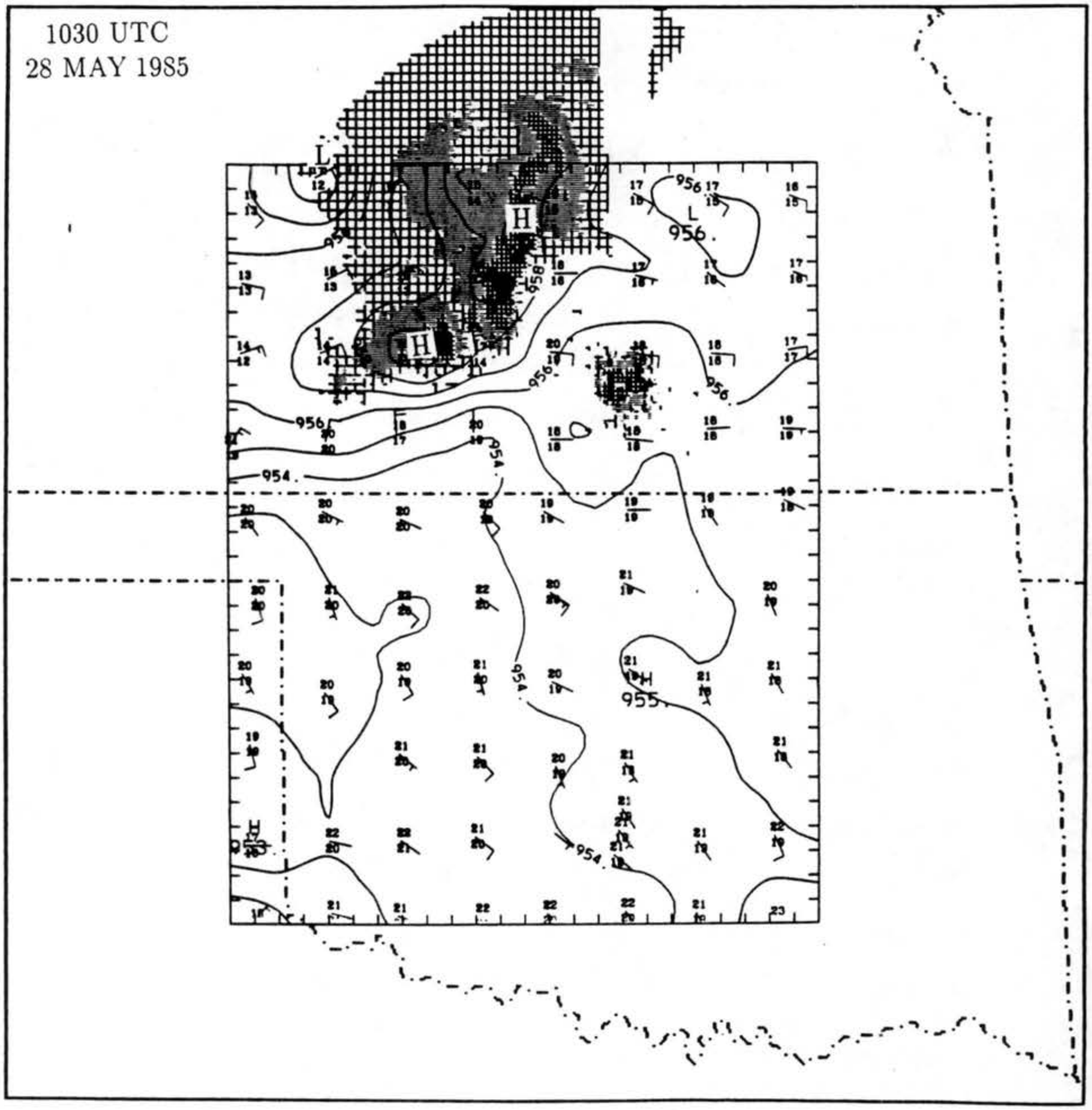

Figure 4.49: Same as Fig. 4.5 except for 1030 UTC 28 May.

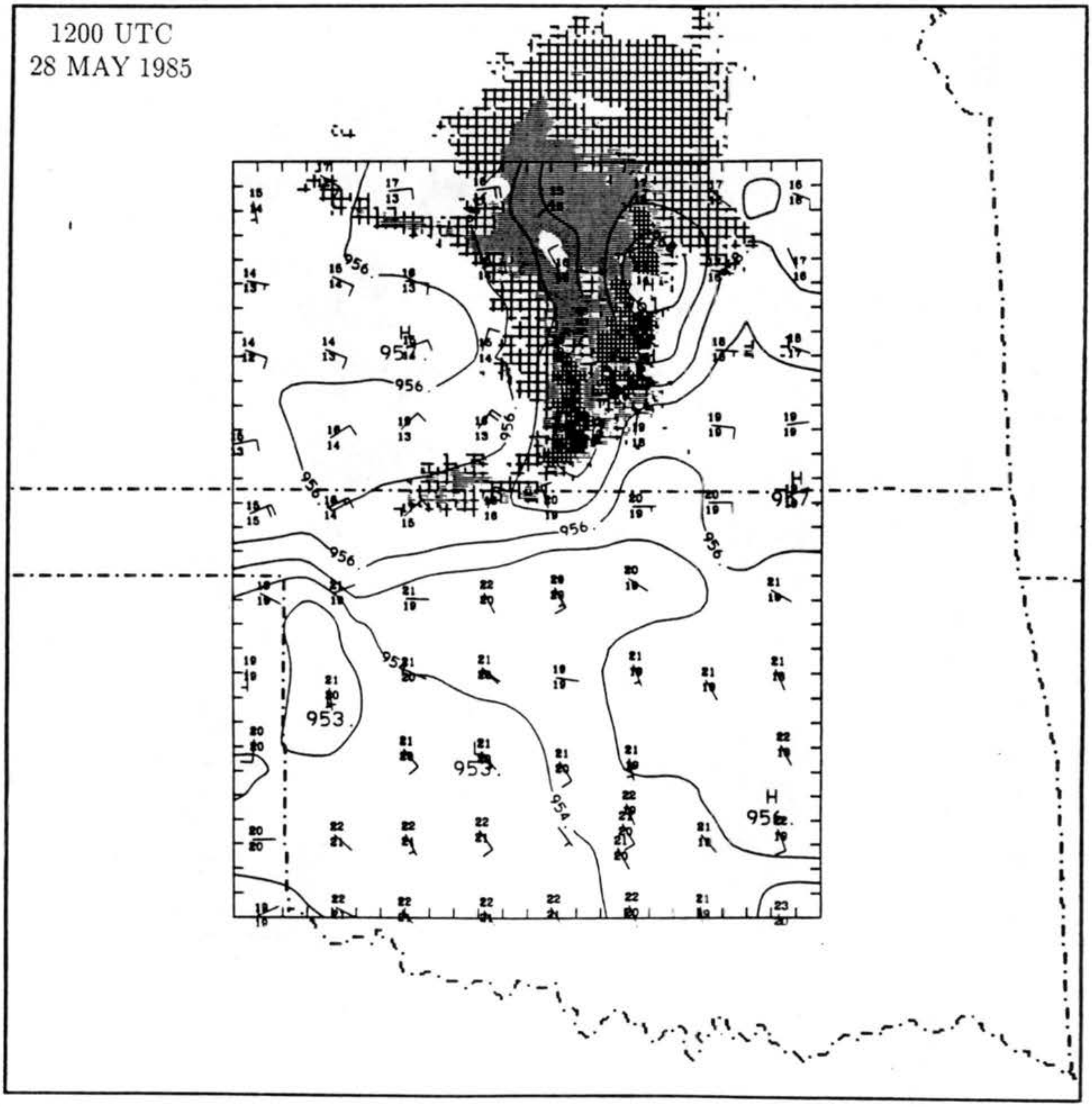

Figure 4.50: Same as Fig. 4.5 except for 1200 UTC 28 May.

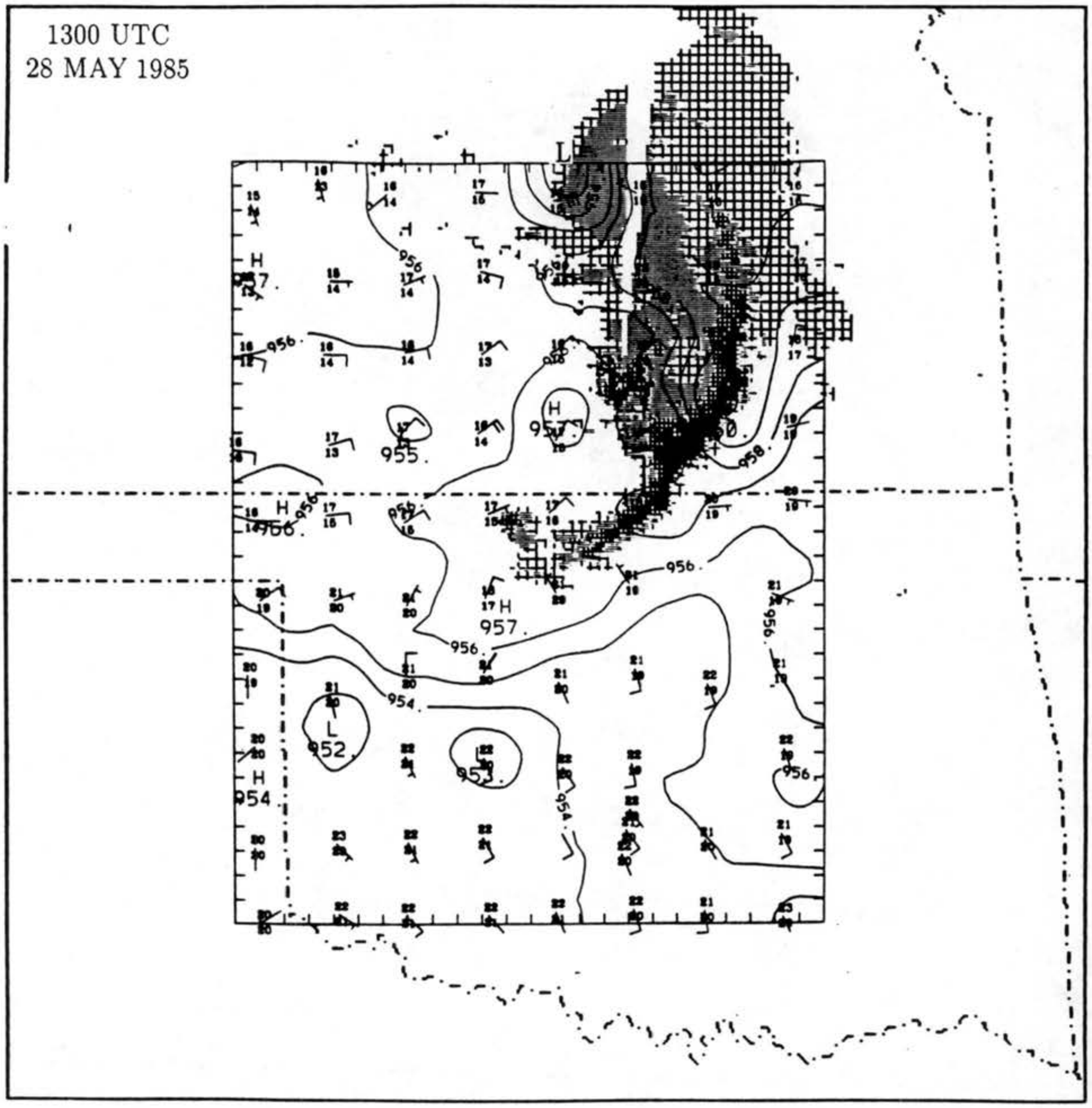

Figure 4.51: Same as Fig. 4.5 except for 1300 UTC 28 May.

mb since it last was there. It was positioned along the back edge of the core of enhanced stratiform precipitation. As the gradient increased there was a strong flow through the low of 15 m s^{-1}. There was no hint of a vortex circulation at the surface. A second, much weaker wake low developed to the rear of the enhanced stratiform precipitation area behind the center of the line. Strong divergence was still present behind the mesohigh.

Houze et al. (1989) examined dual-Doppler radar data for this case at 1308. They found that a 10 m s^{-1} system-relative rear inflow jet was present as the southern branch of a mesoscale cyclonic vortex. The mesovortex had a closed cyclonic circulation at the rear of the stratiform region, and it extended from the lowest level they observed (1.4 km) to approximately 8 km. They also observed that the mesovortex led to changes in the reflectivity pattern, particularly the development of hook-like features.

Intense wake low (1400-1500)

The wake low was at its deepest point at 1400 (Fig. 4.52) with another 2 mb drop in pressure. It was found in the far northwest portion of the system. There continued to be 15 m s^{-1} flow through the low. There was also a region of strong gradient in the transition region. The low to the rear of the central portion of the enhanced stratiform precipitation region was also still present. Note also the hook-like feature in the northern portion of the stratiform region. This was presumably due to the airflow structure of the mesovortex. By 1500 (not shown) the mesohigh started to weaken, leading to a reduction in the gradient and a lowering of the wind speed.

4.6.4 Mesonet time series

Stations P05 (Fig. 4.53, see Fig. 3.1) and P06 (Fig. 4.54) are examined to discover the conditions associated with the system. At P05 the mesohigh (1010) was accompanied by a 3 mb increase in 30 minutes, a 1°C temperature and dewpoint drop, a 14 m s^{-1} wind gust as well as a shift from east to northwest flow. The wake low (1300) passed by a couple of hours after the mesohigh and was accompanied by a 6 mb drop in 30 minutes, a 0.5°C temperature (dewpoint) increase (decrease), a shift from northwest to east flow, as well as a 20 m s^{-1} wind gust. The tempertaure/dewpoint signature again may have been

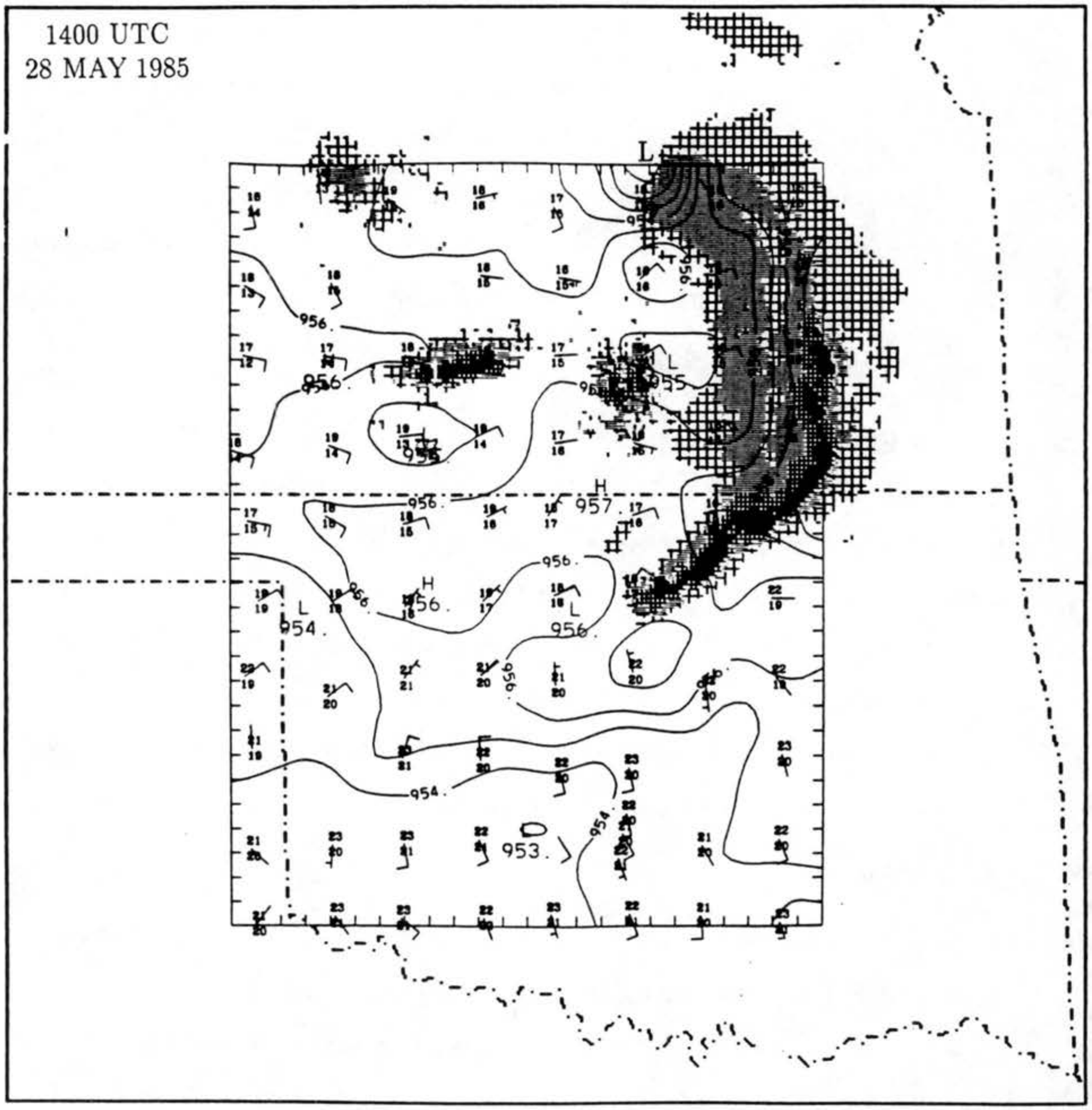

Figure 4.52: Same as Fig. 4.5 except for 1400 UTC 28 May.

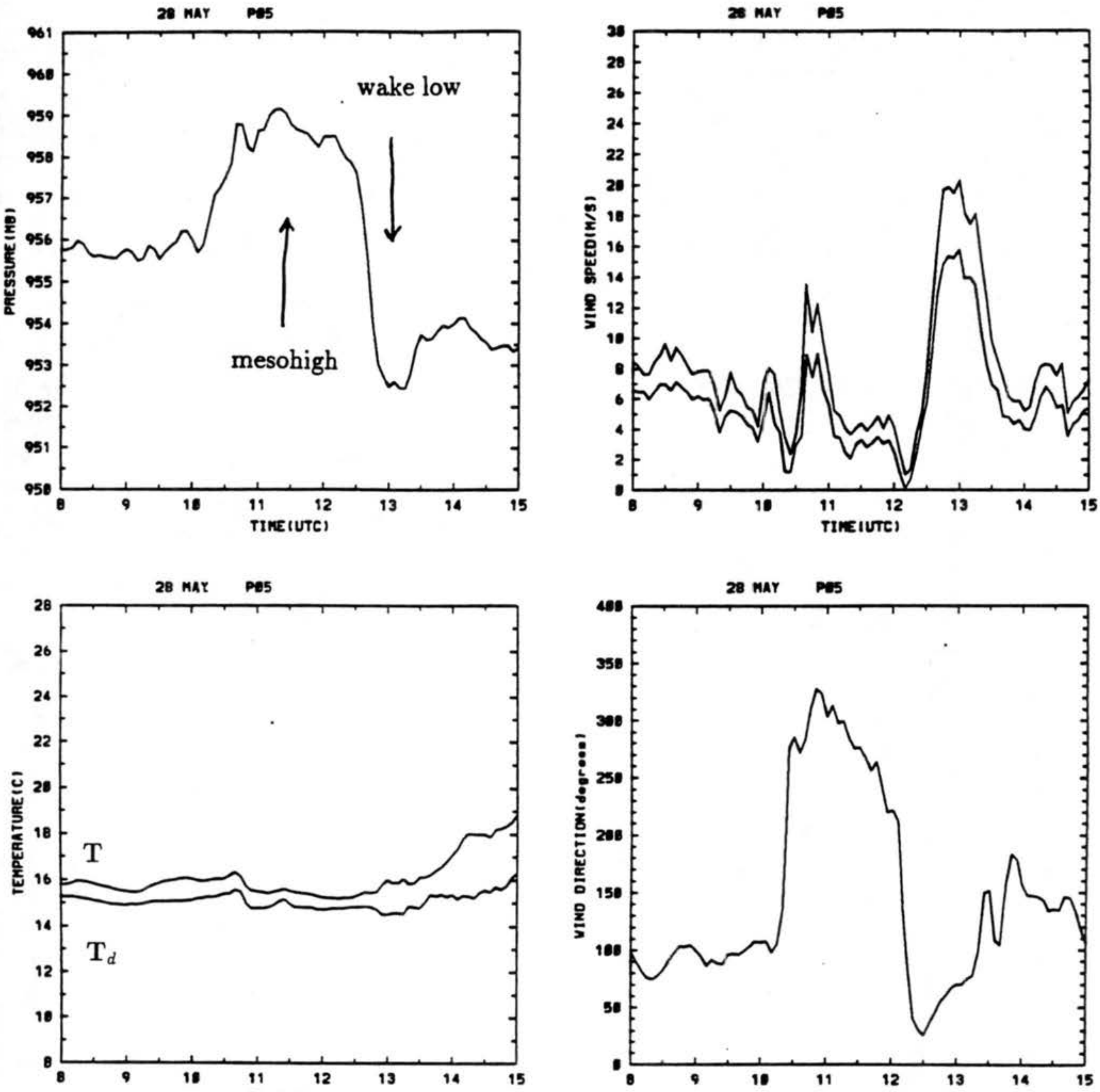

Figure 4.53: Same as Fig. 4.16 except for 28 May at station P05. Note different time scale as each tick mark represents 30 minutes.

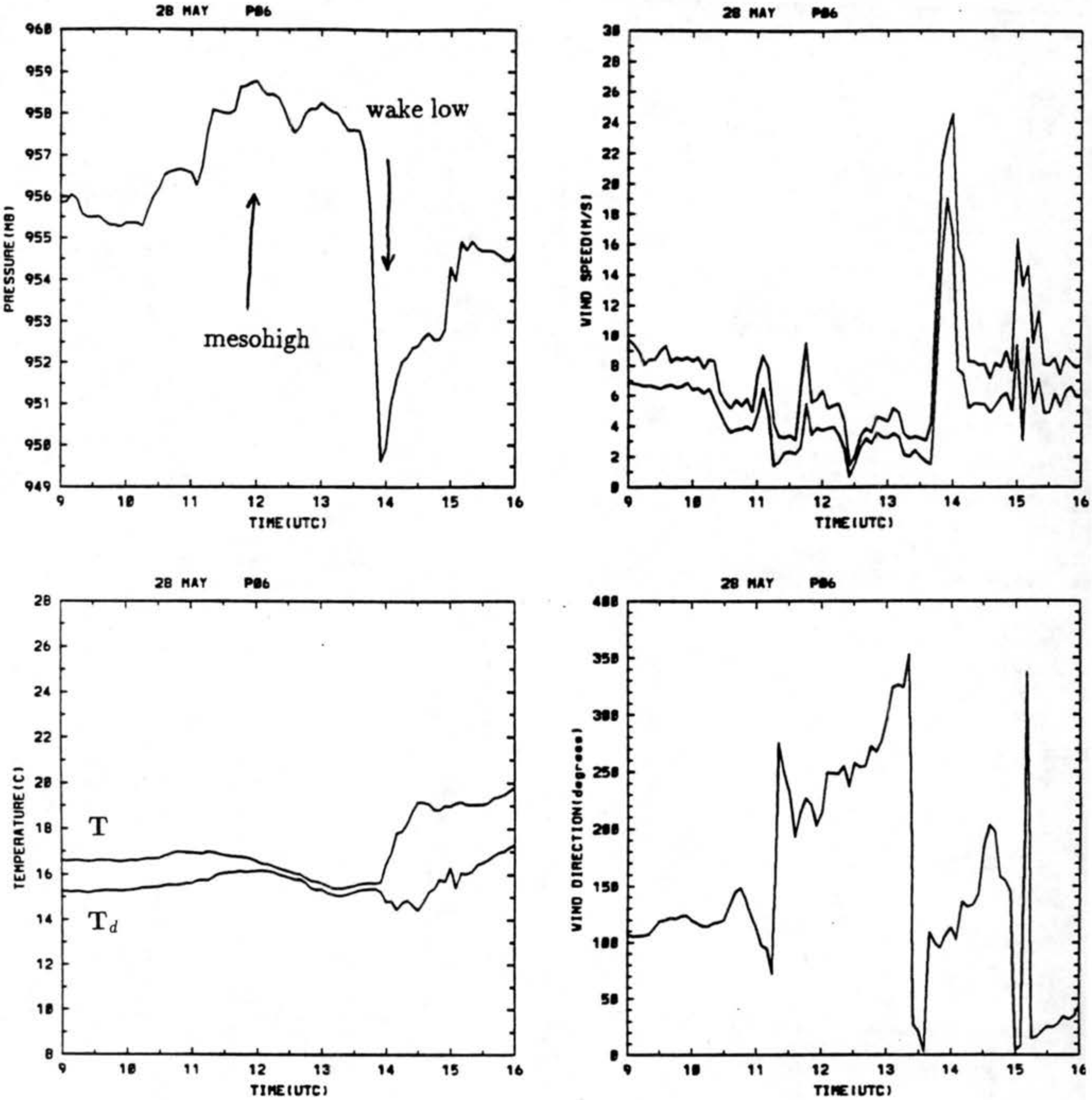

Figure 4.54: Same as Fig. 4.16 except for 28 May at station P06. Note different time scale as each tick mark represents 30 minutes.

associated with a weak heat burst type event. At P06 the mesohigh (1100) was about the same strength as it was at P05, although it did not have the attendant strong winds nor the sharp temperature/dewpoint drop off. The wake low (1400) was 3 mb deeper and had a 8 mb drop in 15 minutes, the second largest gradient observed during PRE-STORM. It also had a 25 m s^{-1} wind gust, and a shift from north to east flow.

4.7 May 29 case

4.7.1 Synoptic situation

The conditions associated with the initial development of the MCS are seen at 0000 29 May. At the surface (Fig. 4.55a), a 999 mb low was over southeastern North Dakota, with a weak cold front extending through northwestern Nebraska into northern Colorado. A dry line was present across western Kansas into the Oklahoma and Texas panhandles. Southeasterly flow was across the PRE-STORM area.

At 850 mb (Fig. 4.55b) a sharp trough was seen from eastern Wyoming to eastern Colorado and western Texas. A moist tongue of air extended from central Texas north to South Dakota, with a strong south to southeast flow of 10-15 m s^{-1} across Nebraska and South Dakota. Warm advection was evident across Kansas, Nebraska, and South Dakota. At 500 mb (Fig. 4.55c) the region from South Dakota to Texas was under a weak ridge. A weak short wave trough was in central Wyoming and eastern Colorado.

The synoptic conditions just before the MCS entered the PRE-STORM area are indicated by the 1200 29 May maps. At the surface (not shown) the conditions were quite similar to the 0000 conditions. At 850 mb (Fig. 4.56a) the main trough rotated to the northeast and was centered in north-central North Dakota, but a weak trough was still extending through the Kansas-Colorado border to western and central Texas. Just ahead of the system at DDC and OMA a strong low-level jet developed, streaming in very warm and moist air. This was more evident within the PRE-STORM area (Fig. 4.56b) with all of Kansas covered by dewpoints greater than 15°C. At 500 mb (Fig. 4.56c) the trough was only weakly visible from North Dakota to Nebraska.

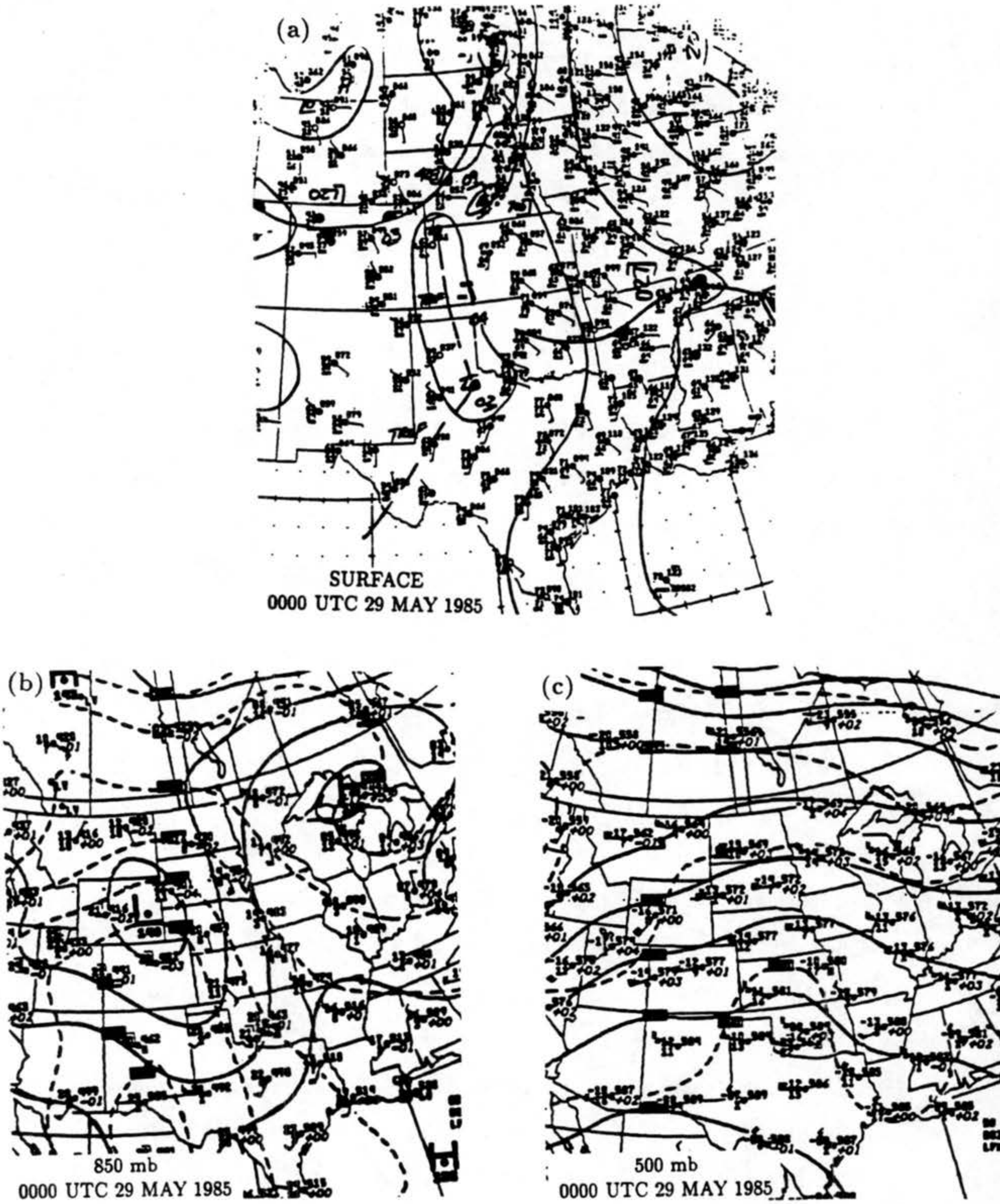

Figure 4.55: Same as Fig. 4.1 except for 0000 UTC 29 May.

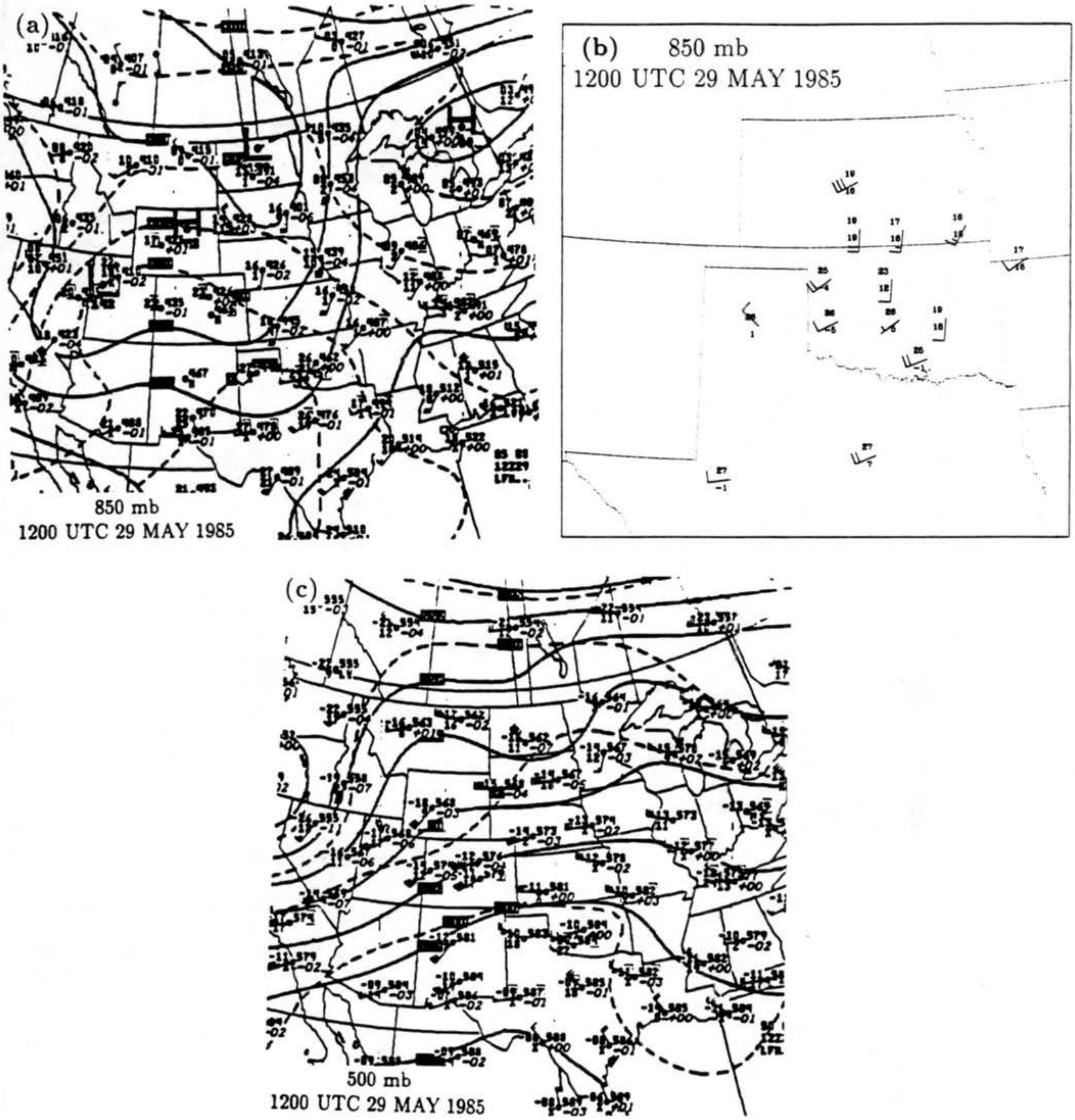

Figure 4.56: For a. and c.: Same as Fig. 4.1 except for 1200 UTC 29 May at: a) 850 mb; c) 500 mb. For b.: Same as Fig. 4.2 except for 1200 UTC 29 May at 850 mb.

4.7.2 Radar overview

The initial convection associated with this MCS developed in the extreme southwestern panhandle of Nebraska to the south of several convective systems in the Dakotas at 0130 (not shown). By 0530 (Fig. 4.57a) it developed into a symmetric-type system (recognizing the deficiences in the NMC radar analysis) with a leading convective line and a trailing stratiform region located behind the center of the line, and was on the southern end of a dissipating area of convection to its north. By 0930 (not shown) it continued to move southeast into south-central Nebraska and north-central Kansas and weakened considerably. Stratiform precipitation now seemed to be tending more to the north side of the MCS.

By 1410 (Fig. 4.57b) it restrengthened and moved into range of the Wichita radar. The stratiform precipitation at this time was limited in extent and was located on the northern portion of the MCS. At 1610 (Fig. 4.57c) it can be seen that the convective line was continuing to build on its southern flank, while a more well developed stratiform area formed to the rear of its northern end, giving this system its strongly asymmetric features. By 1740 (Fig. 4.57d) the stratiform area expanded and was now to the rear of the central portion of the MCS as well, but it was still mostly on the northern end. Also the strongest convection was still building on its southern flank.

4.7.3 System overview

Unfortunately, this MCS was not well covered by either the surface or upper-air data. No special soundings were taken while the MCS was within the network and it brushed the northeast corner of the mesonet. It was felt, however, that enough of the pressure structure was observed for the MCS to be included here.

MCS in mesonet (1500-1630)

The first time all pressure features were visible was at 1500 (Fig. 4.58). There was a weak pre-squall low ahead of the convective line, as well as a mesohigh along and just behind the convective line. Also, there was the suggestion of a wake low, but the stratiform precipitation area as well as the wake low are of outside the network. The flow features

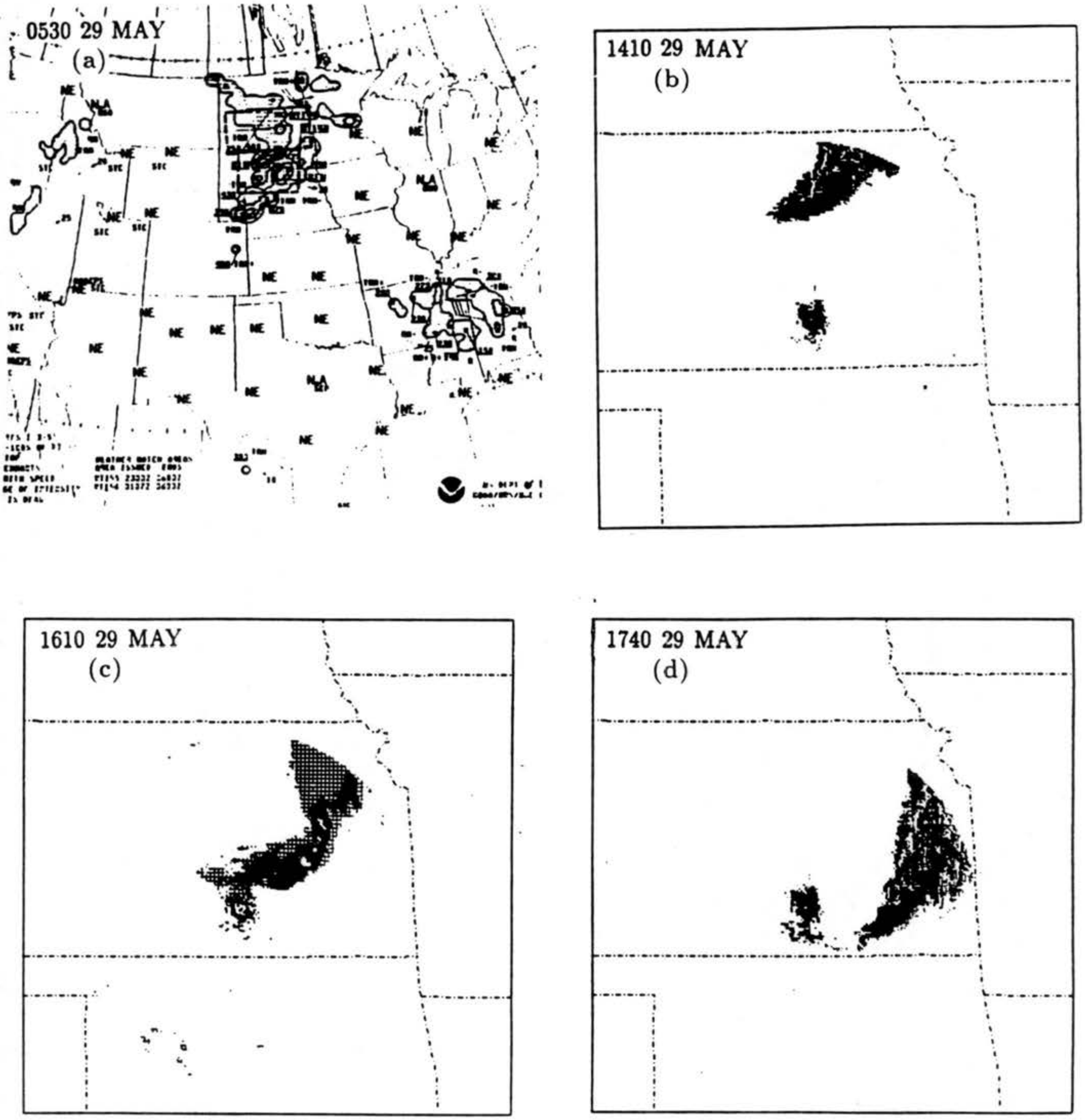

Figure 4.57: In a. NMC radar summary chart for 0530 UTC 29 May. In b-d. Same as Fig. 4.3 except for 29 May at: b) 1410 UTC; c) 1610 UTC; d) 1740 UTC. All using Wichita KS.

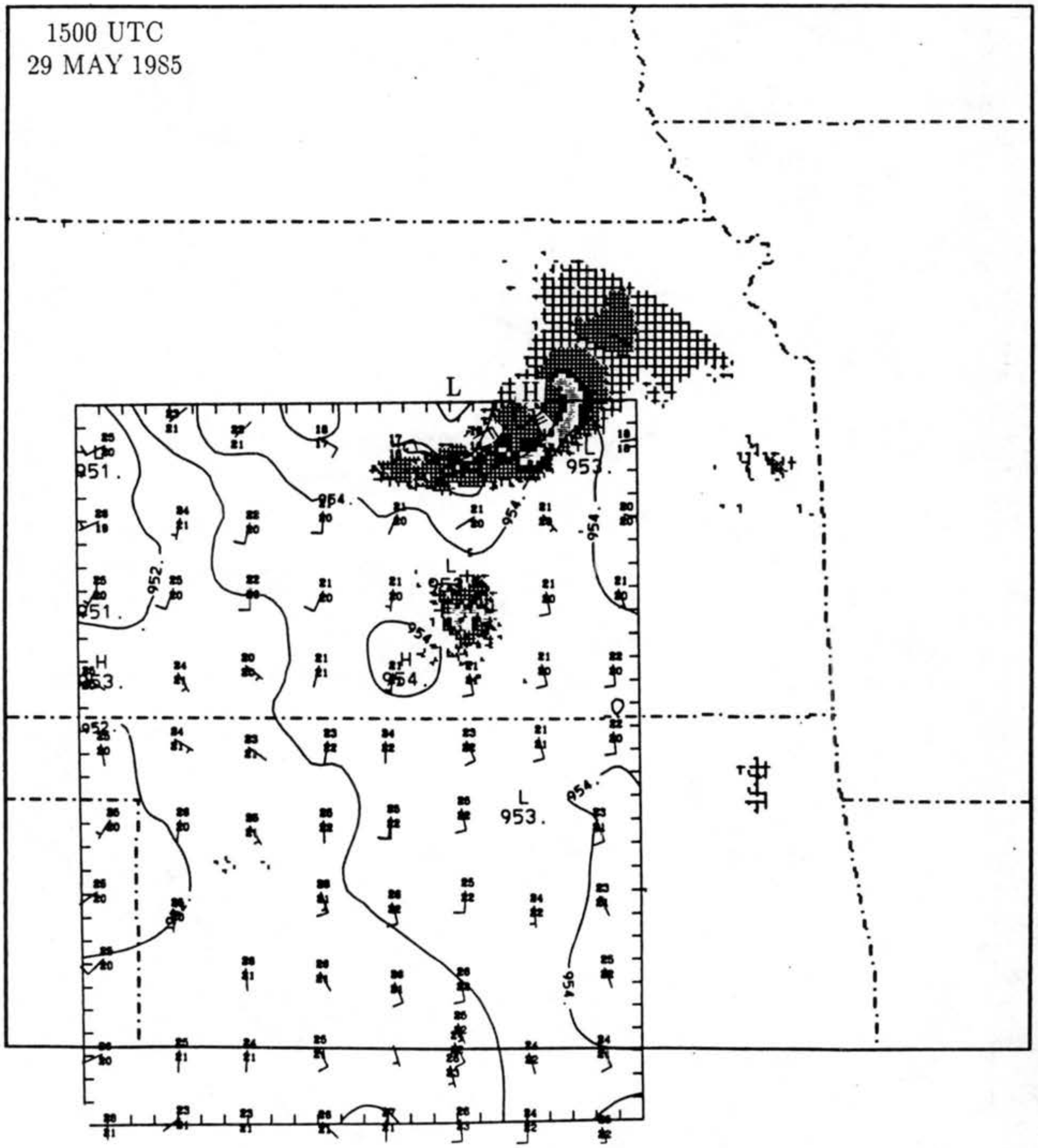

Figure 4.58: Same as Fig. 4.5 except for 1500 UTC 29 May.

were a southerly to southeasterly flow ahead of the system, a strong outflow from the convection (10 m s^{-1}), strong divergence to the rear of the mesohigh, and strong flow through the wake low (10 m s^{-1}). By 1600 (Fig. 4.59) the wake low became visible in the northern part of the network behind the northern part of the convective line and the southern tip of the stratiform area. As the stratiform area approached the mesonet, the gradient tightened considerably. Also note the intense divergence occurring to the rear of the mesohigh with 7.5 m s^{-1} easterlies in the wake low and 15 m s^{-1} northwesterlies in the mesohigh. The 1630 plots (Fig. 4.60) also tended to support the placement of the wake low as the low was now definitely positioned somewhere along the back edge of the stratiform precipitation area to the north of the mesonet, since as the stratiform precipitation area was moving across the northeast portion of the mesonet, the wake low was moving along with the back edge of it.

4.7.4 Mesonet time series

The best station to view the wake low is the station in the far northeast part of the mesonet, P08 (Fig. 4.61, see Fig. 3.1). The mesohigh (1600) was quite sharp, with a 4 mb increase in 15 minutes, a 3°C temperature and dewpoint drop, a shift from east to northwest flow and a 28 m s^{-1} wind gust. Then there was a sharp 6.5 mb drop in 15 minutes (1620), a wind shift back to the east and a 22 m s^{-1} wind gust. But this station still did not get the full effect of the wake low since it passed to the north and to the east of it, but due to the sharp pressure drop even in this position, this was probably a very intense wake low case.

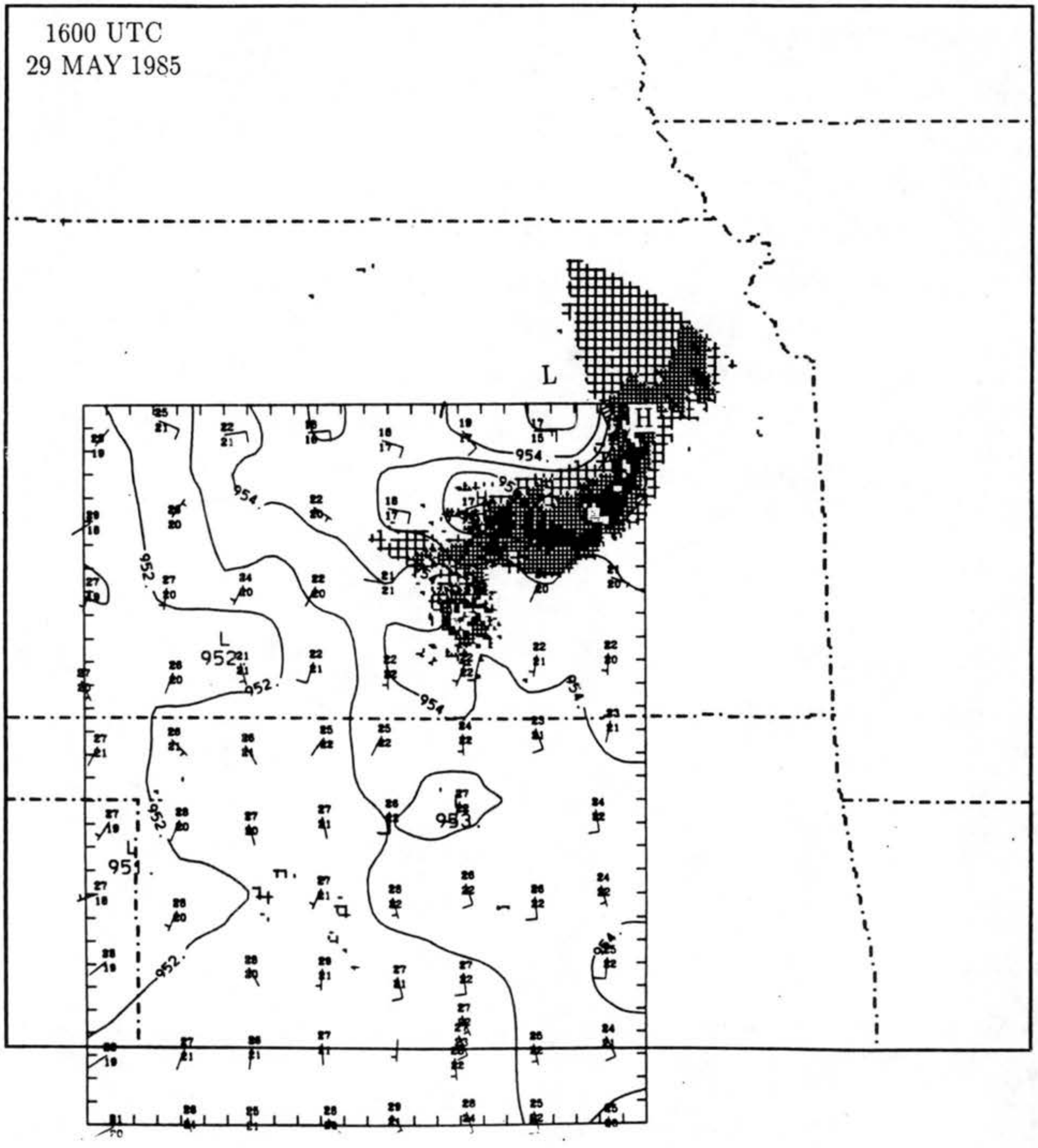

Figure 4.59: Same as Fig. 4.5 except for 1600 UTC 29 May.

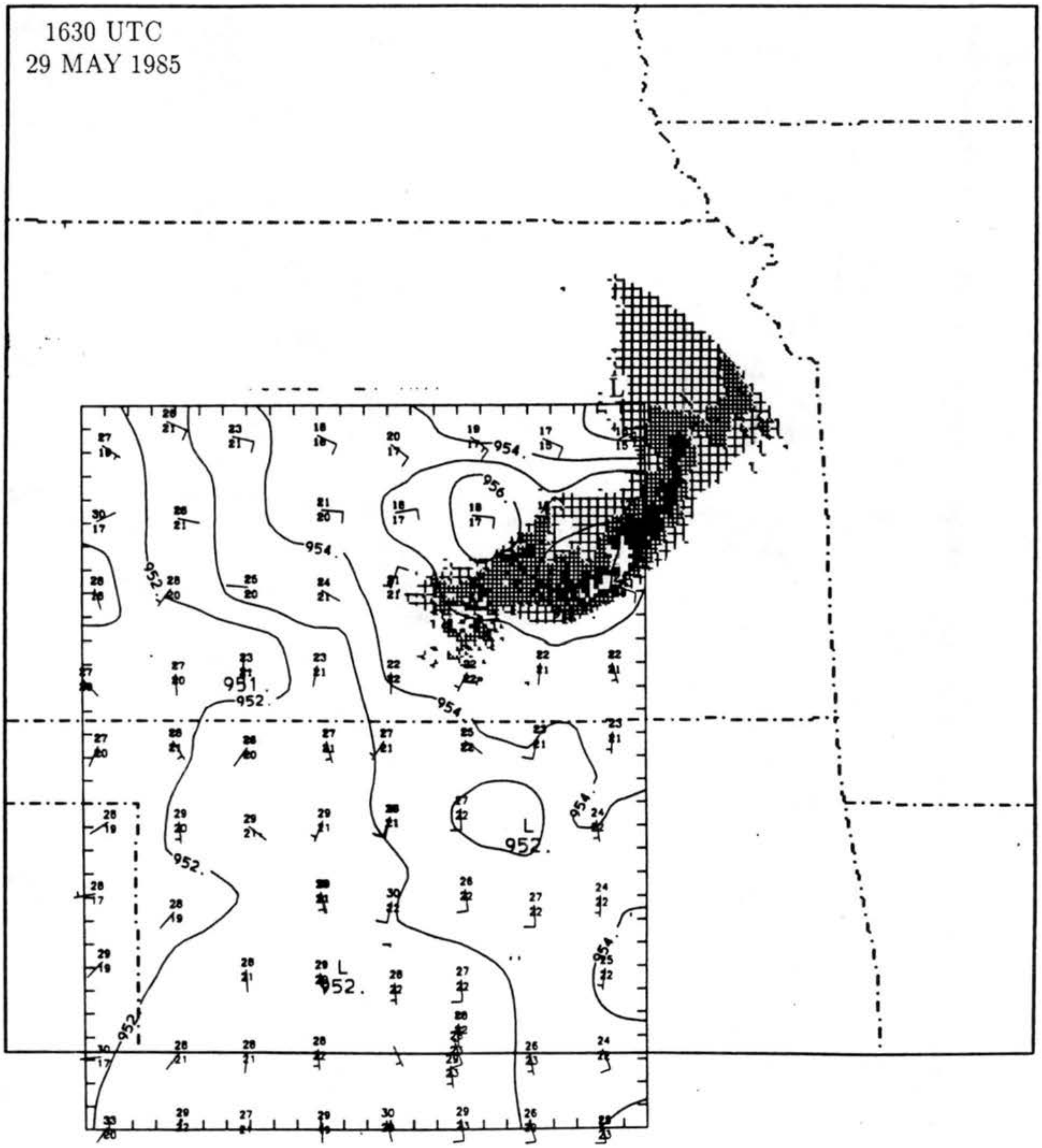

Figure 4.60: Same as Fig. 4.5 except for 1630 UTC 29 May.

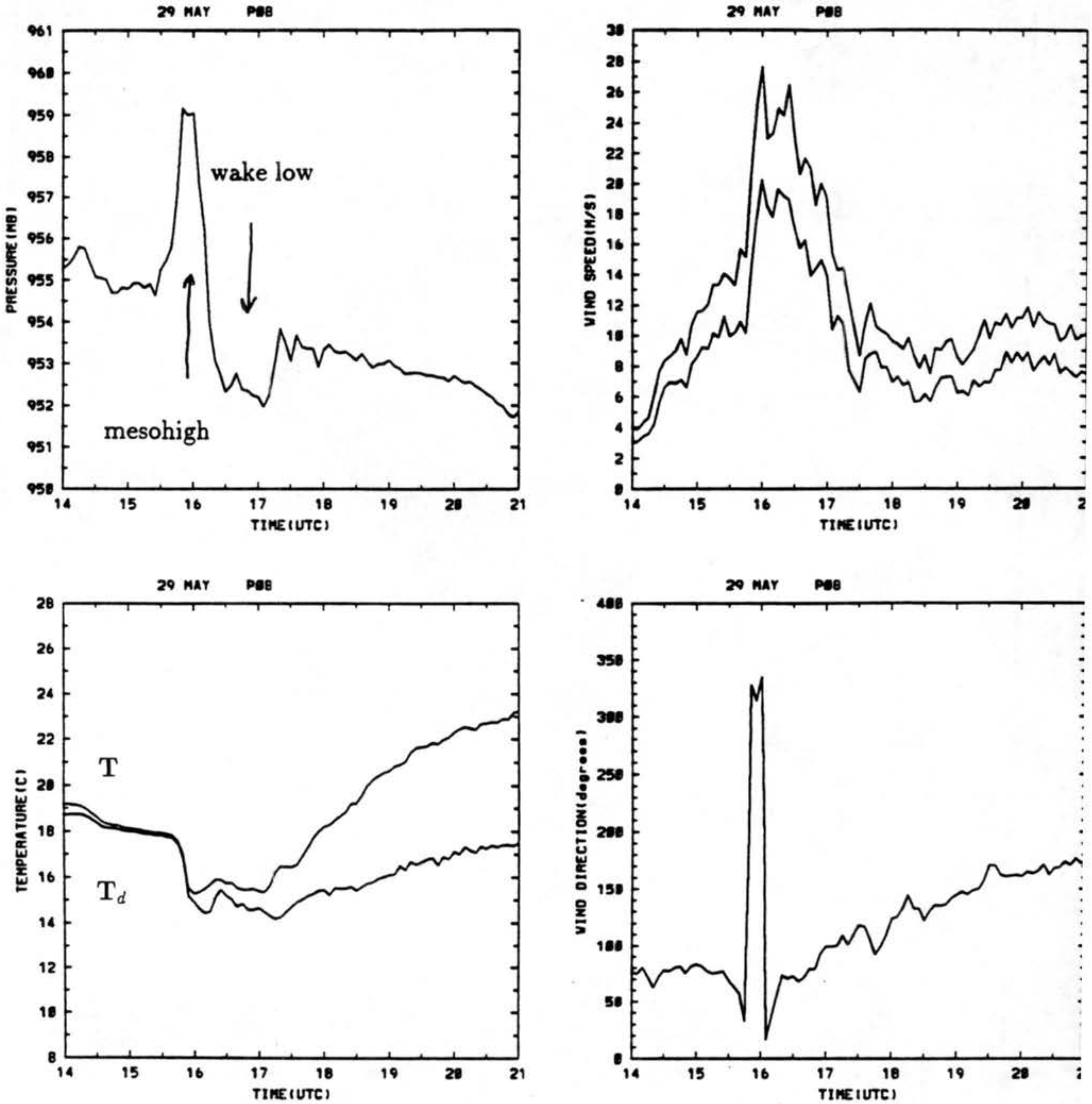

Figure 4.61: Same as Fig. 4.16 except for 29 May at station P08. Note different time scale as each tick mark represents 30 minutes.

Chapter 5

MCS CASES: JUNE 1985

5.1 Introduction

During the month of June 1985, nine separate MCSs passed through the PRE-STORM network. These cases occurred on 3, 3-4, 4, 9, 11, 15, 22, 24, and 26-27 June. Several other systems occurred during this period, but were not adequately observed by the intensive PRE-STORM network. These included cases on 10, 16-17, 22 (eastern system), and 24 (eastern system) June. Each of these systems developed along the periphery of the mesonet and it could not be determined if the features of interest here, particularly the wake low, existed with these systems.

The purpose of this chapter is to give an overview of each of the nine major systems. The synoptic situation leading to the development of the MCSs, the radar reflectivity structure, the surface pressure and ground-relative flow features, the system-relative upper air flow, as well as time series of the mesonet data are examined.

5.2 June 3 case

5.2.1 Synoptic situation

The environmental conditions associated with the development of this MCS are summarized with the 1200 3 June maps. At the surface (Fig. 5.1a) a stationary front extended from northeastern Oklahoma southwest to the Texas panhandle. The temperatures were 22-25°C to the south of the front, with dewpoints of 18-21°C (except in western Texas where they were 12-15°C) and a south-southeast flow of 5 m s^{-1}. To the north of the front the temperatures were 12-18°C, the dewpoints were 7-15°C and there was a northeast flow.

At 850 mb (Fig. 5.1b) a weak trough extended from the Texas panhandle to western Oklahoma, as the winds were cyclonically curved from northern Texas to Kansas. There

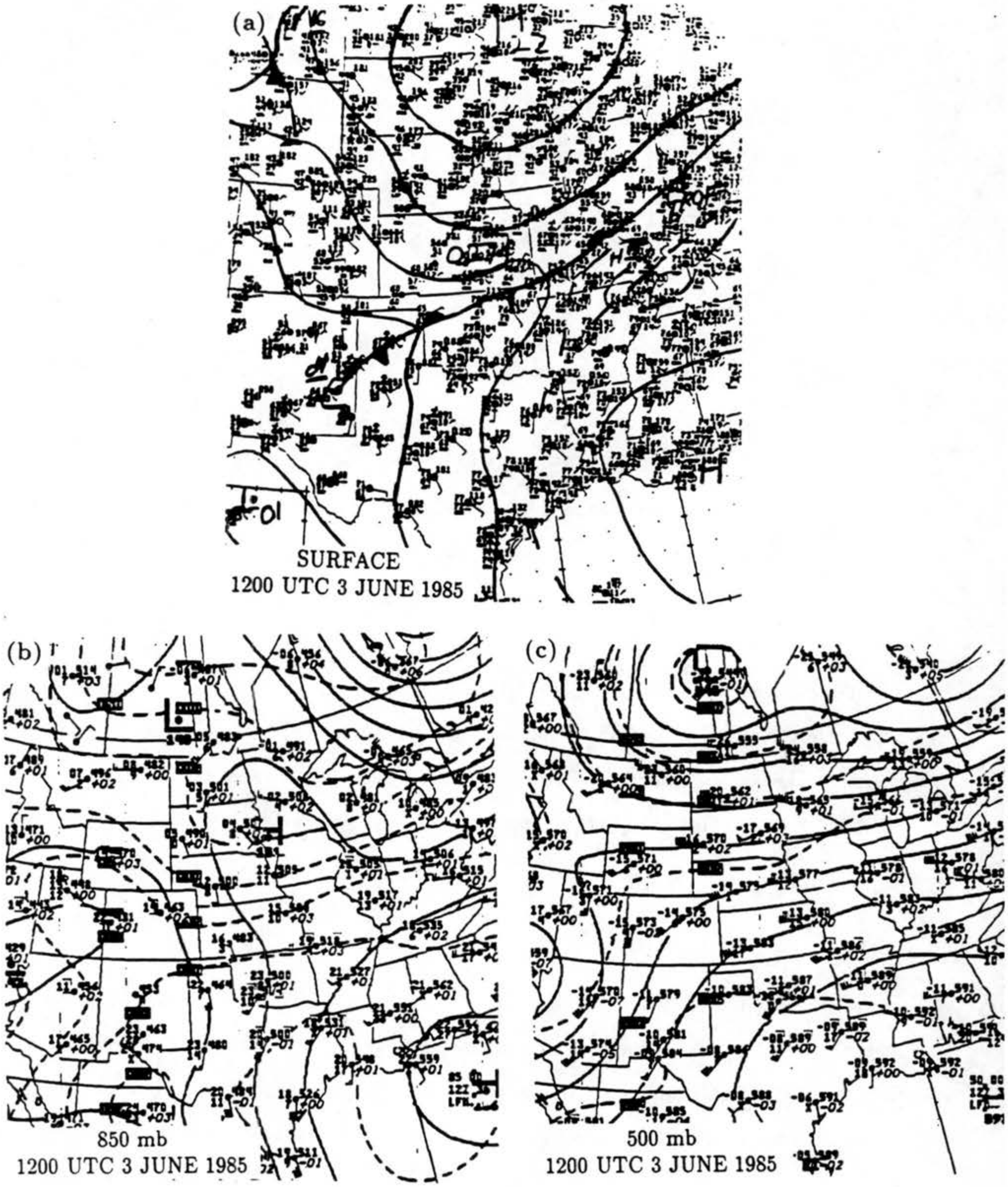

Figure 5.1: 1200 UTC 3 June 1985 NMC analyses: a) surface; b) 850 mb; c) 500 mb. Solid contours represent: in a. sea-level pressure and in b. and c. geopotential height. Dashed contours in b. and c. represent temperature in °C.

was a strong (8-15 m s^{-1}) southerly flow from Texas north to southwestern Kansas. A tongue of very moist air with dewpoints exceeding 10°C extended from western Texas north to Oklahoma and western Kansas. Significant warm advection was occurring over western and central Kansas. At 500 mb (Fig. 5.1c) a ridge was present over the south-central and southeastern U.S. with the flow being strongly anticyclonically curved over Kansas and Oklahoma. The flow was out of the west to southwest at 10-20 m s^{-1}. A deep closed low was centered over southern California.

5.2.2 Radar overview

The initial development of convection associated with this system occurred around 1230 (not shown) in southwestern Kansas, just to the north of the surface front and within the area of strong 850 mb warm advection. By 1330 (Fig. 5.2a) the convection moved within the radar range and was characterized by its small size and several disorganized convective precipitation cores. Stratiform precipitation was non-existent at this time. By 1520 (Fig. 5.2b) there were three separate cores of convection along the northern and eastern flanks of the system. These areas of convection were diverging, as the northern cell moved towards the north, whereas the remainder of the system moved more to the northeast. This divergent movement of the areas of convection was leading to an expansion in the areal coverage of the MCS. The northern convection was more intense than the southern convection at this time. Stratiform precipitation started to fill in the central portion of the MCS, but its areal coverage was still quite small. By 1630 (Fig. 5.2c) the expansion of the MCS became more obvious, mostly due to the northerly movement of the northern area of convection. The area of stratiform precipitation expanded to fill the space between the convection and, as well, there was the development of a fairly large area of enhanced stratiform precipitation. Just to the west of this enhanced core there was the development of a rear echo notch feature. By 1800 (Fig. 5.2d) the structure of the MCS had changed dramatically. The areas of convection on the northern and eastern sides of the system had nearly completely dissipated. Conversely, the convection on the southern end of the system rapidly intensified. This development tended to give the impression that the system had evolved from largely random convection into an asymmetric-type system,

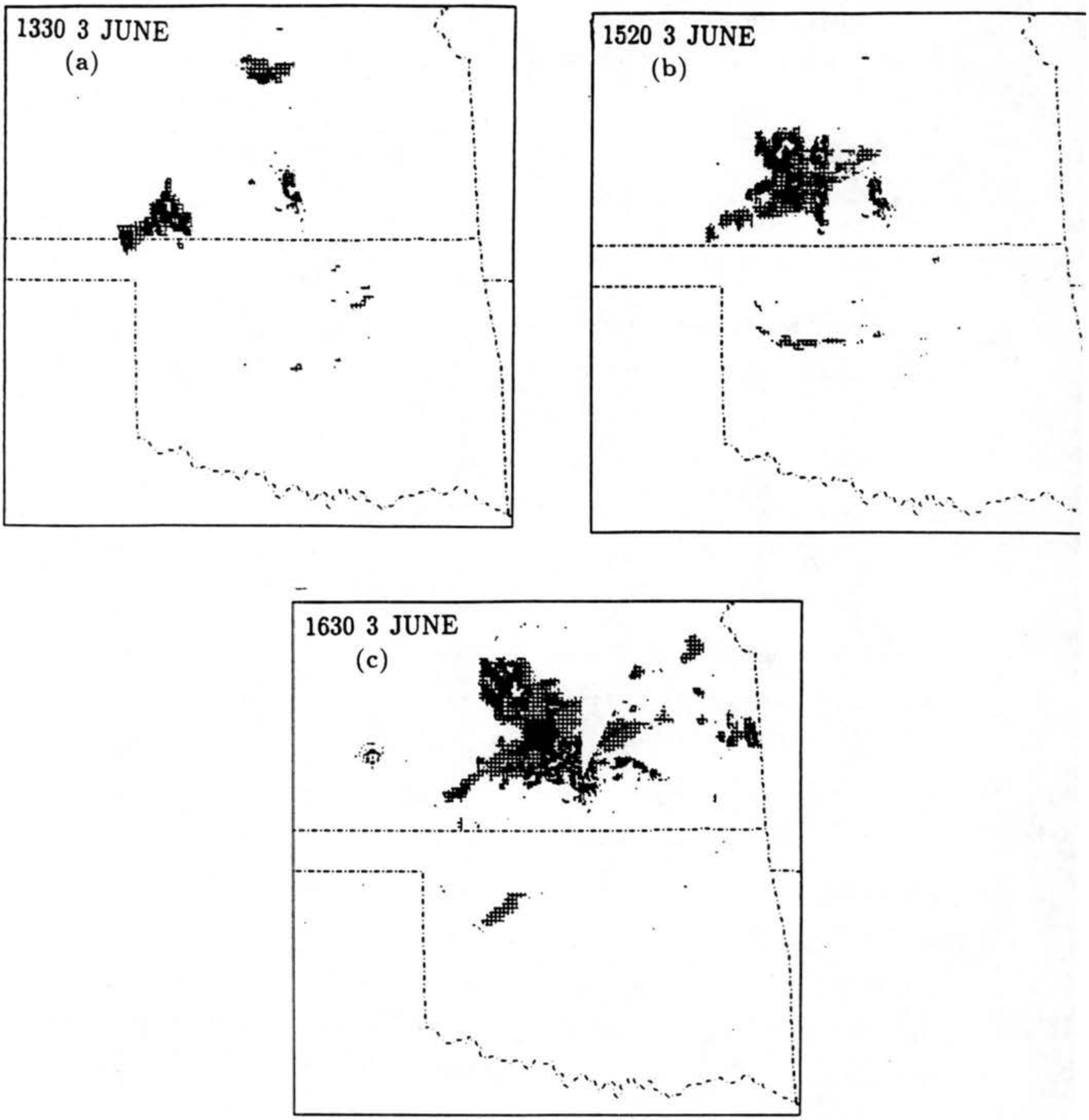

Figure 5.2: Radar composites for 3 June. Figures include: a) 1330 UTC Wichita KS; b) 1520 UTC Wichita KS; c) 1630 UTC Garden City and Wichita KS; d) 1800 UTC Amarillo TX and Wichita KS; e) 1930 UTC Amarillo TX and Garden City and Wichita KS. Reflectivity thresholds are 15, 25, 40 and 49 dBZ.

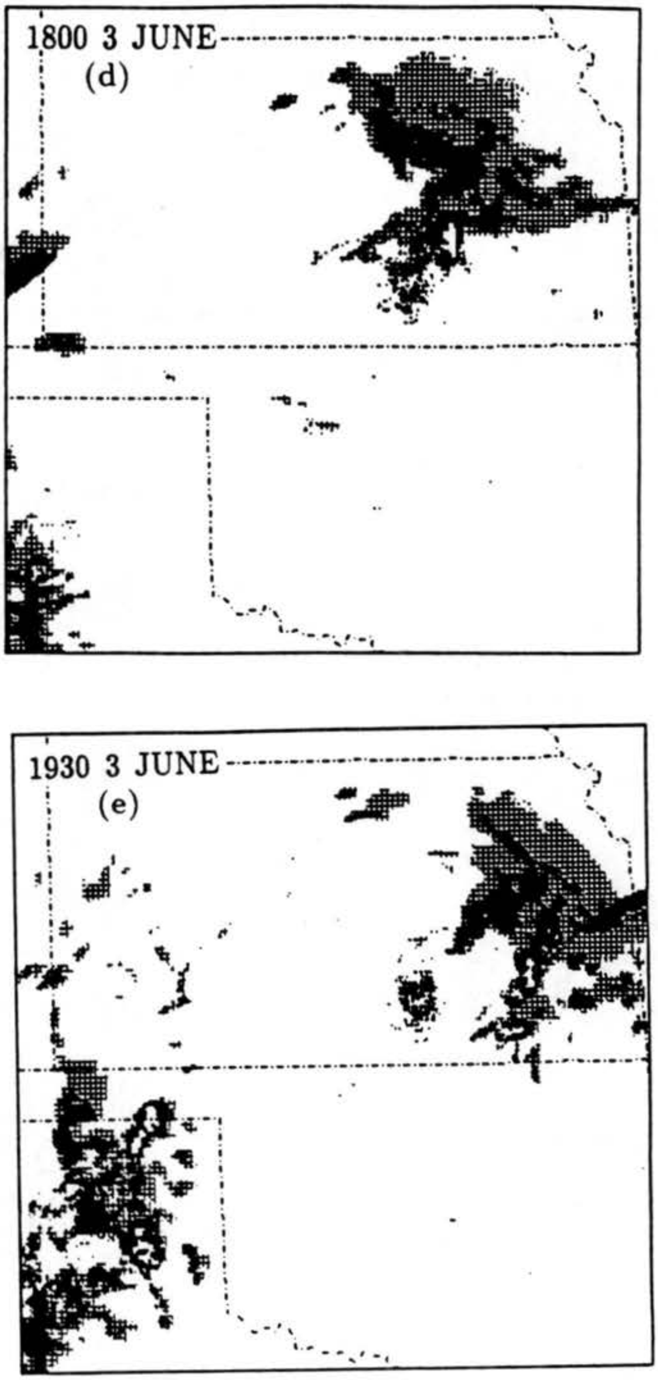

Figure 5.2: Continued.

although not in the sense as shown by Houze et al. (1990), as there was stratiform precipitation both leading and trailing the area of convection that was now present. The stratiform precipitation area was confined to the north of the convection. The enhanced stratiform precipitation was to the north-northwest of the convection, and the rear echo notch was to the west of that. By 1930 (Fig. 5.2e) the MCS took on more of a well-defined asymmetric structure. There has been the development of a northeast-southwest convective line extending to the south of the stratiform precipitation area. The region of enhanced stratiform precipitation was now placed to the rear of the northern portion of this convective line, with a transition zone separating the two areas. The convection in the Texas panhandle was the beginning of the development associated with the 3-4 June case. There were not any reports of severe weather in the PRE-STORM area associated with this MCS.

5.2.3 System overview

Initiation conditions (Prior to 1600)

As discussed by Green (1989), the pressure structure prior to the development of this MCS was largely zonal in nature, with the lowest pressure in the southwest and the highest in the northeast area of the mesonet. There was a general easterly flow across Kansas with cool and moist conditions, while across Oklahoma there was a southerly flow and warm and moist conditions. These features were changed very little by the MCS during this period due to its small size and the relative weakness of the gradients associated with it. There was not a strong gust front, and there were only weak, but slowly strengthening mesohighs.

Early stage (1600)

By this time (Fig. 5.3) the mesohighs, while still weak, strengthened by 1 mb but the gradients were still very weak. There were also two very weak pre-squall lows present, each found ahead of the intense areas of convection at the northern and southern ends of the system. The mesohighs were located coincident with the areas of strong convection at the northern and southern ends of the MCS. There was not a wake low feature at this

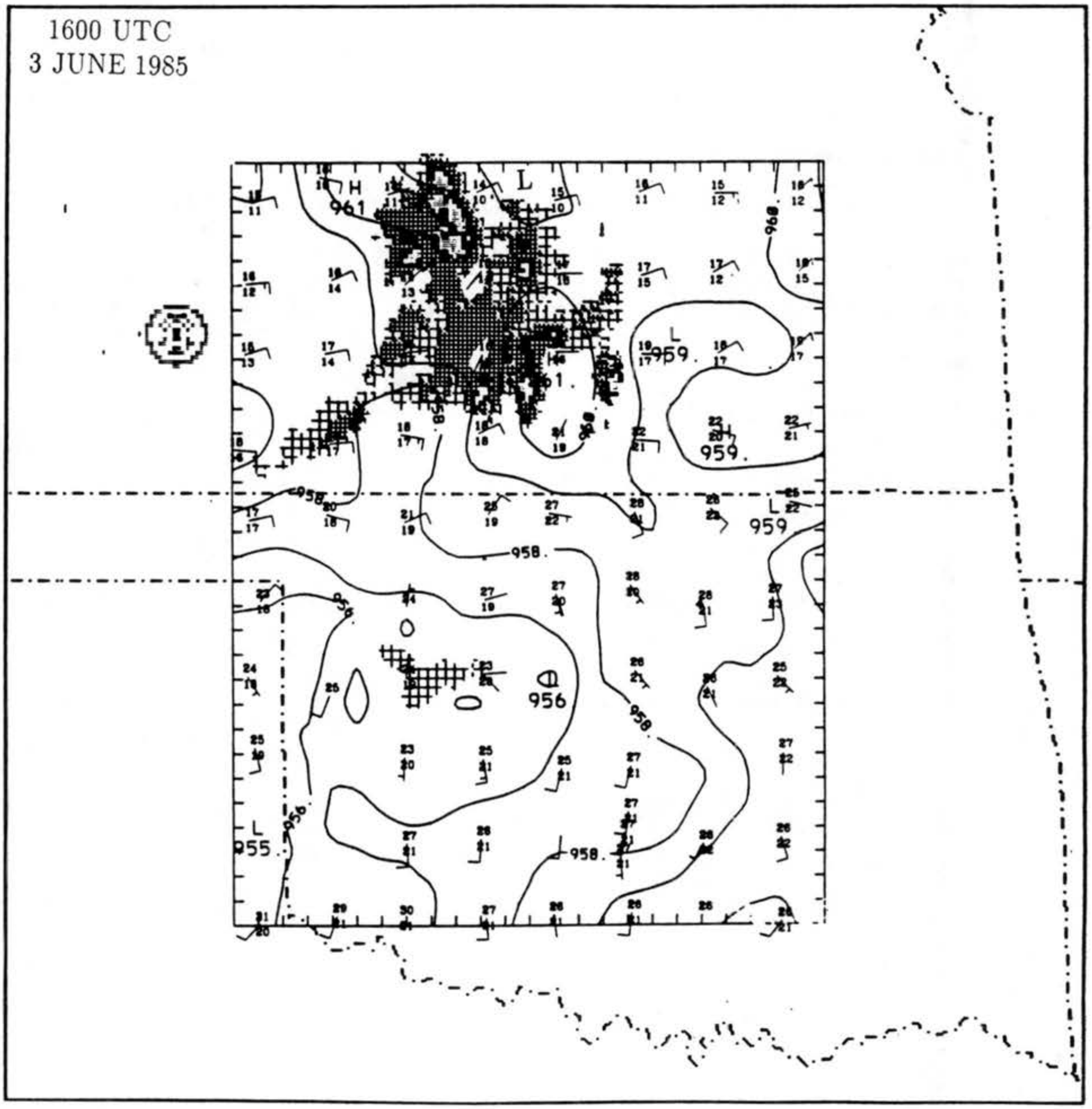

Figure 5.3: Pressure at 480 m, in millibars, at 1600 UTC 3 June. Reflectivity thresholds are 15, 25, 40 and 49 dBZ. Temperature and dewpoint (°C) are plotted at individual stations. Winds are in m s^{-1} with a full barb being 5 m s^{-1}.

time, although there was a weak trough of lower pressure along the southwest edge of the system with a weak gradient along the back edge of the stratiform precipitation. The flow was still largely undisturbed by the system due to the very weak gradients associated with it.

Due to the lack of upper-air soundings taken during the lifetime of this MCS, its rear inflow structure is only obtainable from the dual-Doppler study of this system by Nachamkin (1992). He found that in the southern portion of the system the rear inflow penetrated the stratiform precipitation region and descended. This system-relative rear inflow was generally weak-to-moderate (less than 10 m s^{-1}) and its rate of descent was also weak. Farther to the north, near the rear echo notch, the rear inflow actually ascended dramatically. The flow here was quite strong (10-15 m s^{-1}). The lack of a pronounced descending rear inflow helps to explain why there was not a wake low present at this time (Johnson and Hamilton 1988, Stumpf et al. 1991).

Wake low formation stage (1700-1800)

By 1700 (Fig. 5.4) the mesohighs merged into one large feature covering not only the areas of convection, as they did 60 min earlier, but also the areas of stratiform precipitation in between. A weak northerly outflow developed on the southern end of the system leading to a weakly convergent flow across extreme southern Kansas. The pre-squall low moved to the northeast portion of the MCS, to the north of the approximately east-west oriented convective line. A wake low rapidly developed in the echo notch region on the back edge of the enhanced stratiform precipitation area. The shape of the wake low tended to conform to the shape of the echo notch. The flow was weakly affected by the somewhat larger gradient, giving rise to 7.5 m s^{-1} flow through the wake low. The wake low feature developed at the same time that the enhanced stratiform precipitation region and the echo notch became prominent features in the system.

By 1730 (Fig. 5.5) there was a distinct amplification of all of the pressure features. A pre-squall low redeveloped ahead of the rapidly strengthening convection at the southern end of the system. The mesohigh strengthened by 1-2 mb and covered the entire central portion of the MCS and was now centered within the stratiform precipitation region.

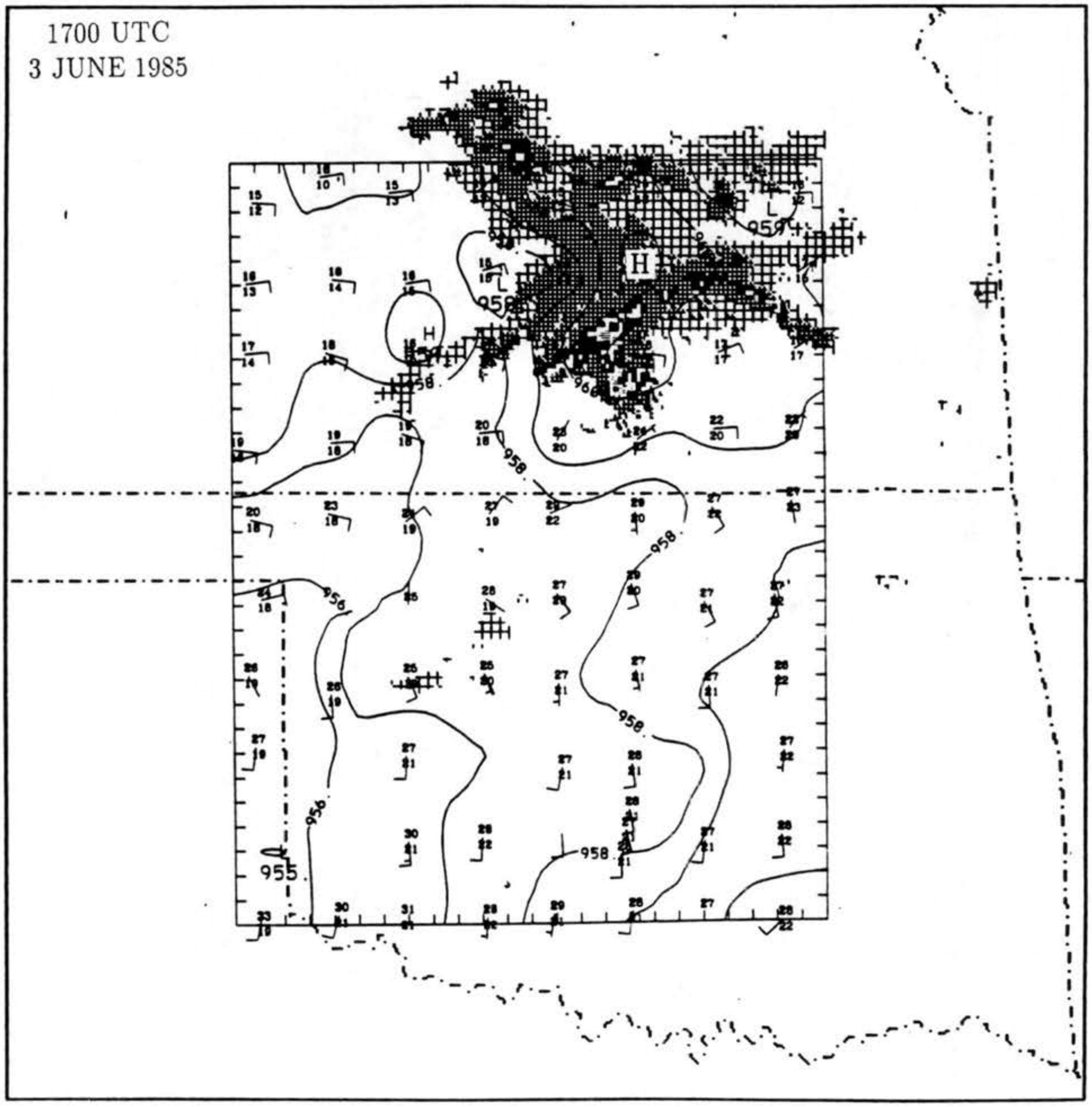

Figure 5.4: Same as Fig. 5.3 except for 1700 UTC 3 June.

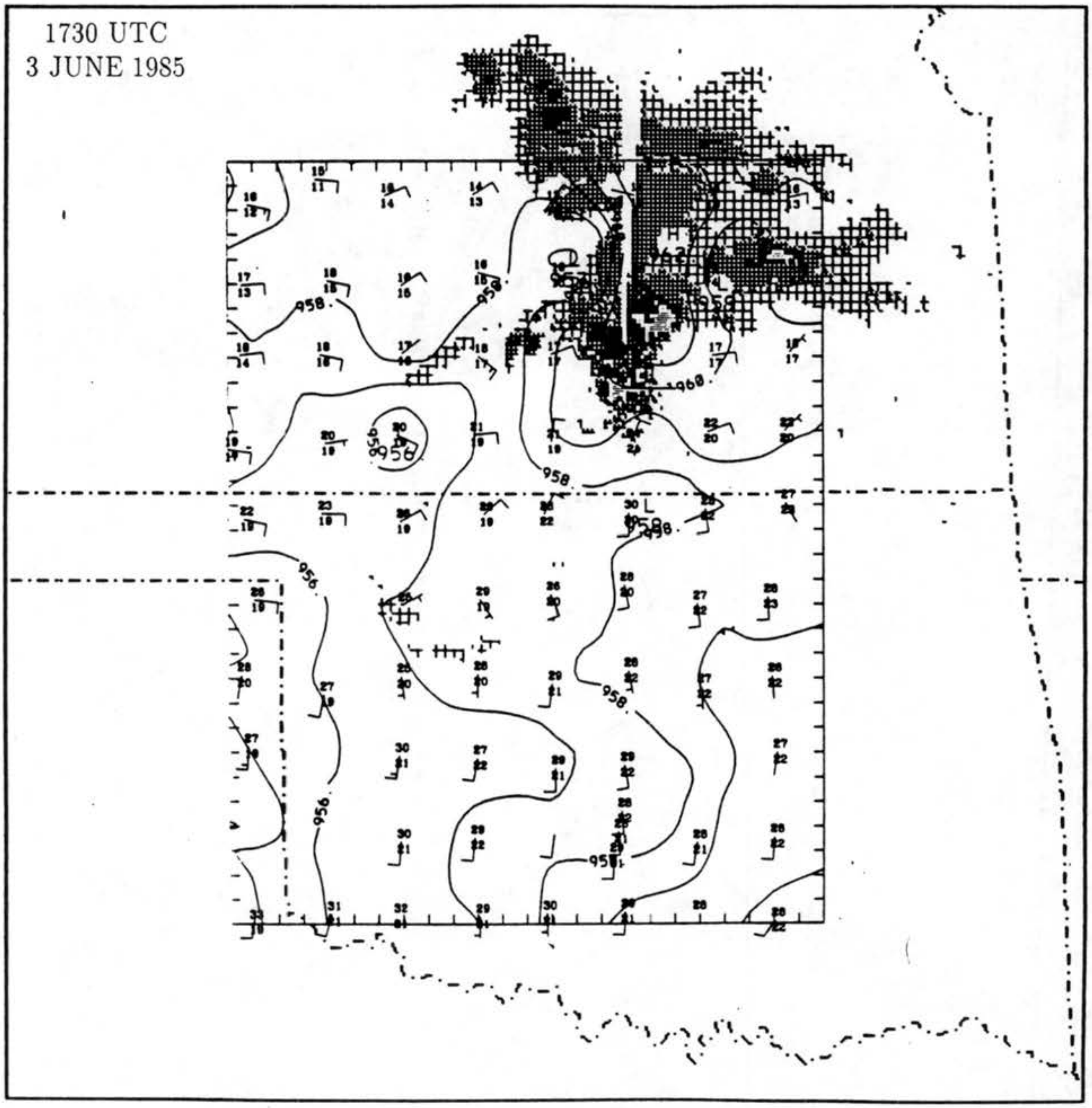

Figure 5.5: Same as Fig. 5.3 except for 1730 UTC 3 June.

The wake low also deepened by 1-2 mb. The strengthening of these features led to the development of a strong gradient along the back edge of the system, which was still tending to curve and conform to the shape of the echo notch. Oddly, there was not a corresponding increase in the strength of the flow to the rear of this stronger gradient. There was, however, more pronounced divergence occurring to the rear of the mesohigh as the wind shifted from northwesterly in the mesohigh to more easterly in the wake low. The outflow from the southern end of the system also strengthened (5 m s^{-1}) corresponding to the stronger convection which developed. This was associated with a gust front emanating from the southern convection with the enhanced northerly flow as well as an enhanced pressure gradient.

Nachamkin (1992) shows that there was a dramatic change in the structure of the rear inflow from 1630 to 1730. In the region of the rear echo notch, where earlier the inflow was rapidly ascending, the rear inflow became a descending flow along the back edge of the stratiform anvil. In the southern portion, the rear inflow increased in speed by 5-10 m s^{-1}. So overall, the entire rear inflow (both north and south) became a descending westerly jet with system-relative speeds of 10-15 m s^{-1}. Now that there was a strong, descending rear inflow, the necessary warming and drying was able to occur to allow the observed decrease in surface pressure to occur via hydrostatic effects.

By 1800 (Fig. 5.6) the pressure gradient weakened somewhat, although the pressure features maintained their same intensities. The wake low became a more diffuse feature and was more of a trough. There was a further strengthening of the northerly outflow from the southern end of the system (5-10 m s^{-1}), and as the flow 50 km to the south was southerly at 5 m s^{-1}, there was enhanced convergence occurring in this region.

Structure as system exits mesonetwork (1930)

By 1930 (Fig. 5.7) further convection developed along the southern flank of the MCS along the region where there was enhanced convergence due to the outflow from the system. This led to the development of a convective line structure at the southern end of the MCS. There was also a strengthening of the gradient near the back edge of the system due to a restrengthening of the wake low. Two wake lows were actually present

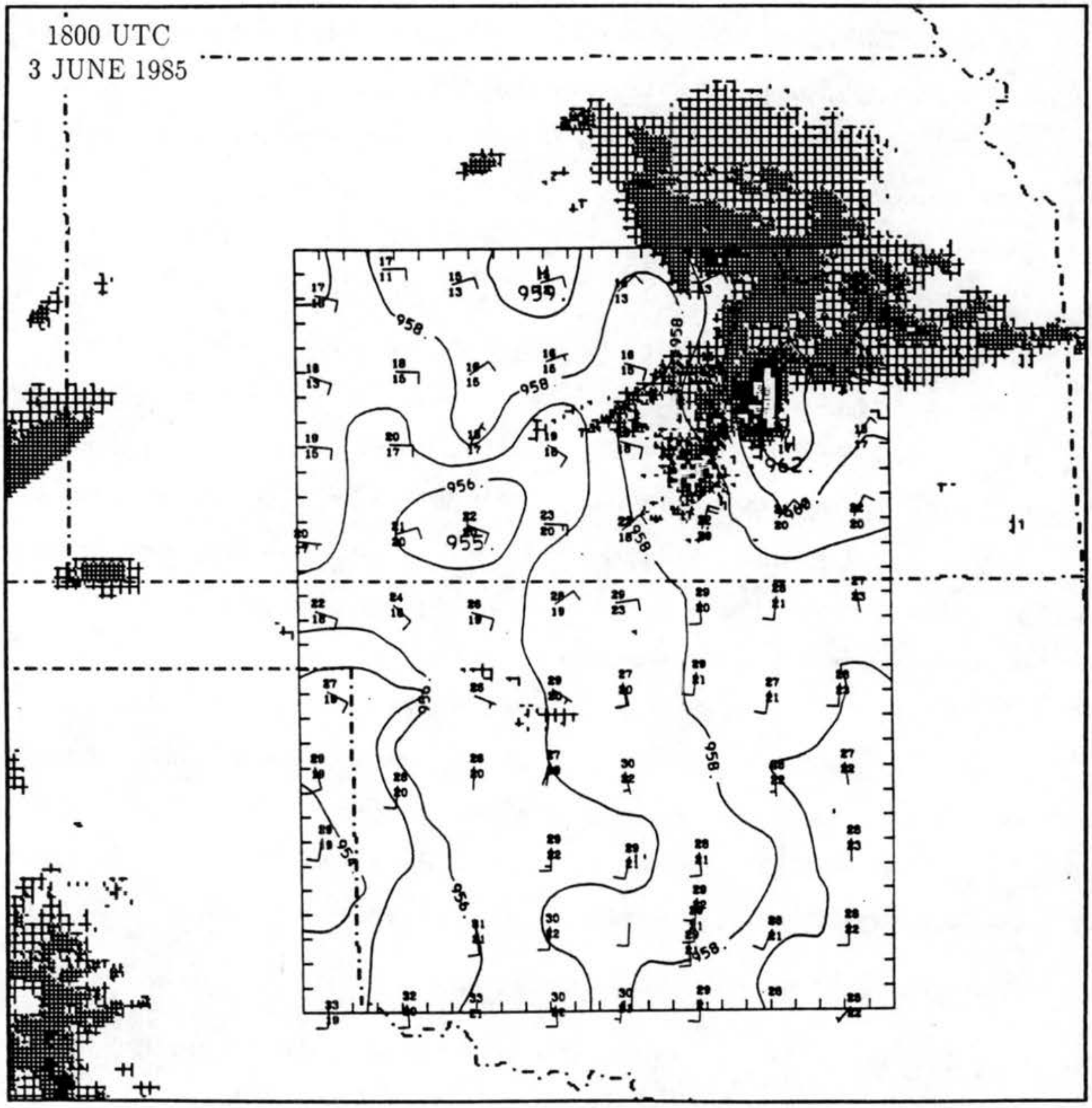

Figure 5.6: Same as Fig. 5.3 except for 1800 UTC 3 June.

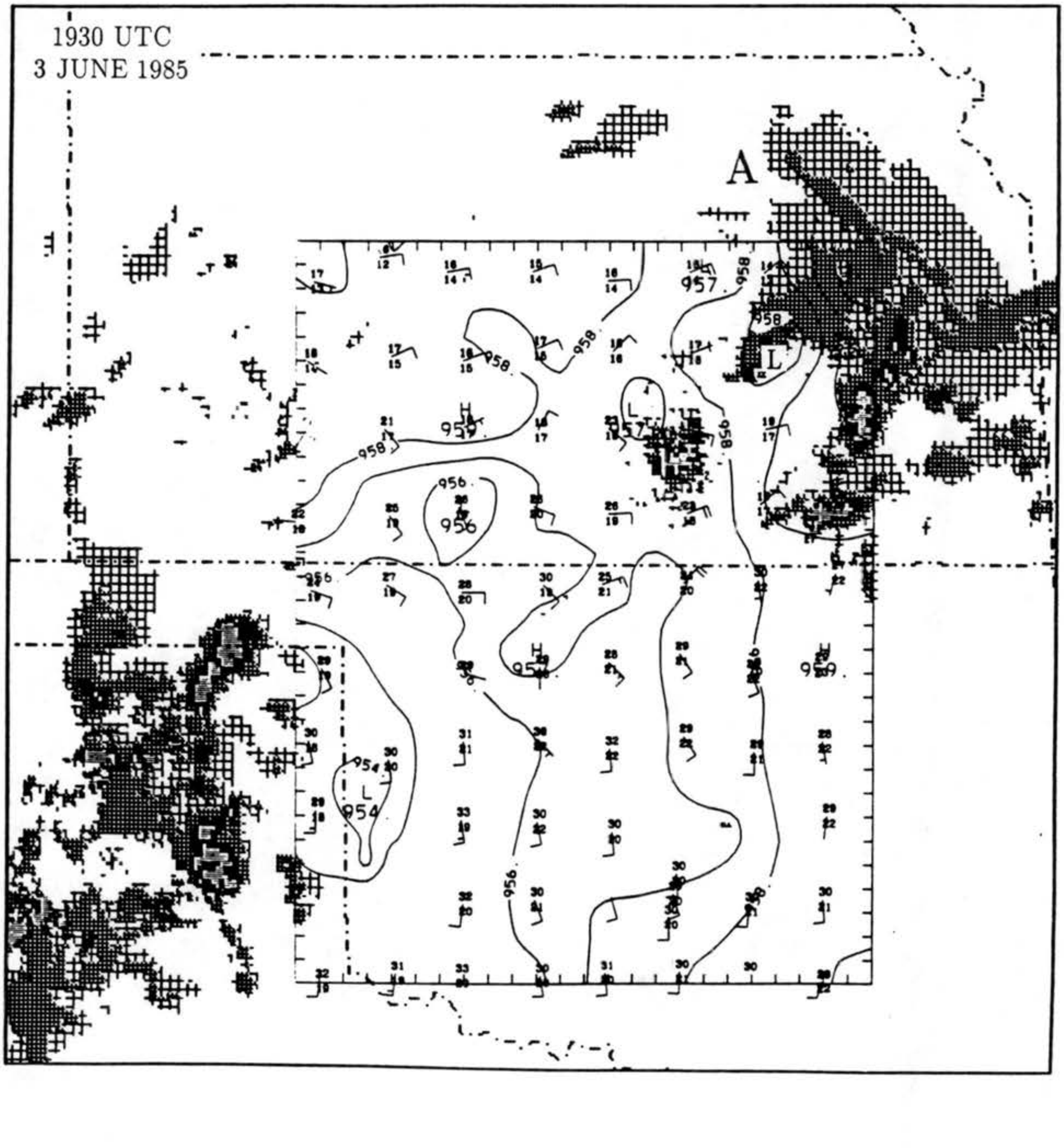

Figure 5.7: Same as Fig. 5.3 except for 1930 UTC 3 June.

at this time, one to the south and the other to the north of a region where the enhanced stratiform precipitation region extended back to the west. The flow through the northern wake low was now at its strongest (10 m s^{-1}) even though a stronger gradient was present earlier. The flow through the southern wake low was still quite weak (2.5-5 m s^{-1}).

The only sounding to sample the rear inflow structure was from FRI (Fig. 5.8), which was located at the back edge of the stratiform precipitation area in the northern portion of the system near the wake low (point A in Fig. 5.7). A distinct rear inflow jet was found at 425 mb (12 m s^{-1}), which is typical for a sounding in this position relative to a wake low. The strong RTF flow above 200 mb was due to the presence of a strong westerly jet at these levels, which accounted for a significant amount of leading stratiform precipitation in this case.

5.2.4 Mesonet time series

The station where the wake low first developed is P12 (Fig. 5.9, see Fig. 3.1). The pressure structure prior to the wake low shows the presence of many areas of higher pressure. This is indicative of the very random nature of the convection at the system's early stages of development. These pressure changes were accompanied by generally light winds, which is indicative of the lack of strong gradients in this case, as well as the presence of a frontal zone which decoupled the surface flow from the flow aloft. The second of the pressure rises (1530) (0.8 mb in 10 min) was accompanied by a 1°C temperature (dewpoint) decrease (increase) but had virtually no signal in the wind. The third pressure increase (1600), while being much more substantial (2 mb in 10 min), was actually accompanied by a weakening of the winds, although there was a dramatic shift in the flow from northeasterly to southwesterly. It also was not accompanied by any temperature or dewpoint signature, which is again an indication of a decoupling of the surface from the system. The wake low (1700) also did not exhibit a strong (relative to other wake low pressure gradients) pressure gradient (2.6 mb in 25 min) but there was a weak strengthening of the winds (11 m s^{-1} gust). The only other change was a shift back to easterly flow, but this was just the background flow. The features at other stations throughout the remainder of the lifespan of this system in the wake low region were very similar.

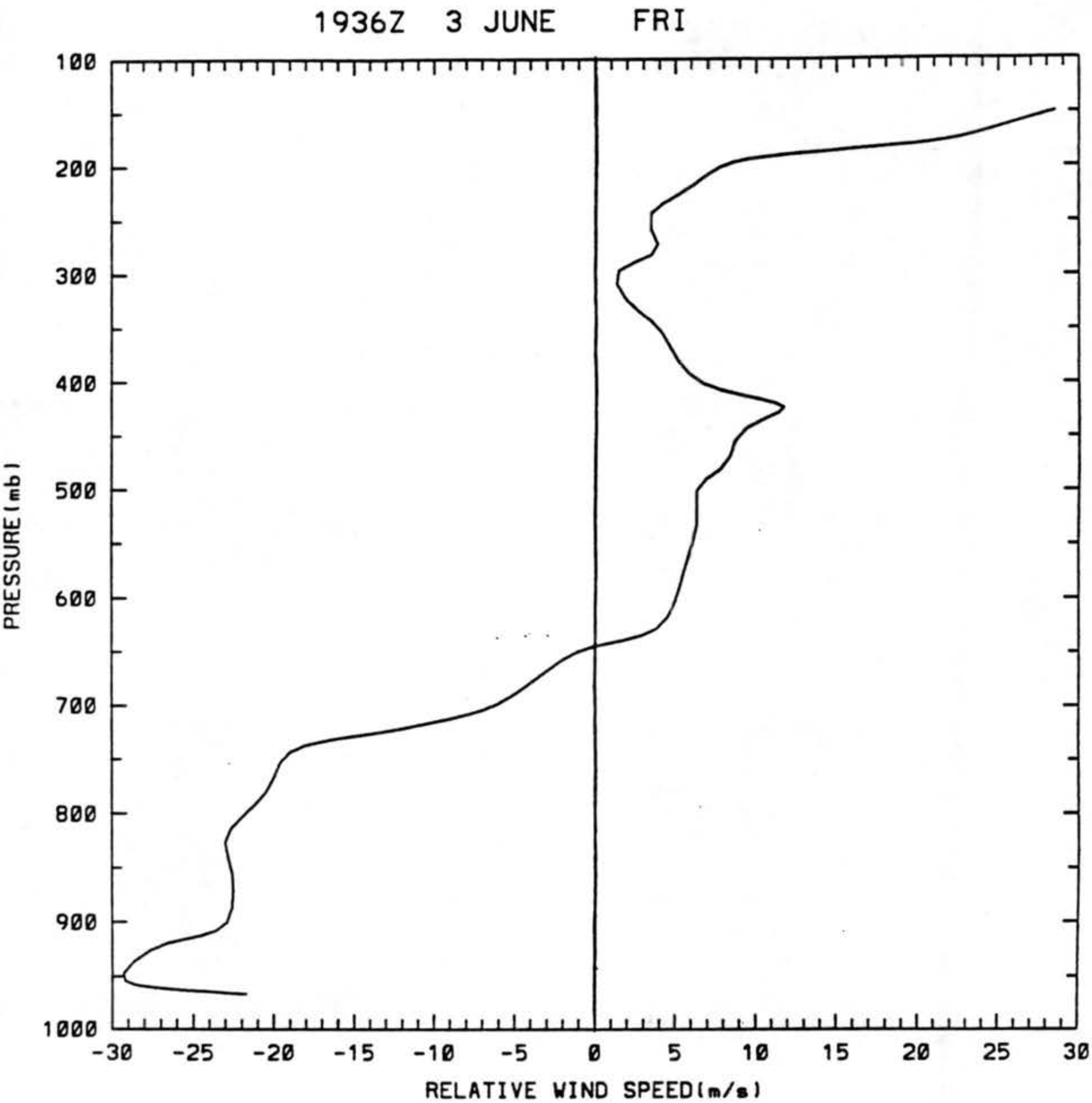

Figure 5.8: System-relative upper-air winds, in m s^{-1}, for FRI at 1936 UTC 3 June. Positive (negative) values imply RTF (FTR) flow. The 0 m s^{-1} line is highlighted.

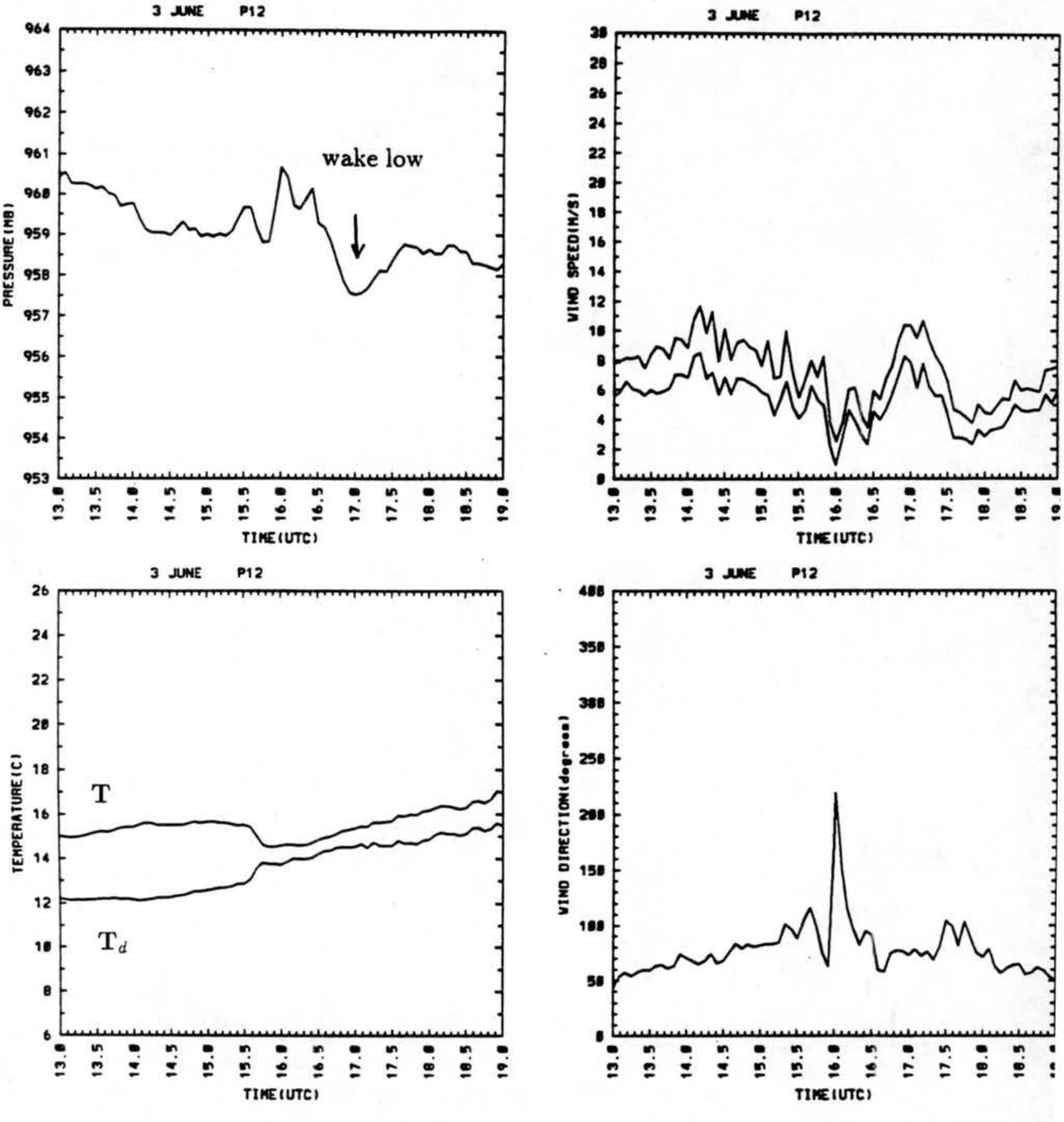

Figure 5.9: Time series data for 3 June at station P12. Data are: In upper-left 480 m pressure with wake low highlighted; in upper-right 5-minute average wind speed (lower curve) and 5-minute maximum wind gust (upper curve) in m s^{-1}; in lower-left 5-minute average temperature (upper curve) and dewpoint (lower curve) in °C; in lower-right 5-minute average wind direction in degrees.

5.3 June 3-4 case

5.3.1 Synoptic overview

The large-scale conditions associated with this case are the same as those associated with the 3 June case. For a discussion of this see section 5.2.1. One important change which occurred was the rapid recovery of very warm and moist air to the rear of the 3 June system. This can be seen on the 2100 3 June 850 mb map (Fig. 5.10), when the PRE-STORM area was between the two systems. The air in northeastern Kansas was still greatly affected by the 3-4 June MCS and was very dry. But elsewhere the atmosphere was able to rapidly recover and was very warm and moist, especially in northern Oklahoma and southwestern Kansas. This rapid recovery was helped by a strong (10-15 m s^{-1}) southerly flow. Strong warm advection was continuing to occur over Kansas.

5.3.2 Radar overview

The initial development associated with this MCS occurred to the southwest of Amarillo, Texas at about 1700 3 June (not shown). At 1900 (Fig. 5.11a) the system became apparent in the Texas panhandle. The convection was highly disorganized and had several cores. The stratiform precipitation was limited, but was found between the areas of convection. By 2000 (Fig. 5.11b) the convection developed a banded structure in the eastern Texas panhandle and replaced most of the earlier stratiform precipitation. By 2230 (Fig. 5.11c) the system started to become more organized. Several lines of convection were evident. At the northern and southern ends of the system small east-west oriented convective lines formed and there was a north-south line extending between them on their western ends. Light stratiform precipitation was beginning to develop on the western side of the system. By 0010 (Fig. 5.11d) the system became well developed, with a wave-cyclone structure (Smull and Augustine 1992). There were now two basic lines of convection, with the weaker one extending northeast-southwest through central Kansas and the stronger one extending to its south into northern Oklahoma. ¿From the intense convective cell in the southern portion of the north-south oriented convective line there were several reports of large hail as well as one F1 tornado (Storm Data, June 1985). An expansive area of

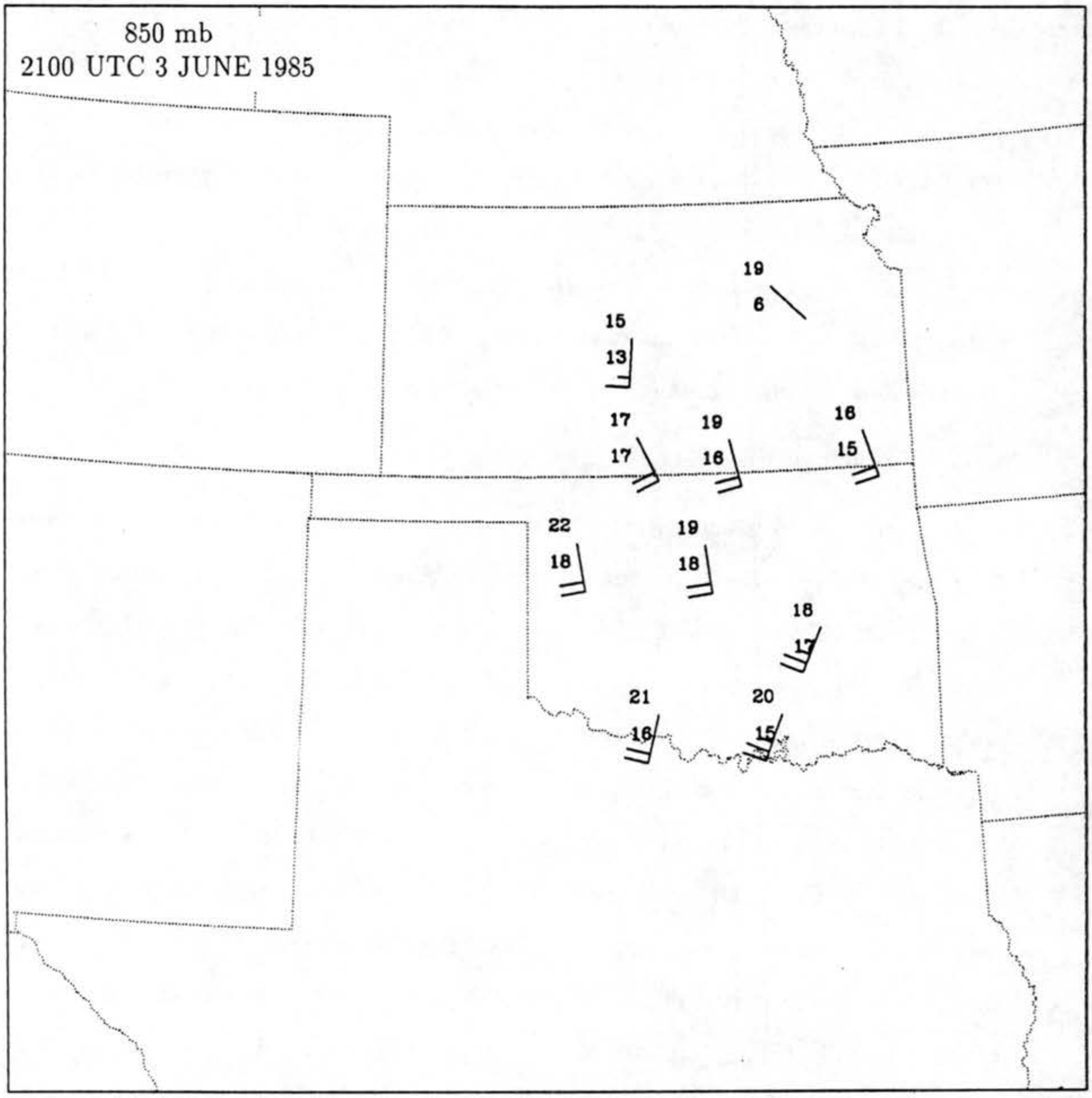

Figure 5.10: 2100 UTC 3 June 850 mb PRE-STORM data. Full wind barb is equivalent to 5 m s^{-1}. Temperature and dewpoint in °C.

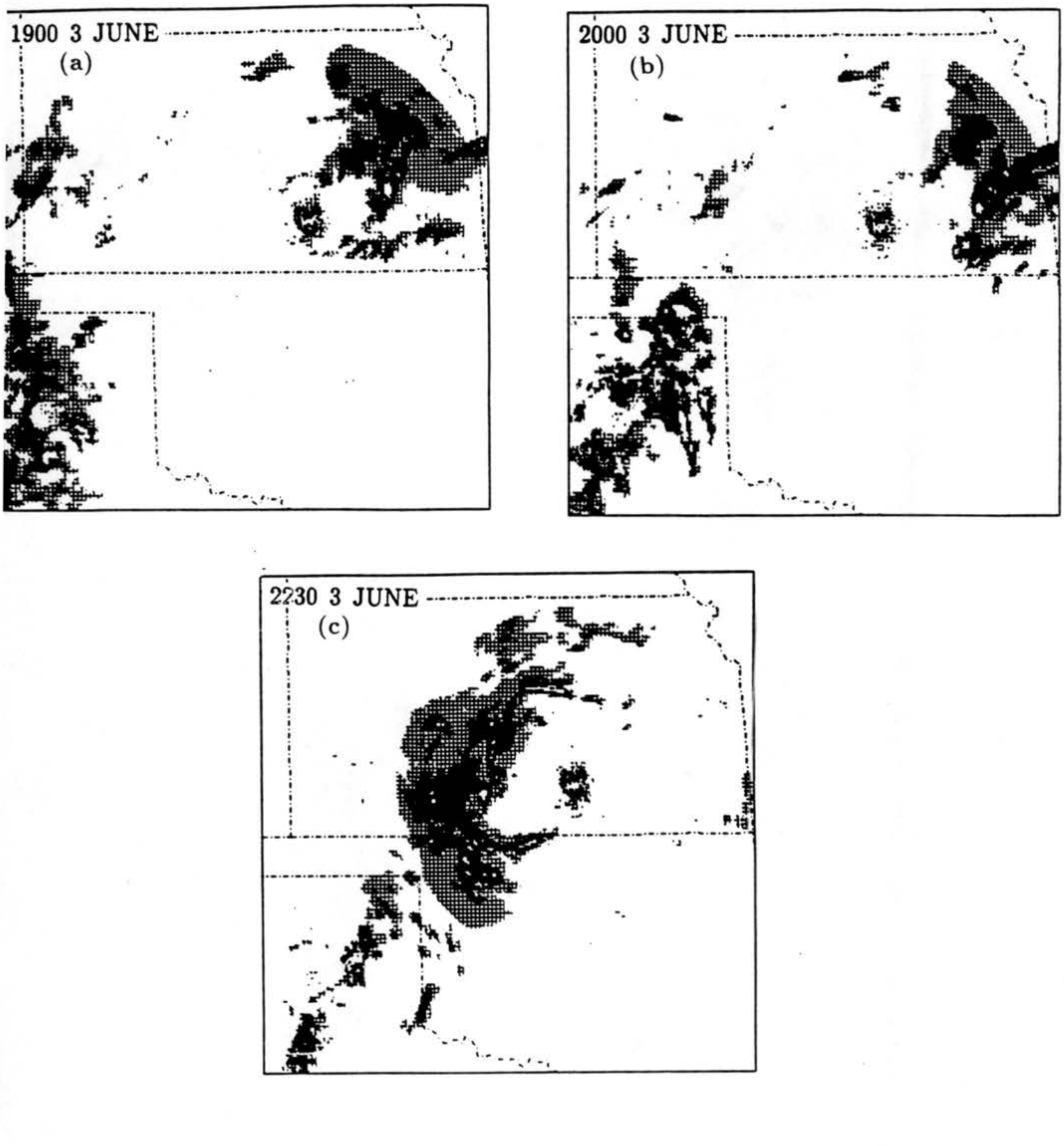

Figure 5.11: Same as Fig. 5.2 except for: a) 1900 UTC 3 June Amarillo TX, Garden City and Wichita KS; b) 2000 UTC 3 June Amarillo TX, Garden City and Wichita KS; c) 2230 UTC 3 June Amarillo TX, Garden City and Wichita KS; d) 0010 UTC 4 June Amarillo TX, Oklahoma City OK, Wichita KS; e) 0130 UTC 4 June Amarillo TX, Oklahoma City OK, Wichita KS; f) 0340 UTC 4 June Amarillo TX, Oklahoma City OK, Wichita KS.

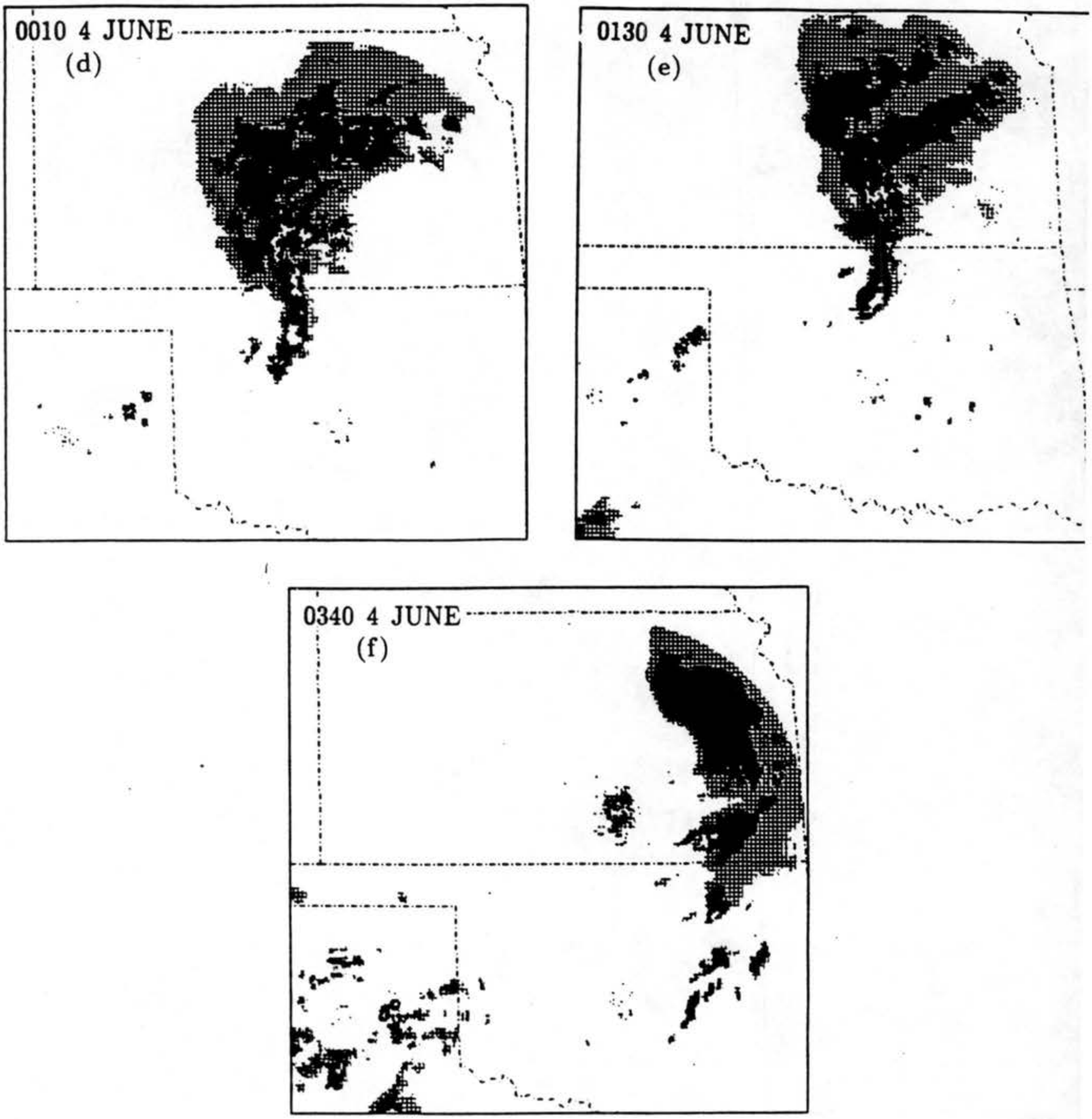

Figure 5.11: Continued.

stratiform precipitation developed to the north and west of the northeast-southwest oriented convective line as well as to the north of the north-south line. By 0130 (Fig. 5.11e) the basic convective structure was the same, but an extensive area of enhanced stratiform precipitation developed to the northwest of the apex of the two convecitve lines. With this, this system took on more of an asymmetric structure. By 0340 (Fig. 5.11f) the convection had largely dissipated but an extensive area of enhanced stratiform precipitation remained over northeastern Kansas.

5.3.3 System overview

Early developing stage (2200)

At this time (Fig. 5.12) there were several areas of localized high pressure, each associated with an area of intense convection. A low was found ahead of the southern portion of the system, but as has been mentioned by Stumpf et al. (1991), this was not a pre-squall low as it was present both well before and after the system passes. The surface flow was characterized by southerly flow throughout all but extreme northern Oklahoma, backing to east-northeast flow to the north, indicative of the front. The southern east-west convective line formed along the convergence area associated with this front. The flow within the system was ill-defined at this time, although there was a moderate (10 m s^{-1}) outflow from the southern end of the MCS leading to convergence in this region.

Late developing stage (2330)

By this time (Fig. 5.13) the mesohighs consolidated into three main centers, one associated with the northern area of convection, another associated with the north-south convective line, and the third, and most prominent, associated with the more stratiform apex area. A weak pre-squall low was present ahead of the north-south convective line. The wake low first appeared at this time along the back edge of the small area of enhanced stratiform precipitation. It appears that this low may have first developed outside the mesonet as a very weak feature, but underwent a rapid deepening at this time as the small enhanced region of stratiform precipitation first developed. A strong gradient was found all along the back edge of the stratiform precipitation region, leading to a 7.5 m s^{-1}

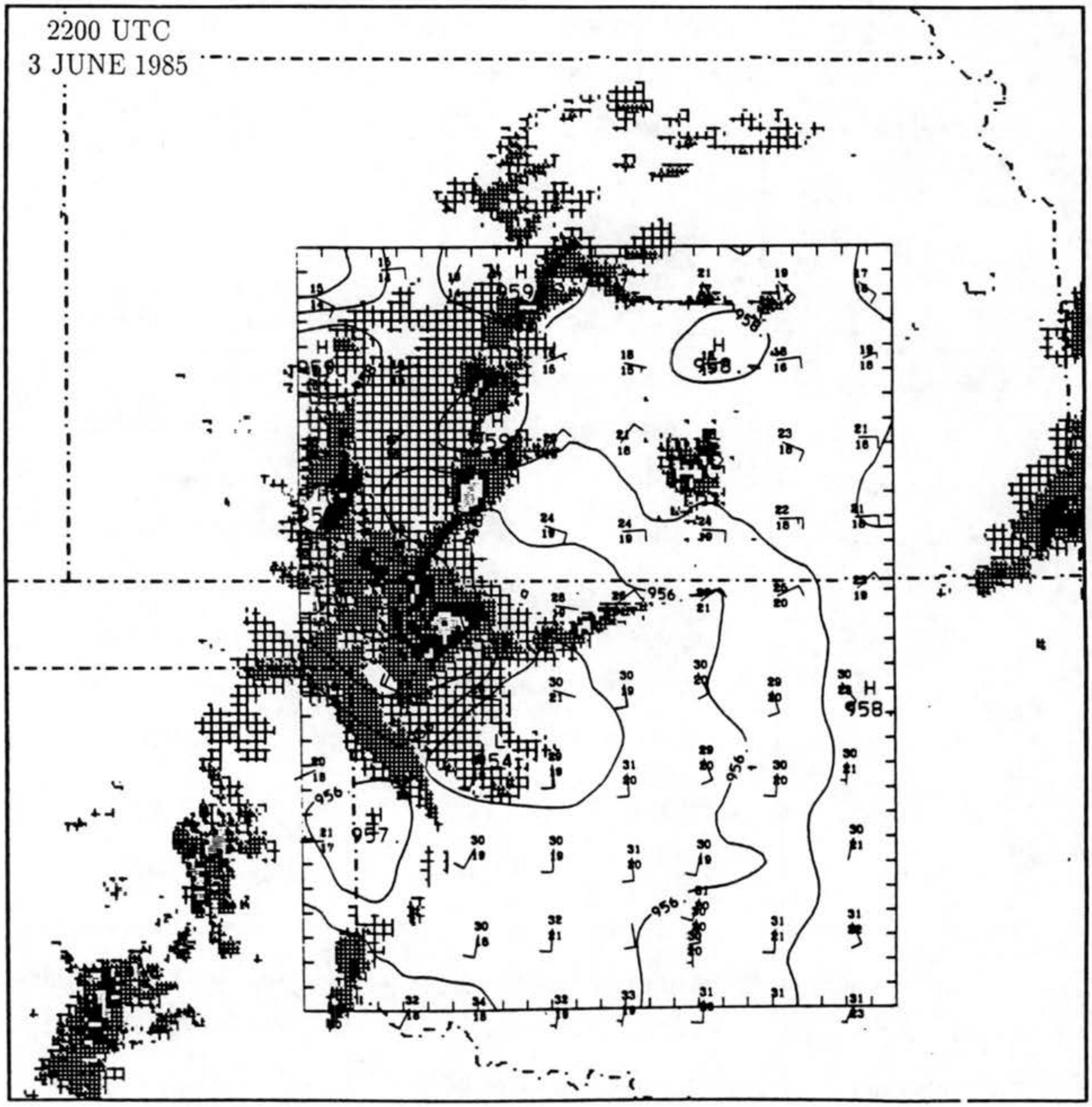

Figure 5.12: Same as Fig. 5.3 except for 2200 UTC 3 June.

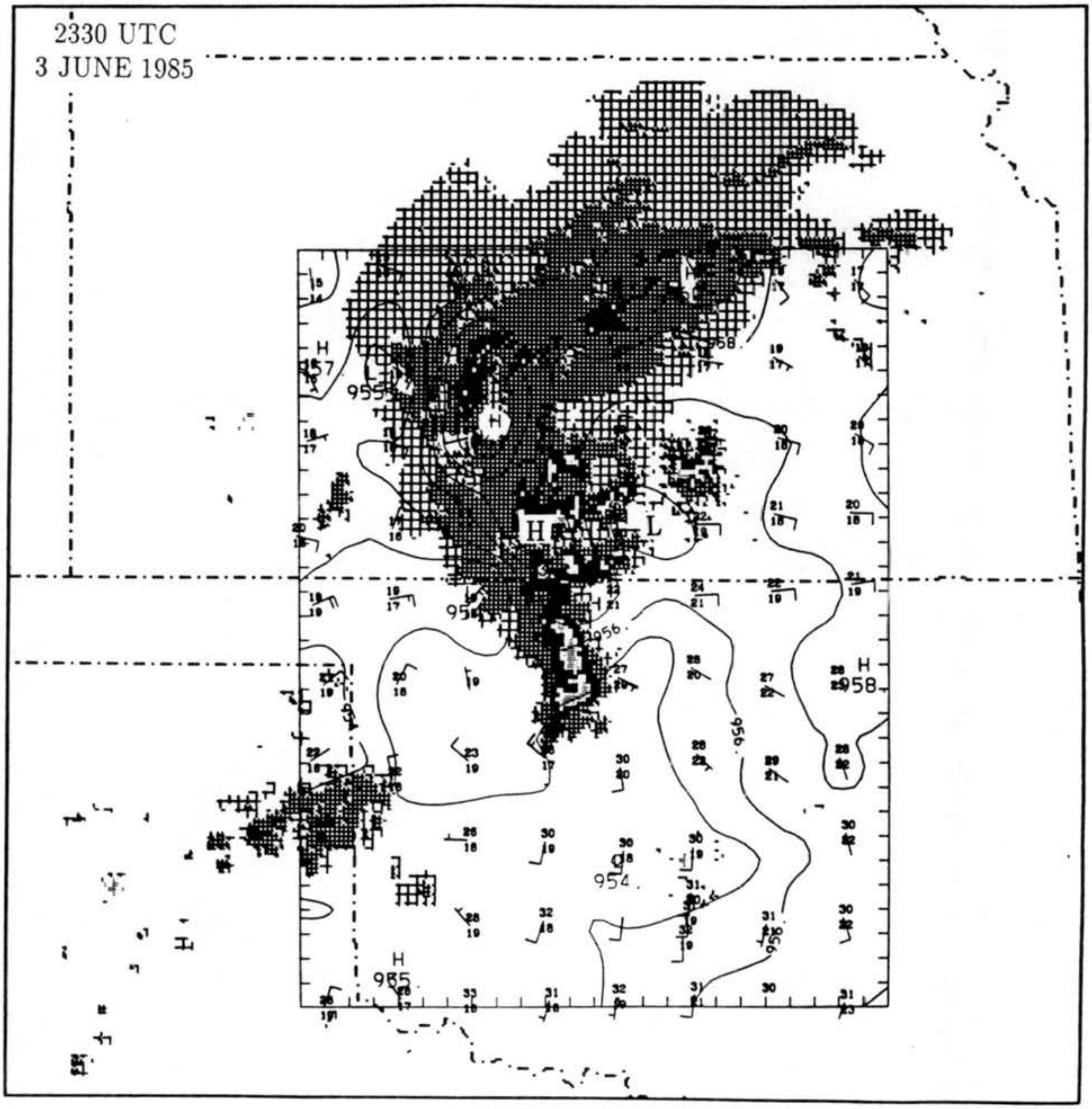

Figure 5.13: Same as Fig. 5.3 except for 2330 UTC 3 June.

easterly flow through the wake low. There was also pronounced divergence occurring to the rear of the mesohigh region.

Mature stage (0130-0300)

By 0130 (Fig. 5.14) the pressure gradient further intensified as the mesohigh strengthened by 1 mb and the wake low deepened by 1 mb. This led to a strengthening of the easterly flow through the wake low to 10 m s^{-1}. The further deepening of the wake low coincided with an expansion of the enhanced stratiform region, and it was situated on the back edge of this region. The southern convection started to weaken, and lost its mesohigh, as it only had a finger of higher pressure extending along it.

By 0300 (Fig. 5.15) the convection rapidly dissipated but a strong gradient still existed in the northern portion of the MCS, and both pressure features were of the same strength as earlier, although both moved out of the mesonet. The wake low was found to the rear of the far northern area of enhanced stratiform precipitation. The flow was still strongly through the wake low (10 m s^{-1}).

In this case there was an opportunity to compare the rear inflow structure within the wake low region to that found to the rear of the southern convective line which did not have any stratiform precipitation nor a wake low. The rear inflow structure to the rear of the southern convective line was profiled by the soundings at END at 0138 (Fig. 5.16a) and 0302 (Fig. 5.16b). At 0138, END was located just to the rear of the convective line (point A in Fig. 5.14), and shows a very high rear inflow (for this location) 250 mb deep with a maximum at 450 mb (10 m s^{-1}). While 90 min later at 0302 END was located 100-150 km to the rear of the now dissipated convective line (point A in Fig. 5.15) and shows a 200 mb deep layer of very weak (3 m s^{-1}) rear inflow peaking at 450 mb. So in this section of the MCS the rear inflow was weak-to-moderate and did not descend as it approached the convective line.

The flow within the wake low region is shown by the RSL soundings taken at 0130 (Fig. 5.16c) and 0300 (Fig. 5.16d). At 0130 RSL was located along the back edge of the stratiform precipitation region, near the wake low (point B in Fig. 5.14). It shows a 200 mb deep layer of strong rear inflow maximized at 425 mb (15 m s^{-1}). While at 0300 RSL

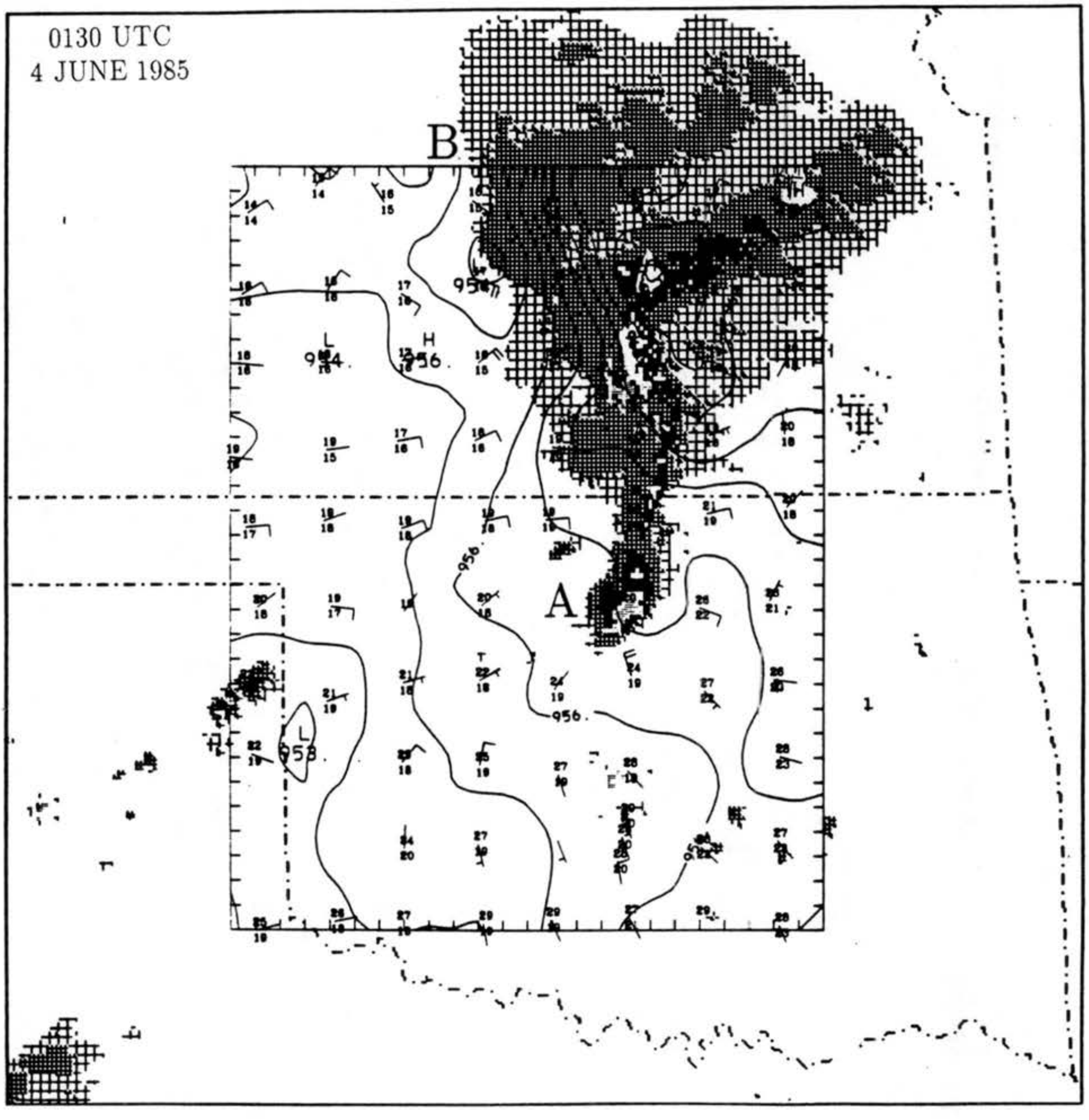

Figure 5.14: Same as Fig. 5.3 except for 0130 UTC 4 June.

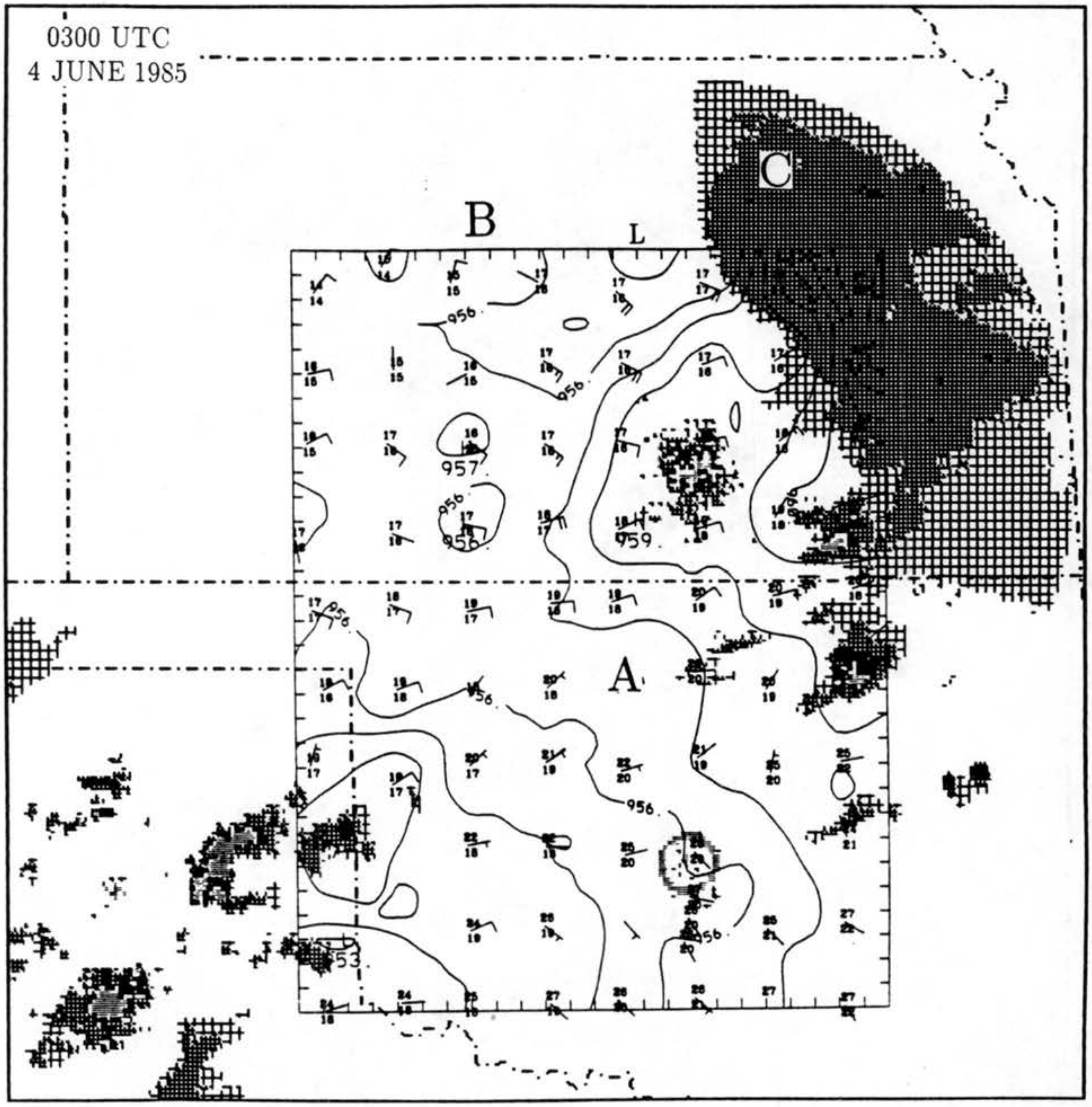

Figure 5.15: Same as Fig. 5.3 except for 0300 UTC 4 June.

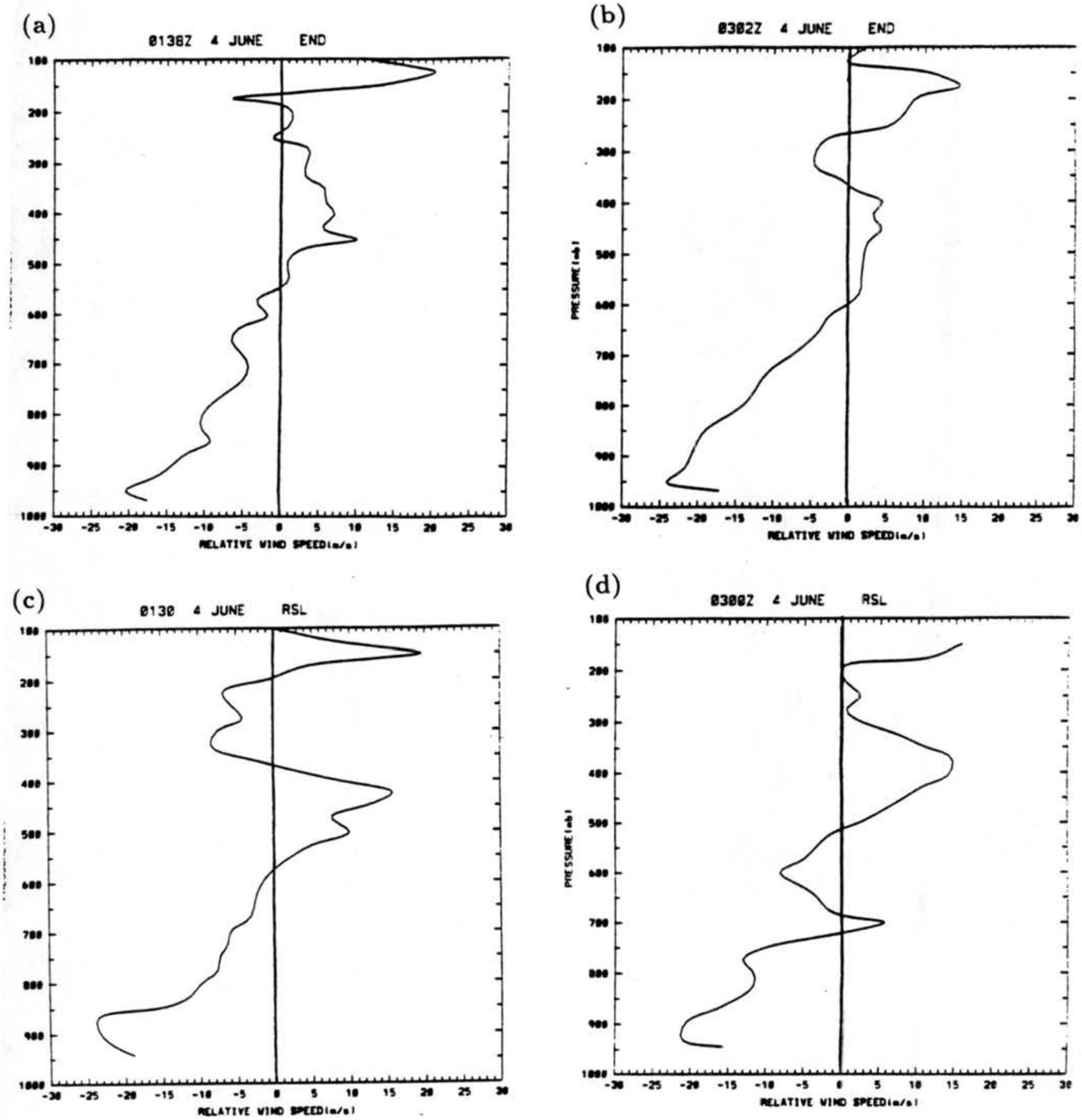

Figure 5.16: In a-e) Same as Fig. 5.8 except for 4 June at: a) 0138 UTC at END; b) 0302 UTC at END; c) 0130 UTC at RSL; d) 0300 UTC at RSL; e) 0319 UTC at FRI. In f) Same as Fig. 5.10 except for 0130 UTC 4 June at 850 mb.

(e)

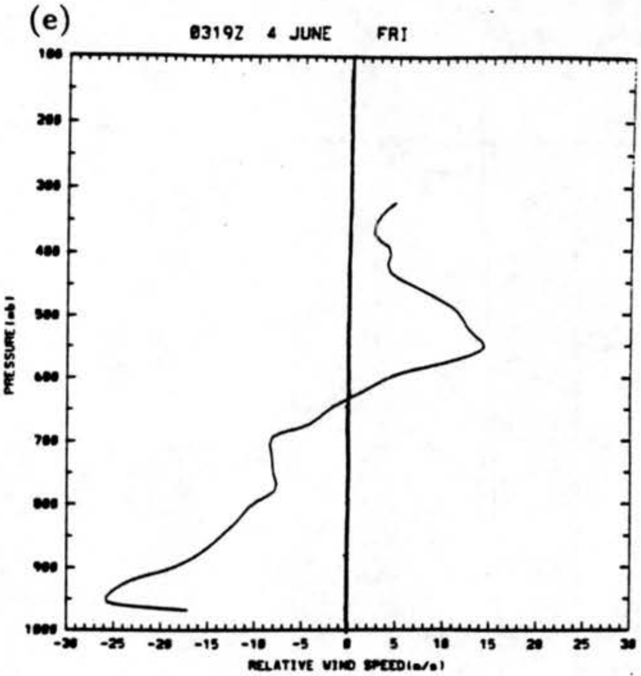

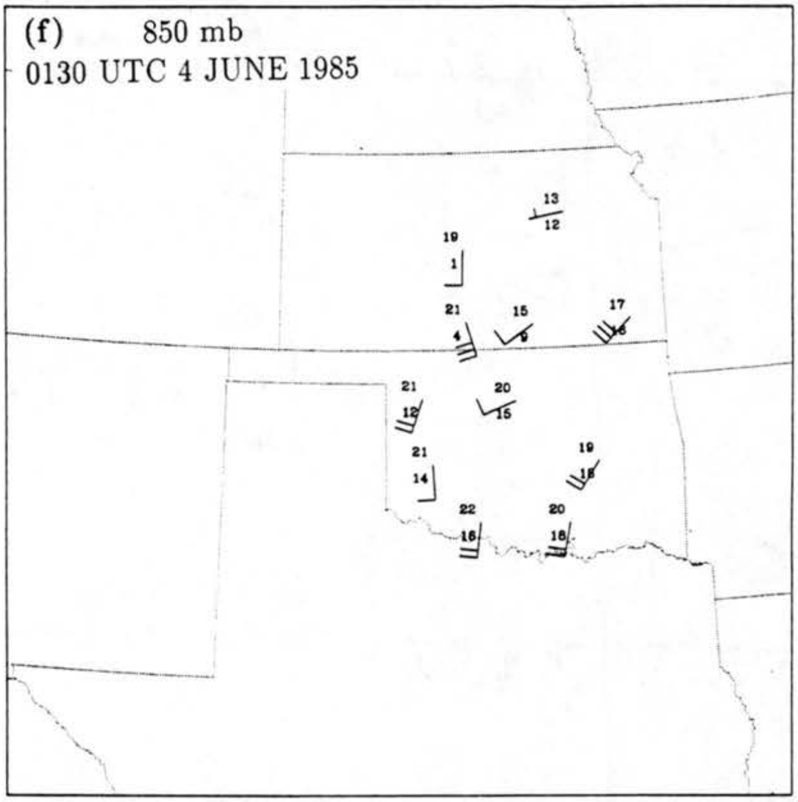

Figure 5.16: Continued.

was located about 100 km to the rear of the stratiform precipitation area (point B in Fig. 5.15) and shows continued strong rear inflow peaking at 375 mb (15 m s^{-1}). So in the wake low region the rear inflow was found to be quite strong and was descending as it approached the convective line. A further indication that the rear inflow was descending as it moved into the system is the FRI 0319 sounding (Fig. 5.16e), which was located within the region of the strong pressure gradient, in the stratiform precipitation region (point C in Fig. 5.15). It shows a deep layer (over 300 mb) of strong rear inflow maximized at 550 mb (14 m s^{-1}). Comparing this to the RSL sounding taken at this time (Fig. 5.16d) shows that the rear inflow had descended another 125 mb.

A way to further demonstrate that the rear inflow was descending is to show that there was strong warming and drying occurring in the lower troposphere in this region due to the hydrostatic effects of the descending airflow. This did, in fact, occur and it was most profound at 0130 at RSL at 850 mb (Fig. 5.16f). RSL had a dewpoint 7.7°C lower than any other station except PTT, and was also much warmer than any other Kansas stations except PTT. PTT may still have had lingering effects from wake low passage over here about 1 h earlier. Also notice that at END in the region to the rear of the southern convection there was not any warming or drying relative to the other stations near it.

5.3.4 Mesonet time series

The conditions associated with the north-south oriented convective line which did not have a wake low are summarized by P41 (Fig. 5.17, see Fig. 3.1). The mesohigh (0020) in this area was a very sharp, short-lived feature with a 3 mb increase in 10 min and was accompanied by a very sharp 8°C temperature and 3°C dewpoint decrease, a shift from east-southeast to northwest flow and a 24 m s^{-1} wind gust. Then the fields became largely unchanged after this time.

The wake low region conditions are sumarized by P05 (Fig. 5.18). A weak pre-squall low feature was evident with a 1.5 mb decrease in 40 minutes. It was accompanied only by a light increase in the winds. The first mesohigh (2300) which was associated with the east-west convective line was fairly sharp, with a 2.5 mb increase in 60 min and was accompanied by 1°C temperature (dewpoint) decrease (increase), a very brief 9 m s^{-1}

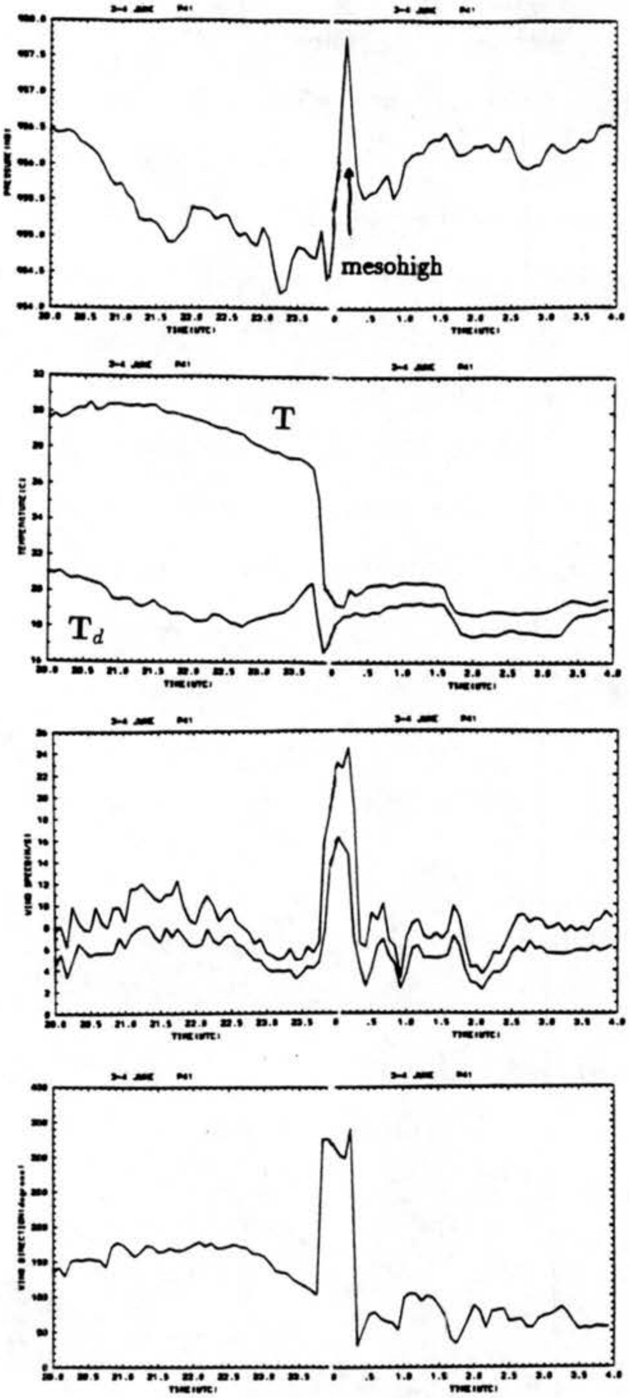

Figure 5.17: Same as Fig. 5.9 except for 3-4 June at station P41. Note the different scales of pressure, temperature and wind speed.

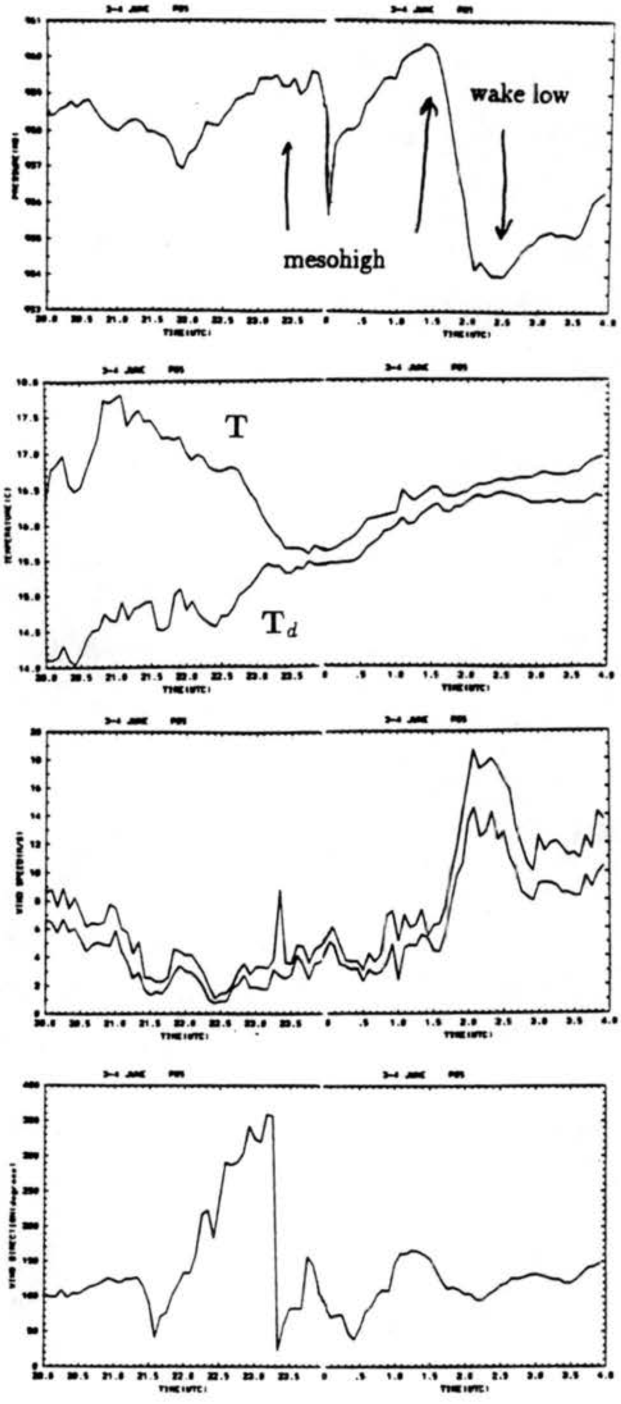

Figure 5.18: Same as Fig. 5.9 except for 3-4 June at station P05. Note the different scales of pressure, temperature and wind speed.

wind gust and a shift from east to northwest flow. Then there was a sharp pressure drop (0000) of 3.5 mb in 15 min and a shift back to easterly flow. Then the mesohigh associated with the center of the MCS passed over (0130) with a 4 mb increase in 75 min and was accompanied by very light winds and a shift to south-southeast flow and a 1°C temperature and dewpoint increase. Then the wake low (0200) passed over with a 6.5 mb decrease in 35 minutes, and was accompanied by a sustained strengthening of the winds to 13 m s^{-1}, a 19 m s^{-1} wind gust and a shift back to east-southeast flow.

5.4 June 4 case

5.4.1 Synoptic situation

The synoptic conditions associated with the development of this MCS are shown from the 0000 4 June maps. At the surface (Fig. 5.19a) the quasi-stationary front was still in about the same position as it was 12 h earlier, extending from a low in southeastern Colorado through extreme northern Oklahoma. To the south of the front it was very warm (29-33°C) and moist (18-24°C) with a southerly flow. To the north of the front it was cooler (18-24°C) but still moist (12-18°C, although the farther north of the front, the drier it becomes) with an easterly flow.

At 850 mb (Fig. 5.19b) there was a strong low-level southerly jet (10-20 m s^{-1}) across Texas and Oklahoma and these same areas were quite moist with dewpoints of around 15°C, except in the Texas panhandle where it was quite dry. Considerable warm advection was still occurring across Oklahoma and especially western and central Kansas. At 500 mb (Fig. 5.19c) a general ridge extended over most of the south central and southeastern U.S., with a continued pronounced anticyclonic curvature to the flow over Oklahoma and Kansas. The closed low moved only slightly to the east and was now along the California-Arizona border. The flow was generally out of the southwest in Oklahoma and Texas, switching to more westerly in Kansas.

5.4.2 Radar overview

The initial development associated with this MCS occurred around 0500 (Fig. 5.20a) as a northeast-southwest oriented convective line in the northern Texas panhandle. The

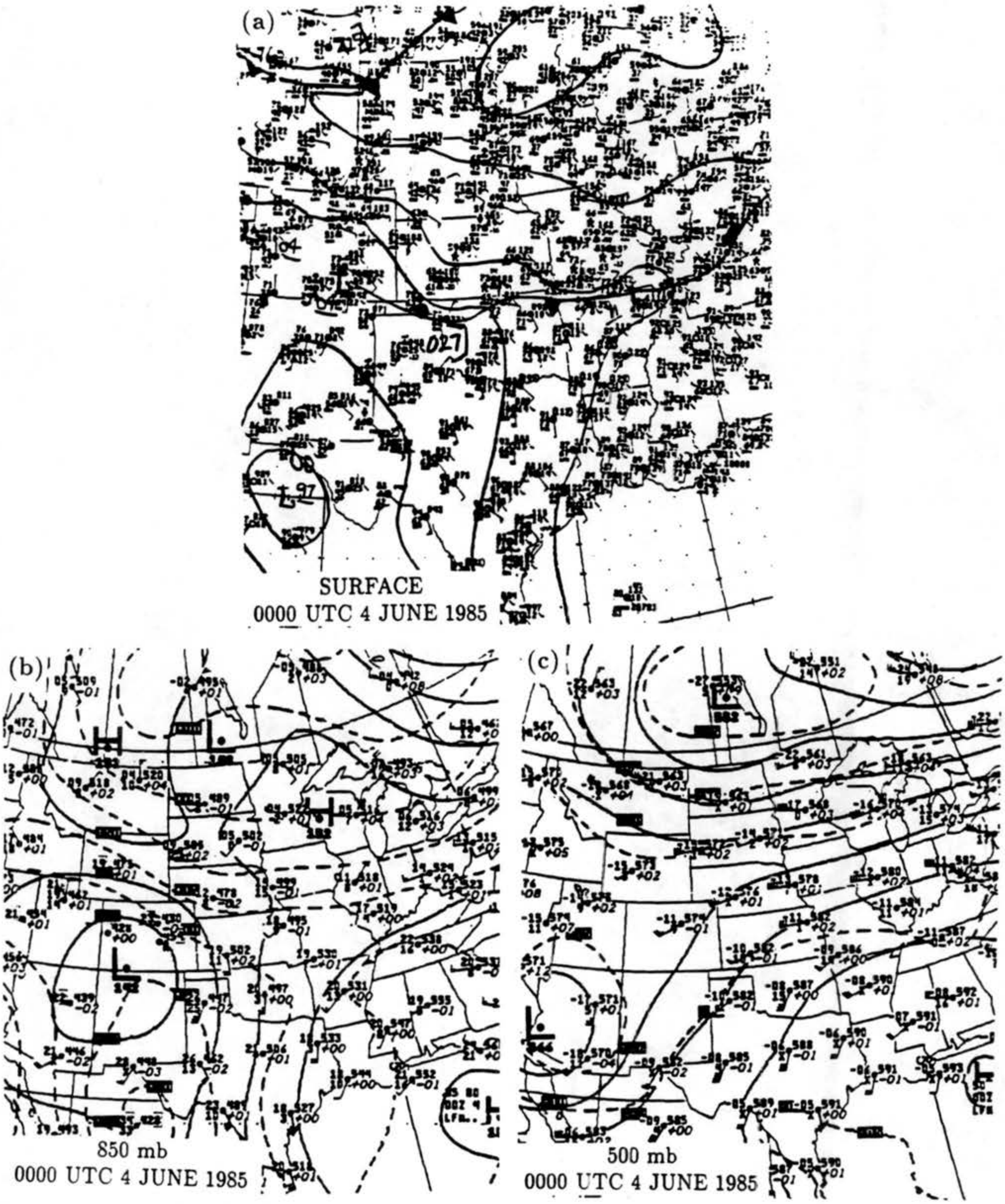

Figure 5.19: Same as Fig. 5.1 except for 0000 UTC 4 June.

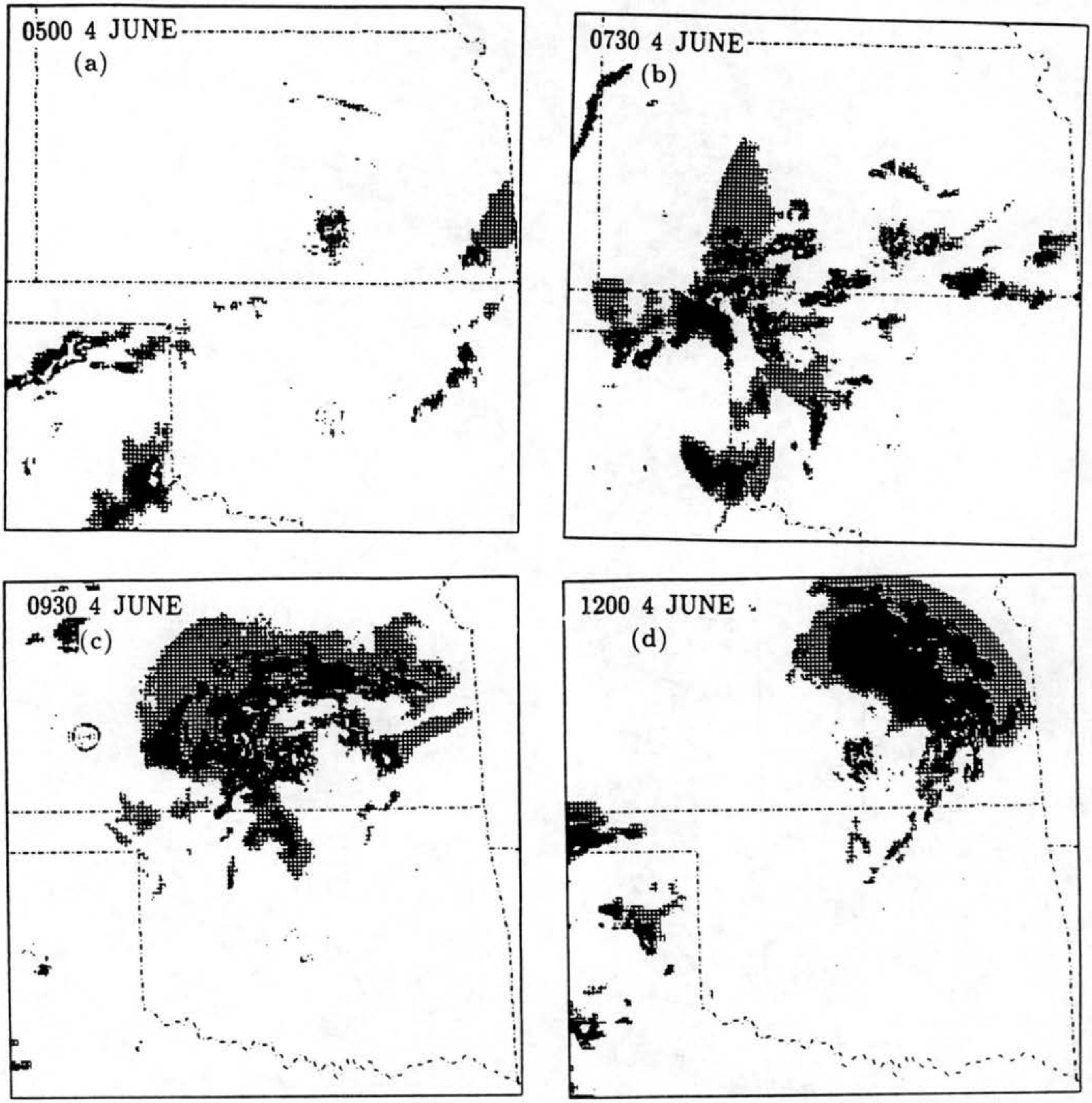

Figure 5.20: Same as Fig. 5.2 except for 4 June at: a) 0500 UTC Amarillo TX, Oklahoma City OK and Wichita KS; b) 0730 UTC Amarillo TX, Garden City and Wichita KS, Oklahoma City OK; c) 0930 UTC Amarillo TX, Garden City and Wichita KS, Oklahoma City OK; d) 1200 UTC Amarillo TX and Wichita KS.

3-4 June MCS was still evident in extreme southeastern Kansas, and a portion of another MCS which never entered the mesonet was visible in the southern Texas panhandle. By 0730 (Fig. 5.20b) several areas of disorganized convection developed in southern Kansas and northern Oklahoma. The MCS itself was visible in central and western Kansas with largely random convection also associated with it. The extent of the stratiform precipitation was difficult to determine due to the inability of the Garden City, Kansas radar to detect the light precipitation. By 0930 (Fig. 5.20c) an east-west oriented convective line formed in the northern portion of the MCS, and it had a limited area of light stratiform precipitation to its north. There was also a fairly linear north-south oriented convective structure in the south-central portion of the MCS. There was a region of enhanced stratiform precipitation to the rear of the northern portion of this line. By 1200 (Fig. 5.20d) the east-west convective line dissipated. Just after 0930 the southern convection also had largely dissipated except for an intense single cell. But by 1200 a small, broken line of convection redeveloped. Also an area of enhanced stratiform precipitation was found to the rear of the northern portion of this line, giving this system an asymmetric structure, from what had been very random convection. After 1230 the entire system rapidly dissipated.

5.4.3 System overview

Low-level flow prior to MCS development (0430-0600)

After the passage of the 3-4 June MCS, the atmosphere in Kansas became stabilized due to the pronounced drying associated with the mesoscale downdrafts in its wake. This can be seen in the 850 mb map at 0430 (Fig. 5.21a) which shows that the dewpoints in Kansas were fully 4-10°C lower than in Oklahoma. There was a very strong southerly flow (10-15 m s^{-1}) in Oklahoma, however, advecting moist air into Kansas. By 0600 at 850 mb (Fig. 5.21b) the low-level jet veered to the south or southwest in Kansas and strengthened to 15-20 m s^{-1}. Notice the approximately 6°C dewpoint rise in southern Kansas. As pointed out by Trier and Parsons (1992), this, combined with the horizontal speed convergence over Kansas, and the ascent of the southerly flow over the front, led to a destabilization of the atmosphere along and to the north of the surface front.

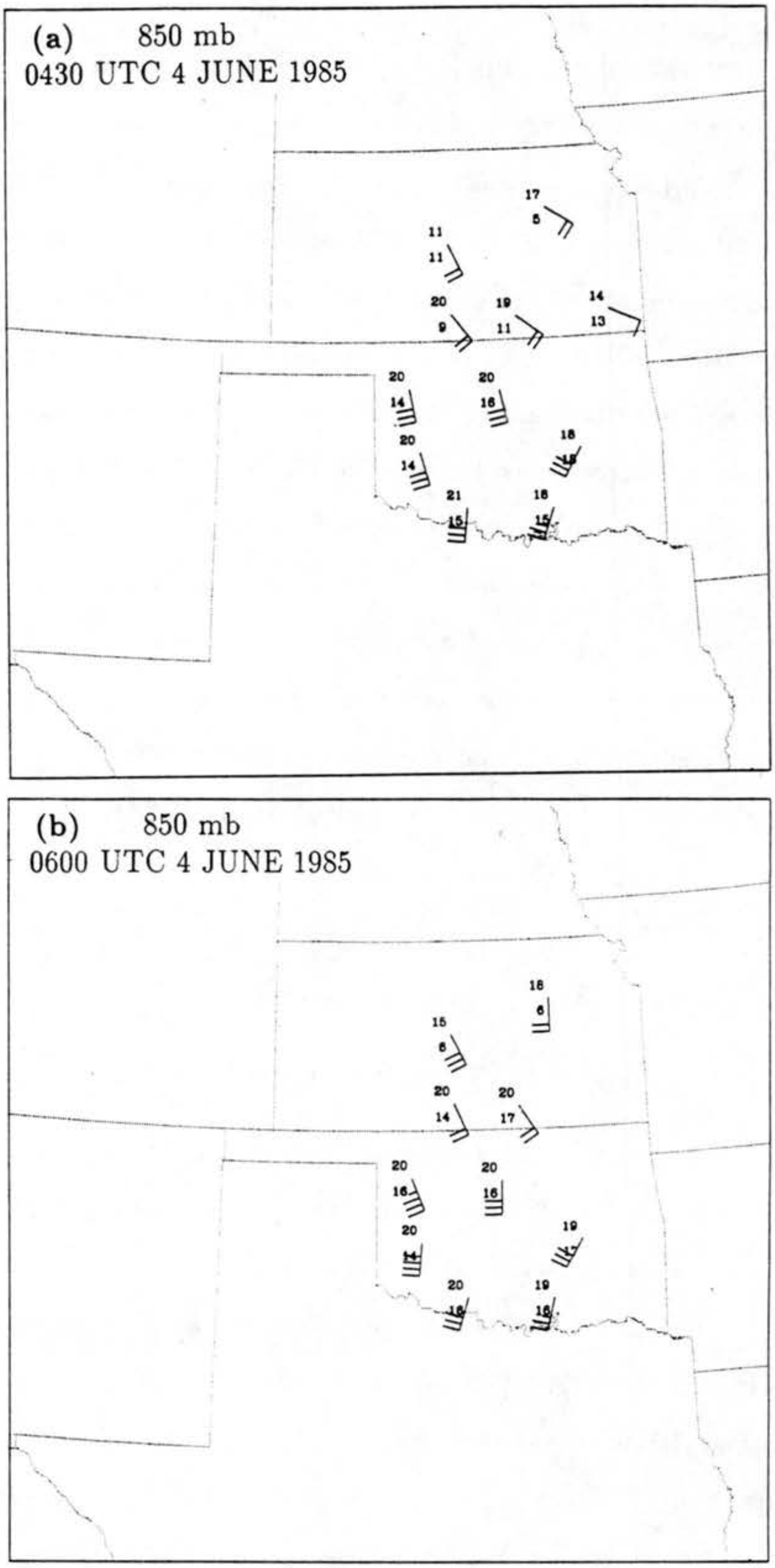

Figure 5.21: Same as Fig. 5.10 except for 4 June at: a) 0430 UTC at 850 mb; b) 0600 UTC at 850 mb.

Development stage (0800)

At this time (Fig. 5.22) there was a weak low in eastern Kansas which in all likelihood arose from the subsidence to the rear of the 3-4 June case convection. A pre-squall low was found in between two areas of intense convection in extreme southern Kansas. Another low was found on the southern end of the system, which was a semi-permanent feature along the front, but it was a little deeper at this time, possibly also due to compensating subsidence from adjacent deep convection. The mesohighs were quite weak and highly localized, being associated with the areas of convection. The flow was southerly only in southern Oklahoma, to the north it was easterly. The flow within the system was disorganized due to the disorganized nature of the system itself.

Intensification of mesohigh and wake low (0830-0930)

This was a period of rapid change in the pressure structure of this MCS. At 0830 (Fig. 5.23) the flow within the system was still very disorganized. The mesohighs were of about the same strength and still centralized over the convective areas. A wake low feature also appeared on the back edge of a small area of stratiform precipitation. By 0930 (Fig. 5.24) the mesohighs extended their coverage and were now centered within the areas of stratiform precipitation. There were now two wake lows with one on the south side and the other on the north side of an area of enhanced stratiform precipitation. There was quite intense divergence occurring to the rear of the mesohigh in the central portion of the MCS. Strong convergence was occurring just to the rear of the southern wake low axis. All three of these features strengthened by 1-2 mb, giving rise to a strong gradient which tended to conform to the shape of the back edge of the stratiform precipitation region.

Expansion of stratiform region (1030-1230)

By 1030 (Fig. 5.25) the southernmost of the two wake lows dissipated, and the remaining one filled by 1 mb. The mesohigh also moved more towards the eastern portion of the MCS, thereby weakening the gradient considerably. Hence the divergence to the rear of the mesohigh weakened. The wake low was still along the back edge of an enhanced region of stratiform precipitation. The flow through the wake low was weak (5 m s^{-1}).

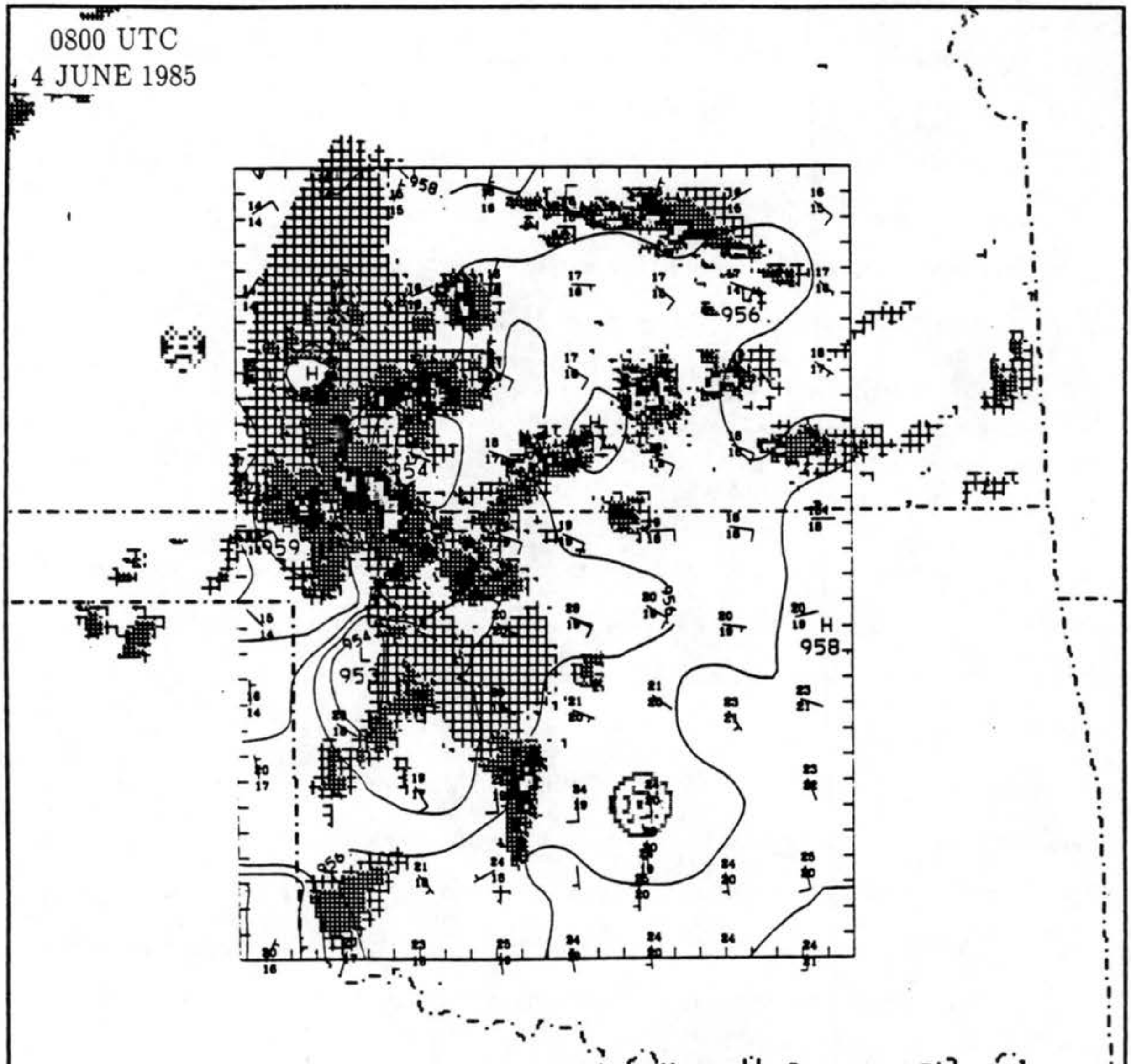

Figure 5.22: Same as Fig. 5.3 except for 0800 UTC 4 June.

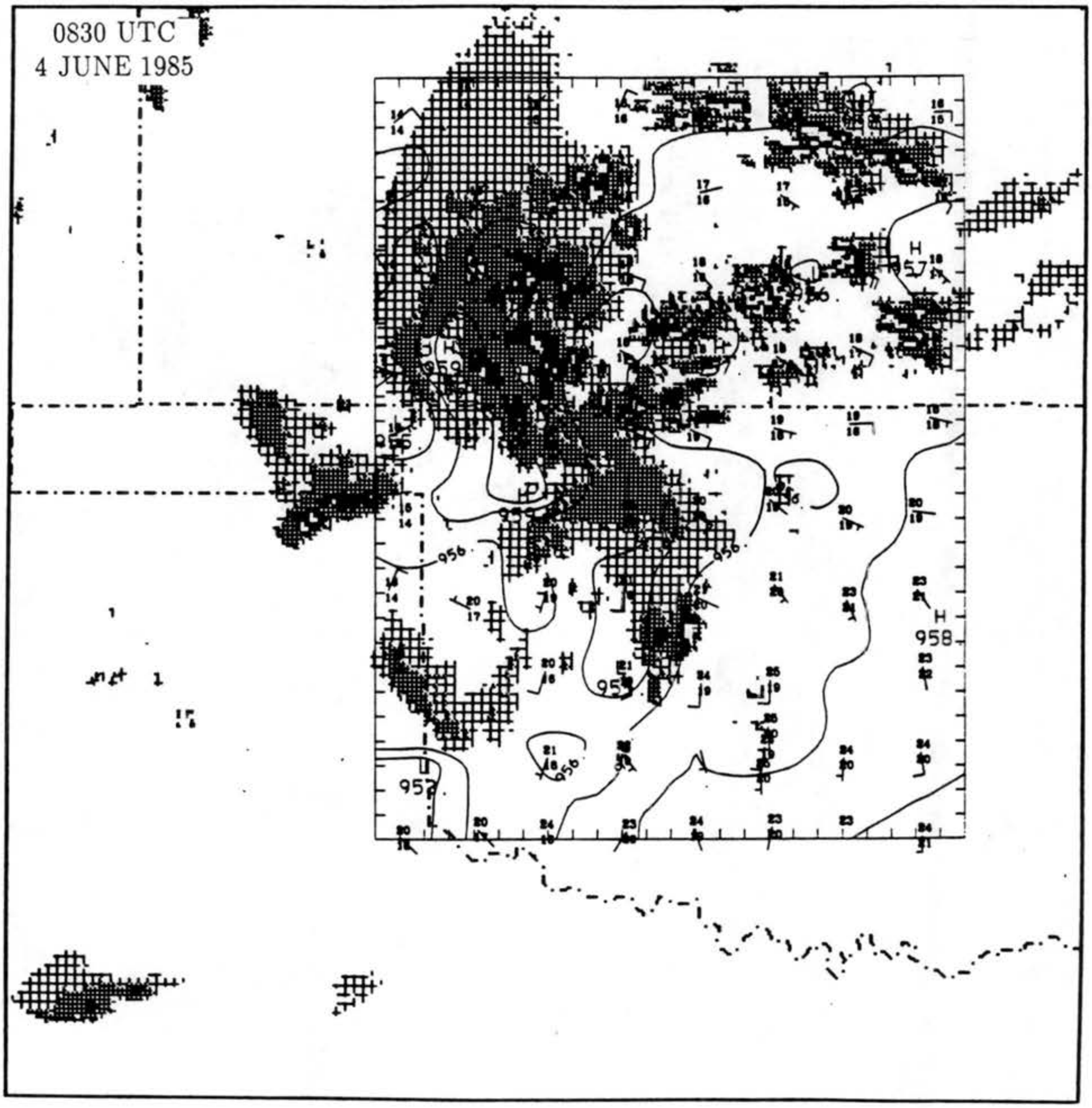

Figure 5.23: Same as Fig. 5.3 except for 0830 UTC 4 June.

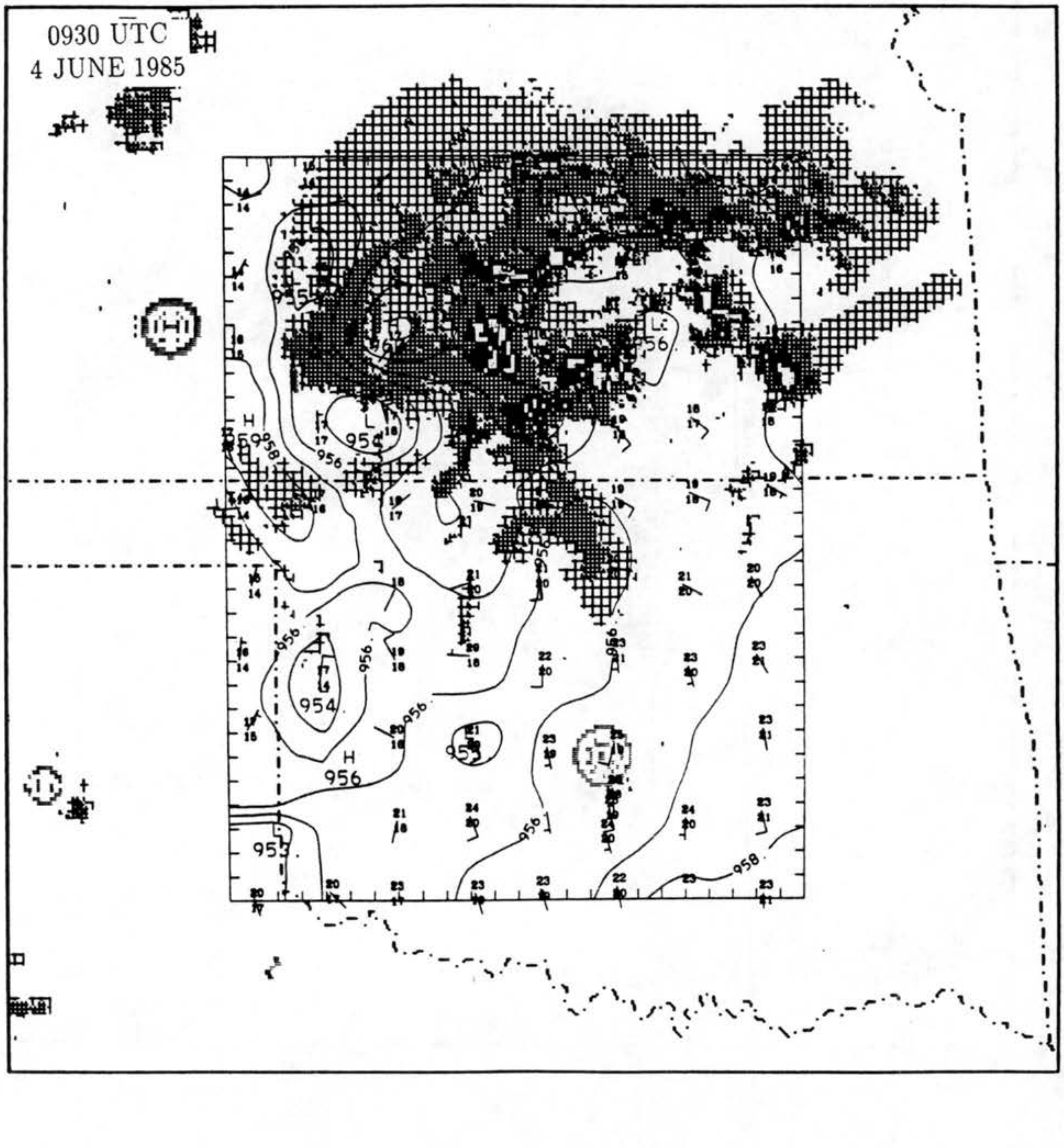

Figure 5.24: Same as Fig. 5.3 except for 0930 UTC 4 June.

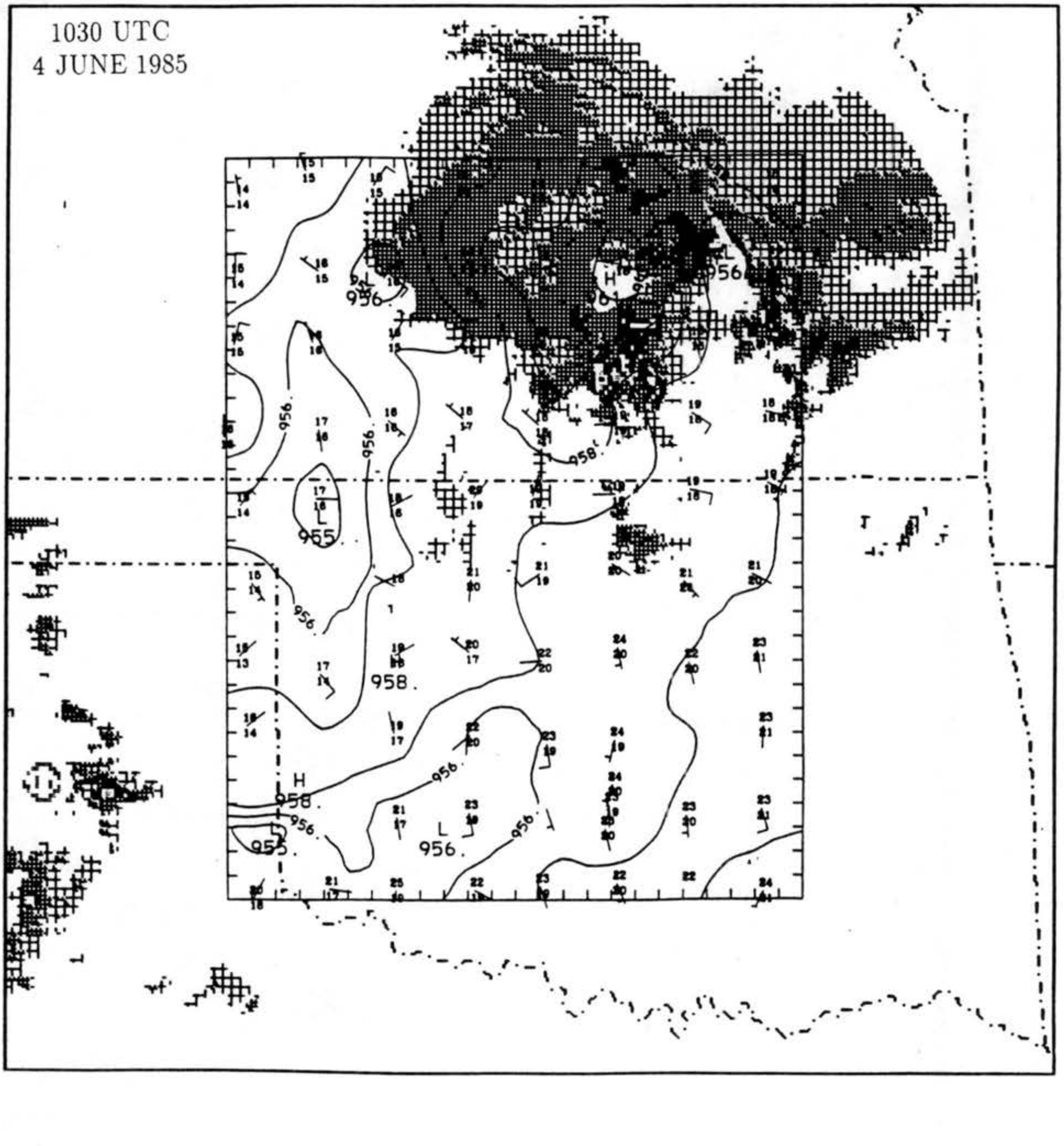

Figure 5.25: Same as Fig. 5.3 except for 1030 UTC 4 June.

There was also some convergence to the rear of the wake low as the wind shifted to northeasterly to the rear of the wake low. There was no pronounced surface outflow ahead of this system. By 1130 (Fig. 5.26) the wake low deepened by 1 mb and the mesohigh again associated itself with an area of strong convection. There was a rapid increase in pressure to the rear of the MCS and a shift to north-northwest flow. This feature did not reflect the passage of a cold front though, since there was no change in the temperature nor dewpoint in this area. By 1230 (Fig. 5.27) the pressure features mostly moved outside of the mesonet. The wake low was still partially present at the back edge of the region of enhanced stratiform precipitation. The patterns to the rear of the system were quite complex with two troughs of low pressure separating the southerly flow to the south from the easterly flow to the north. The southern trough was along the quasi-stationary front, while the northern trough was of unknown origin.

5.4.4 Mesonet time series

The conditions in the northern wake low region are summarized by station P10 (Fig. 5.28, see Fig. 3.1). In this region there was not a mesohigh feature since the convection passed to the south and east of this station. The pressure gradient associated with the wake low (0940) was fairly weak with a 3 mb decrease in 30 min, concentrated in a 2 mb decrease in 10 min. The wind shifted from northwest to southeast as the low passed, and there was a 17 m s^{-1} gust. Then after the low passed there was a shift to northwest flow and a 1°C temperature and 0.5°C dewpoint increase which occurred in advance of the passage of the post-MCS northern trough (the lower pressure at 1100) and then the values recovered to previous levels.

The southern wake low and trough are shown by P19 (Fig. 5.29). The convection did pass through this region and hence there was a mesohigh (0900) with a 2.5 mb increase in 15 min and was accompanied by a 0.5°C temperature and dewpoint decrease, a shift from easterly to southwesterly flow and a 14 m s^{-1} wind gust. Then the wake low (1020) passed by with a 4 mb decrease in 15 min, a weak 9 m s^{-1} wind gust and a shift from southwest to northeast flow. Then there was a short pressure increase of 1 mb in 10 min which was accompanied by a 1°C drying and a temporary shift to northwesterly flow. Then the

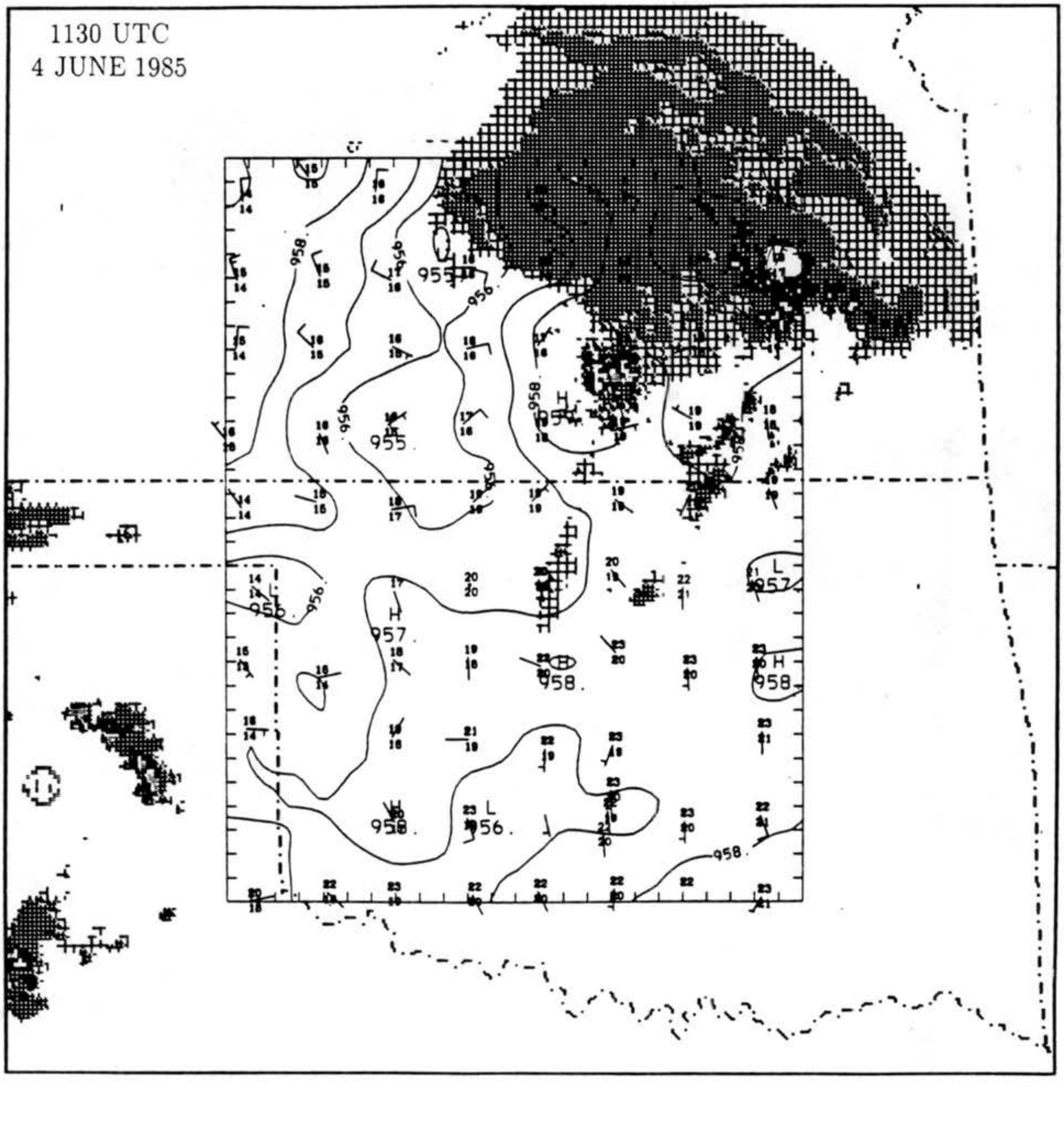

Figure 5.26: Same as Fig. 5.3 except for 1130 UTC 4 June.

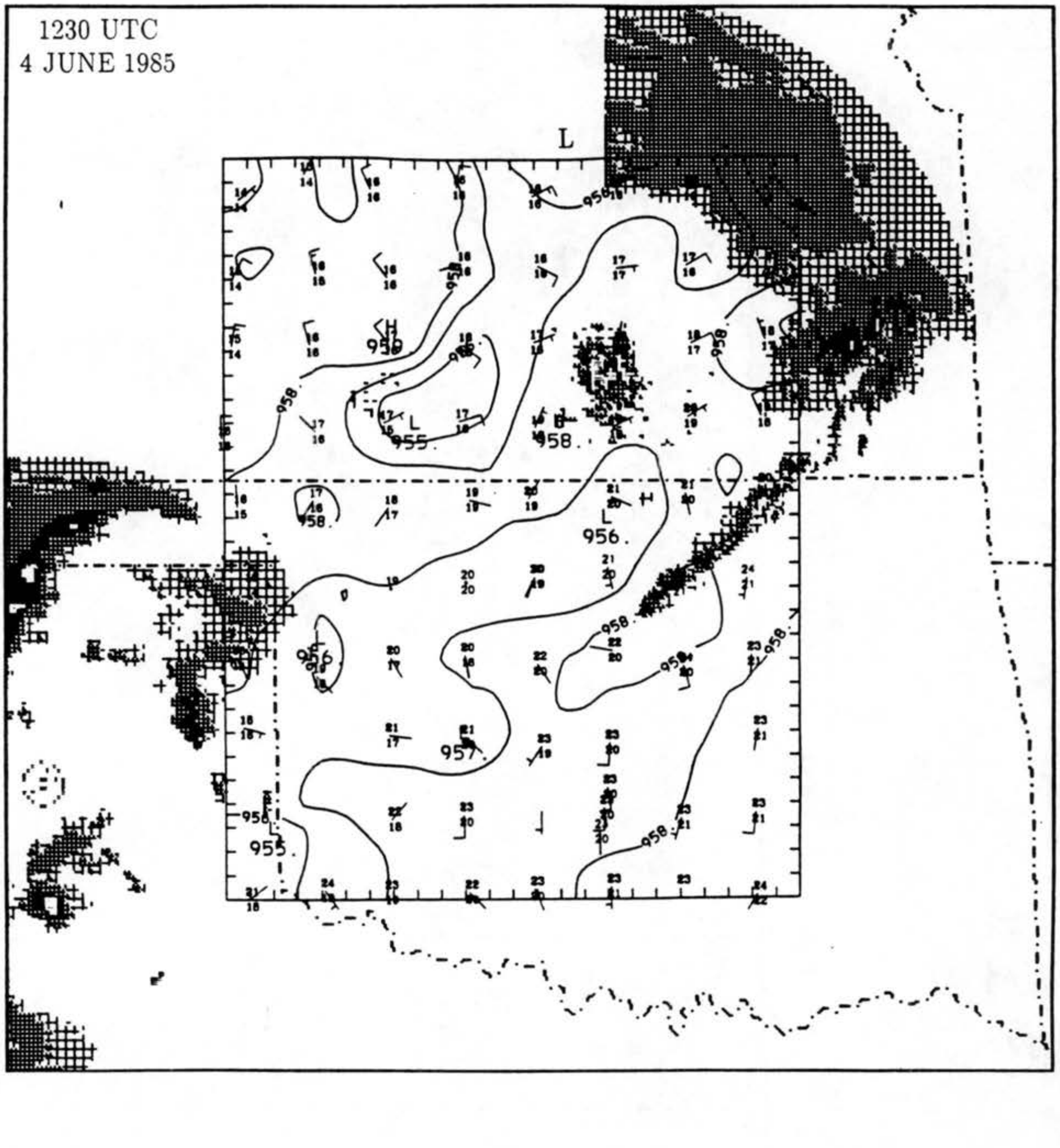

Figure 5.27: Same as Fig. 5.3 except for 1230 UTC 4 June.

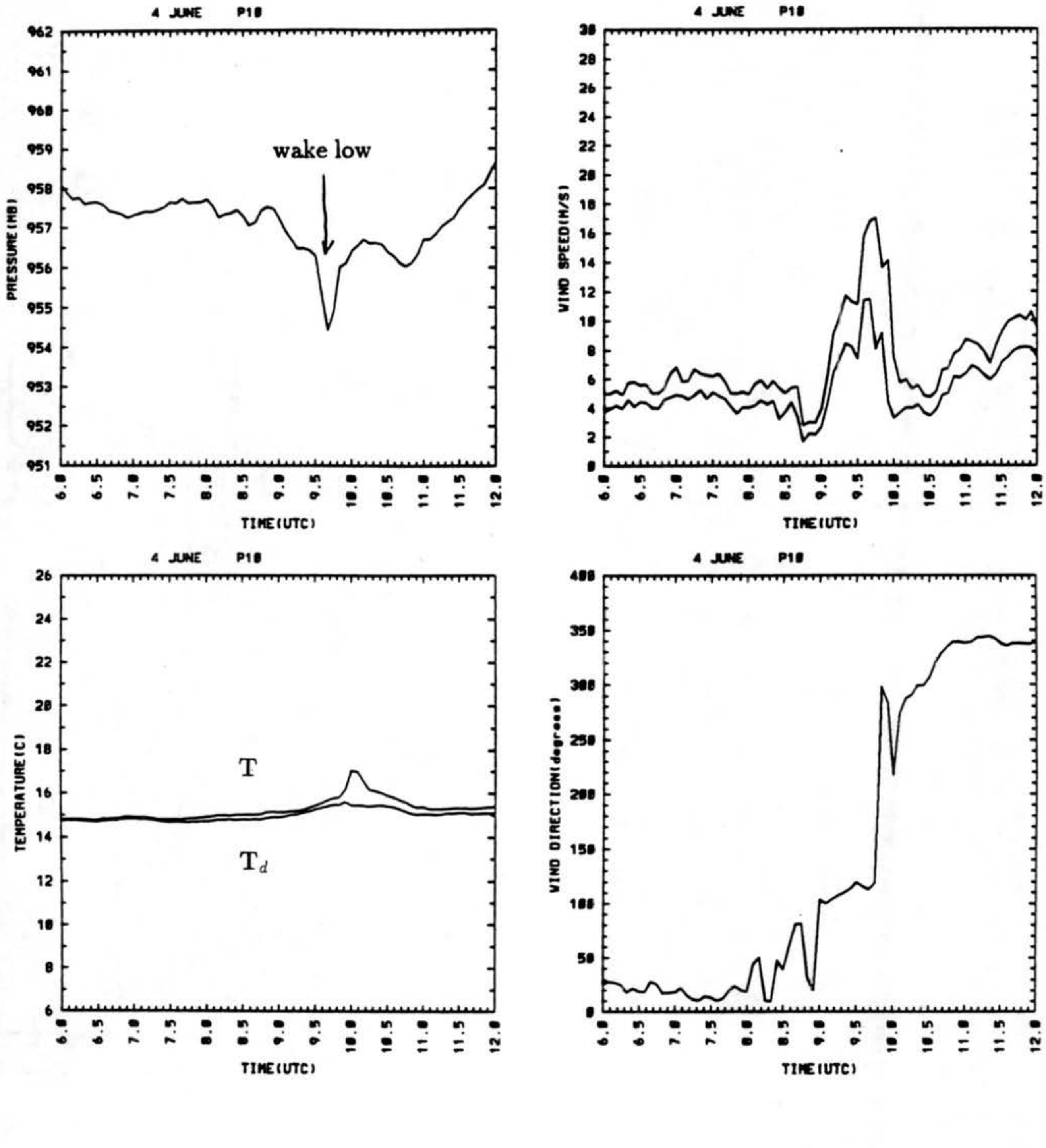

Figure 5.28: Same as Fig. 5.9 except for 4 June at station P10.

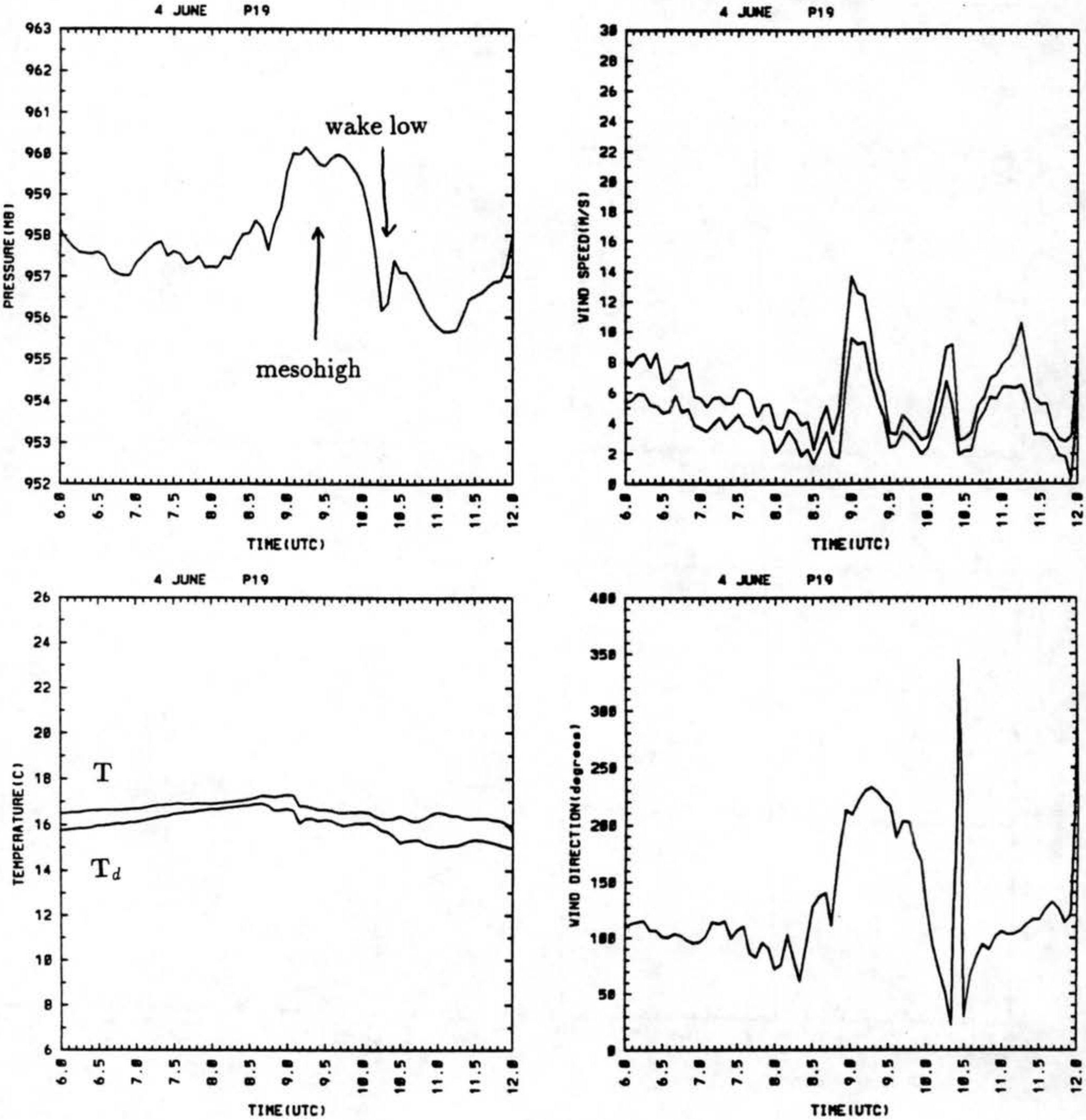

Figure 5.29: Same as Fig. 5.9 except for 4 June at station P19.

trough feature (1100) passed over with a 2 mb decrease in 30 min, a 0.5°C temperature (dewpoint) increase (decrease), a 11 m s^{-1} gust and a shift back to southeast flow. Then as the pressure rose again, there was a 0.5°C decrease in the temperature and dewpoint, a 10 m s^{-1} wind gust as well as a shift back to northwest flow.

5.5 June 9 case

5.5.1 Synoptic overview

The large-scale environment associated with the initial development of this system is summarized by the 0000 9 June maps. At the surface (Fig. 5.30a) there was a deep 990 mb low over central Canada (not visible) with an occluded front extending southward to northern Wisconsin, then a cold front extended to the southwest through southeastern Nebraska and northwestern Kansas. It was very warm on both sides (except far to the north) of the front (26-32°C north; 32-41°C south). To the south of front in eastern Kansas it was very moist (18-26°C) while it was considerably drier to the west (12-18°C), and it was even drier to the north of the front (7-12°F). The flow was southerly to the south and northerly to the north of the front.

At 850 mb (Fig. 5.30b) a closed low was indicated over central Colorado and there was a strong southwest flow across northwestern Texas, Oklahoma and Kansas, which becomes a northeast flow in western Nebraska. At 500 mb (Fig. 5.30c) the flow over Kansas, Oklahoma and northern Texas was very light (5 m s^{-1}) and was out of the north-northwest. A general ridge existed over the southwestern and south-central U.S.

5.5.2 Radar overview

The initial development of this MCS occurred along the Front Range in Colorado as disorganized convection around 2200 8 June (not shown). By 0635 (Fig. 5.31a) there were two distinct MCSs. The northern one (over southern Nebraska and northern Kansas) was much more intense but passed to the north of the mesonet. The system of interest here was in southeastern Colorado, and was shown as having two cores of convection surrounded by a small amount of light stratiform precipitation. By 1035 (Fig. 5.31b) both MCSs were progressing to the east. The system of interest here seems to have taken on an

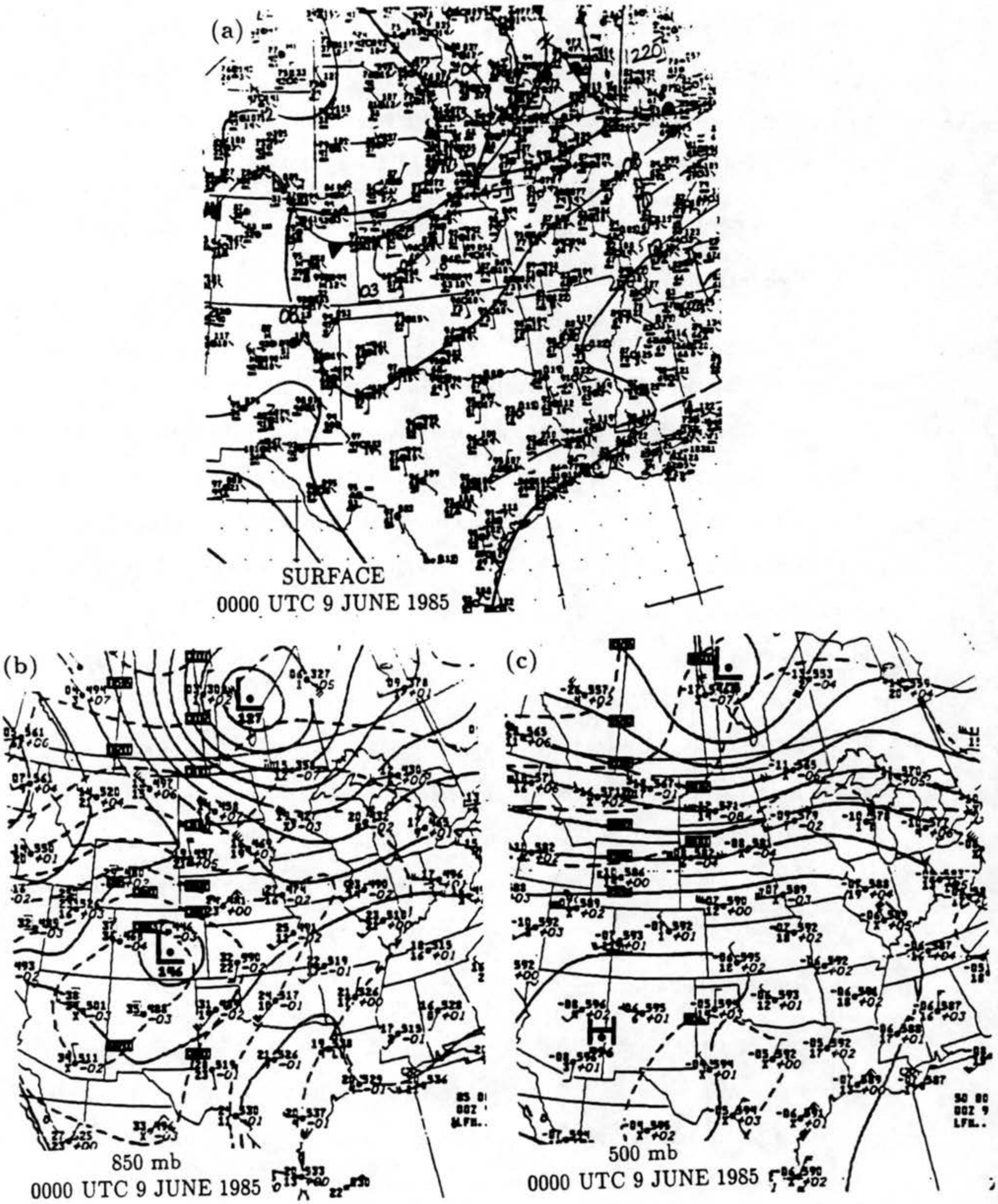

Figure 5.30: Same as Fig. 5.1 except for 0000 UTC 9 June.

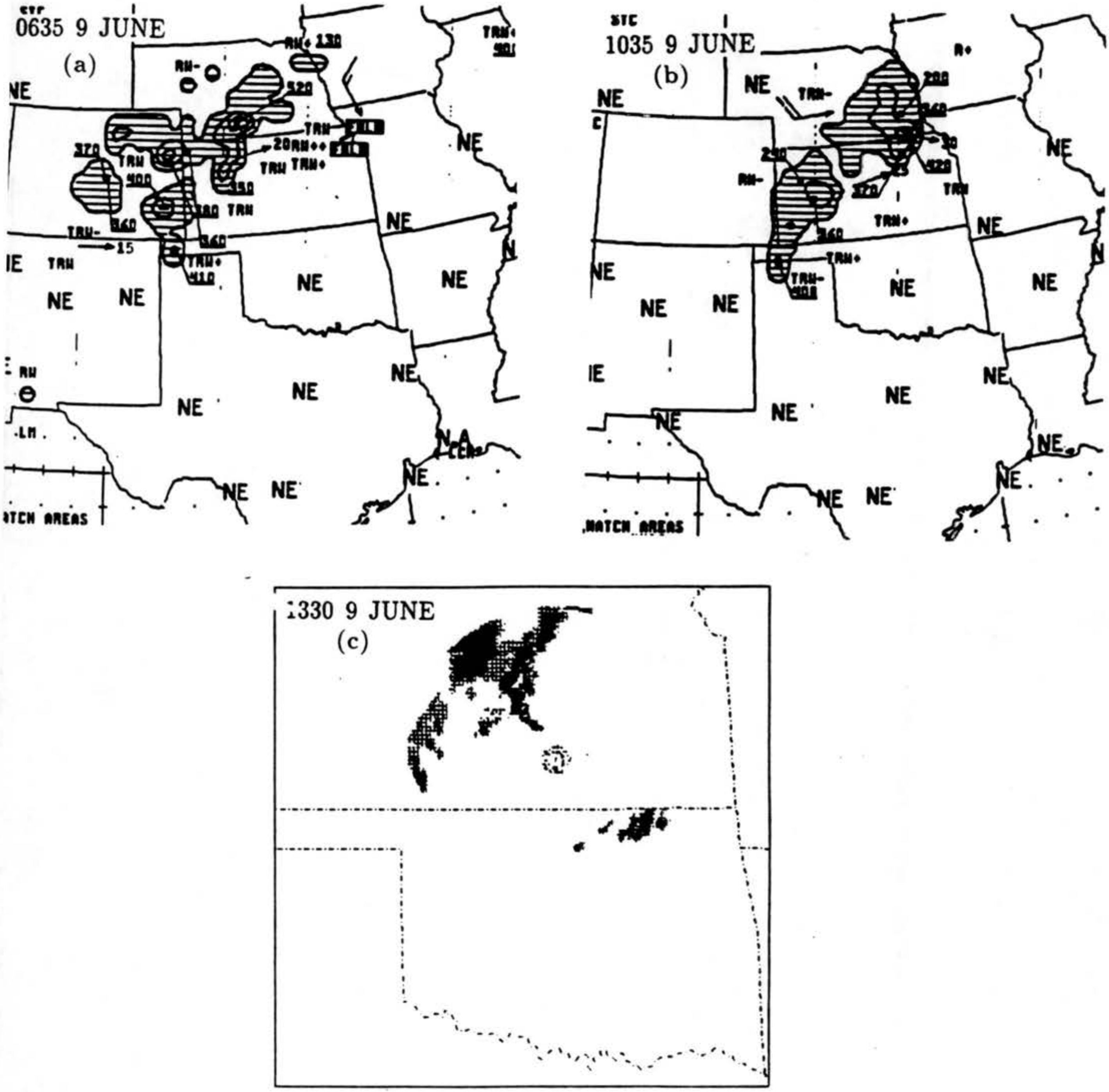

Figure 5.31: In a-b) NMC radar summary charts for 9 June at: a) 0635 UTC; b) 1035 UTC. In c-g) Same as Fig. 5.2 except for 9 June at: c) 1330 UTC; d) 1500 UTC; e) 1630 UTC; f) 1730 UTC; g) 1930 UTC. All using Wichita KS.

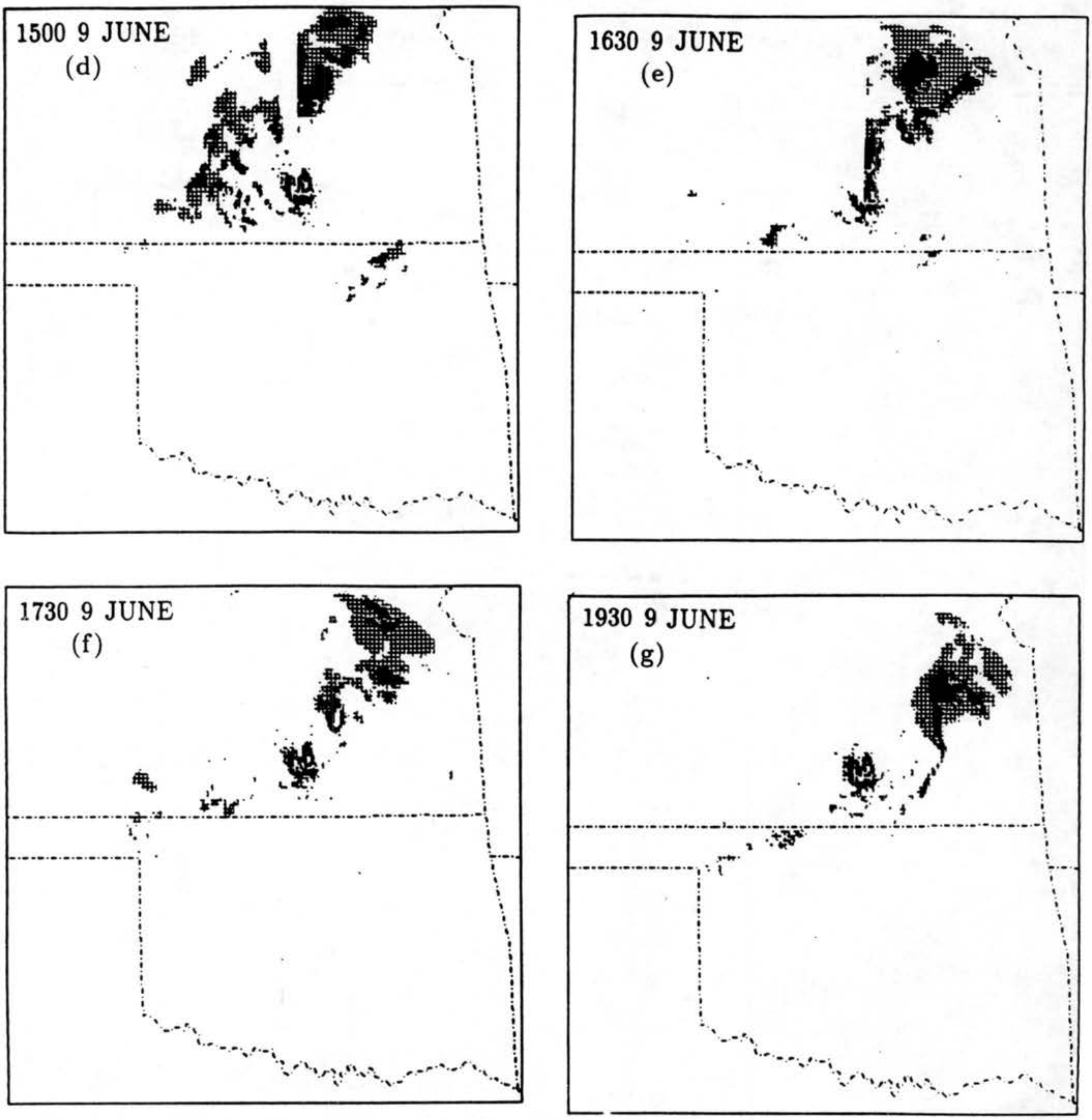

Figure 5.31: Continued.

asymmetric structure, but the resolution of the NMC analyses is insufficient to precisely determine its structure. There was a leading, broken line of convective cells that was quite weak and an area of light stratiform precipitation to the rear of the northern portion of this line. By 1330 (Fig. 5.31c) the MCS moved into the range of the Wichita radar. The system was composed of a leading convective line, a transition zone and a trailing region of enhanced stratiform precipitation, although the precipitation covered a small area. There was another, weaker area of convection to the southwest. By 1500 (Fig. 5.31d) there was a broken line of northeast-southwest oriented convection with a small area of stratiform precipitation trailing each of the convective areas, but there did not appear to be any organized structure. By 1630 (Fig. 5.31e, part of the data are missing at this time) the convection on the northern end had largely dissipated and the system appeared to have an asymmetric structure with a leading line of very weak convection, except on its southern end where the cells were more intense, and a region of enhanced stratiform precipitation to the rear of its northern end. By 1730 (Fig. 5.31f) the original MCS was exiting the mesonet in extreme northeastern Kansas. A very intense single convective cell developed to its southwest, just to the northeast of the ground clutter associated with Wichita. By 1930 (Fig. 5.31g) the earlier MCS had dissipated, except for the convection on its southern end which evolved over a two-hour period to a completely separate asymmetric-type MCS. This MCS was of such small scale (100-150km) that it is not included in the conclusions derived from this summary.

5.5.3 System overview

Stong mesohigh/wakelow just entering mesonet (1200)

At this time (Fig. 5.32) the cold front extended from southeastern Kansas through northwestern Oklahoma as evidenced by the shift from southerly to northeasterly flow. The air north of the front was extremely dry with dewpoints of 5-10°C. The MCS had a very well defined mesohigh associated with it. It also had a weak (5 m s^{-1}) outflow, as shown by the shift from northeast to northerly flow at the southern end of the system. The flow to the rear of the system, in response to the strong pressure gradient, shifted to easterly.

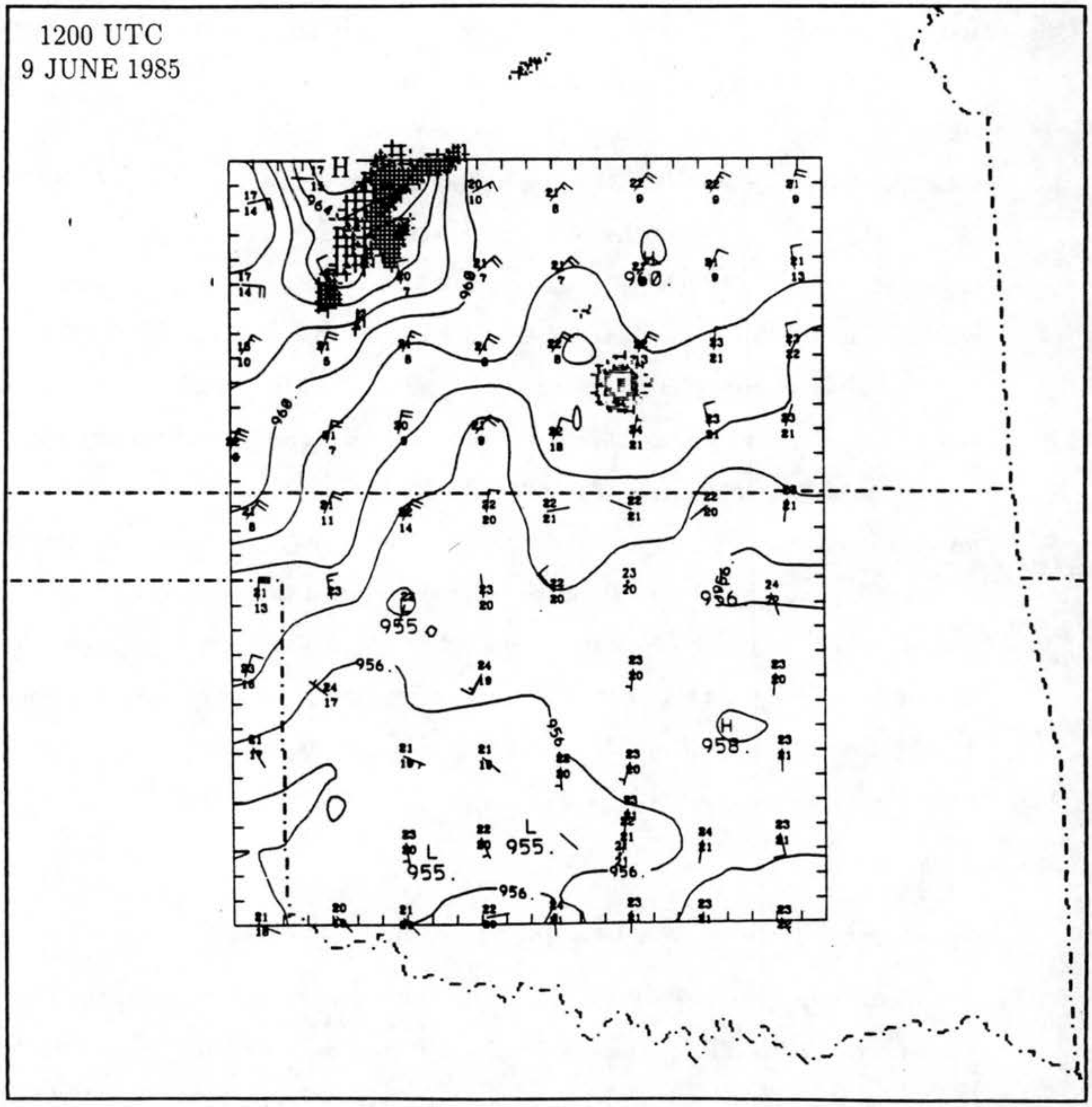

Figure 5.32: Same as Fig. 5.3 except for 1200 UTC 9 June.

Southward growth of convection (1330)

At this time (Fig. 5.33) a weak pre-squall low developed. The mesohigh was still of the same intensity and was spread over the convective and stratiform precipitation regions. The convective regions intensified and expanded farther to the south in the past 90 min. There was still a westerly outflow ahead of the system (10 m s^{-1}) as well as a northerly outflow to the south of the MCS (5-10 m s^{-1}). The pressure pattern to the rear of the MCS was quite complex. A wake low was found at the back edge of the region of enhanced stratiform precipitation. A much deeper low was found to the rear of the southern portion of the system. Due to the lack of radar data, its positioning cannot be determined, but it was affecting the flow leading to 10-12.5 m s^{-1} easterly flow in this region.

Expansion of mesohigh/wake low (1430)

By this time (Fig. 5.34) it is seen that the intense low in southern Kansas was along the back edge of the southern portion of the system. But this feature differs from the previous wake lows since there was actually minimal precipitation of any sort occurring at the southern end of the MCS. This low was also not associated with the cold front since the cold front was already well into central and southern Oklahoma. The low was still leading to a shift from the prevailing northeast flow to a more easterly flow. The mesohigh was still of the same strength and now covered an expansive area.

Appearance of mesovortex (1730)

By this time (Fig. 5.35) the cold front was completely through western Oklahoma. The original MCS was now just visible in extreme northeastern Kansas. There was earlier a redevelopment of an enhanced stratiform precipitation region as well as a wake low along its back edge, but it was never viewed well by the mesonet. The new small scale system mentioned in the radar section was just developing. The pressure features associated with this small scale feature were quite intense, extremely complex, and were not always positioned as expected. The low which was to the rear of the southern portion of the system slowed its movement considerably, but was still moving slowly to the east. The true nature of this low was now becoming more clear. The visible satellite picture at

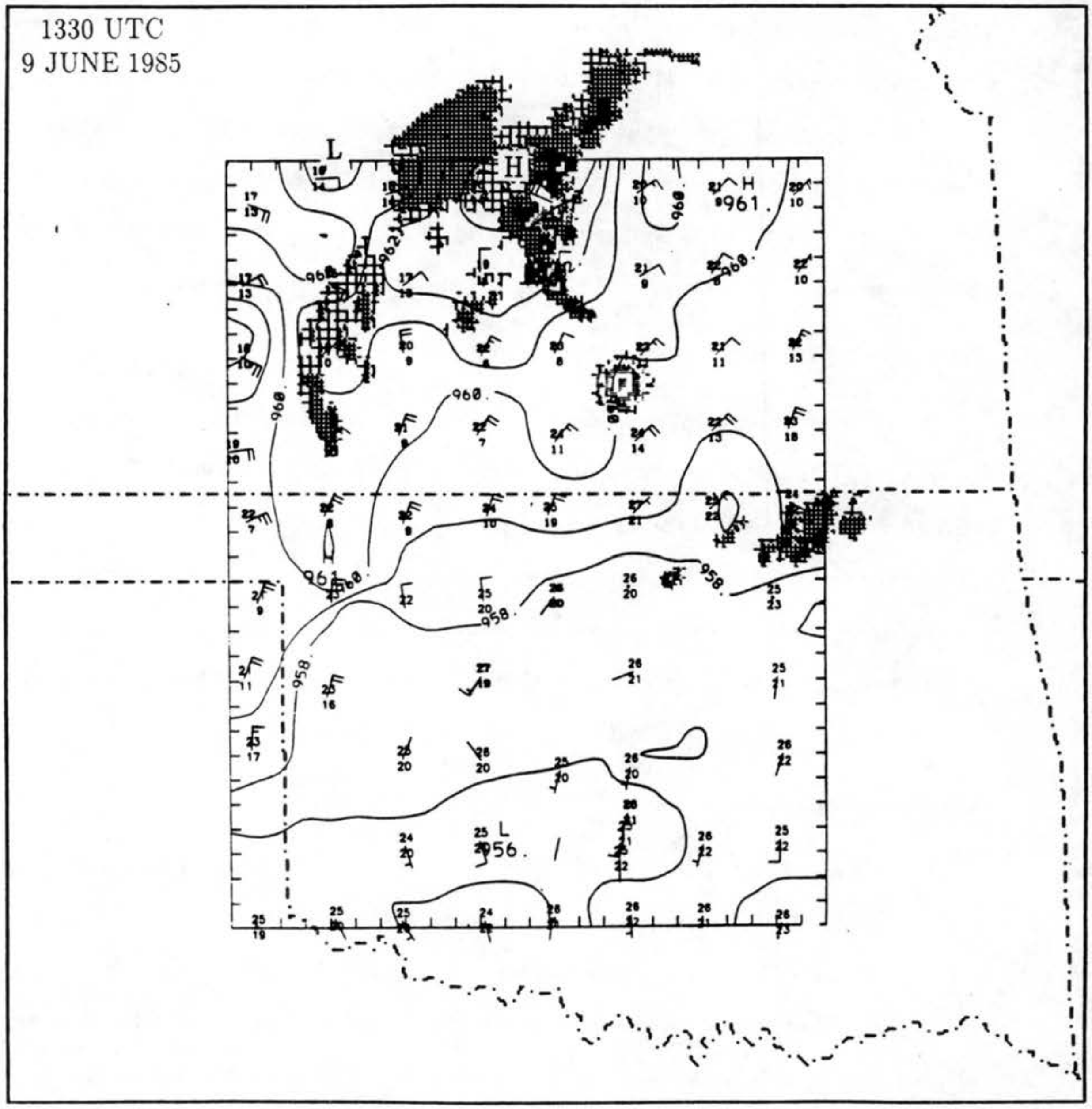

Figure 5.33: Same as Fig. 5.3 except for 1330 UTC 9 June.

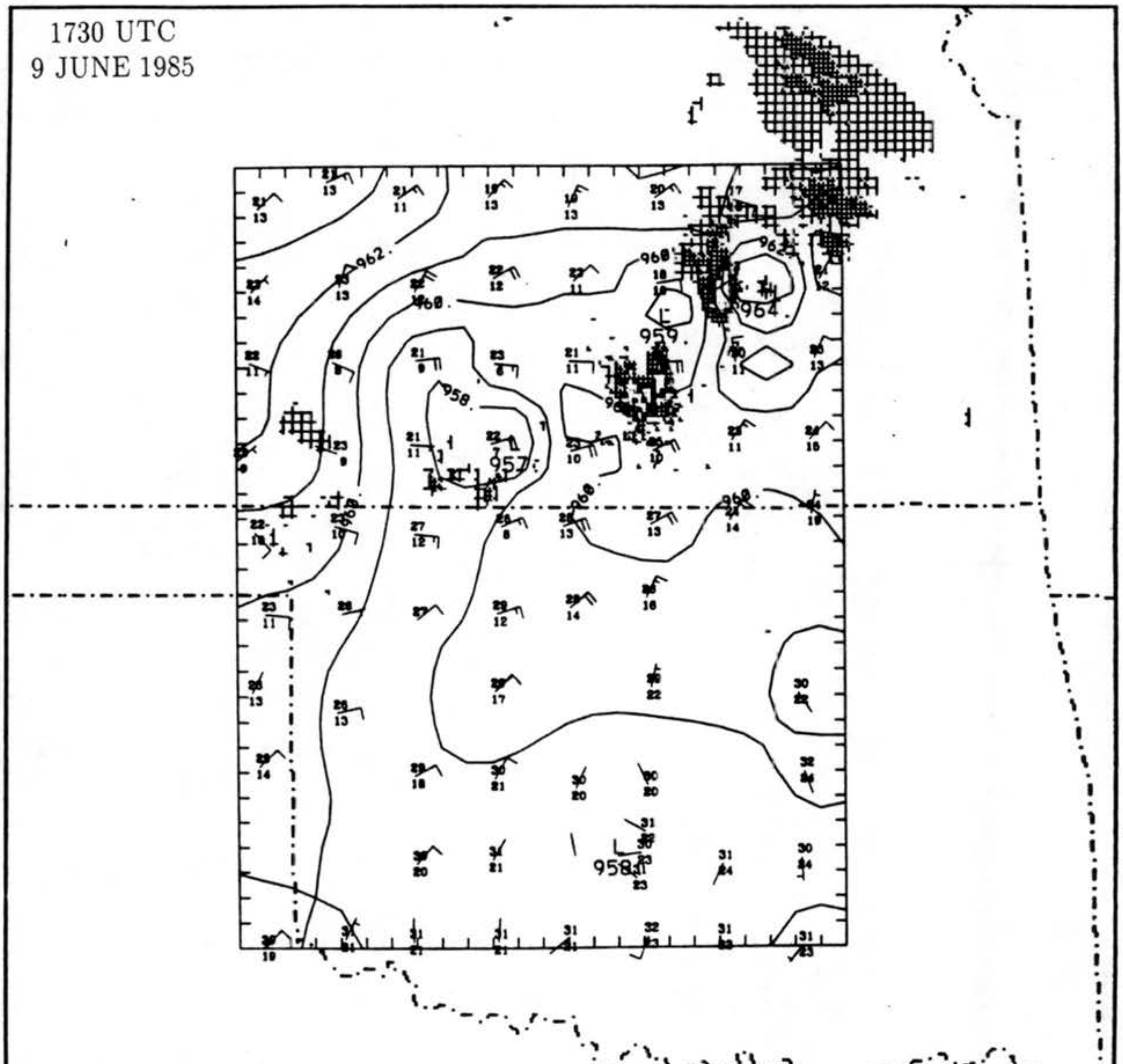

Figure 5.35: Same as Fig. 5.3 except for 1730 UTC 9 June.

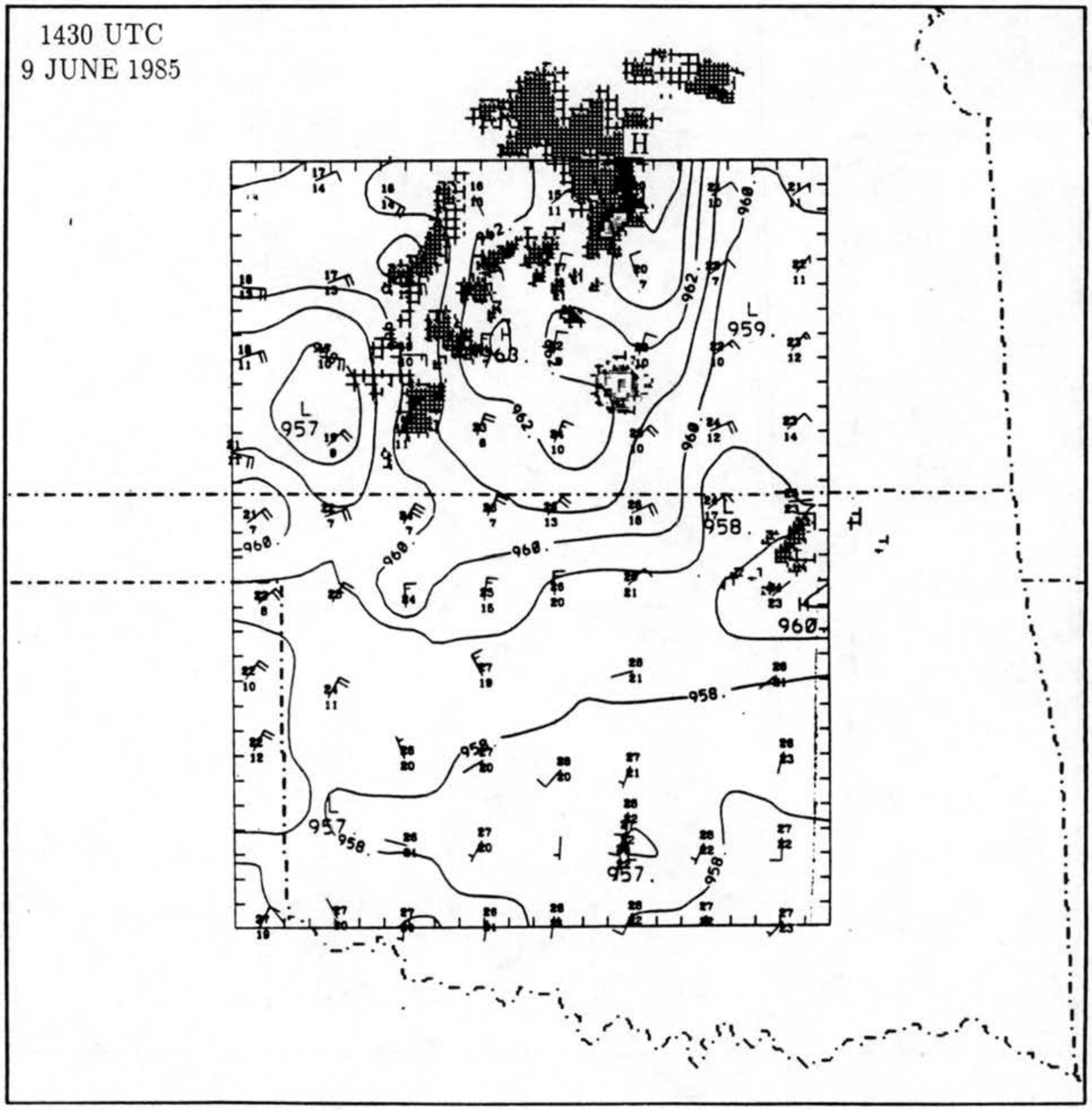

Figure 5.34: Same as Fig. 5.3 except for 1430 UTC 9 June.

this time (Fig. 5.36) shows a cyclonic curvature to the cloud field over central Kansas. This was apparently a mesovortex feature as was identified for this case by Bartels and Maddox (1991). There was not a mesovortex signature in either the 1200 9 June nor the 0000 10 June regular synoptic sounding network and, unfortunately, there were no special soundings taken. Given that this was a mesovortex, the low in southern Kansas appears to be a very intense surface representation of this mesovortex. It was positioned to the southwest of the presumed mesovortex center (the actual center was unclear due to the lack of sounding coverage). This apparent tilt of the mesovortex to the northeast with height is consistent with the observational findings of Johnson and Bartels (1992) as well as the modeling study of Zhang and Fritch (1988b).

5.5.4 Mesonet time series

The conditions associated with the northern portion of the MCS are summarized by station P01 (Fig. 5.37, see Fig. 3.1). The mesohigh (1100) was quite strong in this region with a 5 mb increase in 25 min, and it was accompanied by a 4°C temperature (dewpoint) decrease (increase) and a shift from northeast to westerly flow. There was also a drop in the wind speed which was probably partially due to the strength of the northeast flow ahead of the system as the wind was unable to adjust fast enough to the pressure field to allow for a stronger outflow. Then the wake low (1230) passed over with a 4.5 mb decrease in 30 min as well as a 14 m s^{-1} wind gust and a shift to easterly flow.

The conditions to the rear of the southern portion of the system are shown by P17 (Fig. 5.38). The first pressure increase (0930) was associated with the inital arrival of the mesohigh and the second (1200) was associated with the expansion of the coverage of the mesohigh. The first pressure increase was accompanied by a sharp dewpoint decrease but this was more due to the earlier cold frontal passage. There was a general strong flow to the rear of the cold front, but there was a weak shift from northeasterly to northerly flow. The second pressure increase was accompanied by a cooling of 4°C and a dewpoint increase of 6°C. The wake low was shown by a 5 mb decrease in 30 min, and was accompanied by a shift from northeast to southeast flow and a gust to 28 m s^{-1}.

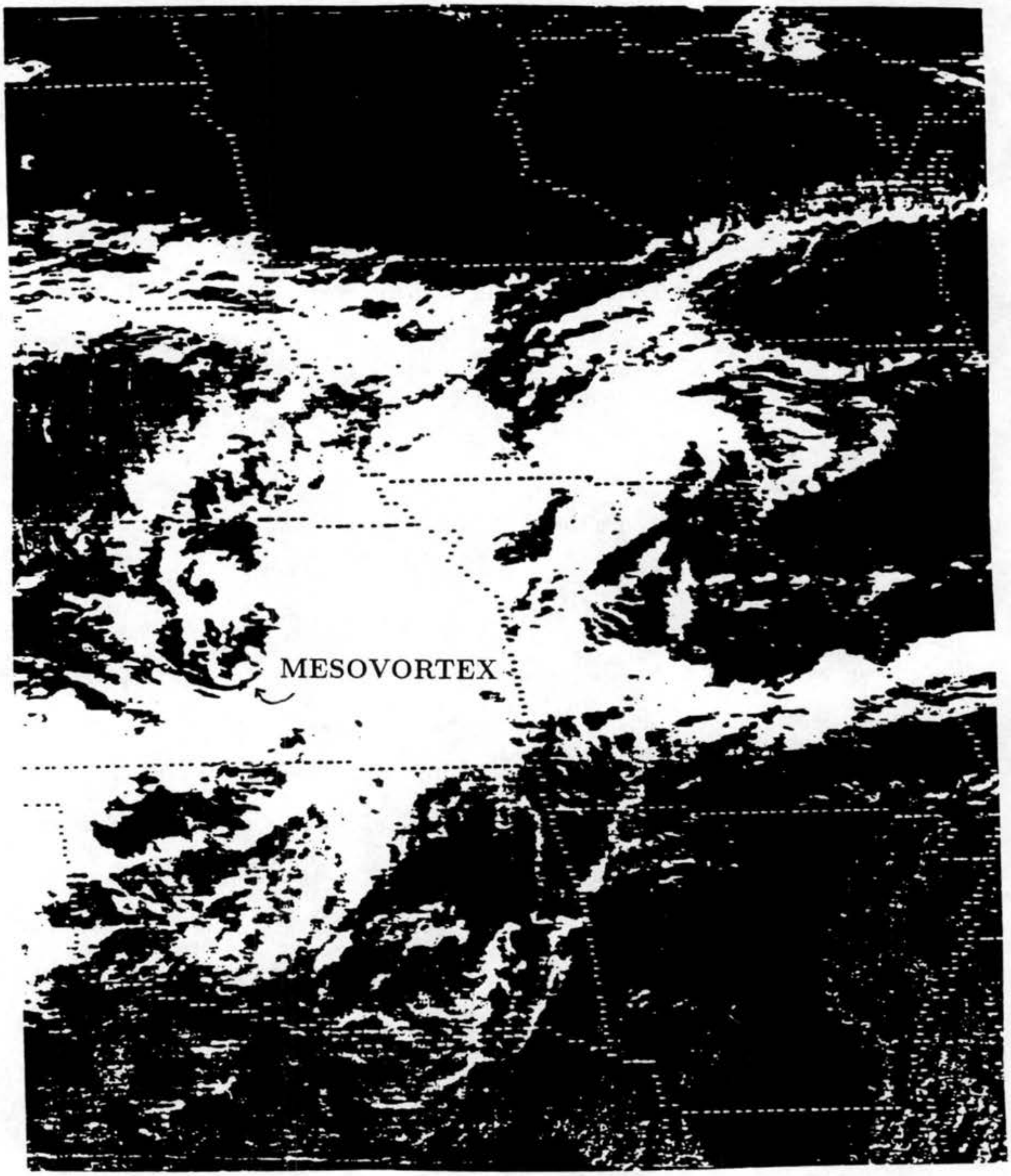

Figure 5.36: 1730 UTC 9 June 1985 visible satellite image.

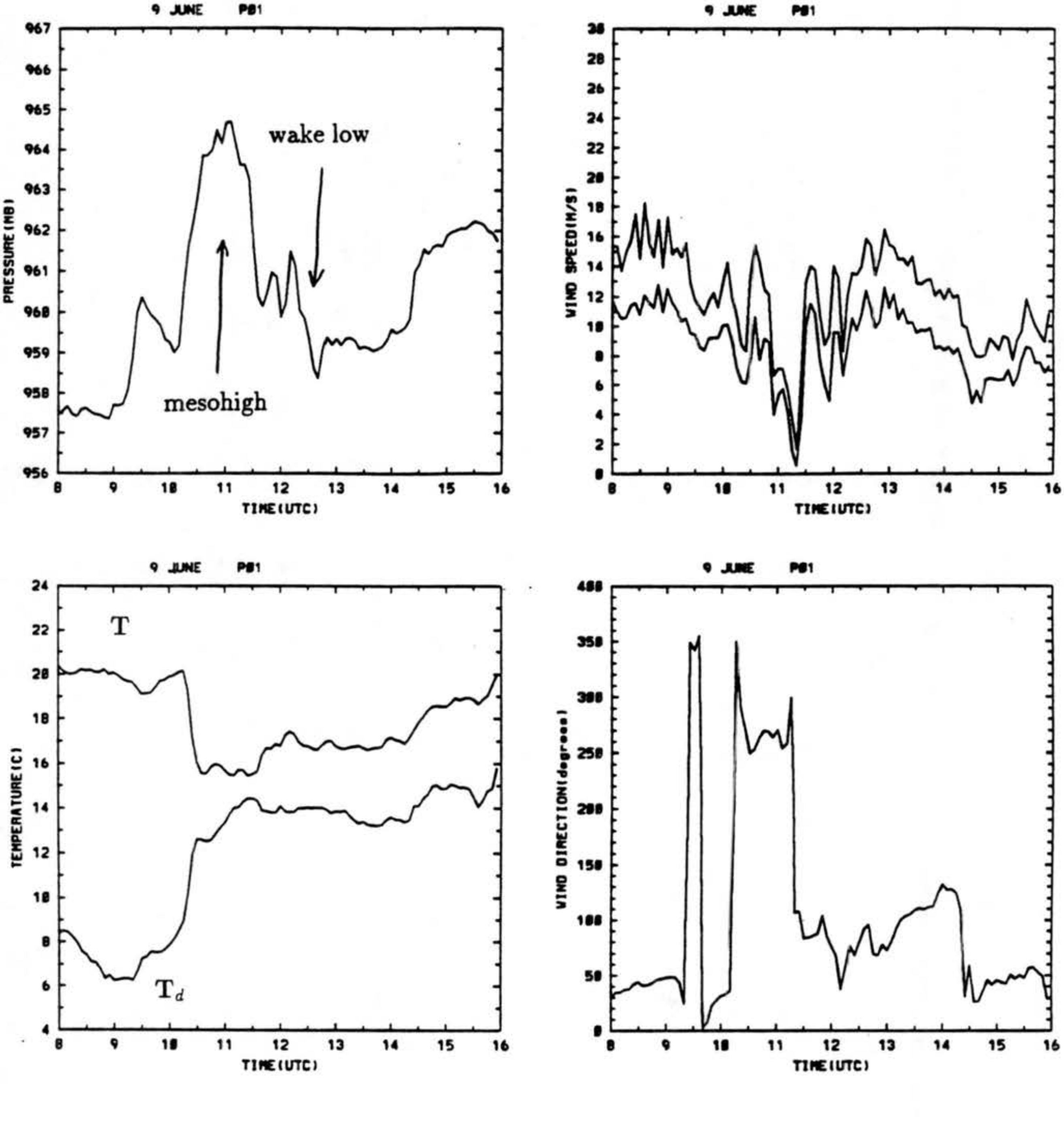

Figure 5.37: Same as Fig. 5.9 except for 9 June at station P01. Note different time scale as each tick mark represents 30 minutes.

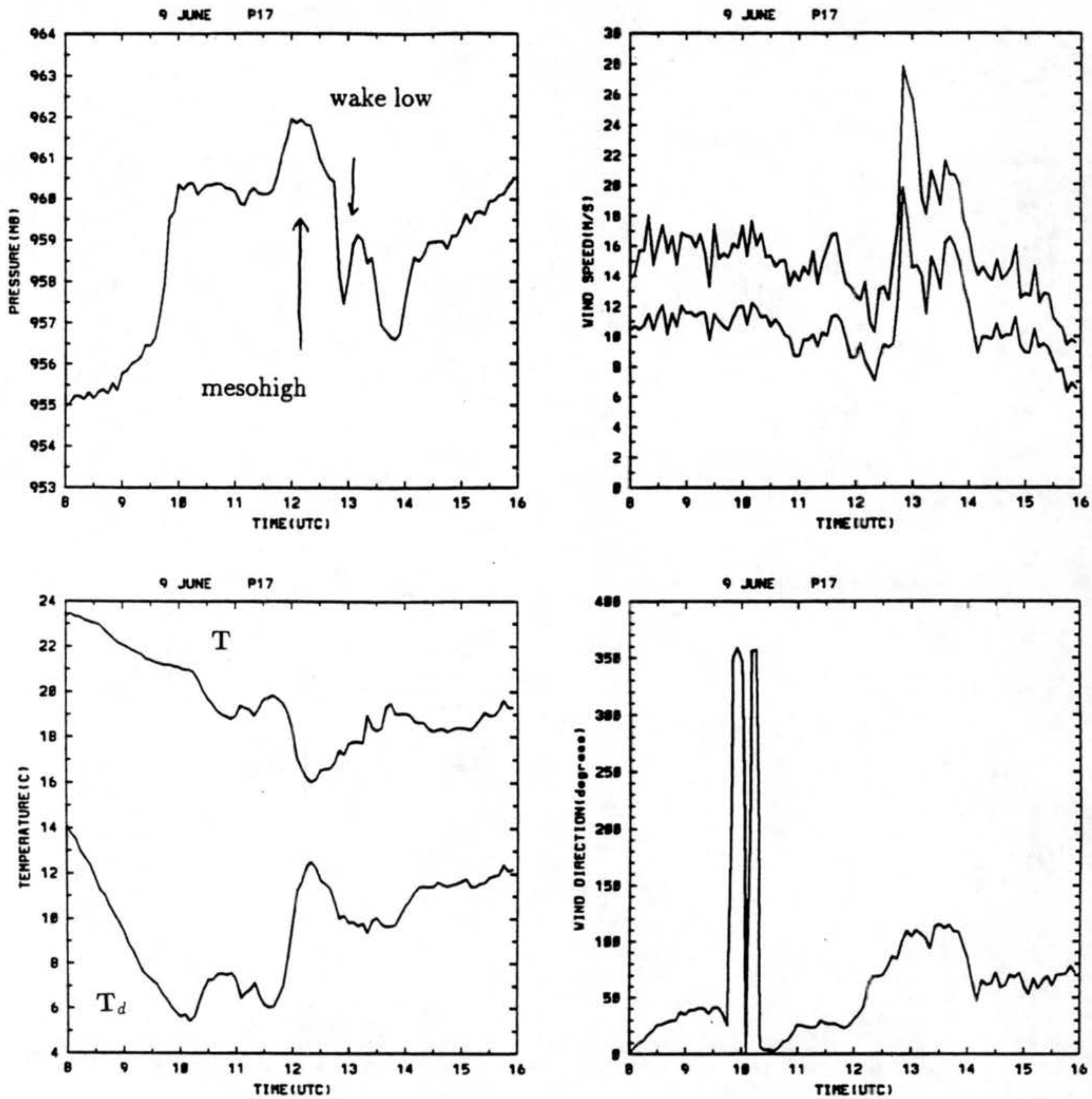

Figure 5.38: Same as Fig. 5.9 except for 9 June at station P17. Note different time scale as each tick mark represents 30 minutes.

5.6 June 11 case

5.6.1 Synoptic overview

The synoptic conditions associated with the initial development of this MCS are closely approximated by the 0000 11 June maps. At the surface (Fig. 5.39a) there was a stationary front extending across southeastern Kansas, with a cold front extending to its southwest across south-central Kansas and the Oklahoma and Texas panhandles. South of the front the temperatures were 29-33°C and the dewpoints were 18-24°C and there was a southerly flow. North of the front it was much cooler (18-24°C) and drier (15-18°C) with a northerly flow.

At 850 mb (Fig. 5.39b) there was a closed low over northeastern New Mexico giving rise to a moderate (5-15 m s^{-1}) southerly flow over Texas and Oklahoma. Very moist (dewpoints over 10°C) air extended over eastern Texas, north to Kansas. At 500 mb (Fig. 5.39c) the flow was mostly out of the northwest over Oklahoma and Texas. A relatively sharp trough extended from western North Dakota south to eastern Colorado.

5.6.2 Radar overview

The initial convective development associated with this case occurred around 2100 10 June just ahead of the cold front (not shown). By 0000 (Fig. 5.40a) there was a nearly solid line of convection from central Kansas to the Texas panhandle. The extent of the stratiform precipitation was difficult to surmise due to the lack of Garden City, Kansas radar data, but it appeared to be limited in its extent. The large convective cell in extreme southern Kansas, just ahead of the convective line produced a weak (F0) tornado at this time. Up until this time, the severe weather reports were mostly due to large hail, while after this time the reports became limited to strong winds. By 0200 (Fig. 5.40b) the convective line was still quite intense and had expanded more along its southwestern flank. There was also the beginnings of the development of a region of enhanced stratiform precipitation to the rear of the convective line. By 0400 (Fig. 5.40c) the convective line started to dissipate. There was now an expansive area of enhanced stratiform precipitation to the rear of the entire convective line. There was also a very

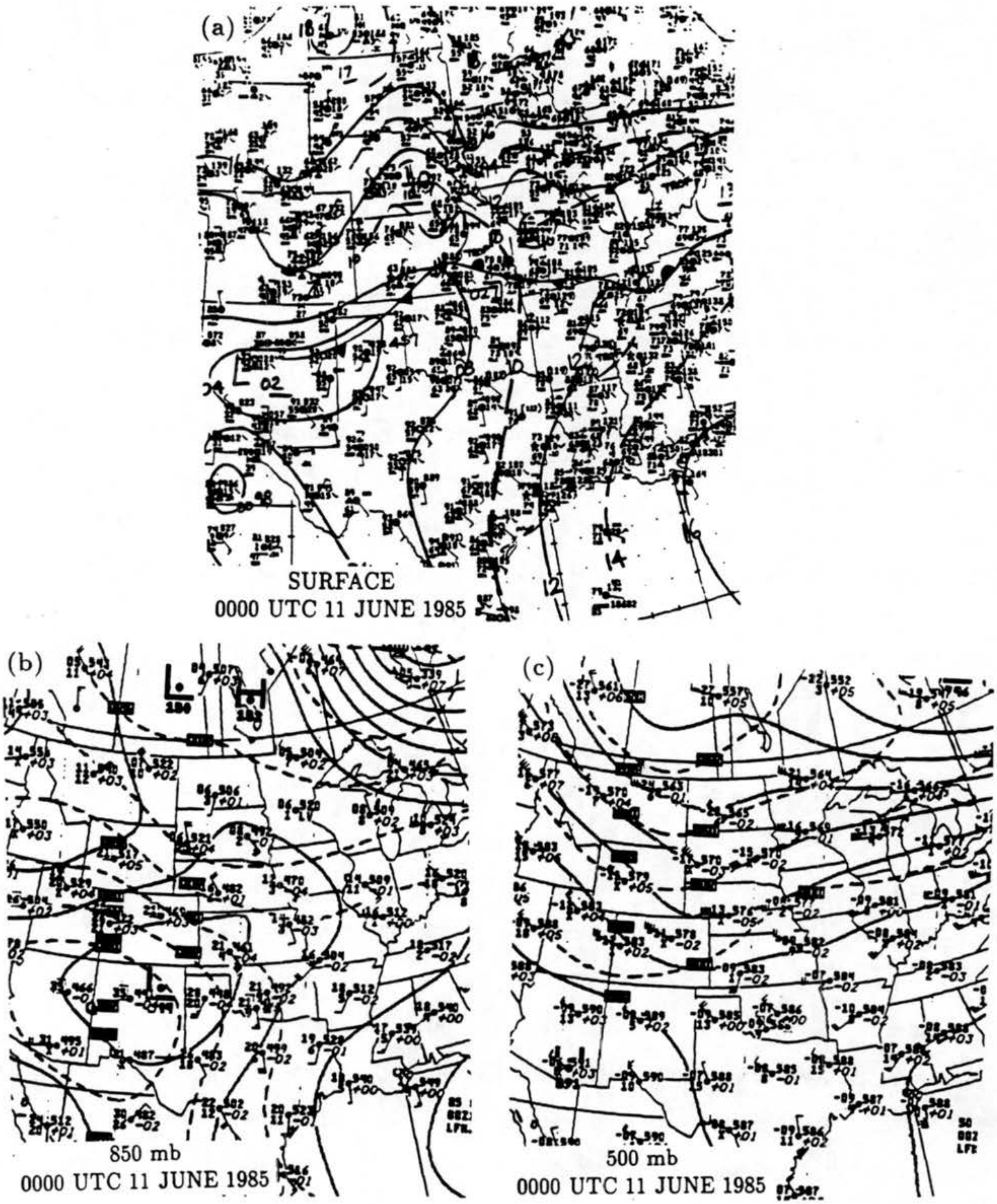

Figure 5.39: Same as Fig. 5.1 except for 0000 UTC 11 June.

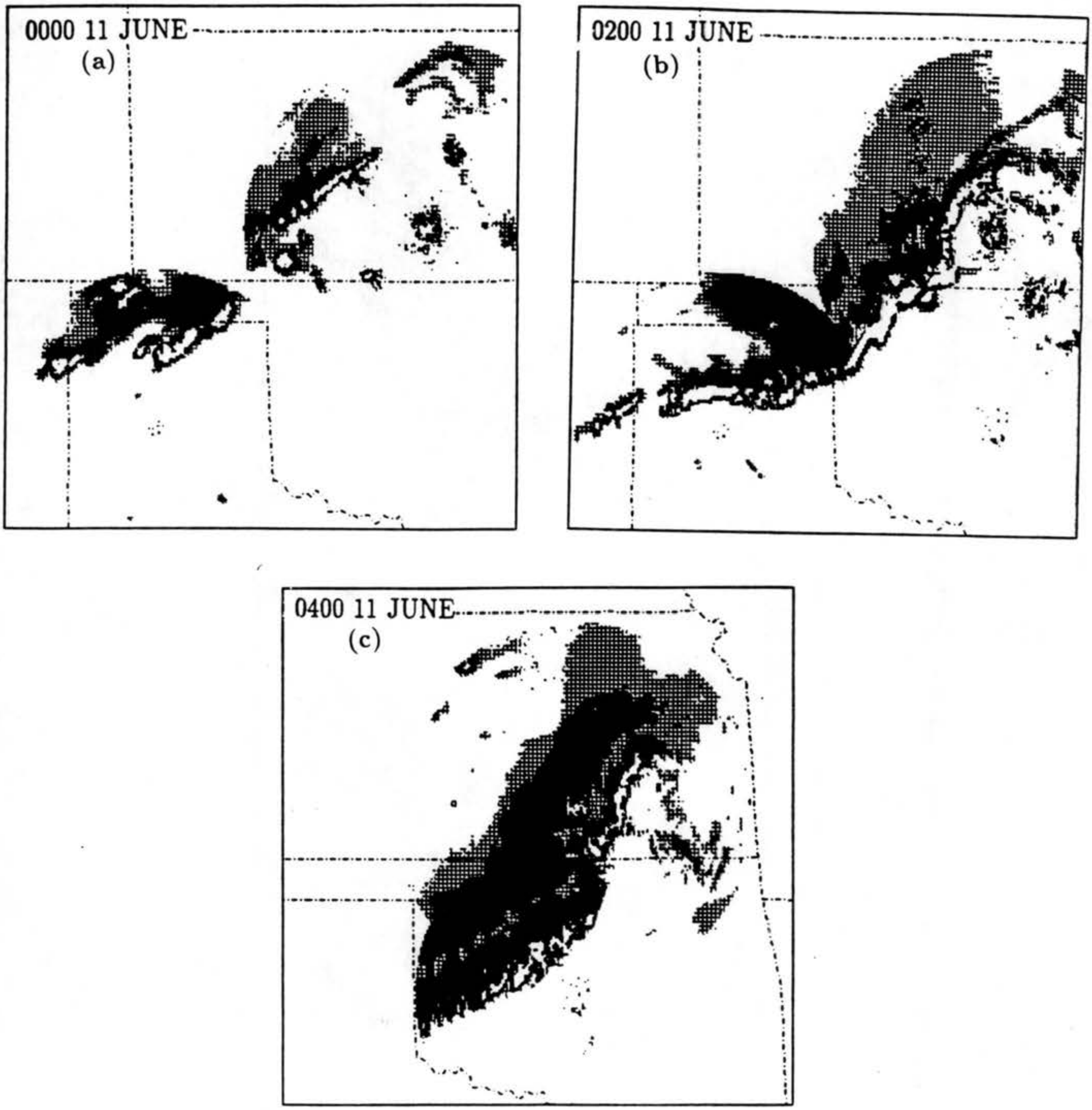

Figure 5.40: Same as Fig. 5.2 except for 11 June at: a) 0000 UTC; b) 0200 UTC; c) 0400 UTC; d) 0530 UTC; d) 0730 UTC. All using Oklahoma City OK and Wichita KS.

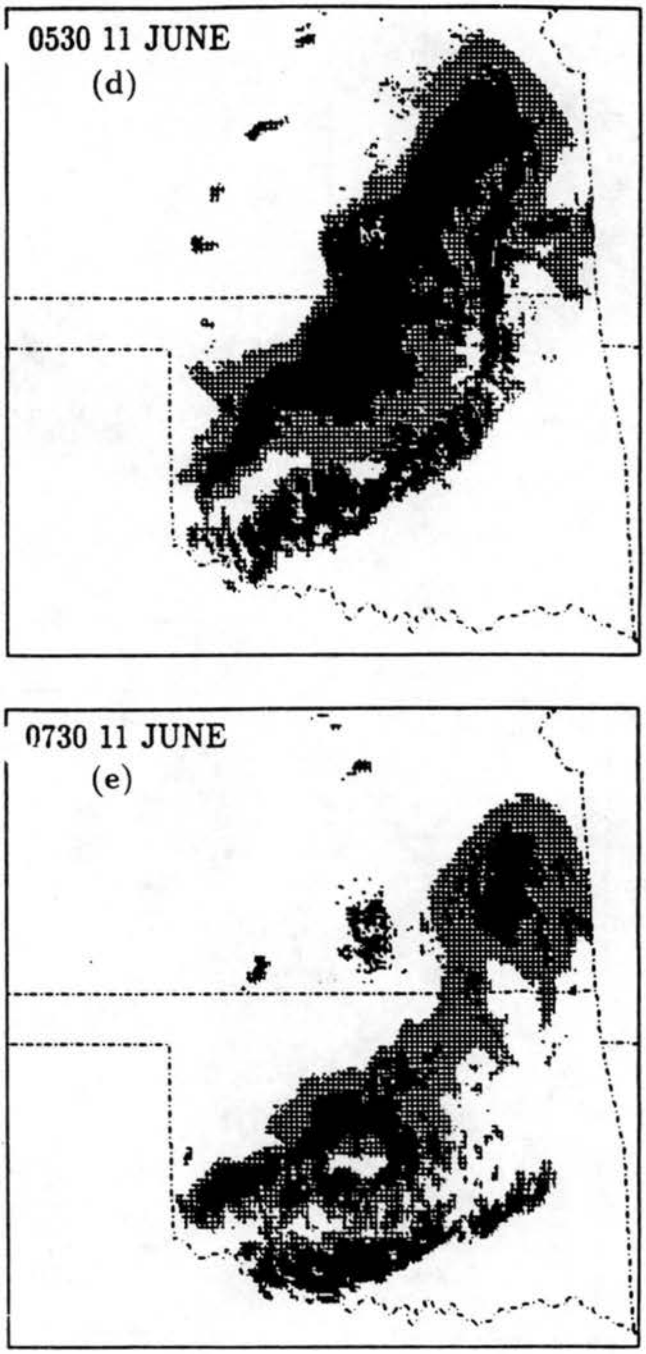

Figure 5.40: Continued.

distinct transition zone of very low reflectivities between the convection and the enhanced region. This system was by far the largest of those occurring during the PRE-STORM experiment. By 0530 (Fig. 5.40d) the convection had largely dissipated, but it was still fairly intense on its southern end. Now the transition zone had greatly expanded as the convective line propagated faster than the stratiform region. By 0730 (Fig. 5.40e) the convection was continuing to dissipate. There was also a distinct splitting of the stratiform area into northern and southern sections, and there was a rear echo notch between the two segments. The northern section was then cut-off from the remainder of the system.

5.6.3 System overview

Wake low formation (0130)

At this time (Fig. 5.41) the flow ahead of the system was southerly in central and southern Oklahoma, becoming more easterly to the north. Two strong pre-squall lows were evident, one ahead of the southern, the other ahead of the northern portion of the system. A mesohigh was found to be mainly associated with the leading convective line. There was a 5 m s^{-1} northerly outflow from the system and there was some divergence occurring to the rear of the mesohigh but due to the weak gradient at this time it was also weak. A fairly weak wake low was found to be centered in an area characterized by an echo notch. The flow was about 5 m s^{-1} through this low and there was some convergence to its rear.

Expansion of stratiform region and strengthening of the wake low (0230)

By this time (Fig. 5.42) the pre-squall lows became weaker and more diffuse. The mesohigh split into two cores, became significantly stronger (by 2 mb) and covered a wider area. The outflow from the system also increased to 10 m s^{-1} from the north-northwest. The wake low also deepened considerably (2 mb) and was positioned along the back edge of the newly developed region of enhanced stratiform precipitation. Despite the presense of a stronger gradient, the flow here was still quite weak (2.5-5 m s^{-1}).

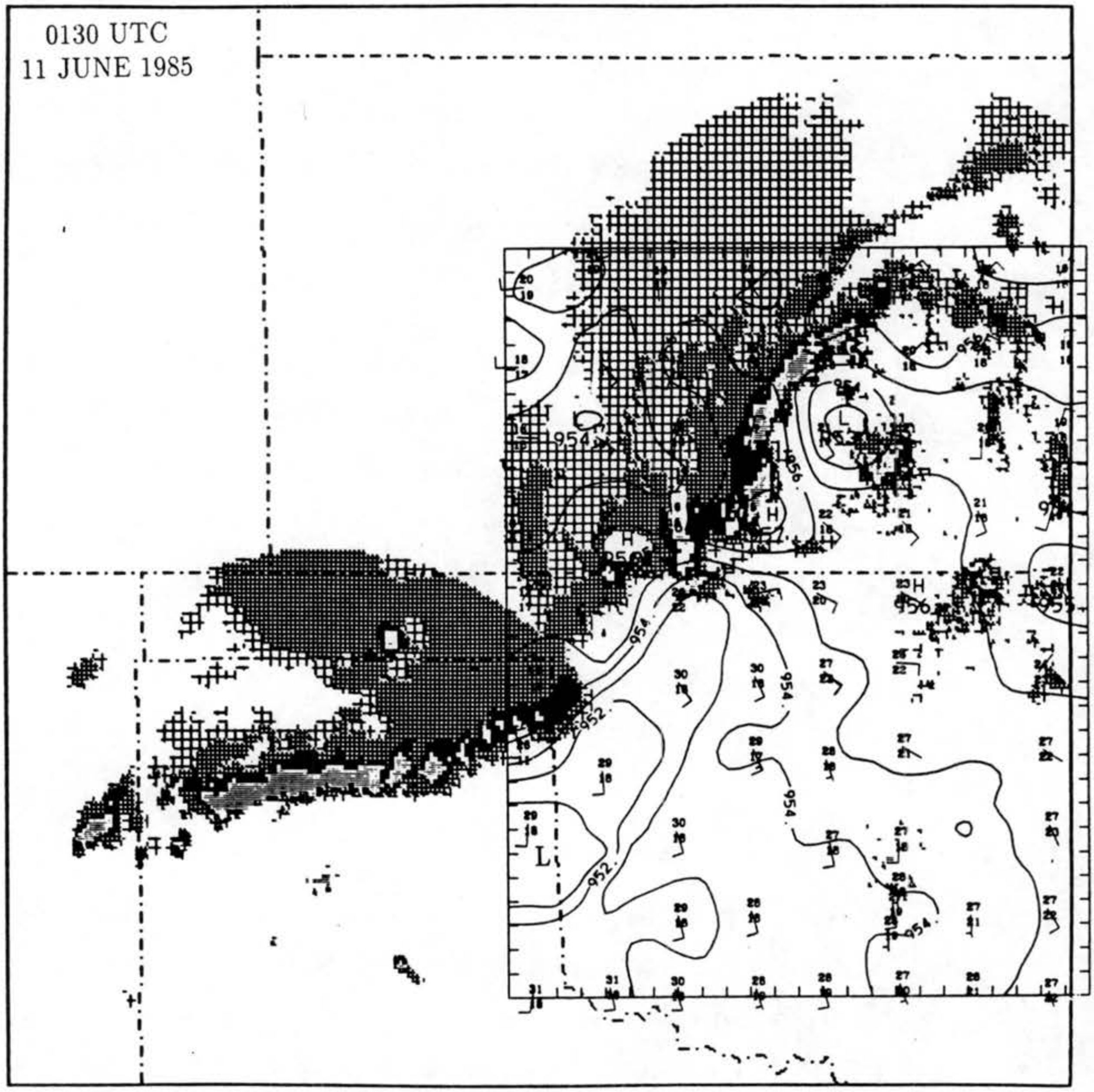

Figure 5.41: Same as Fig. 5.3 except for 0130 UTC 11 June.

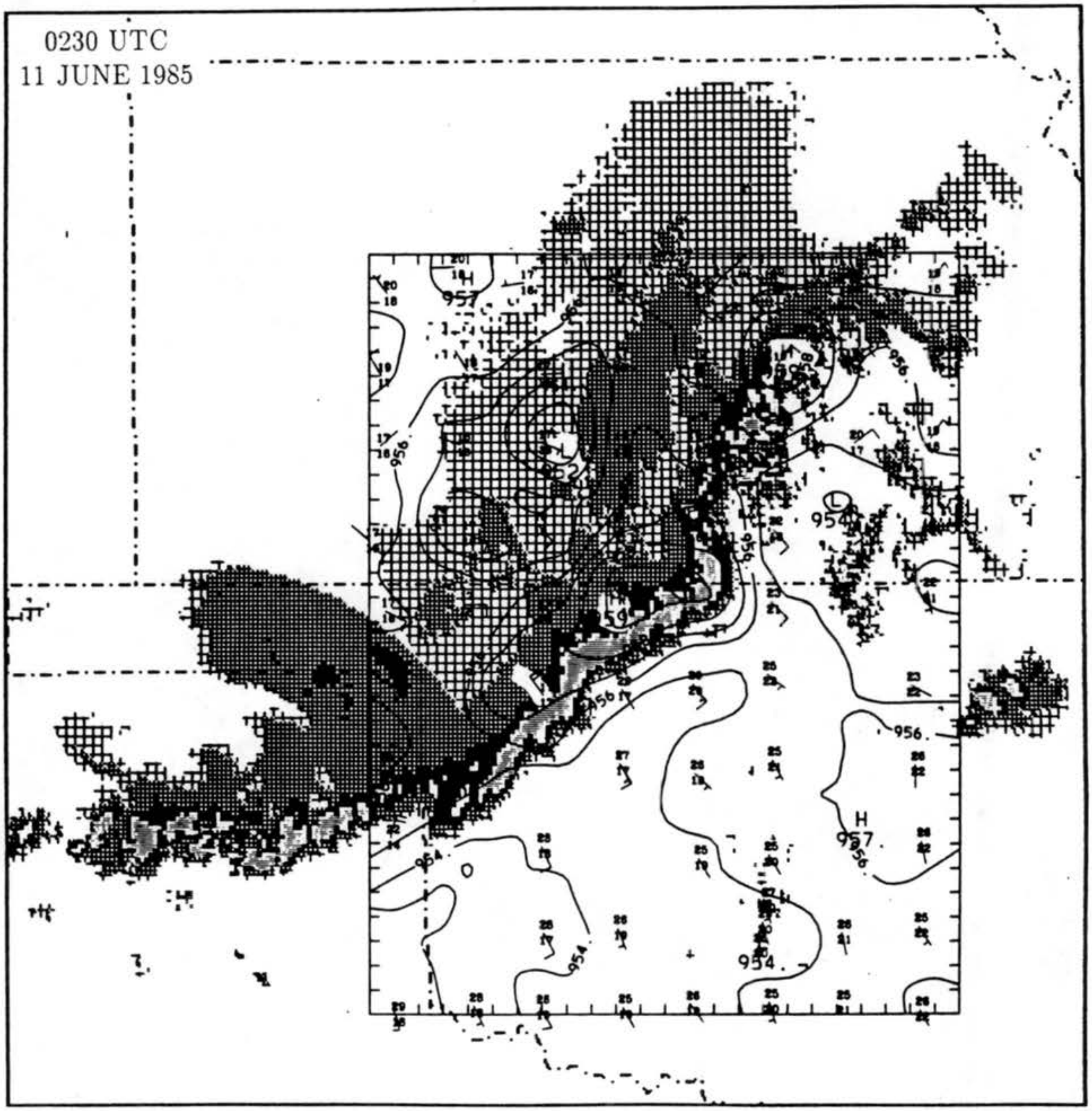

Figure 5.42: Same as Fig. 5.3 except for 0230 UTC 11 June.

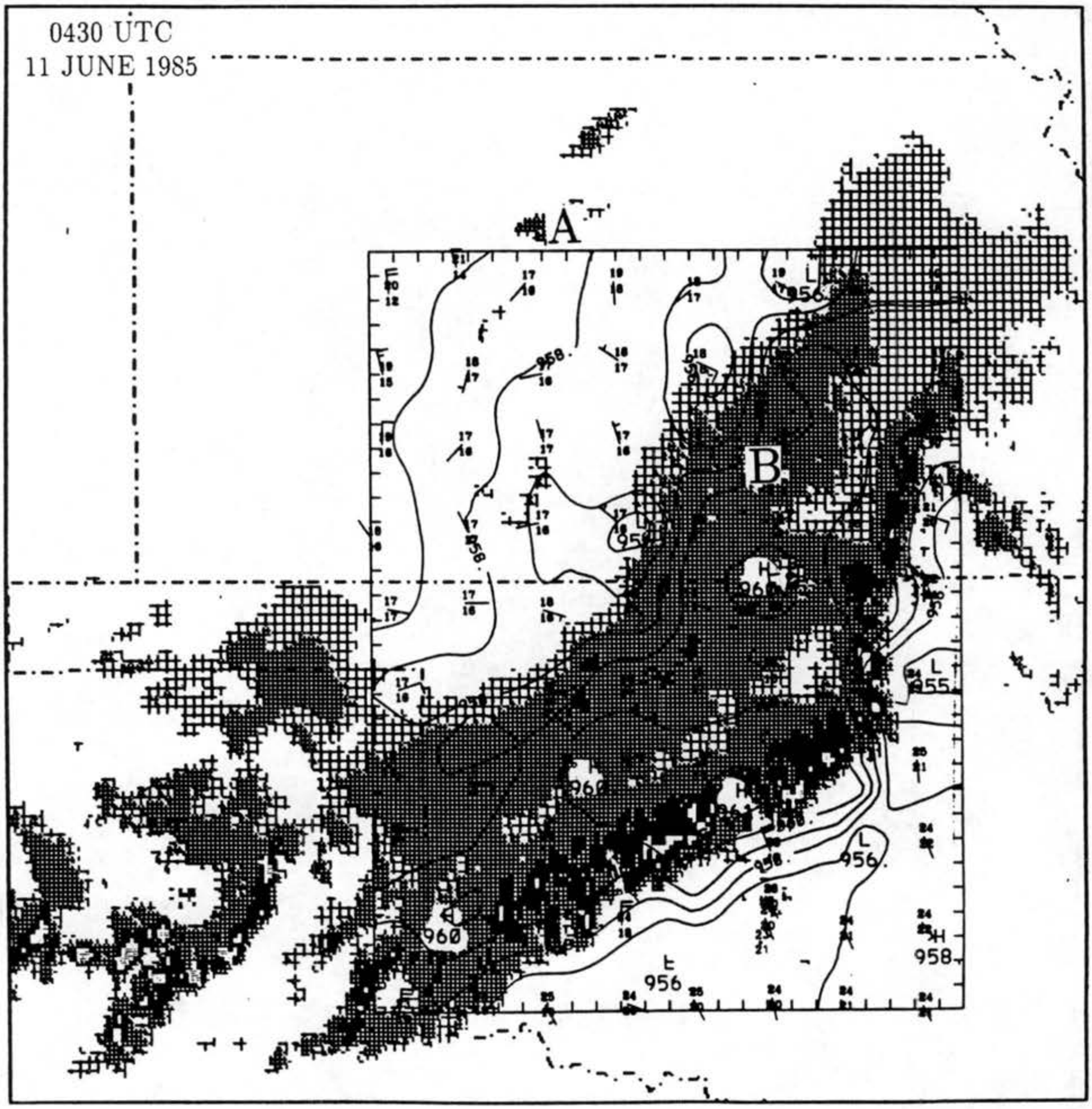

Figure 5.43: Same as Fig. 5.3 except for 0430 UTC 11 June.

Splitting of mesohigh/wake low (0430-0600)

By 0430 (Fig. 5.43) the mesohighs further strengthened (1-2 mb) and now encompassed much of the stratiform precipitation region in addition to the convective region. There was a strong (10-15 m s^{-1}) northerly outflow from the entire system, and it was strongest at the southern end. The wake low weakend considerably (4 mb) and split into two separate segments, both along the back edge of enhanced stratiform regions.

Around 0600 (Fig. 5.44) the pressure patterns became quite complex for a period. There were many separate mesohigh centers in both the convective and stratiform regions (some of these are apparently due to bad data). There were also several wake lows with one each being in the northern, central and southern sections. The northern and southern lows were the deepest, and each low was connected to the back edge of a region of enhanced stratiform precipitation.

To show the structure of the rear inflow associated with the northern wake low the 0430 RSL (Fig. 5.45a) and 0431 IAB (Fig. 5.45b) soundings as well as the 0430 500 mb (Fig. 5.45c) and 850 mb (Fig. 5.45d) maps are examined. RSL was located about 125 km to the rear of the stratiform precipitation (point A in Fig. 5.43) and it shows a 300 mb deep layer of strong rear inflow with a maximum at 400 mb (17 m s^{-1}). While at IAB, which was at the front edge of the heavy stratiform precipitation (point B in Fig. 5.43) there was also a 300 mb deep layer of strong rear inflow peaking at 825 mb (13 m s^{-1}). The 500 mb map shows that at RSL, while the air was actually cool relative to the surrounding stations, it was extremely dry. The 850 mb map shows that at IAB the air was also relatively cool but very dry. So, here the rear inflow was quite strong, carrying in very dry air, and undergoing a rather marked descent in the region of the northern wake low.

Dissipation of MCS and further strengthening and separation of wake lows (0730)

By this time (Fig. 5.46) there was a drastic shift in the structure of the pressure features. The low in south-central Kansas, well to the rear of the system was associated

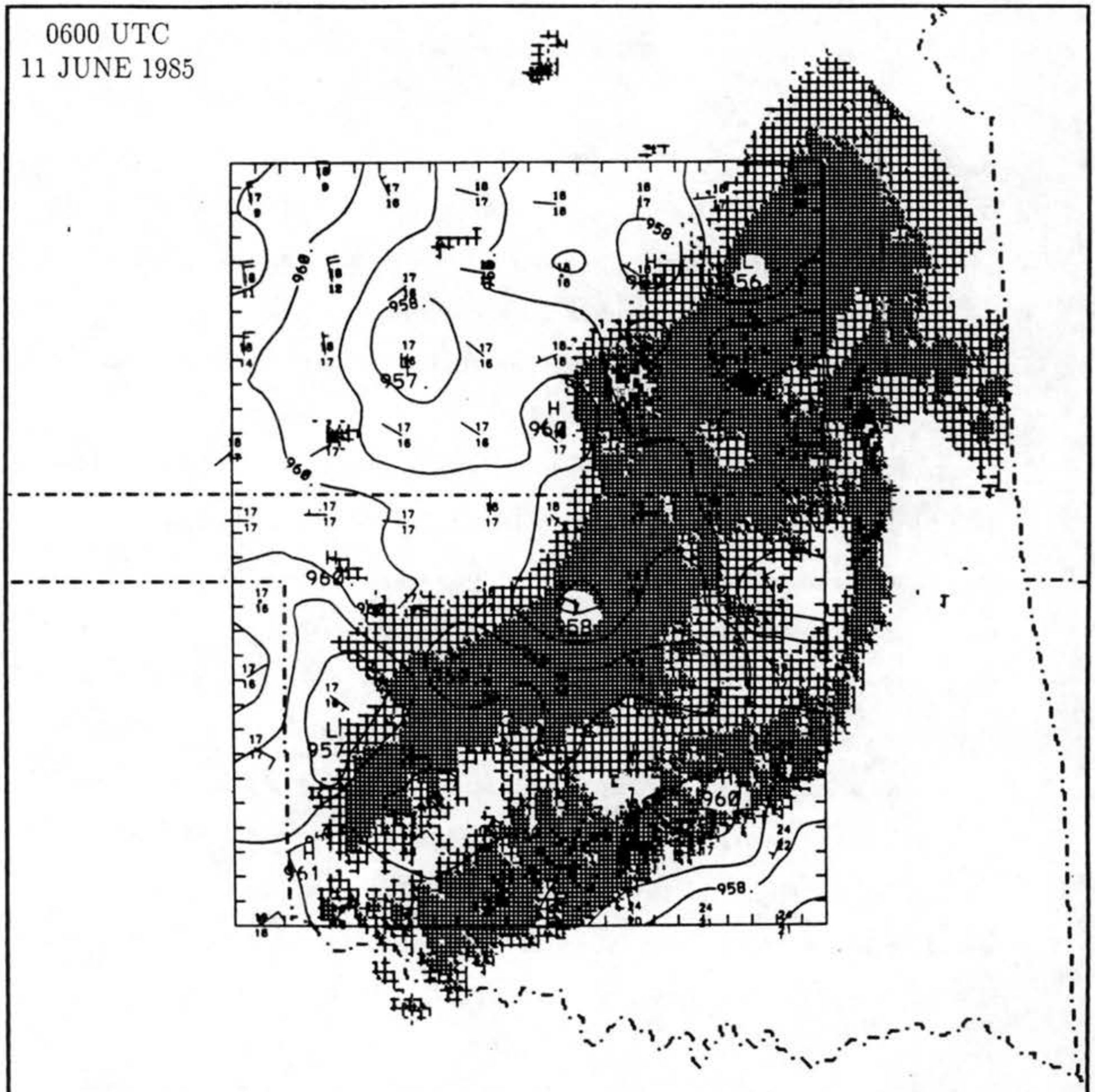

Figure 5.44: Same as Fig. 5.3 except for 0600 UTC 11 June.

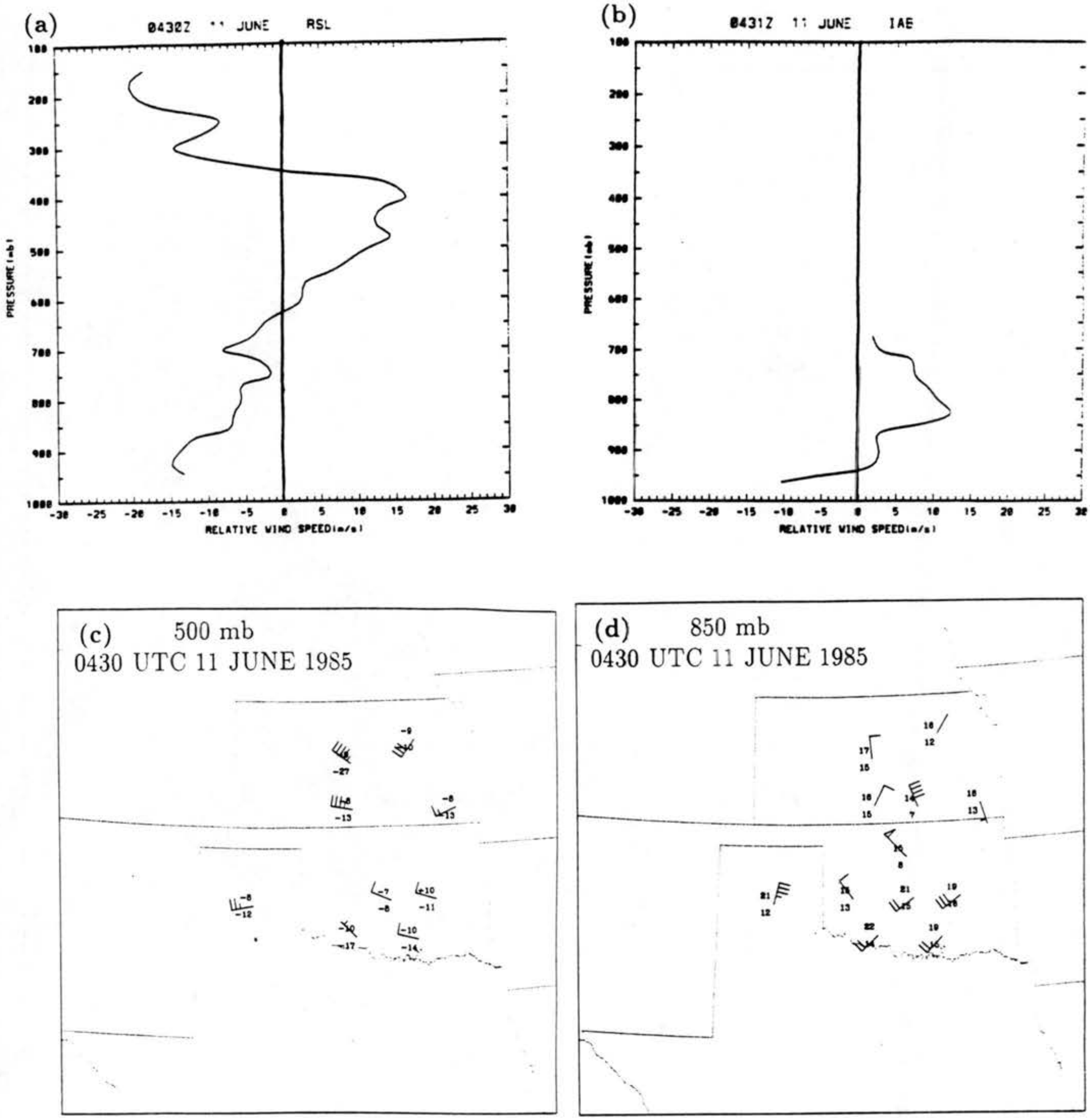

Figure 5.45: In a-b) Same as Fig. 5.8 except for 11 June at: a) 0430 UTC at RSL; b) 0431 UTC at IAB. In c-d) Same as Fig. 5.10 except for 11 June at: c) 0430 UTC at 500 mb; d) 0430 UTC at 850 mb.

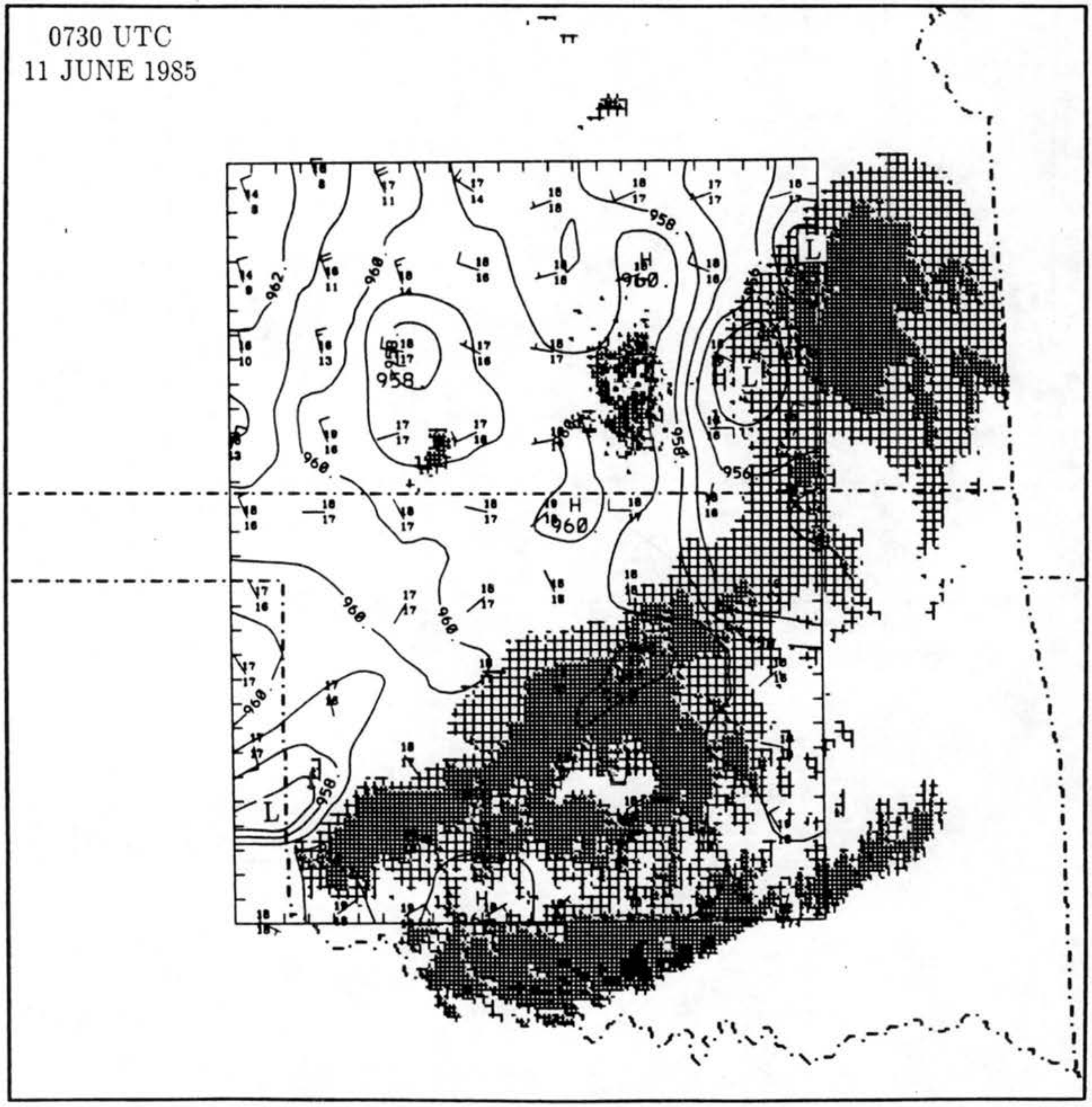

Figure 5.46: Same as Fig. 5.3 except for 0730 UTC 11 June.

with the cold front moving in, as evidenced by the shift to northwest flow, and a significant drying and cooling in the northwest portion of the mesonet.

In the system itself, the mesohighs were fairly weak and covered only very small areas of the stratiform precipitation. The wake low to the rear of the central portions of the system nearly completely filled and was only evident as a very slight lowering of the pressure in this region. The wake low to the rear of the southern portion of the system was still visible in the far southwest portion of the mesonet and it had a very strong gradient positioned along the back edge of the stratiform precipitation region. The most dominant wake low now was the northen one, which deepened by 2-3 mb. Unfortunately, the upper-air coverage at this late stage of the system was limited. The low was found along the northern end of an enhanced region of stratiform precipitation.

5.6.4 Mesonet time series

The conditions associated with the passage of the central portion of this system can be seen at station P19 (Fig. 5.47, see Fig. 3.1). When the system passed through this area, its convective line was still very intense and this was reflected in the very strong changes in the features. There was a sharp mesohigh (0100, 4 mb increase in 10 min) and it was associated with a very sharp 7°C temperature and 5°C dewpoint decrease in a 10 min span. There was also a wind gust of 22 m s^{-1} and a shift from southeast to northwest flow. The wake low (0210) then passed by about 2 hr later with a 5.5 mb decrease in 30 min and it is accompanied by a 11 m s^{-1} wind gust as well as a shift back to southeast flow.

The region in the northern portion of the system, where there was a very deep wake low is examined using the station P23 (Fig. 5.48). The mesohigh (0400) in this region was a broader feature, although there was one rise of 3 mb in 5 min which was accompanied by very intense winds (25 m s^{-1} gusts) as well as a 2°C temperature and dewpoint decrease in 5 min and a sharp shift from east-northeast flow to northwest flow. Although the overall mesohigh was broader, there was one very strong segment. The wake low (0730) here was also very deep with a 5 mb decrease in 90 min (concentrated in a 2.5 mb drop in 15 min) and it was accompanied by a wind gust of 16 m s^{-1} and a shift to easterly flow. There

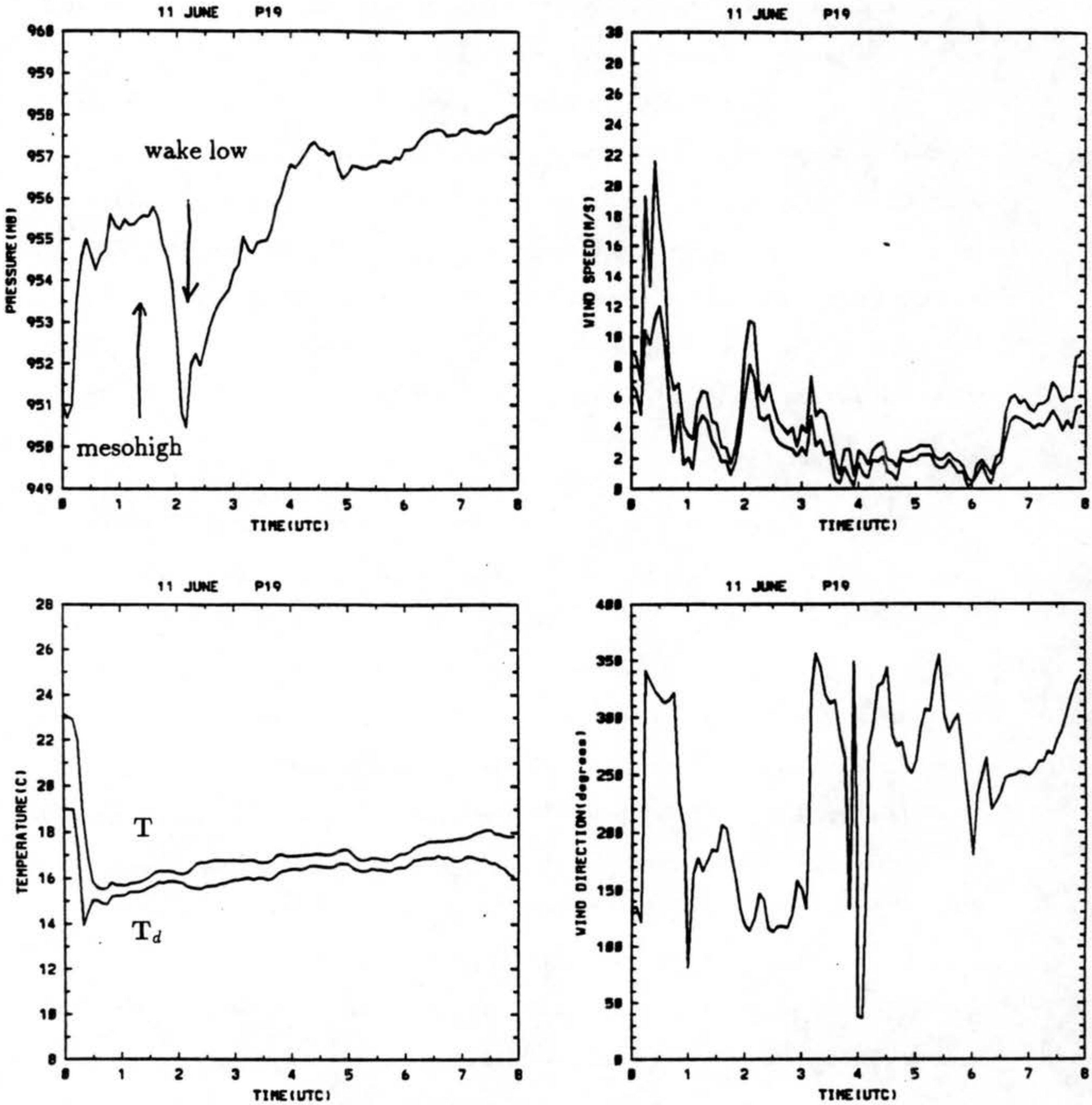

Figure 5.47: Same as Fig. 5.9 except for 11 June at station P19. Note different time scale as each tick mark represents 30 minutes.

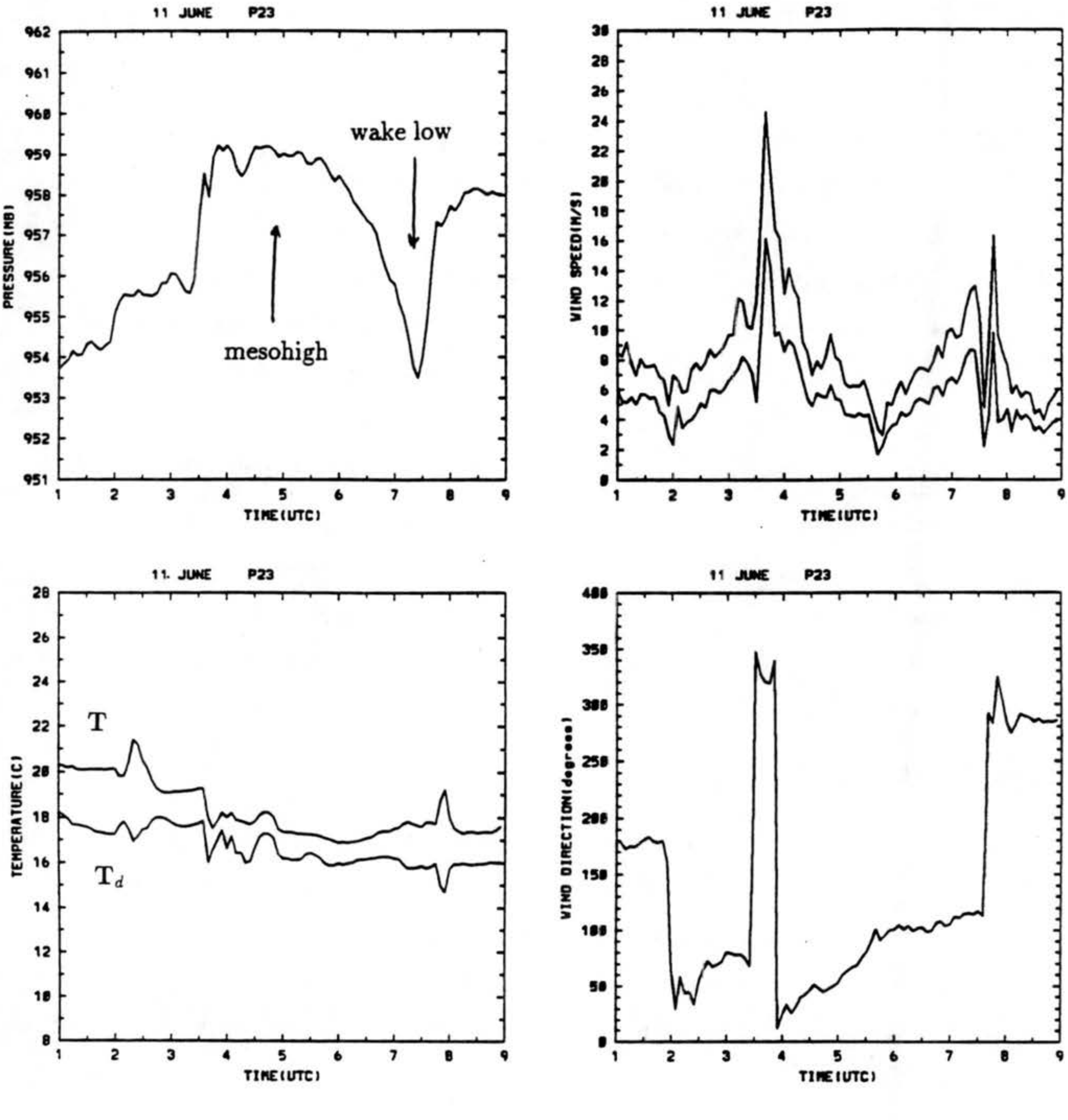

Figure 5.48: Same as Fig. 5.9 except for 11 June at station P23. Note different time scale as each tick mark represents 30 minutes.

was also a 1.5°C temperature (dewpoint) increase (decrease) which is indicative of a weak heat burst event.

5.7 June 15 case

5.7.1 Synoptic overview

The synoptic conditions just after the initial development associated with this MCS are summarized by the 0000 15 June maps. At the surface (Fig. 5.49a) there was a 1005 mb low in southwestern Minnesota with a cold front extending to the south through eastern Nebraska, northwestern Kansas and southern Colorado. South of the front the temperatures were 26-32°C with dewpoints of 12-18°C and a southeast flow, while to its north it was cooler (23-30°C) and drier (7-12°C) with a northerly flow.

At 850 mb (Fig. 5.49b) there was a closed low over northeastern New Mexico giving rise to a moderate (10 m s^{-1}) southerly flow over Texas and Oklahoma, becoming more north-northeasterly in Kansas. A tongue of very moist air extended over most of Texas into Oklahoma. At 500 mb (Fig. 5.49c) there was a ridge over the southwestern U.S. and a deep trough over the central and eastern U.S. The 500 mb jet runs through Kansas with a 20 m s^{-1} kt west-northwest flow. The flow was much weaker over Oklahoma (7-13 m s^{-1}).

5.7.2 Radar overview

The initial convective development occurred around 2100 14 June in north-central Kansas (not shown). By 0000 (Fig. 5.50a) there were two distinct areas of convection, one consisted of a pair of small convective lines in northeastern Kansas, and the other just moving into radar range in the panhandles of Oklahoma and Texas. The Kansas convection had a limited segment of light stratiform precipitation. The leading of the two convective line segments in the Kansas MCS quickly became the dominant of the two. By 0200 (Fig. 5.50b) there were three separate areas of convection, the two earlier areas and another which developed in between them. The eastern Kansas MCS now had a stratiform precipitation region which was on its eastern side. It had a very intense convective line on its southen end, with scattered, weaker convection to its north. The panhandle MCS

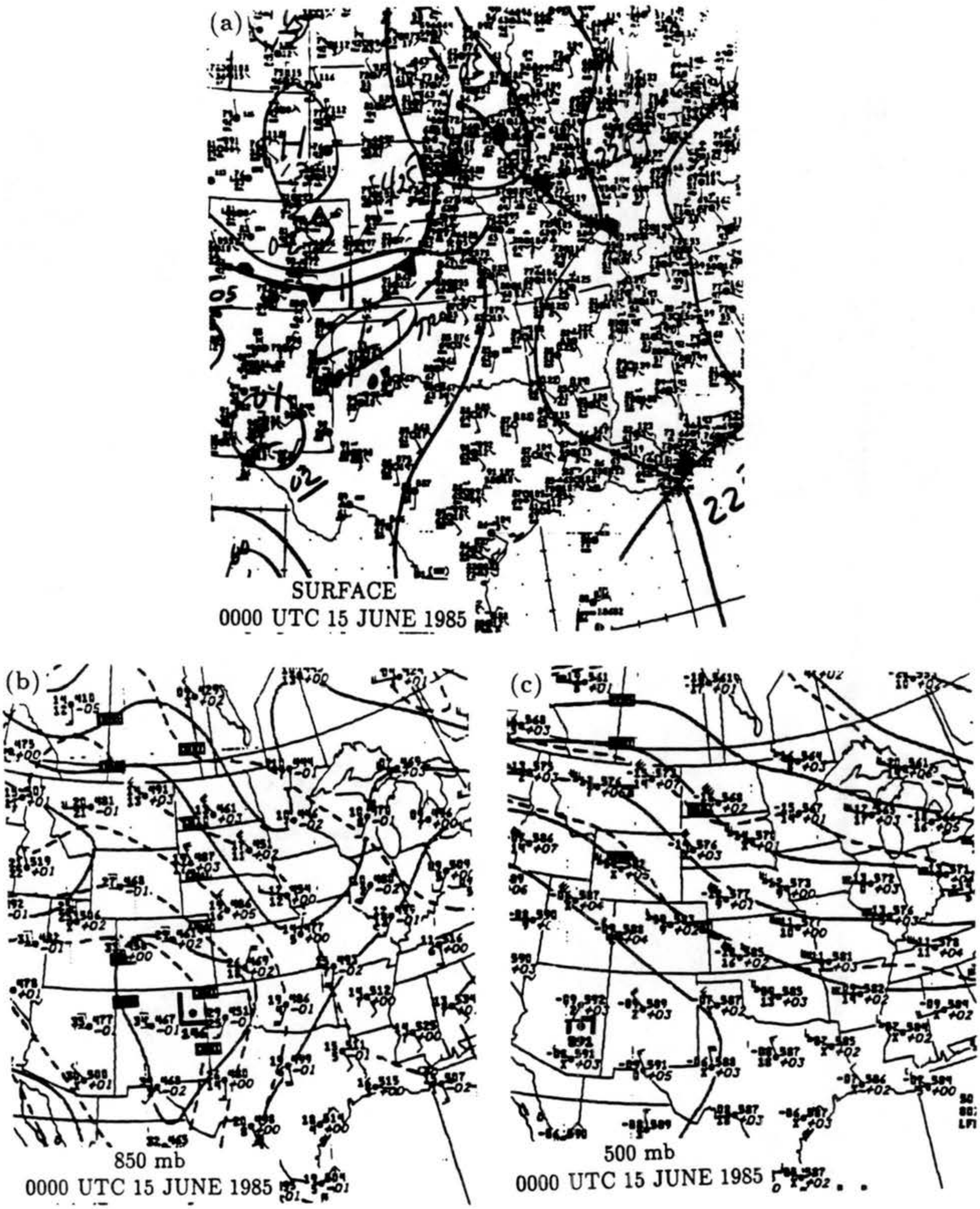

Figure 5.49: Same as Fig. 5.1 except for 0000 UTC 15 June.

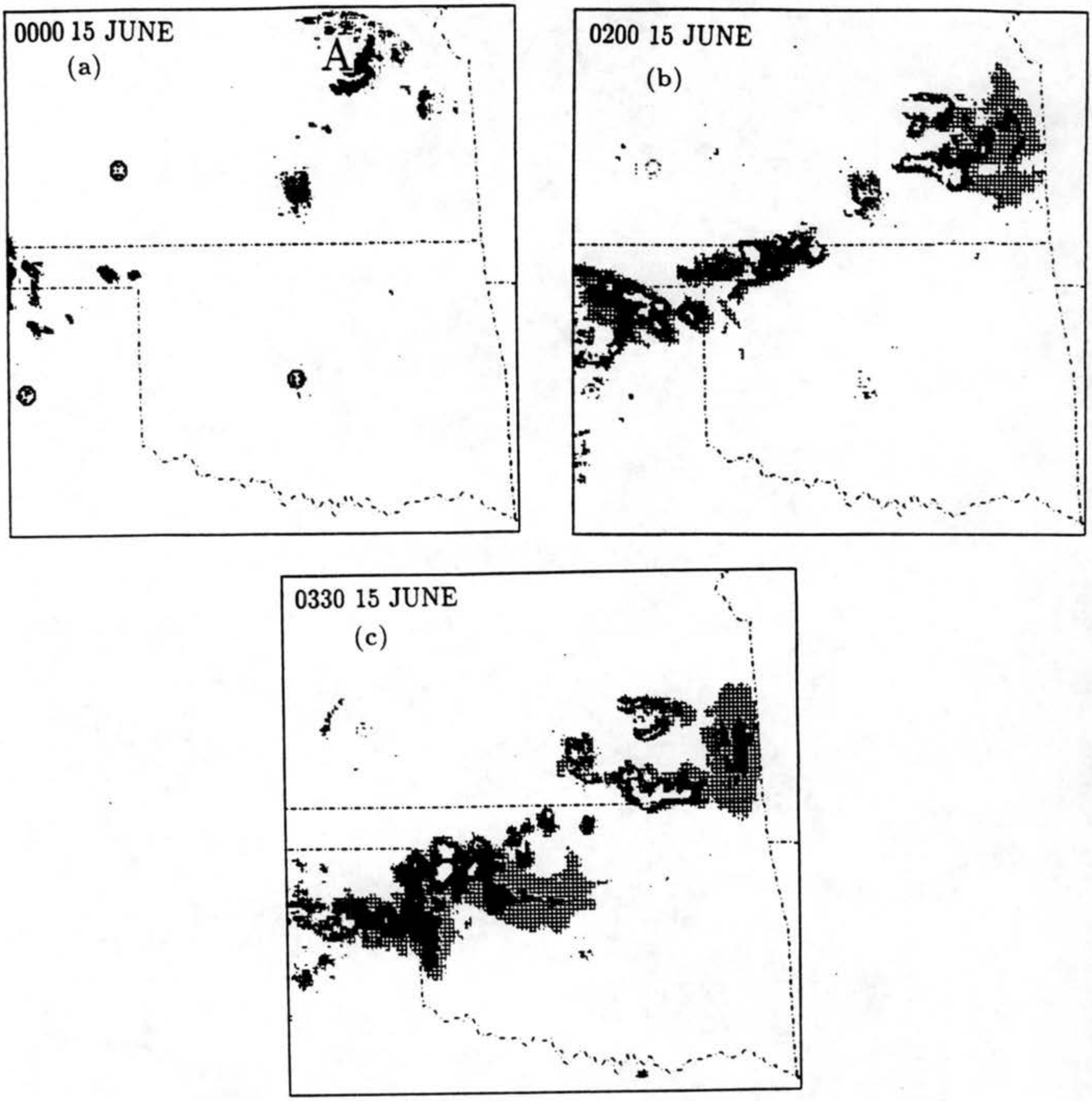

Figure 5.50: Same as Fig. 5.2 except for 15 June at: a) 0000 UTC; b) 0200 UTC; c) 0330 UTC; d) 0500 UTC; e) 0700 UTC. All using Amarillo TX, Garden City and Wichita KS and Oklahoma City OK.

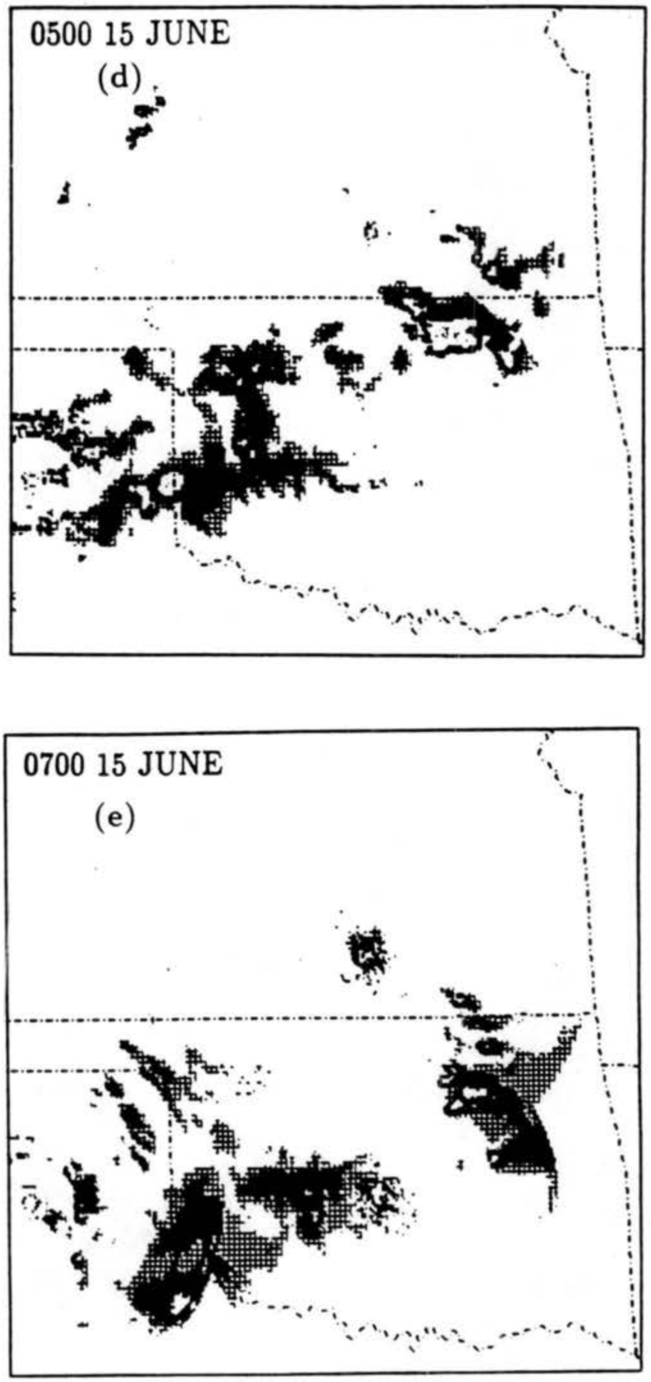

Figure 5.50: Continued.

was composed of largely random convection with some weak stratiform precipitation. The newly developed northern Oklahoma convection was a northeast-southwest line and did not have any stratiform precipitation. By 0330 (Fig. 5.50c) the panhandle MCS merged with the northern Oklahoma convective line. The structure of this MCS was actually a trailing line of convection with a leading band of stratiform precipitation. This was the only case that consisted of only leading stratiform precipitation at any point of its existence. There was some new convection developing on the northern side of this MCS. The Kansas MCS had nearly the same structure it had earlier, with a strong southern convective line with scattered convection to its north and a region of stratiform precipitation to its east. By 0500 (Fig. 5.50d) the convective structure became highly random in nature. The eastern MCS convective line was still visible, but its stratiform precipitation, if there was any, was to the east of the radar range. The western MCS had lost nearly all of its stratiform precipitation as the convective structure had become very random in nature with several areas of scattered intense convective cells. By 0700 (Fig. 5.50e) the eastern MCS was barely visible. The western MCS had now developed a trailing region of enhanced stratiform precipitation. Its convective portion was just visible in extreme northern Texas. The structure of these systems appeared to be more random rather than symmetric or asymmetric.

5.7.3 System overview

Development of leading stratiform precipitation (0300)

At this time (Fig. 5.51) the flow throughout Oklahoma was southerly while in Kansas it was northwesterly, setting up strong convergence in the region where the convection has developed. The pressure structure was quite remarkable. There was a general area of low pressure between the Kansas and Oklahoma MCSs. This feature was presumably due to the compensating subsidence which would have been occurring in this region due to the several areas of intense convection surrounding it. The eastern MCS did not have a mesohigh associated with it, but it still had a strong 10-15 m s^{-1} north-northeasterly outflow. The western MCS had its mesohigh within its leading band of stratiform precipitation and there was not any outflow at all from this region. There was a strong westerly

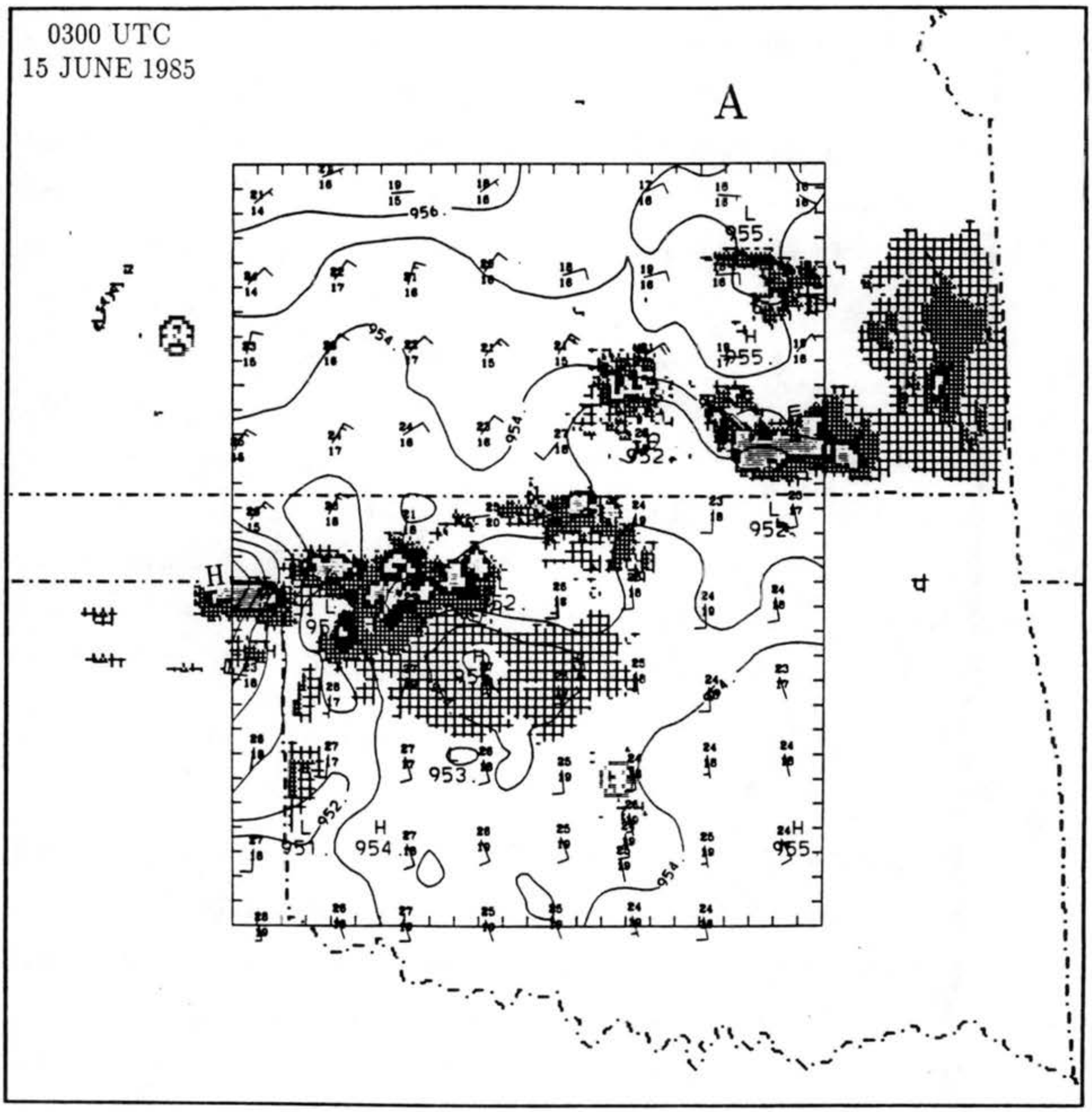

Figure 5.51: Same as Fig. 5.3 except for 0300 UTC 15 June.

outflow (12.5 m s^{-1}) from the western portion of this MCS where there was a very intense mesohigh and a very strong gradient. There was another low found between the areas of convection in the western MCS and, again, this was presumably due to compensating subsidence.

The lack of a trailing stratiform precipitation region as well as a wake low with either system at this time can be explained by examining the FRI soundings at 0001 (Fig. 5.52a) and 0259 (Fig. 5.52b) which were representative of the conditions in all of Kansas and northern and central Oklahoma where the systems were at this time. At 0001 FRI was located just to the rear of the convective line of the eastern MCS (point A in Fig. 5.50a), while at 0259 it was about 200 km to the rear of the MCS (point A in Fig. 5.51). It can be seen that at both times there was a very deep layer of very strong (15-20 m s^{-1}) RTF flow covering virtually the entire troposphere above 800 mb. This deep and strong RTF flow would tend to advect the hydrometeors which were formed in the convective regions, to the south and east of these regions. Hence, the development of leading and eastern stratiform precipitation regions. Also notice that at both times the rear inflow coverage was nearly the same and both peaked at 350 mb. Hence, there was not any descent of the rear inflow at this time and, given that, the warming and drying neccesary for wake low development was not occurring.

Development of mesolow between MCSs (0430)

By this time (Fig. 5.53) an expansive mesohigh covered nearly the entire precipitation area of the western MCS. There were also several localized, weak mesohighs associated with every other area of convection. The hypothesis that the low in between the two systems was being caused by compensating subsidence appeared to be more obvious at this time. The low contours conformed nearly exactly to the edges of the surrounding convection and also the low was at its deepest in the area which was nearly exactly in the middle of the convection. This conforms with the hypothesis suggested by Fritsch and Chappell (1980), that the compensating subsidence from each of the convective cores should add in the area in between the convective cores, leading to more intense subsidence. The surface

(a)

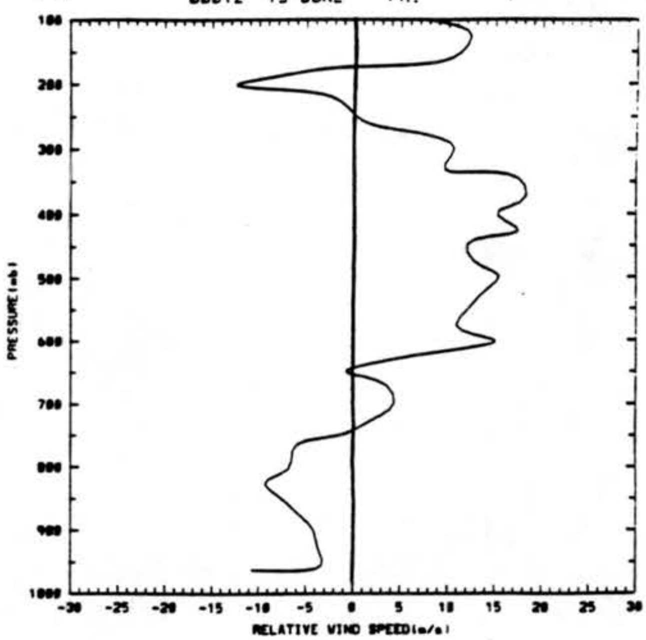

(b)

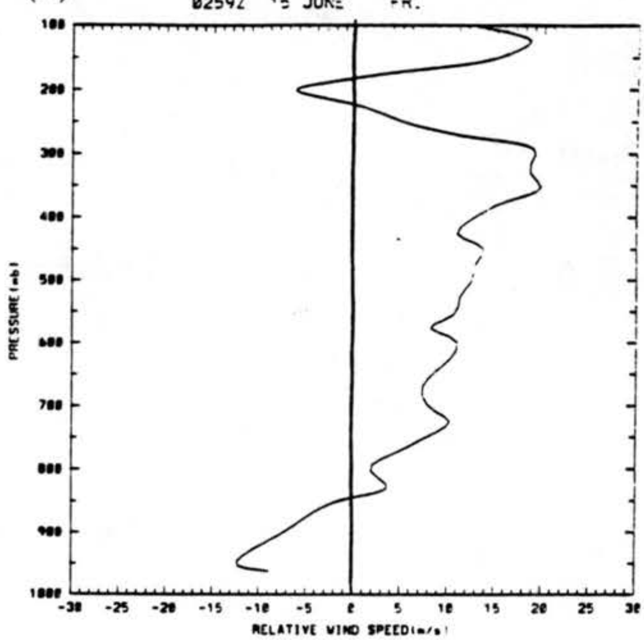

Figure 5.52: Same as Fig. 5.8 except for 15 June at: a) 0001 UTC at FRI; b) 0259 UTC at FRI.

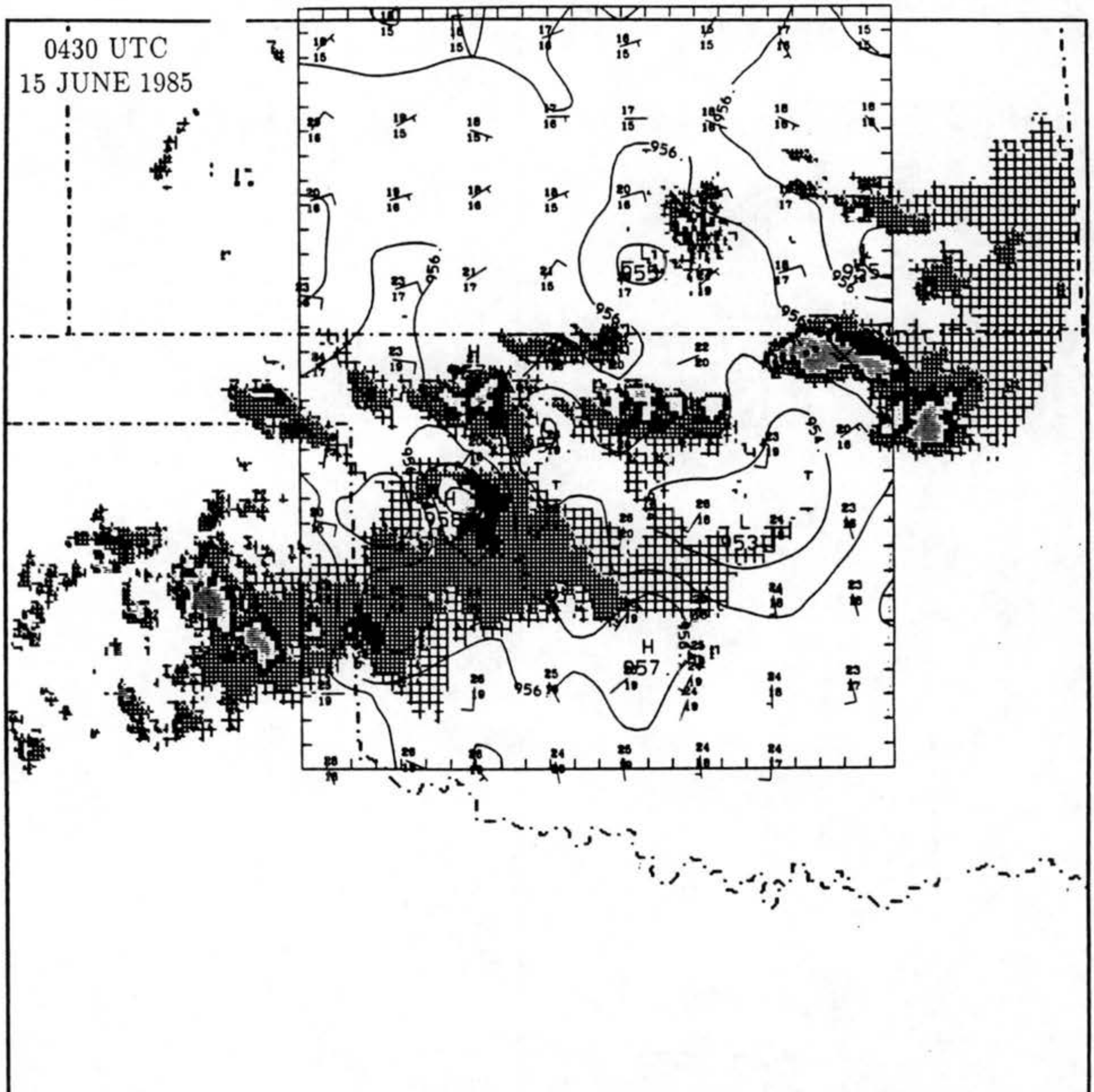

Figure 5.53: Same as Fig. 5.3 except for 0430 UTC 15 June.

flow was still largely unaffected by any of these features other than some moderate outflow from some convective areas.

Development of trailing stratiform precipitation (0730)

By this time (Fig. 5.54) a region of trailing, enhanced stratiform precipitation had been in existence for about 1 hr (see radar discussion) in the western MCS. The convective areas were to the south of the mesonet. Three separate wake lows developed, each on the back edge of a region of enhanced stratiform precipitation. The gradient (which was outside of the mesonet) ahead of the westernmost of these was presumably quite strong since the flow was 10 m s^{-1} through this low. The flow associated with the other lows was weaker and variable in its direction, as would be expected given the weakness of the gradients associated with these lows.

To arrive at an explanation for the sudden shift from a leading to a trailing stratiform precipitation region as well as the formation of the wake lows, the soundings from FSB at 0600 (Fig. 5.55a) and 0840 (Fig. 5.55b) are examined. At 0600 FSB was along the leading edge of the convection associated with the western MCS, and it shows a drastic change in the flow structures from those in Kansas and northern Oklahoma. Here there was a 300 mb deep layer of moderate (10 m s^{-1}) mid-level FTR flow, which advected the hydrometeors to the rear of the convection, hence leading to the development of the trailing stratiform precipitation region. Also notice that there was a weak rear inflow jet maximized at 750 mb (5 m s^{-1}). At 0840, when FSB was along the back edge of the trailing stratiform precipitation, the rear inflow elevated to about 475 mb (4 m s^{-1}). So although this was not a strong rear inflow, it underwent a rapid descent as it approached the convective line and led to a strong enough warming and drying to lower the surface pressure. The 850 mb maps at 0600 (Fig. 5.55c) and 0900 (Fig. 5.55d) show that at FSB there was a significant lower-tropospheric warming and drying, while at the other Oklahoma stations there was cooling and/or moistening. So the descending rear inflow appears to have led to a hydrostatic warming and drying along the back edge of the stratiform precipitation region and hence a lowering of the surface pressure.

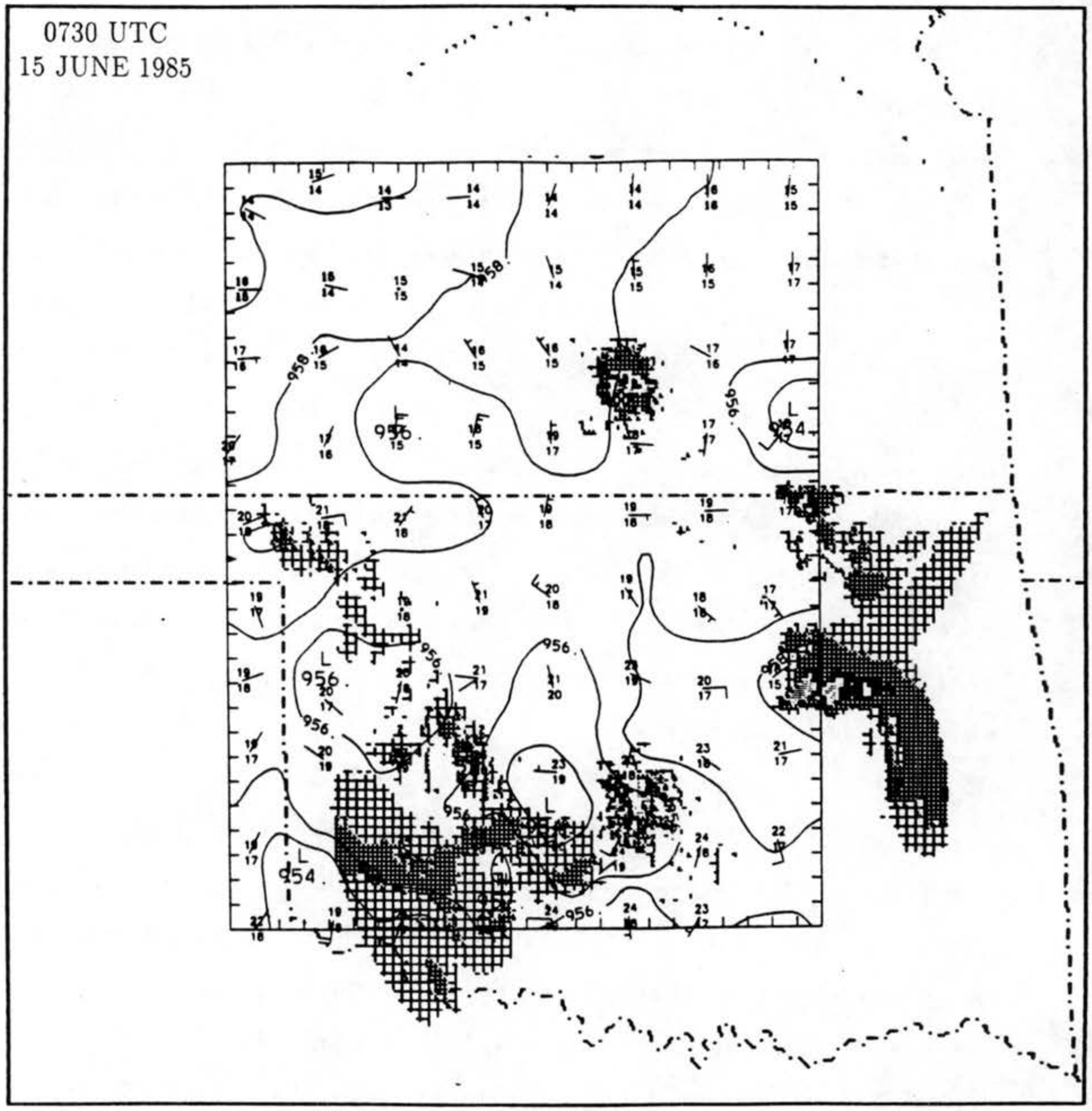

Figure 5.54: Same as Fig. 5.3 except for 0730 UTC 15 June.

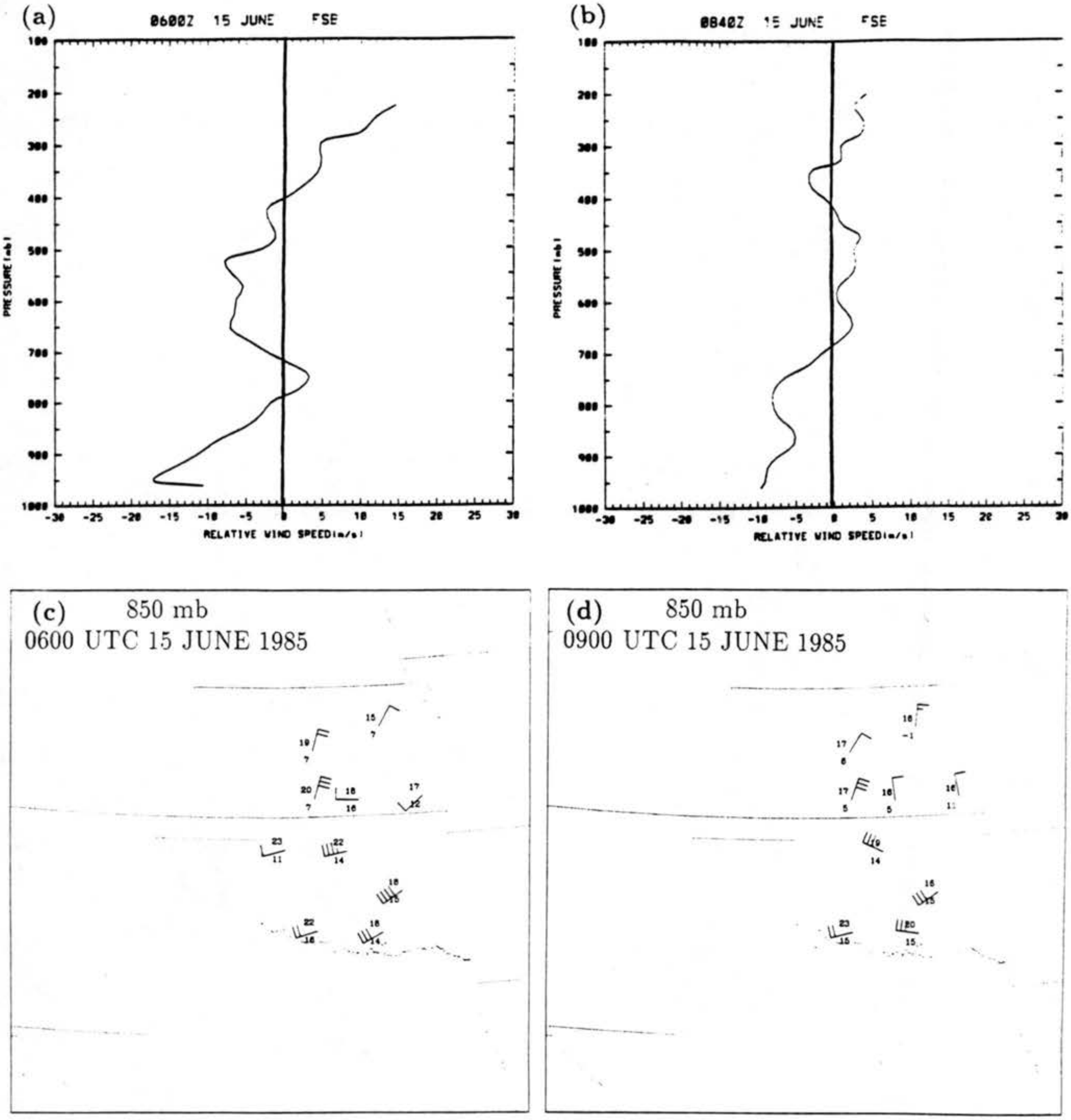

Figure 5.55: In a-b) Same as Fig. 5.8 except for 15 June at: a) 0600 UTC at FSB; b) 0840 UTC at FSB. In c-d) Same as Fig. 5.10 except for 15 June at: c) 0600 UTC at 850 mb; d) 0900 UTC at 850 mb.

5.7.4 Mesonet time series

The region where the wake lows developed is examined with station S03 (Fig. 5.56, see Fig. 3.1). There was a very sharp mesohigh (0610) here with a 3 mb increase in 5 min and a 5°C cooling, 3°C dewpoint decrease, a 25 m s^{-1} wind gust and a shift from southeast to northwest flow. Then the wake low (0730) passed by with a 4 mb decrease in about 60 min, a 14 m s^{-1} wind gust and a shift from northwest to southwest flow.

5.8 June 22 case

5.8.1 Synoptic overview

The large-scale environment associated with the development of this MCS is summarized by the 0000 22 June maps. At the surface (Fig. 5.57a) there was a 992 mb low over central Minnesota with a cold front trailing to its south and west through northeastern to south central Kansas to the Texas panhandle. South of the front there was a strong southerly flow (7-10 m s^{-1}) with temperatures of 26-32°C and dewpoints of 18-21°C. To the north of the front there was a north to northwest flow with temperatures of 21-30°C and dewpoints of 10-16°C.

At 850 mb (Fig. 5.57b) there was a deep trough extending from Minnesota southwest to New Mexico. There was a strong southerly flow over Texas and Oklahoma and a tongue of very moist (dewpoints in excess of 15°C) air extending from south-central Texas north to Oklahoma. In Kansas the flow was out of the north. There was some warm advection occurring over Oklahoma. At 500 mb (Fig. 5.57c) the jet flow was confined to Kansas and north, while the flow in Texas and Oklahoma was very weak (2-5 m s^{-1}) out of the west-northwest. There was a trough from North Dakota south to central Kansas, a portion of which may extend south through western and central Texas where there was a cyclonic curvature to the flow.

5.8.2 Radar overview

There were actually two MCSs which developed during this period. The convection with each system first formed around 2100 21 June (not shown). By 0200 (Fig. 5.58a) both

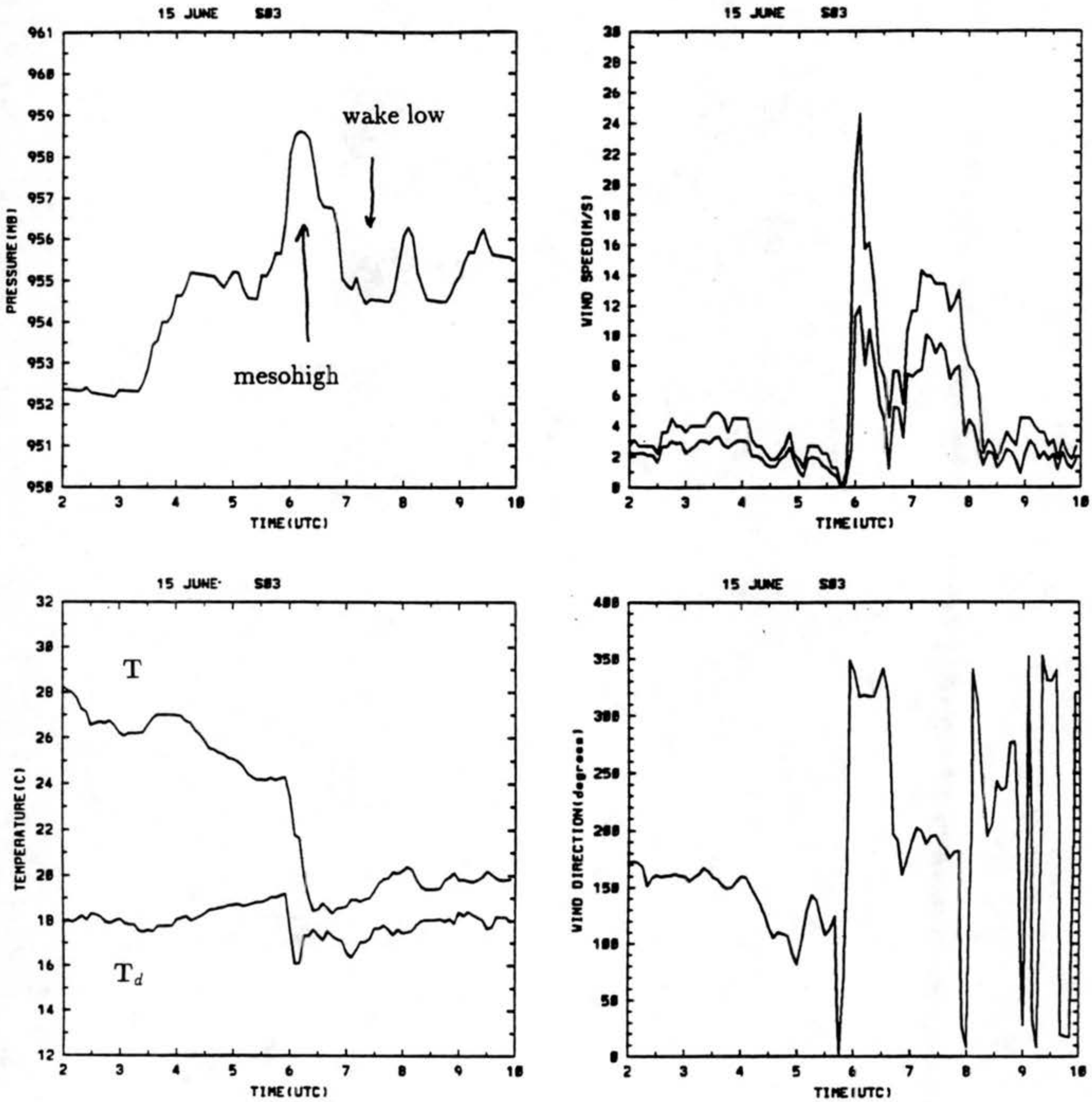

Figure 5.56: Same as Fig. 5.9 except for 15 June at station S03. Note different time scale as each tick mark represents 30 minutes.

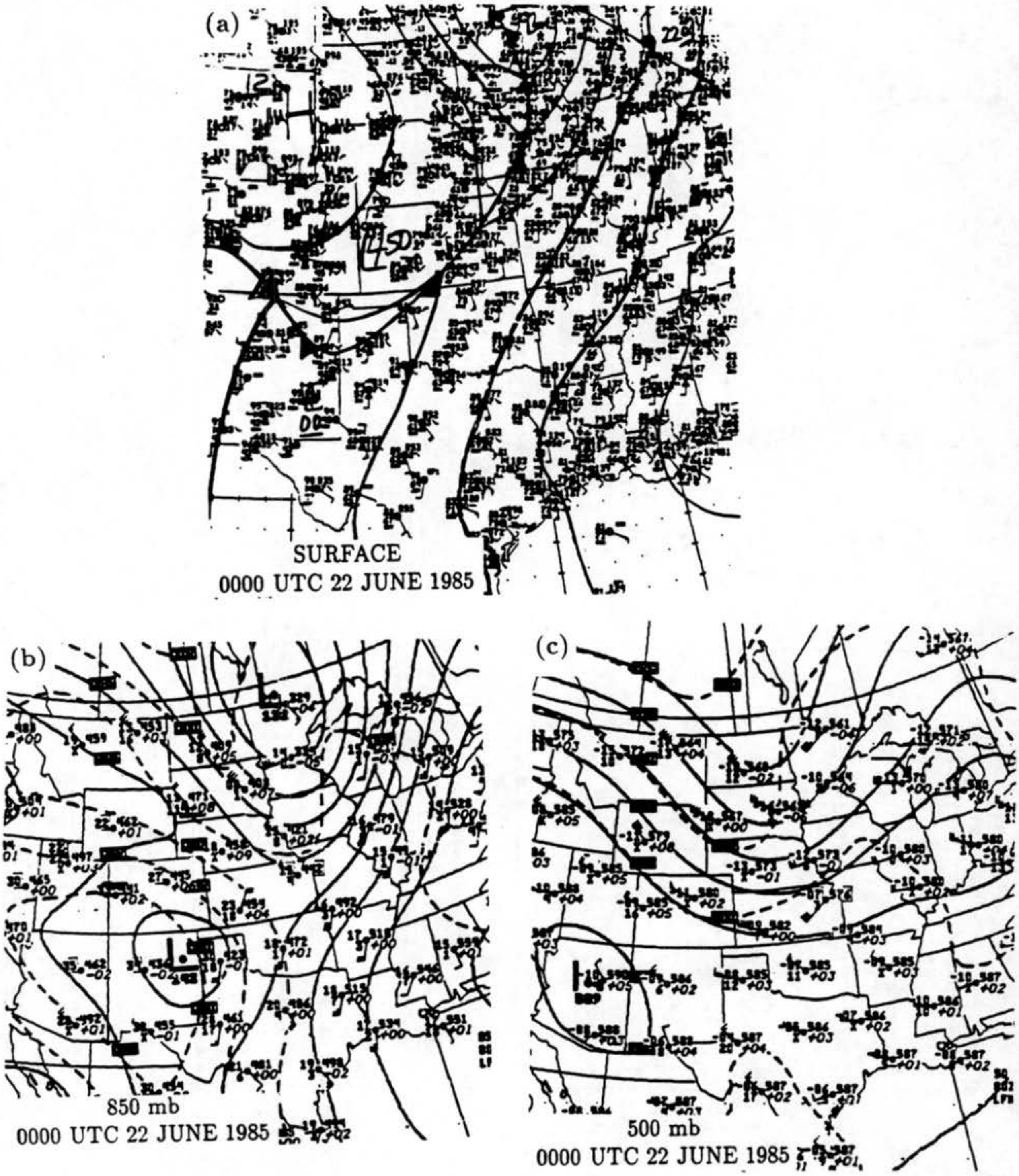

Figure 5.57: Same as Fig. 5.1 except for 0000 UTC 22 June.

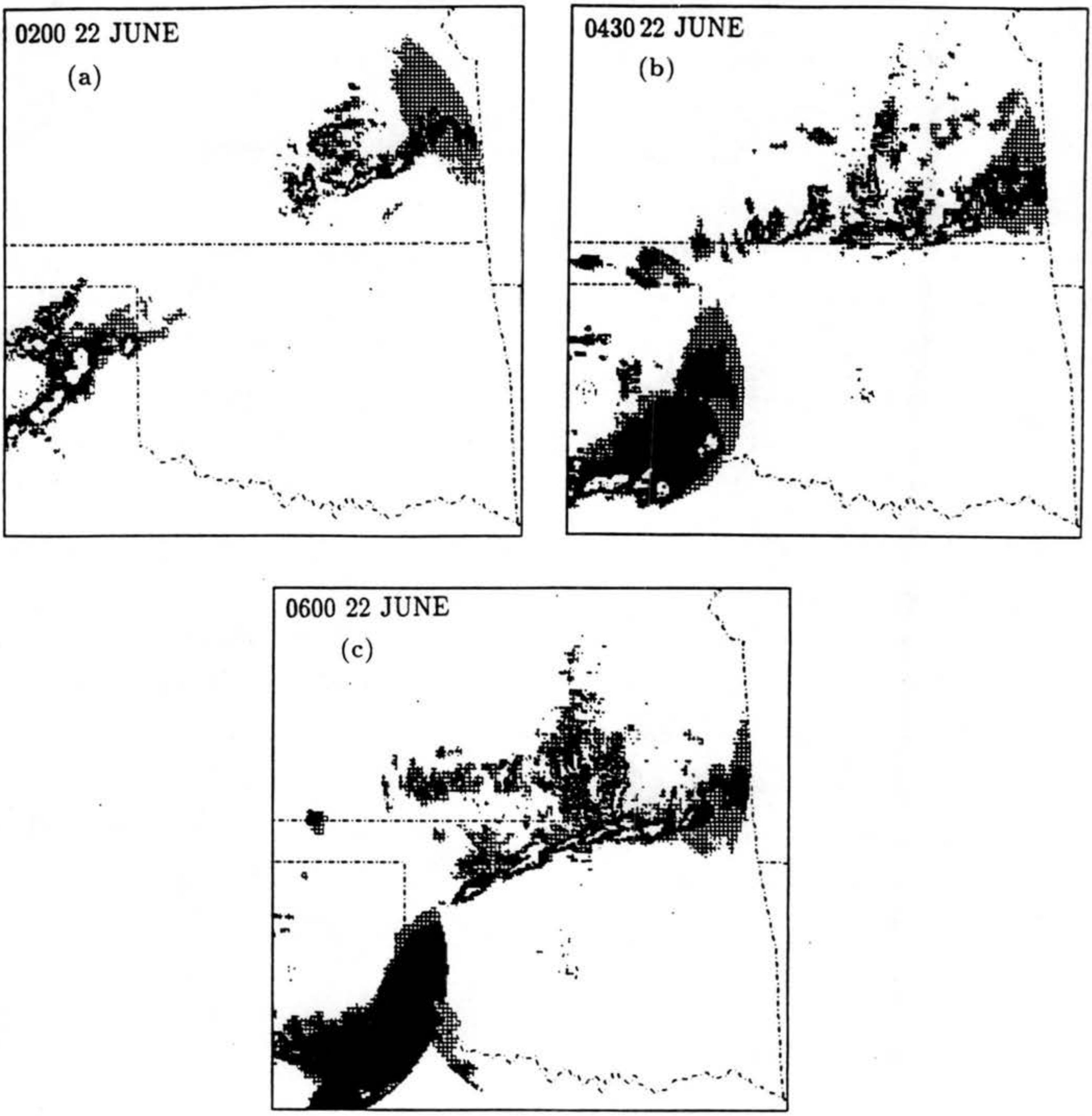

Figure 5.58: Same as Fig. 5.2 except for 22 June at: a) 0200 UTC Amarillo TX and Wichita KS; b) 0430 UTC Amarillo TX and Wichita KS; c) 0600 UTC Amarillo TX, Oklahoma City OK and Wichita KS.

systems were within radar range. The eastern system was earlier a very well developed asymmetric system with an enhanced trailing stratiform precipitation region, but it was beginning to lose that structure. Unfortunately, the stratiform precipitation region of this system never entered the mesonet, so the existence of a wake low could not be determined. There were widespread reports of large hail, severe winds, and funnel clouds with this MCS throughout its existence. The western system was characterized by two separate convective lines at this time, with the southernmost line being the most intense. There was no stratiform precipitation at this time. By 0430 (Fig. 5.58b) the structure of both MCSs changed. The eastern system's stratiform precipitation was now trailing the far eastern portion of the line, while a large, broken line of convection had developed in an east-west line extending to the west of this MCS. The western MCS still had an intense convective line, but had now developed an extensive area of heavy stratiform precipitation. The system had a combined symmetric/asymmetric structure at this time. The symmetric characteristics were that the leading line of convection did not have the tendency for its strongest cells to be on its southern flank. Also there was a region of enhanced stratiform precipitation to the rear of the central portion of this convective line. The asymmetry arose from the tendency for a large area of stratiform precipitation to be confined to the northeastern side of the MCS. By 0600 (Fig. 5.58c) the eastern MCS had a nearly solid east-west line of convection on its western side. The western MCS convection was barely visible and it started to weaken. There was still the enhanced core of stratiform precipitation as well as the extensive area of weaker, but still heavy, stratiform precipitation on the northeast side of the MCS.

5.8.3 System overview

MCS entering Oklahoma portion of mesonet (0400)

At this time (Fig. 5.59) the flow over central and eastern Oklahoma was southerly while the flow over eastern and central Kansas was easterly, becoming northerly in western Kansas. This was indicative of the position of the cold front. The east-west oriented convective line associated with the eastern MCS developed along this front. The western

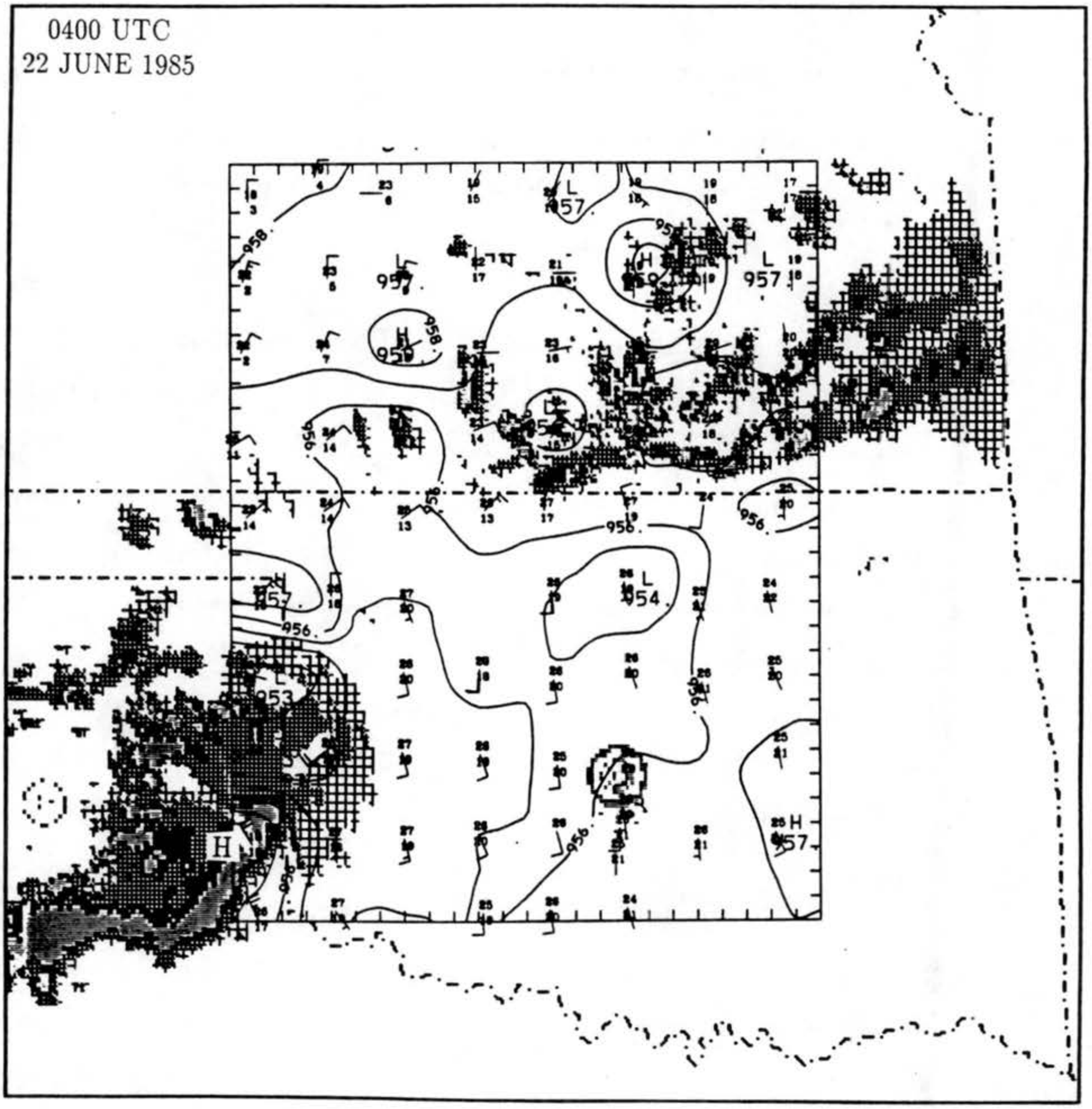

Figure 5.59: Same as Fig. 5.3 except for 0400 UTC 22 June.

MCS had a well developed mesohigh associated with its convective line. There was a 10 m s^{-1} north-northwesterly outflow from the convection, and there was quite strong divergence occurring to the rear of the mesohigh. The first reaches of the wake low appeared on the northern edge of the heavy stratiform precipitation region.

Development of intense mesolow (0600-0630)

By 0600 (Fig. 5.60) a very deep wake low developed in the far northern reaches of the stratiform precipitation region over Oklahoma and there was an enhanced gradient along the back edge of the enhanced stratiform precipitation region. There was a very strong closed vortex around this wake low with 5-7.5 m s^{-1} flow around it. Part of the vortex was due to the front and its associated wind shift, but the low itself was forcing the north and northwest flow on its western side as there was no other comparable flow in the other frontal regions. Also notice that the temperature in the center of the wake low was 2-6°C higher and the dewpoint was 3-8°C lower than any of the surrounding stations. This was indicative of an intense heat burst, and a sample mesonet station will be presented in the mesonet section. There was a mesohigh over the enhanced stratiform region in the far southwest portion of the mesonet.

The only sounding site to give an adequate representation of the rear inflow structure was AMA at 0318 (Fig. 5.61a) and 0600 (Fig. 5.61b). This was indicative of the rear inflow structure to the rear of the central portion of the system where there was also a very deep wake low. At 0318, AMA was about 25 km to the rear of the convective line and shows a 300 mb deep layer of strong rear inflow peaking at 500 mb (10 m s^{-1}). While at 0600 it was about 75 km to the rear of the stratiform precipitation region, and it shows that the rear inflow was maximized at 400 mb (9 m s^{-1}). So there was a moderate descent of the rear inflow as it approached the convective line and it was also a strong rear inflow.

By 0630 (Fig. 5.62) the northern wake low weakened by 2 mb. The wake low to the rear of the central portion of the MCS was along the back edge of the enhanced stratiform precipitation region (not visible due to the lack of AMA radar data) and can be seen as the strong gradient in the extreme southwest corner of the mesonet.

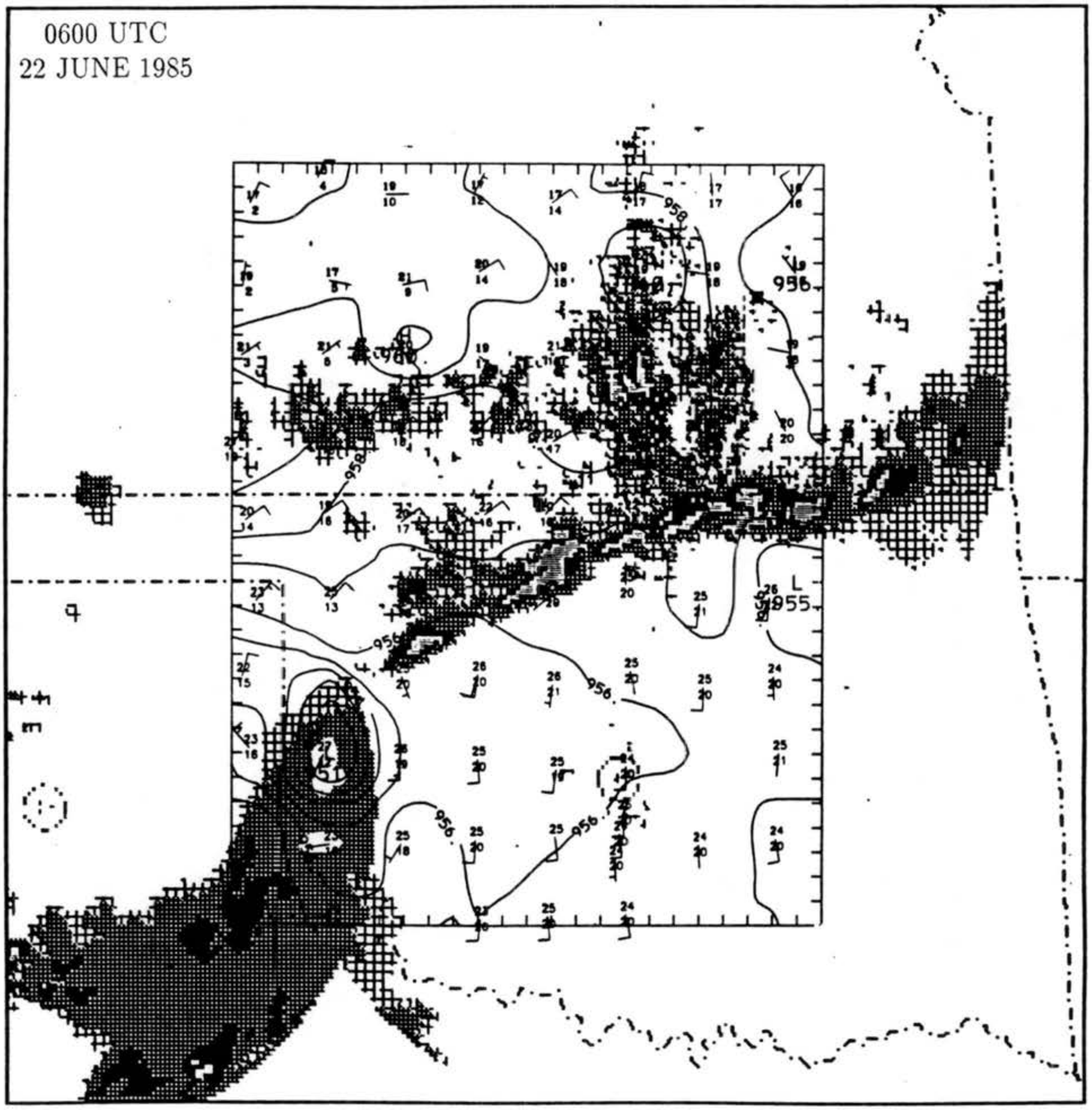

Figure 5.60: Same as Fig. 5.3 except for 0600 UTC 22 June.

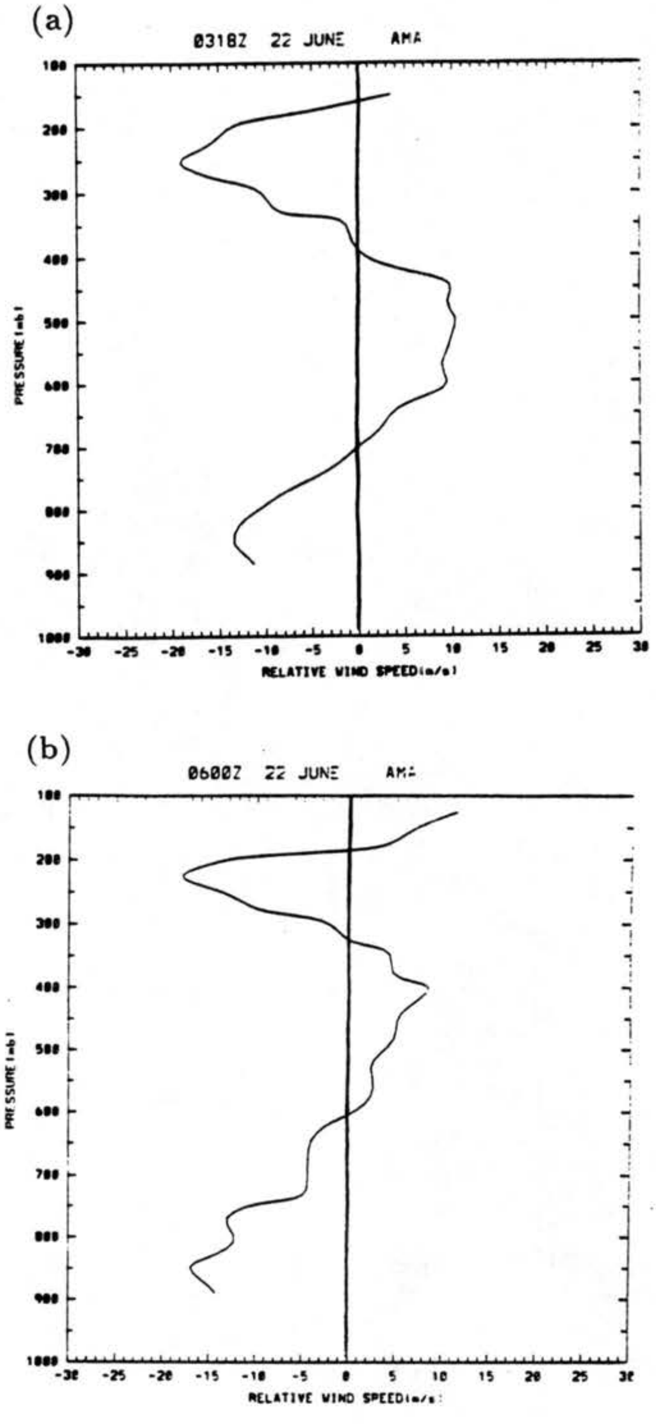

Figure 5.61: Same as Fig. 5.8 except for 22 June at: a) 0318 UTC at AMA; b) 0600 UTC at AMA.

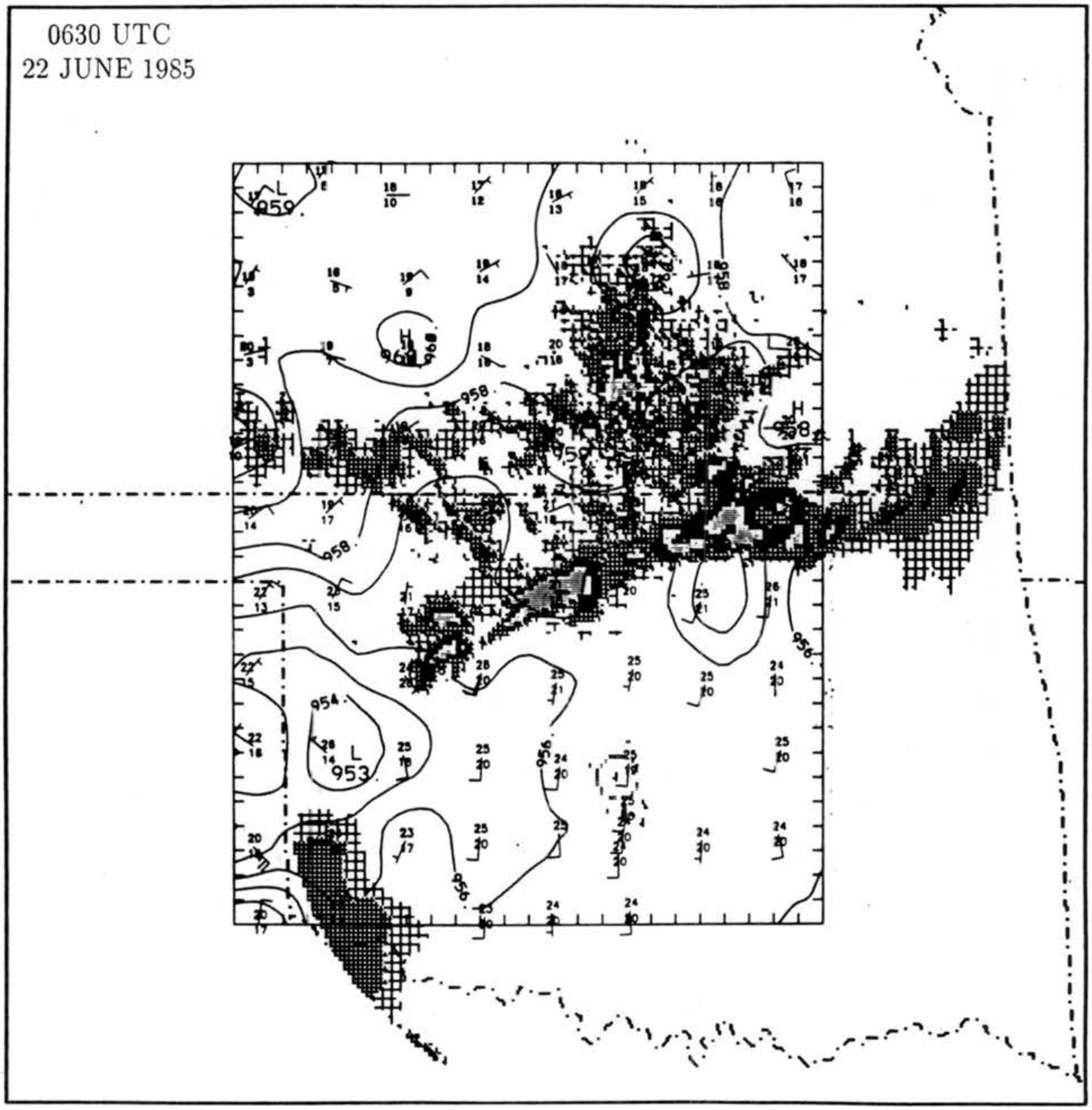

Figure 5.62: Same as Fig. 5.3 except for 0630 UTC 22 June.

Mesovortex structure (0830-0900)

By 0830 (Fig. 5.63) most of the western MCS exited the mesonet, but the back edge of its stratiform precipitation region was still evident as was the intense gradient associated with the wake low.

At 0900 the upper-air maps (Fig. 5.64a-e) show that there was the development of a mesovortex feature with this MCS. At 500 mb (Fig. 5.64a) the mesovortex was clearly visible in southwestern Oklahoma. The exact positioning of the vortex center was highly questionable since it was right along the southern reaches of the sounding network, but it appeared of be in extreme southern Oklahoma which would place it in the northern portion of the stratiform region and well as to the northeast of the surface low. At 600 mb (Fig. 5.64b) the region where the mesovortex was present at 500 mb appeared to be anticyclonic although the analysis is difficult. There was a sharp cyclonic curvature to the flow between AMA and CSM, but whether this was related to a rather sharp tilt to the mesovortex or just to the loss of its structure is unknown. At 700 mb (Fig. 5.64c) there was absolutely no sign of the mesovortex as there was only strong anticyclonic curvature over southern Oklahoma and Texas. At 800 mb (Fig. 5.64d) there was a return to the sharp cyclonic curvature over southwestern Oklahoma. The probable explanation for this odd structure is that there was a mesovortex at midlevels and at low-levels there was a circulation related to the descending rear inflow (as in Johnson and Bartels 1992). Then at the surface (not shown) there was still a weak vortex around the low. There was a very complex structure to this mesovortex as it was strongly visible at 500 mb and below 800 mb, but was replaced by an anticyclone in between. It was also interesting to note that at 500 mb, 800 mb and at the surface where the mesovortex was present, station FSB, which was near the center of the circulation, was typically 1-4°C warmer than any of the surrounding station, while at 600 mb and 700 mb where there was a mesoanticyclone it was 0-1°C cooler than its surroundings. This mesovortex structure resembled that of the 23-24 June 1985 MCS examined by Johnson and Bartels (1992). The 500 mb mesovortex was still present at 1200 (Fig. 5.64e) in north central Texas and it was still a warm core feature.

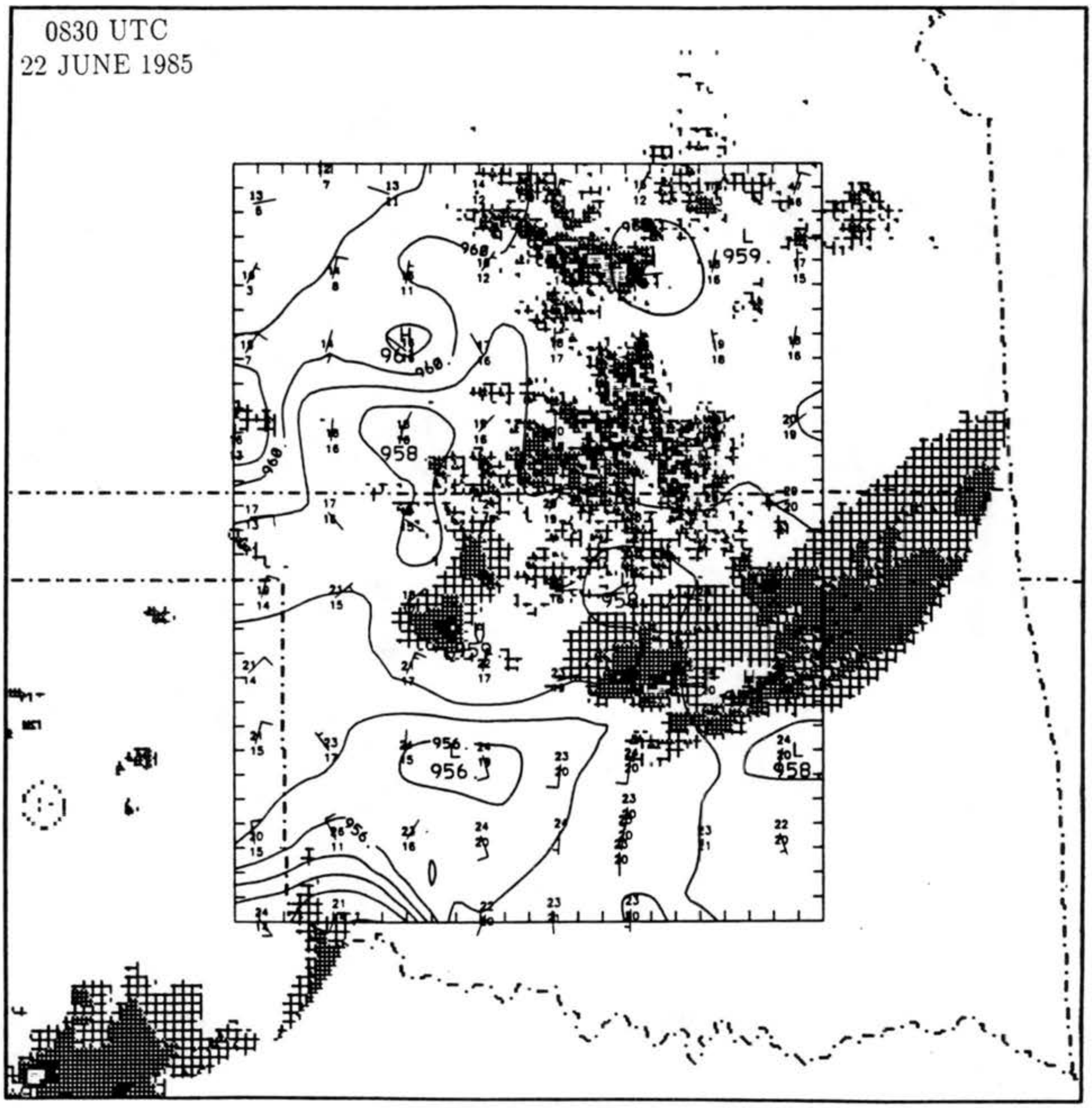

Figure 5.63: Same as Fig. 5.3 except for 0830 UTC 22 June.

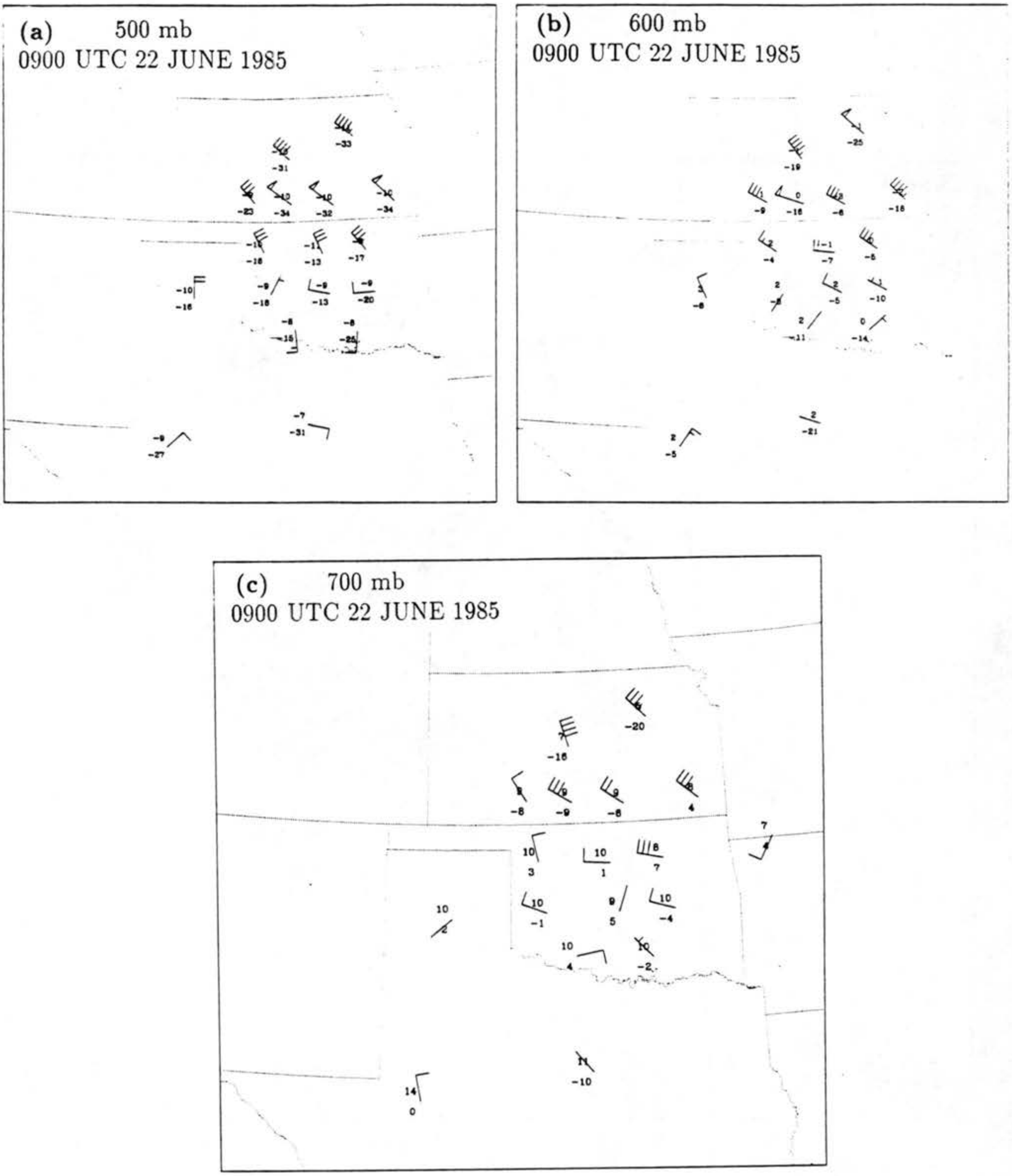

Figure 5.64: In a-d) Same as Fig. 5.8 except for 0900 UTC 22 June at: a) 500 mb; b) 600 mb: c) 700 mb; d) 800 mb. In e) Same as Fig. 5.1 except for 500 mb at 1200 UTC 22 June.

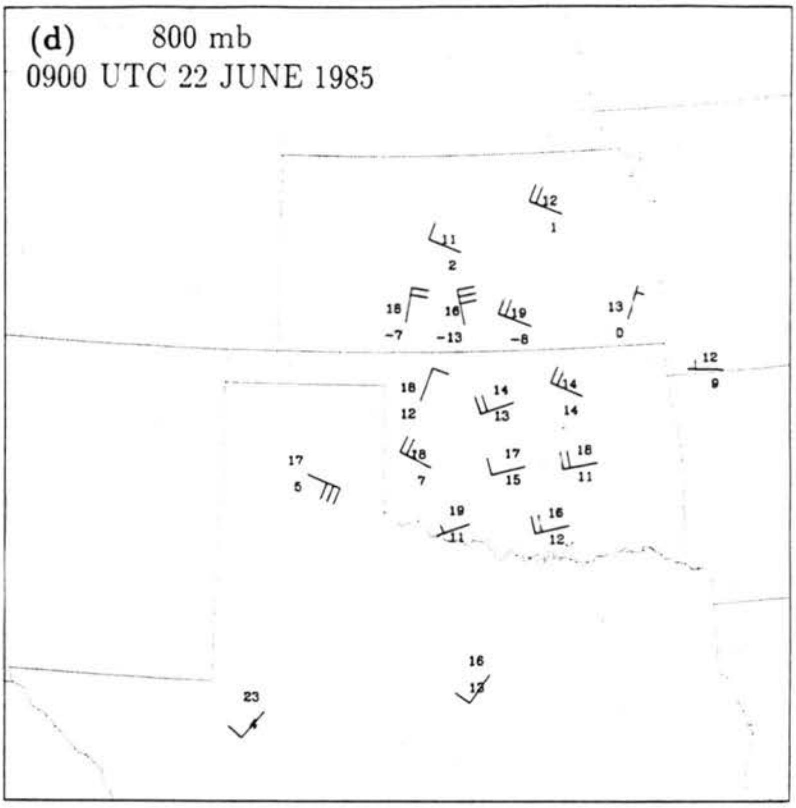

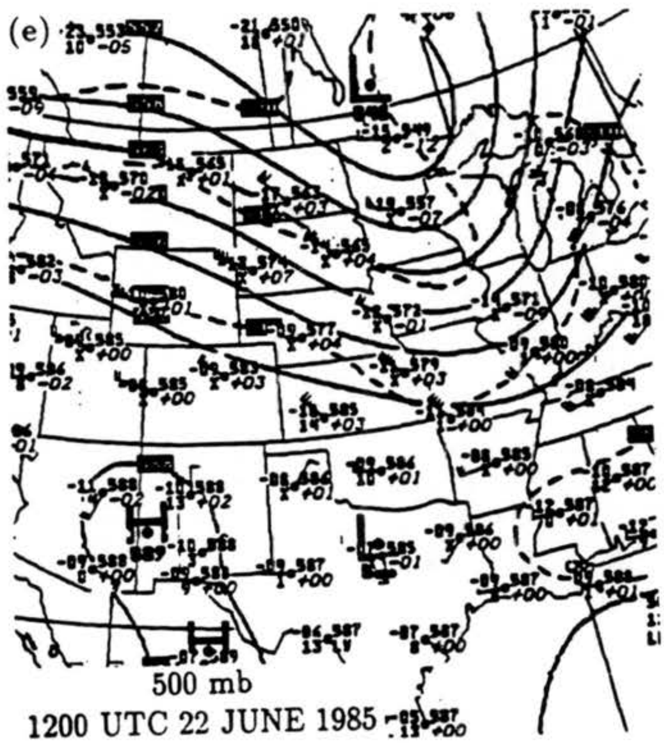

Figure 5.64: Continued.

5.8.4 Mesonet time series

The conditions associated with the southern wake low are shown by station S02 (Fig. 5.65, see Fig. 3.1). The mesohigh (0630) was quite sharp with a 5 mb increase in 60 min and was associated with a 8°C temperature and a 2°C dewpoint decrease in 15 min as well as a 26 m s^{-1} wind gust and a shift from southeast to northwest flow. Then the wake low (0750) passed over with a 8 mb decrease in 40 min and was accompanied by a slow warming of 4°C and a dewpoint decrease of 4°C while the pressure droped, indicative of a fairly large heat burst event. There was also a 23 m s^{-1} wind gust and a shift from north to southeast flow.

The northern wake low conditions are summarized by station S19 (Fig. 5.66). The mesohigh (0400) was less intense here (2 mb increase in 20 min) as the convection did not directly pass over this region. There was an 18 m s^{-1} wind gust, a 2°C cooling and dewpoint decrease and virtually no wind shift. The first pressure drop (0430) was associated with a weak low which passed over and this has very little effect on the other features. The second drop (0600) was the wake low with a 4.5 mb decrease in 60 min and was accompanied by an 18 m s^{-1} wind gust and a very sharp heat burst event which lasted about 10 min and had a 6°C temperature increase and a 7°C dewpoint decrease.

5.9 June 24 case

5.9.1 Synoptic overview

The 0000 24 June maps are used to summarize the conditions associated with the development of this MCS. At the surface (Fig. 5.67a) there was a 1003 mb low over north-central Wyoming with a stationary front extending to the southeast to northwestern Kansas where there was a 1005 mb low with the front extending to the northeast through south-central and northeastern Nebraska. To the south of the front the temperatures were 29-35°C with dewpoints of 18-21°C and a southerly flow. To the north of the front the temperatures were 29-35°C with dewpoints of 7-12°C and a southeast flow.

At 850 mb (Fig. 5.67b) there was a trough extending south from Montana to central Colorado and another trough extending to the east through central Nebraska. There was

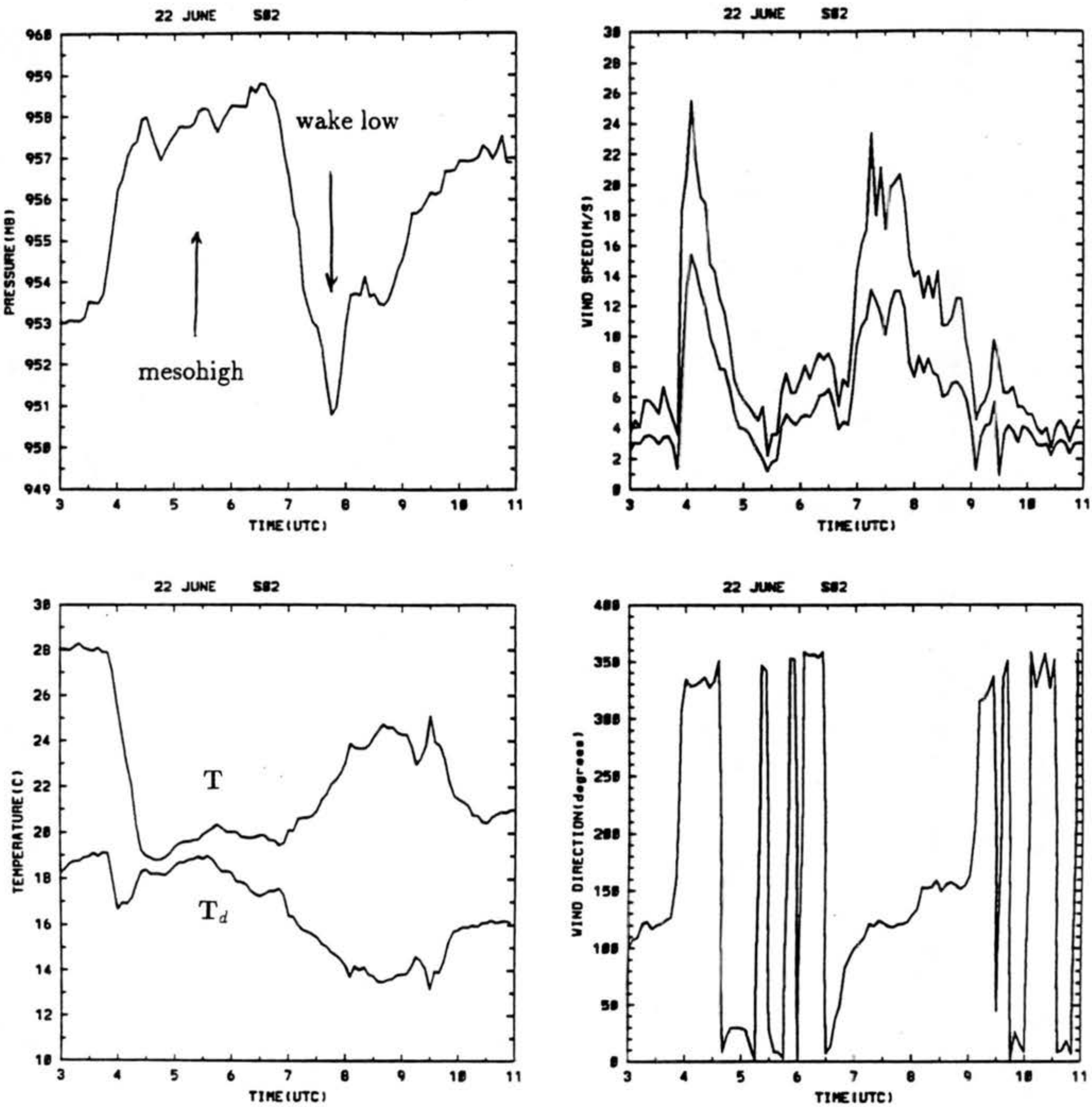

Figure 5.65: Same as Fig. 5.9 except for 22 June at station S02. Note different time scale as each tick mark represents 30 minutes.

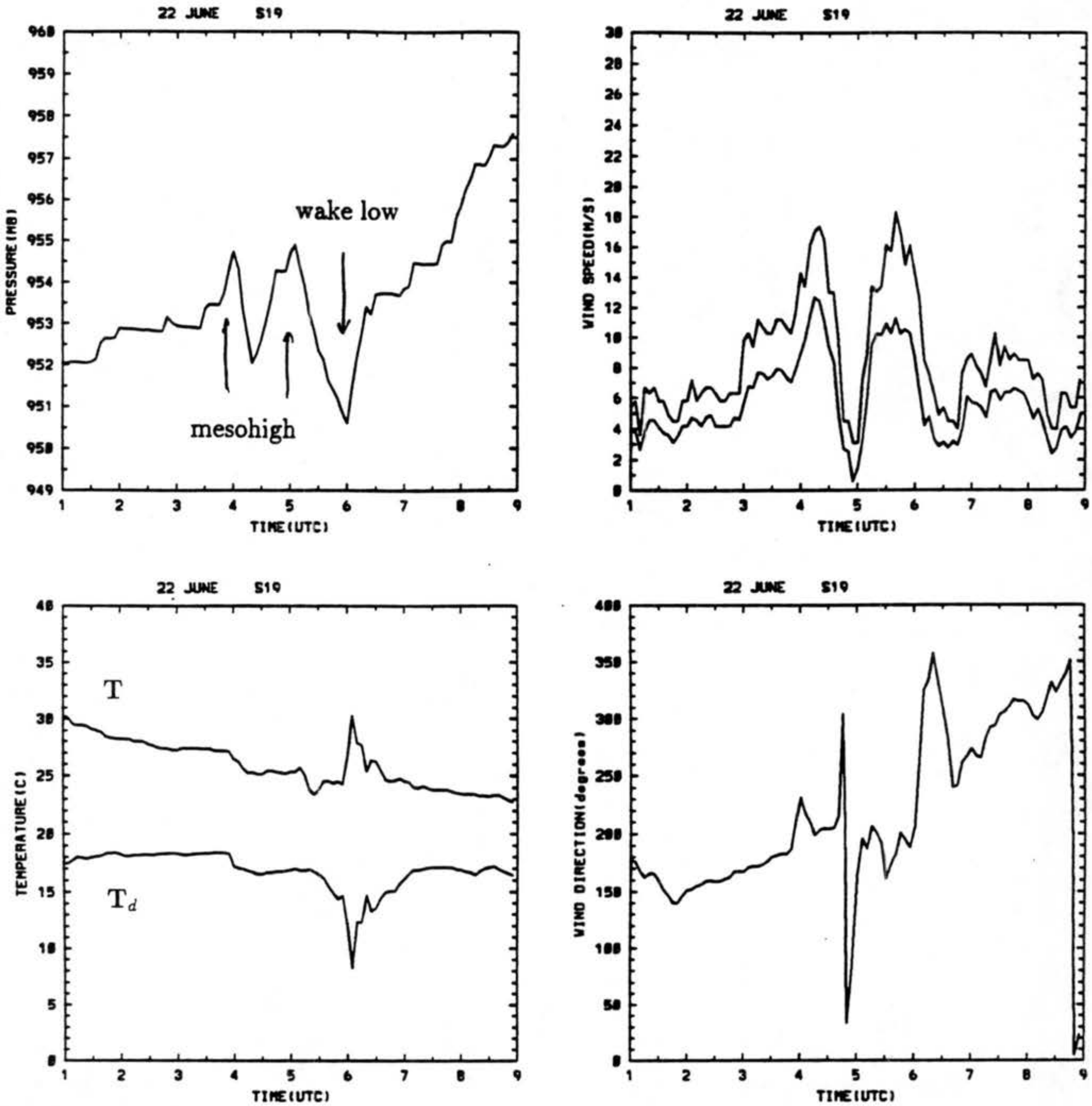

Figure 5.66: Same as Fig. 5.9 except for 22 June at station S19. Note different time scale as each tick mark represents 30 minutes.

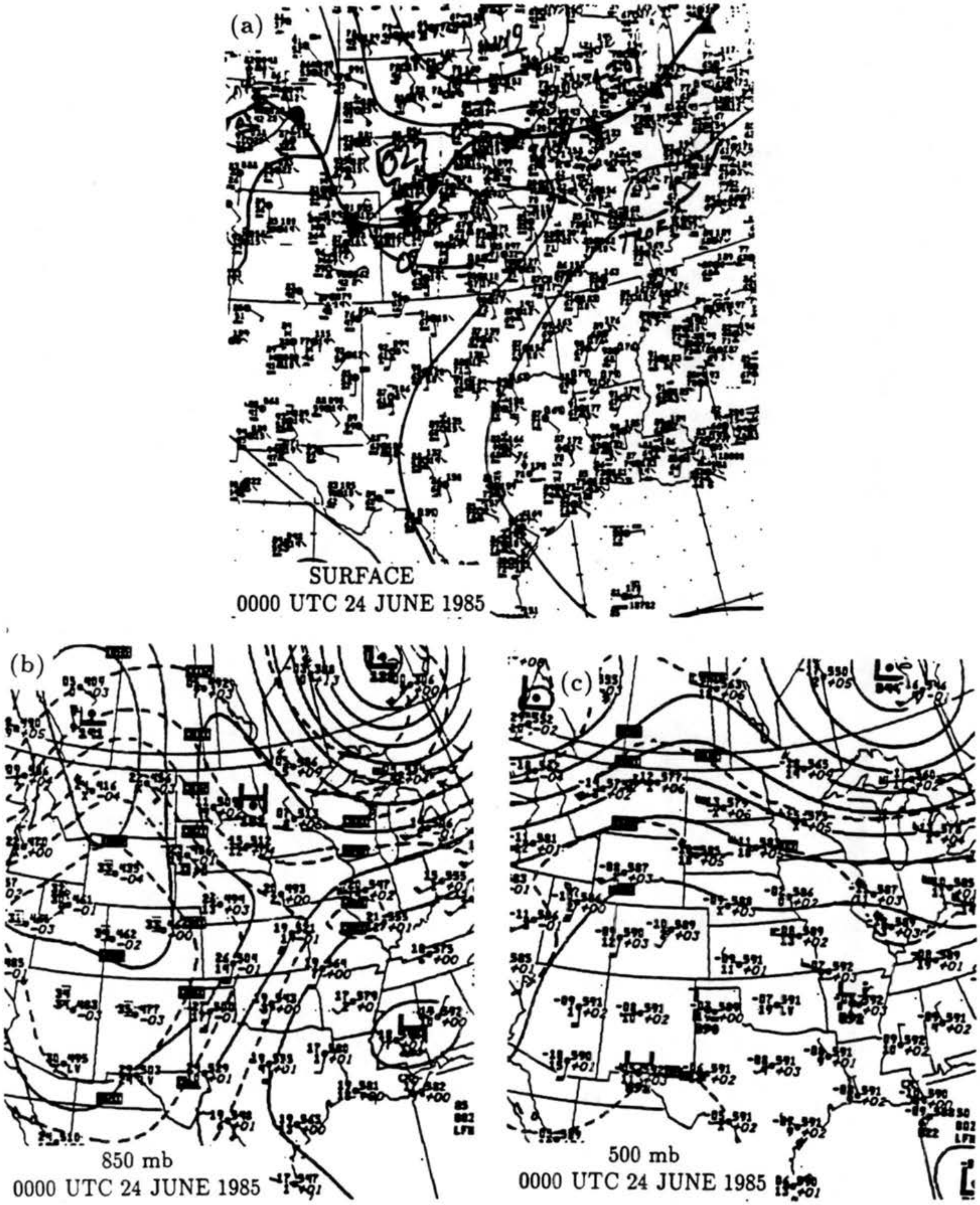

Figure 5.67: Same as Fig. 5.1 except for 0000 UTC 24 June.

a very strong (10-15 m s^{-1}) south-southwest flow over central Texas north to Kansas. This same area was covered by very moist air. At 500 mb (Fig. 5.67c) there was a general ridge over the southern U.S. and there was very weak (0-10 m s^{-1}) west-northwest flow over Kansas south to Texas.

5.9.2 Radar overview

The initial convective development associated with this MCS occurred around 1900 23 June in western Kansas ahead of the cold front (not shown). By 0100 (Fig. 5.68a) there were two separate MCSs evident in Kansas. The eastern MCS did not move through the PRE-STORM network so it is not examined here. The western system at this time had a line of fairly weak leading convection with a limited area of light stratiform precipitation extending to its rear. Due to a problem with the Garden City, Kansas radar data, the true extent of this system was difficult to determine. By 0330 (Fig. 5.68b) the western MCS developed an extensive area of enhanced trailing stratiform precipitation to the northeast of the convective line, giving this system an asymmetric structure, although it was rotated about 90° from the previous cases because of its southerly movement. By 0530 (Fig. 5.68c) the leading line of convection had largely dissipated. The trailing stratiform precipitation continued to expand its areal coverage. An important feature which developed was an arm-like appendage to the stratiform precipitation region on the northeast side of the system. By 0900 (Fig. 5.68d) the entire system largely dissipated with only a small amount of stratiform precipitation remaining.

5.9.3 System overview

MCS entering mesonet with mesohigh/wake low (0100-0200)

At 0100 (Fig. 5.69) there was southerly flow over all of Oklahoma and Kansas. A weak pre-squall low was ahead of the central portion of the convective line. There was a strong mesohigh centered along and just to the rear of the convective line. There was a strong 10 m s^{-1} northerly outflow from the MCS. To the rear of the mesohigh there was very strong divergence as the flow through the wake low shifted to southerly. Notice that at stations P02 and P03 the temperature was very warm and it was also very dry. There

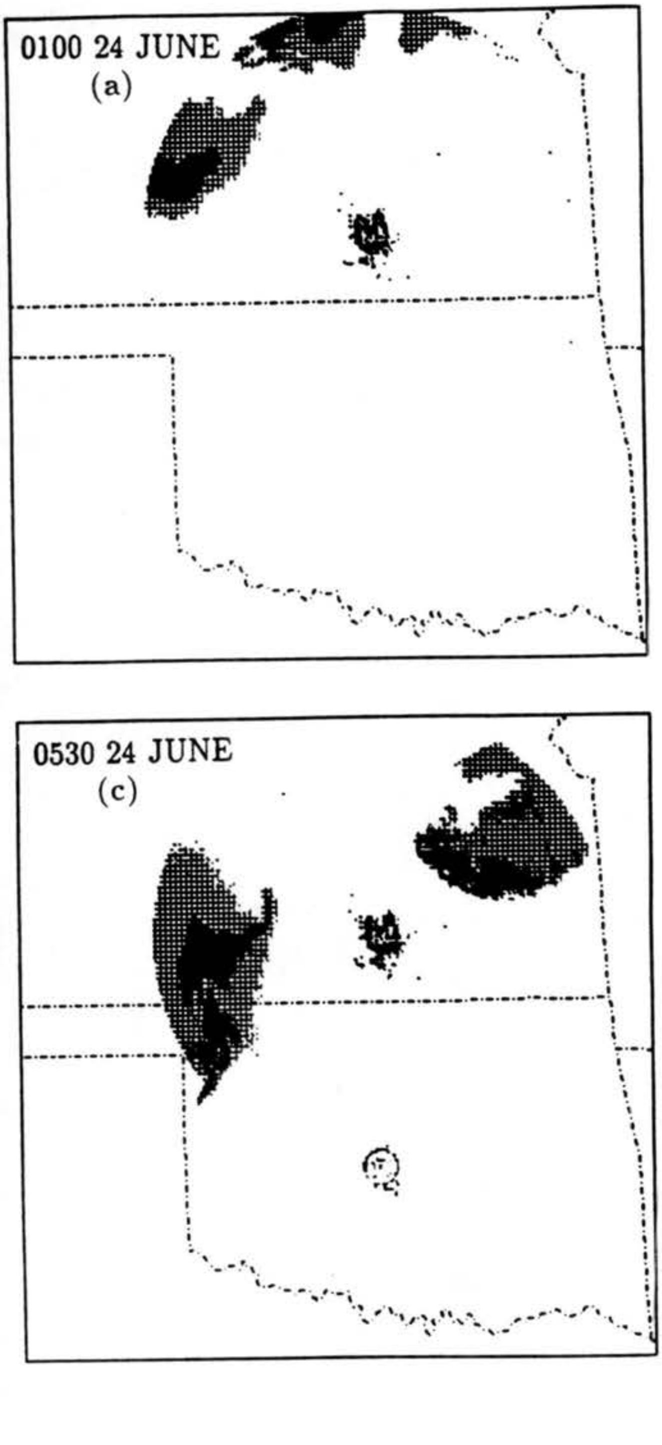

Figure 5.68: Same as Fig. 5.2 except for 24 June at: a) 0100 UTC Wichita KS; b) 0330 UTC Wichita KS; c) 0530 UTC Oklahoma City OK and Wichita KS; d) 0900 UTC Oklahoma City OK and Wichita KS.

0100 UTC
24 JUNE 1985

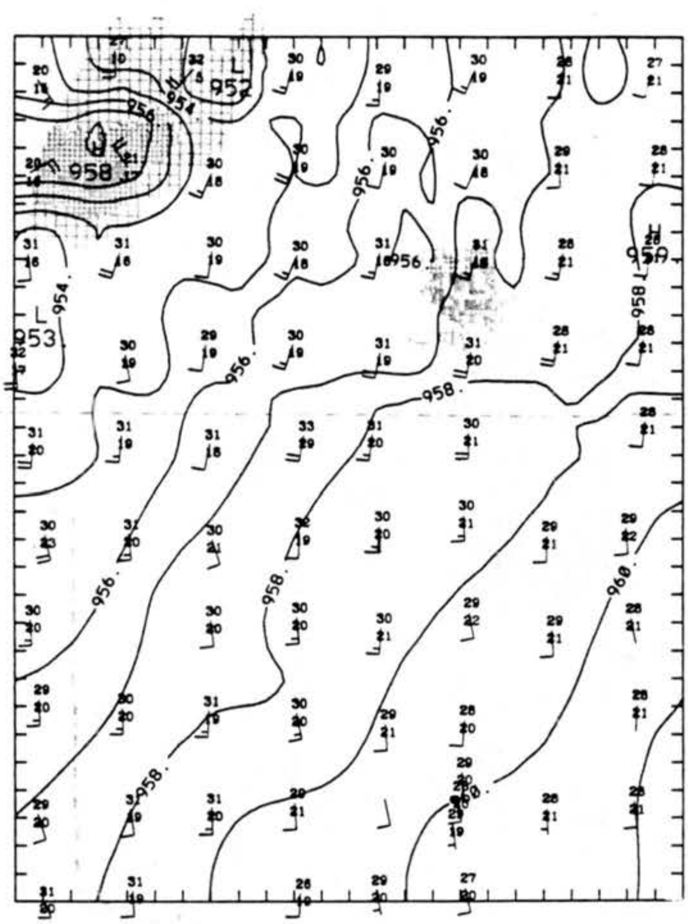

Figure 5.69: Same as Fig. 5.3 except for 0100 UTC 24 June.

were a series of heat bursts which occurred in this region of the wake low. For more on these features see Johnson et al. (1989).

By 0200 (Fig. 5.70), although neither of the pressure features strengthened, the gradient between them greatly increased. This was partially due to the mesohigh center moving to the region of enhanced stratiform precipitation as it developed. The most intense gradient was along the back edge of this newly developed enhanced stratiform precipitation region. The flow in the wake low region responded to the strengthening of the gradient and was now 10-15 m s^{-1}. This further increased the divergence to the rear of the mesohigh.

Development of mesovortex (0400-0530)

By 0400 (Fig. 5.71) the mesohigh strengthened by 4 mb and covered most of the MCS. The wake low weakened by 2 mb and was now in two sections. The region of strong gradient tended to conform to the shape of the enhanced stratiform region. Also notice that in the northeastern portion of the MCS in the enhanced stratiform region there was a mesohigh at this time.

By 0530 (Fig. 5.72) the mesohigh covered the majority of the system. The wake low filled by another 2 mb. But a trough now extended along the region where the arm-like appendage to the stratiform precipitation region was. This trough may have been a surface representation of a mid-level mesovortex which was found to occur in this case by Johnson et al. (1989) and Johnson and Bartels (1992). Johnson and Bartels found that at 4.5 km there was a closed system-relative cyclonic circulation centered just to the west of the arm-like appendage and they hypothesize that the mesovortex was creating this feature. They also found that the mesovortex extended from 3-9 km. A closed vortex never did reach the surface. They also found that the strong reflectivity gradient at low levels marked the northern boundary of the surface rainfall as well as the pronounced zone of midtropospheric convergence of the FTR flow from the south and the RTF flow from the north. This convergent flow strongly descended and was collocated with the band of the strong surface pressure gradient.

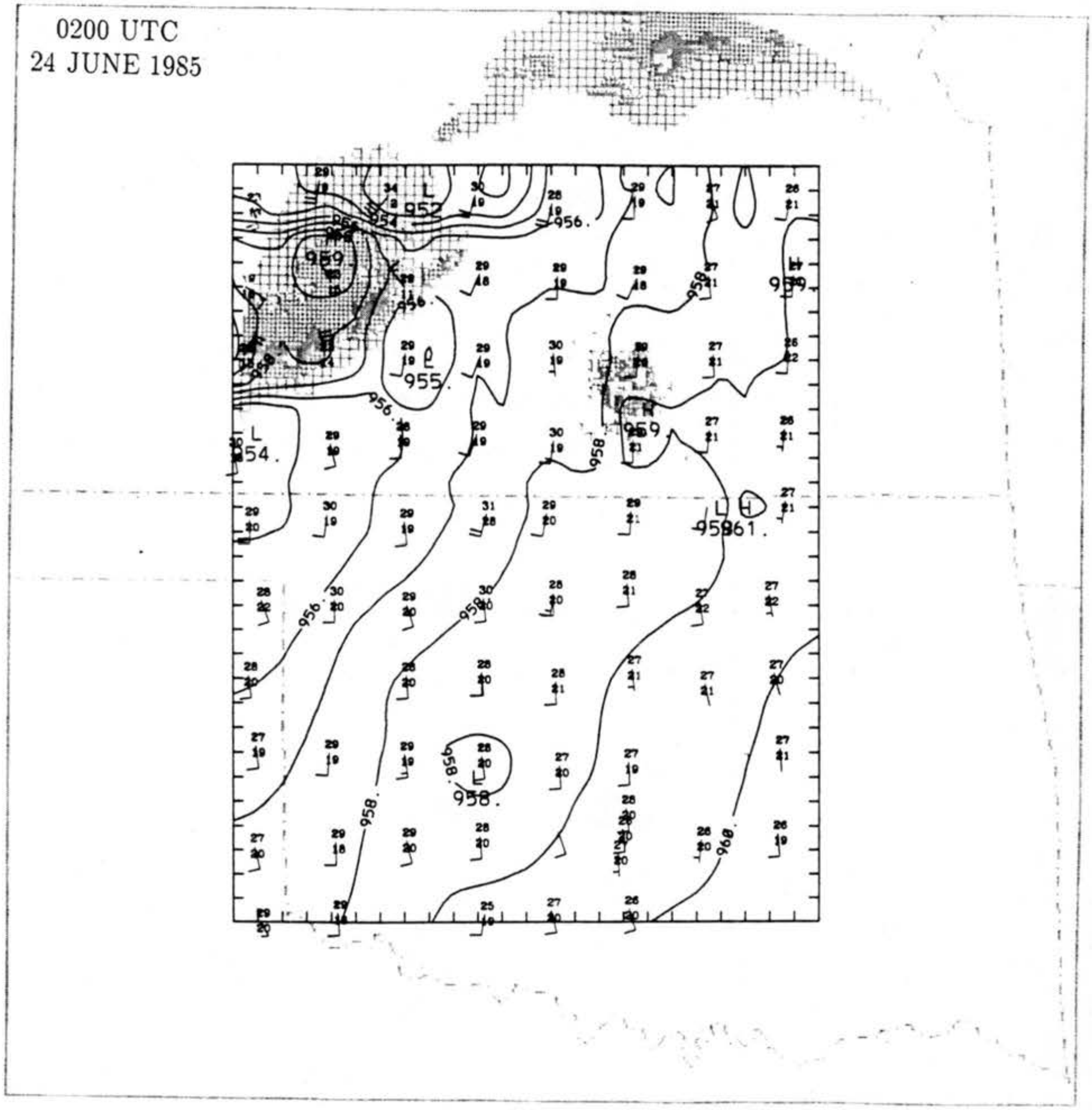

Figure 5.70: Same as Fig. 5.3 except for 0200 UTC 24 June.

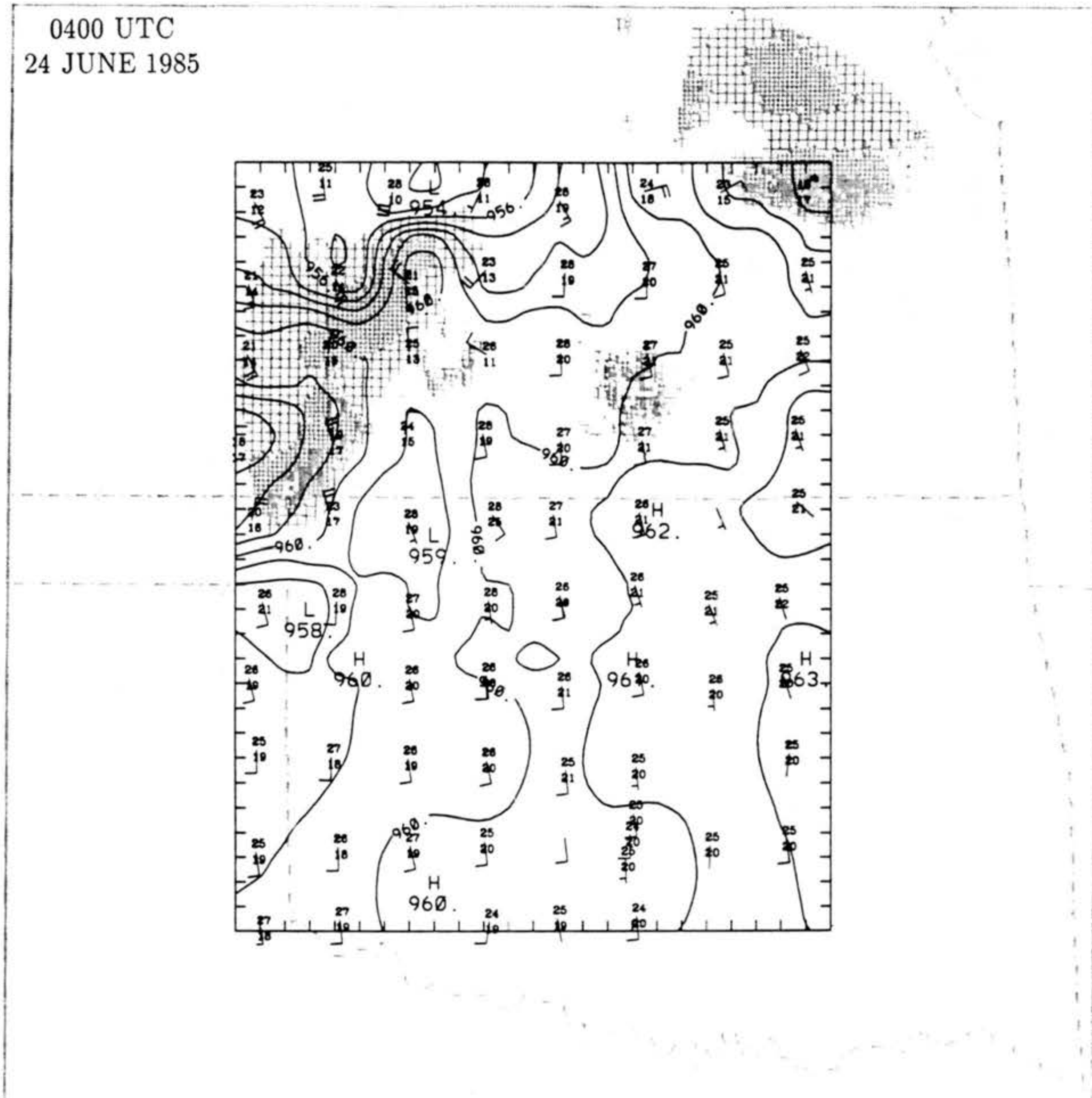

Figure 5.71: Same as Fig. 5.3 except for 0400 UTC 24 June.

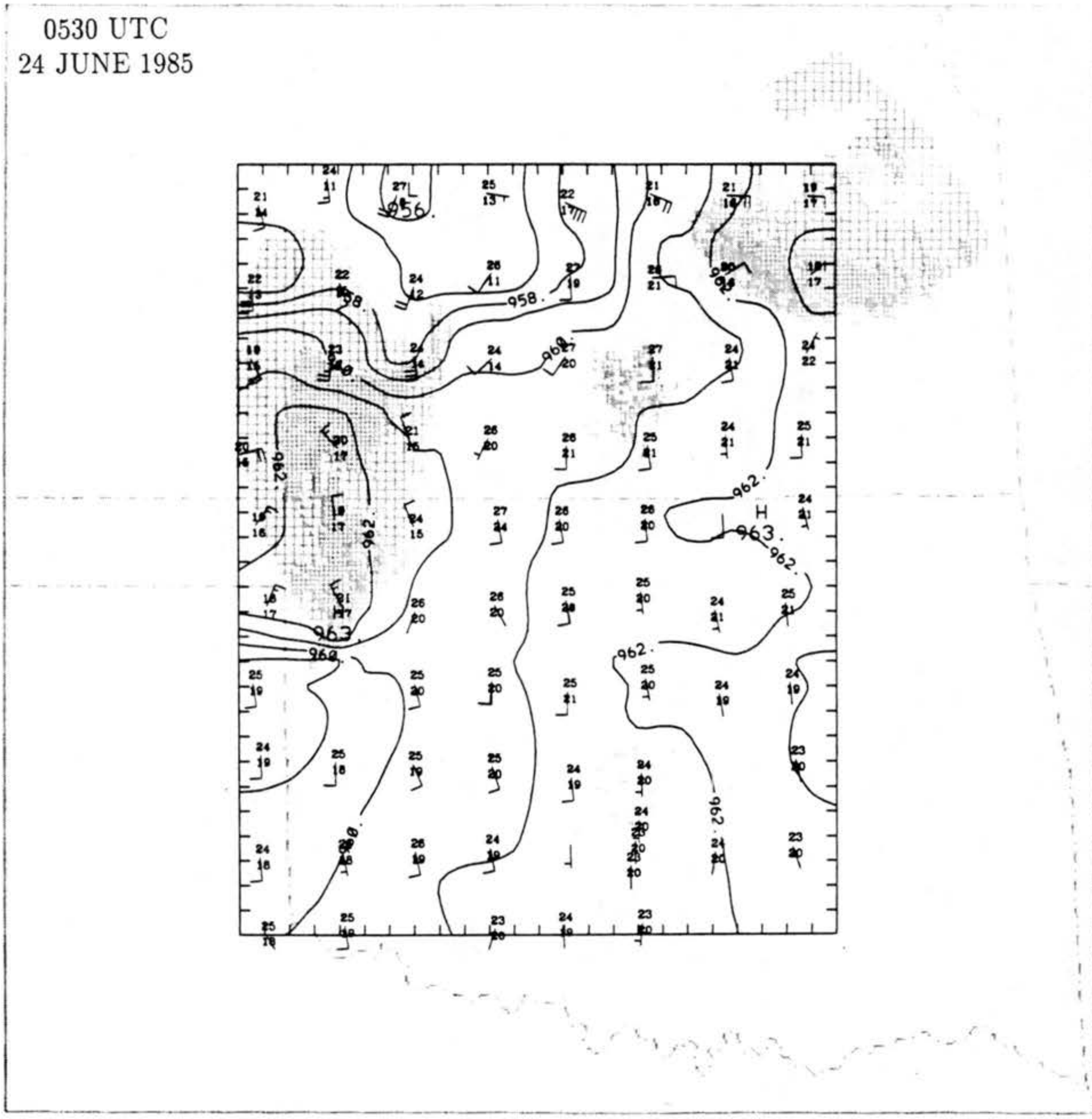

Figure 5.72: Same as Fig. 5.3 except for 0530 UTC 24 June.

Dissipated stage (0900)

The features associated with this MCS remained largely the same from 0530 to 0900 with a strong gradient found along the back edge of the enhanced stratiform precipitation region. By 0900 (Fig. 5.73) the flow field was largely unaffected by the MCS except for a weak (2.5-5 m s^{-1}) northerly outflow along its southern edge. Despite the greatly dissipated nature of the precipitation associated with this MCS, there was still a very deep low with an enhanced gradient found along the back edge of the precipitation that did still exist. This low still remained for another 2-3 hr after this time. Johnson and Bartels (1992) found that at 500 mb the closed cyclonic circulation which was present at 0530 expanded. They also found that this mesovortex sloped to the northeast with height. The mesovortex was visible in the ground-relative framework at 500 mb (Fig. 5.74), and it was centered to the southwest of PTT at this time.

5.9.4 Mesonet time series

There were two separate stages to the surface structure of this system. The early stage is shown by P03 (Fig. 5.75, see Fig. 3.1). Here there were several large fluctuations in the pressure field (from 0000-0400). Each of the areas of low pressure was associated with a heat burst event, each lasting about 10-15 min. The flow was very strong at all times in this region with the sustained flow ranging from 10-18 m s^{-1} and gusts from 14-29 m s^{-1}, the strongest winds found in any case examined here.

At a later stage at P10 (Fig. 5.76) the pressure had much smoother changes. There was a sharp gust front (0030) with a 3.5 mb increase in 40 min and a cooling of 11°C and a dewpoint increase of 6°C as well as a 26 m s^{-1} wind gust and a shift from southerly to northewesterly flow. The wake low (0340) is also sharp in this region with a 6 mb decrease in 40 min and it was accompanied by a 2°C warming and dewpoint decrease as well as a 26 m s^{-1} wind gust and a shift from northerly to southeasterly flow.

5.10 June 26-27 case

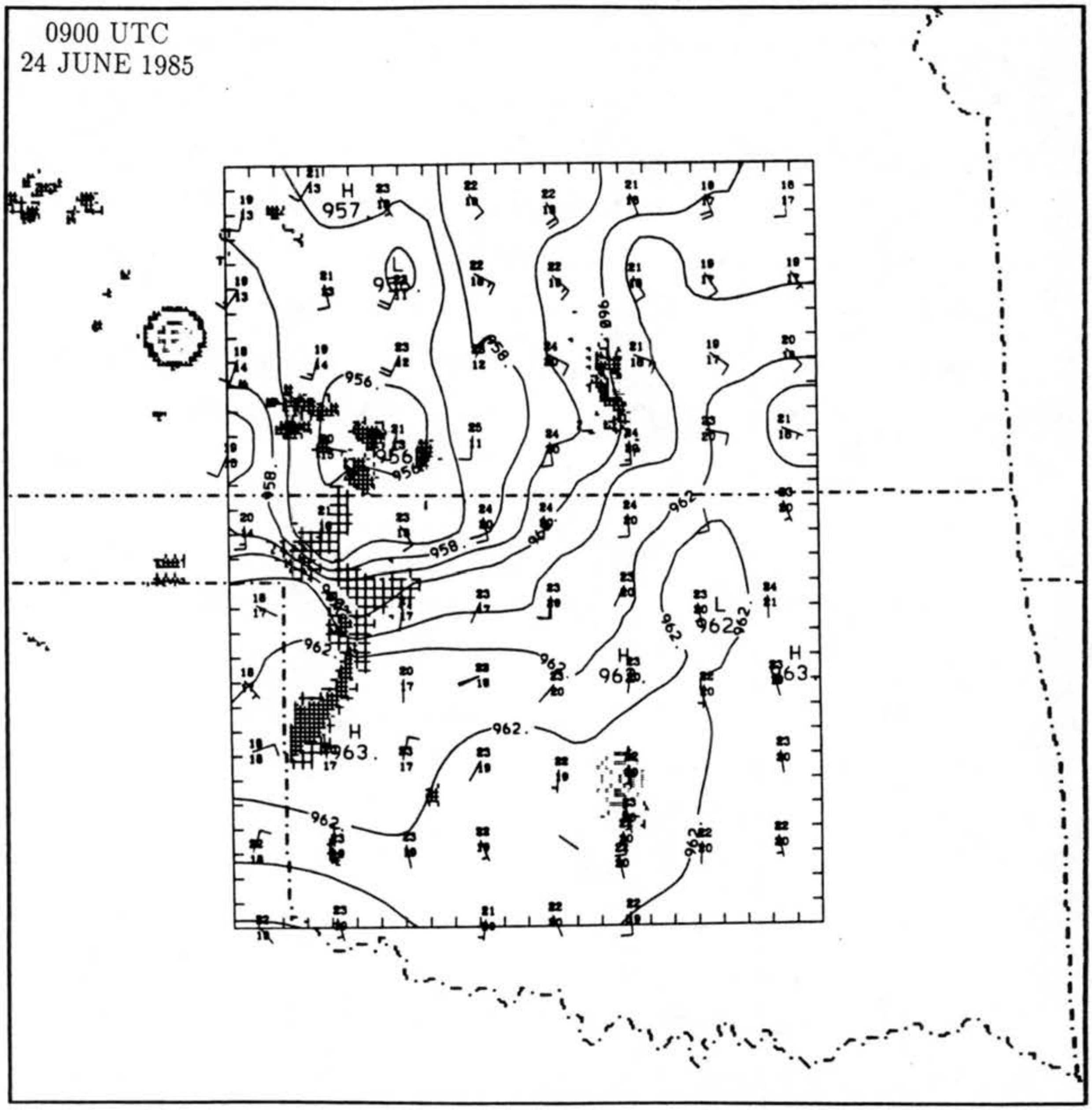

Figure 5.73: Same as Fig. 5.3 except for 0900 UTC 24 June.

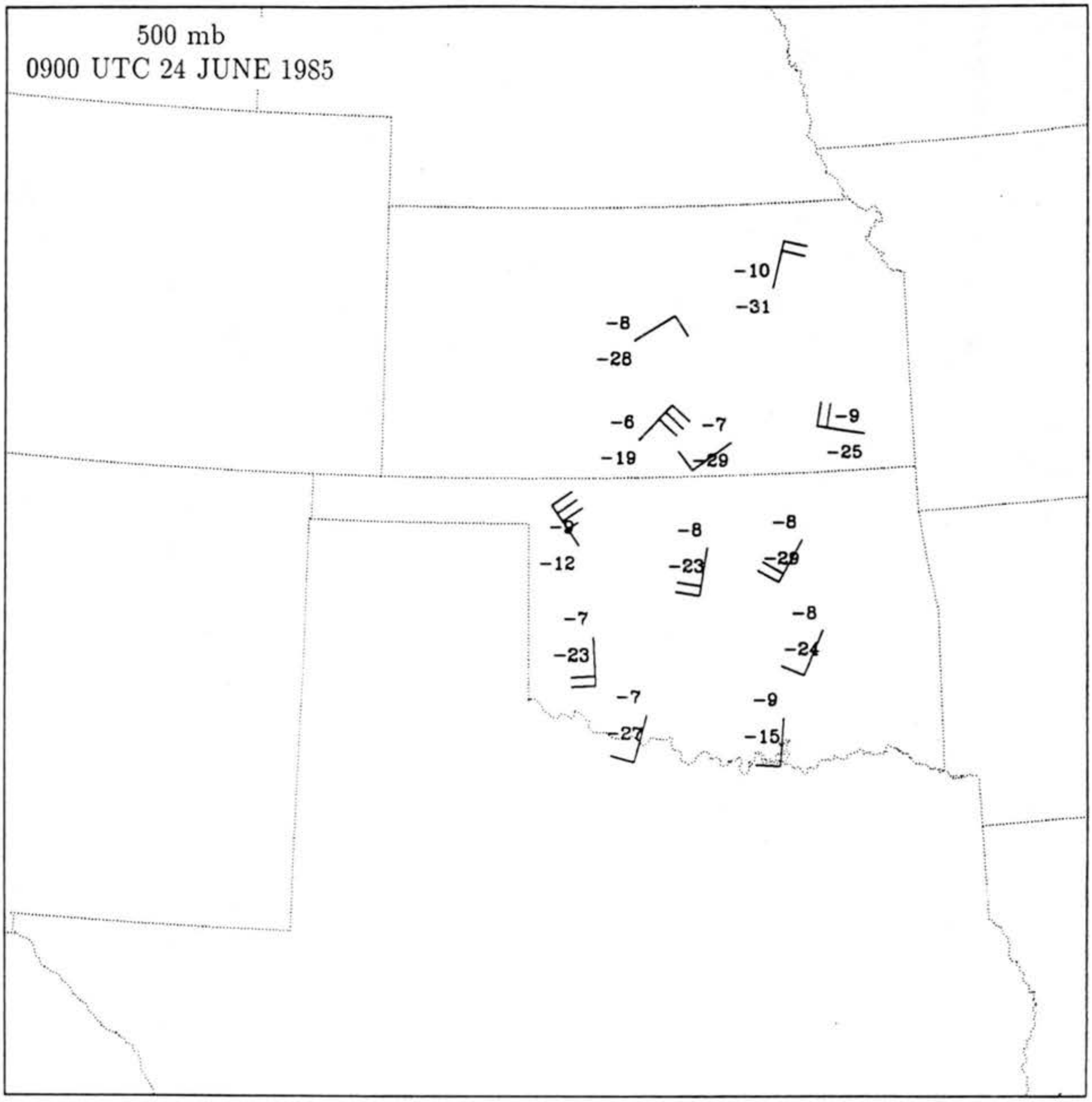

Figure 5.74: Same as Fig. 5.10 except for 500 mb at 0900 UTC 24 June.

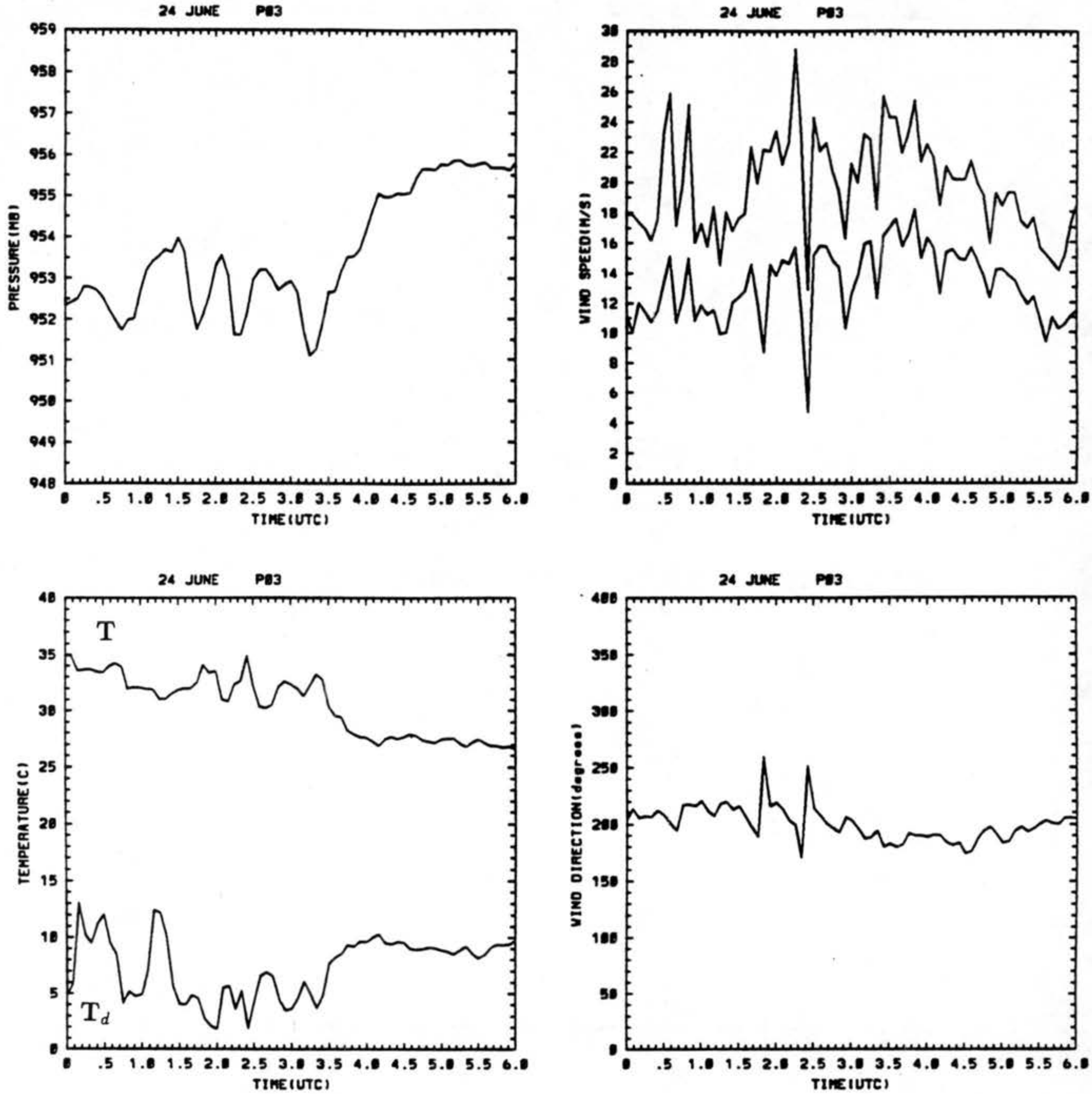

Figure 5.75: Same as Fig. 5.9 except for 24 June at station P03.

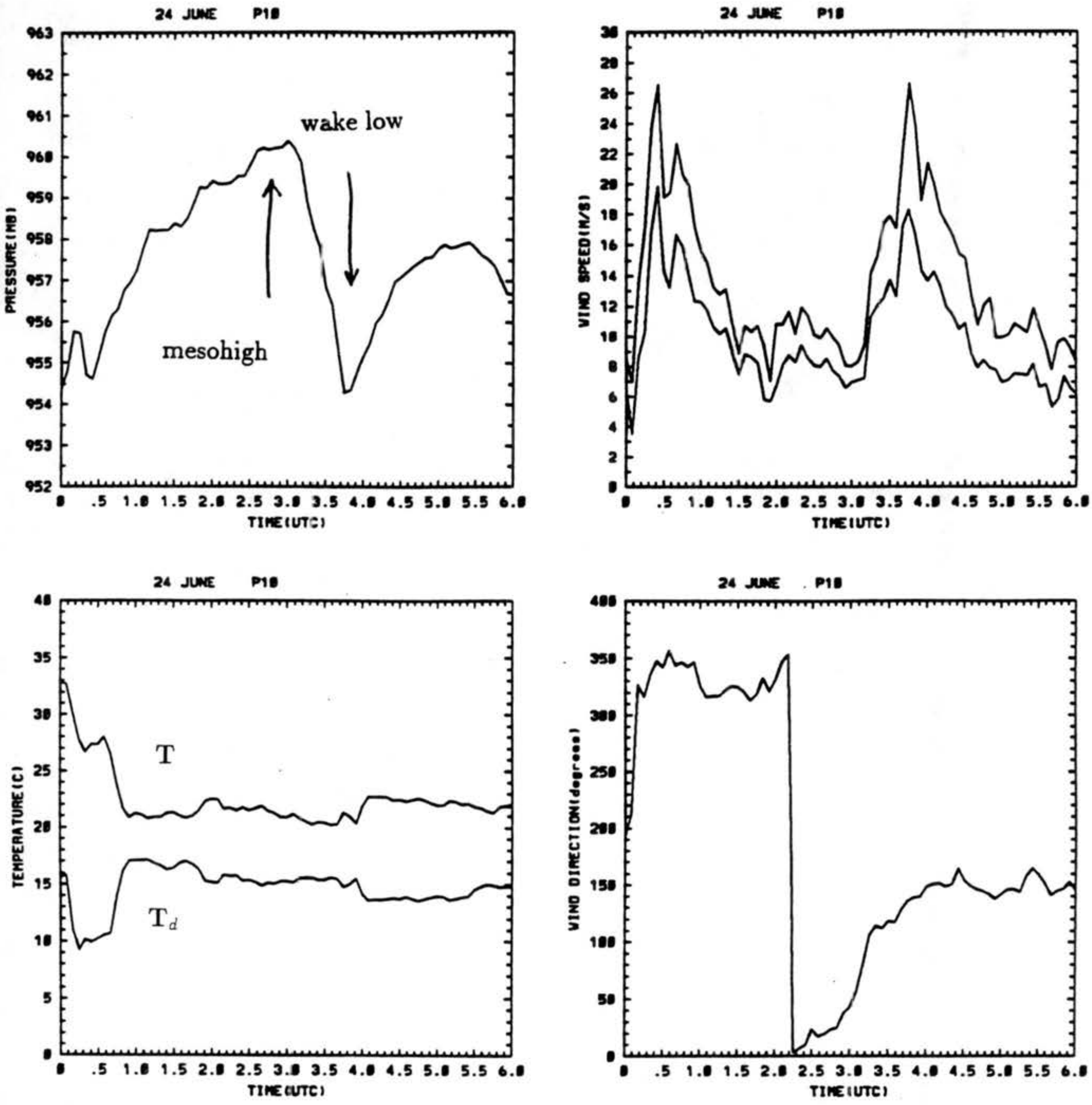

Figure 5.76: Same as Fig. 5.9 except for 24 June at station P10.

5.10.1 Synoptic overview

The 1200 26 June maps are used to summarize the large-scale conditions associated with the development of this MCS. At the surface (Fig. 5.77a) there was a 1007 mb low in east-central Minnesota with a strong cold front extending to the southwest through southeastern Nebraska to north-central and southwestern Kansas. To the south of the front the temperatures were 21-24°C with dewpoints of 15-21°C and a southeast flow. To the north of the front the temperatures were 10-16°C with dewpoints of 7-12°C and a northerly flow.

At 850 mb (Fig. 5.77b) there was a sharp trough extending from central Canada south to western Kansas. Ahead of the trough there was a very strong (15-23 m s^{-1}) southwesterly jet with very moist air also found here. At 500 mb (fig. 5.77c) the sharp trough was across central Wyoming to the Arizona-New Mexico border. There was a southerly flow over Oklahoma and Kansas.

5.10.2 Radar summary

The initial development associated with this MCS occurred around 1200 26 June in the Texas panhandle (not shown). By 1600 (Fig. 5.78a) there were two separate areas of precipitation. There was an approximately east-west oriented line of convection in northern Kansas, and this area was moving northerly and quickly separated from the rest of the system. Then there was a northeast-southwest oriented convective line of scattered convection over southern Kansas into Oklahoma. In between there was a twisting band of stratiform precipitation. By 1900 (Fig. 5.78b) the east-west oriented convective line which was in northern Kansas had now separated itself from the MCS. There were three basic precipitation structures at this time. First, there was a leading line of convection. Second, there was a region of enhanced stratiform precipitation which was separated from the leading convective line by about a 25 km region that was precipitation free. Then right along the back edge of the stratiform precipitation region another line of convection was starting to develop. By 2200 (Fig. 5.78c) the convective line which was trailing the stratiform precipitation region earlier had overtaken it and was now the dominant

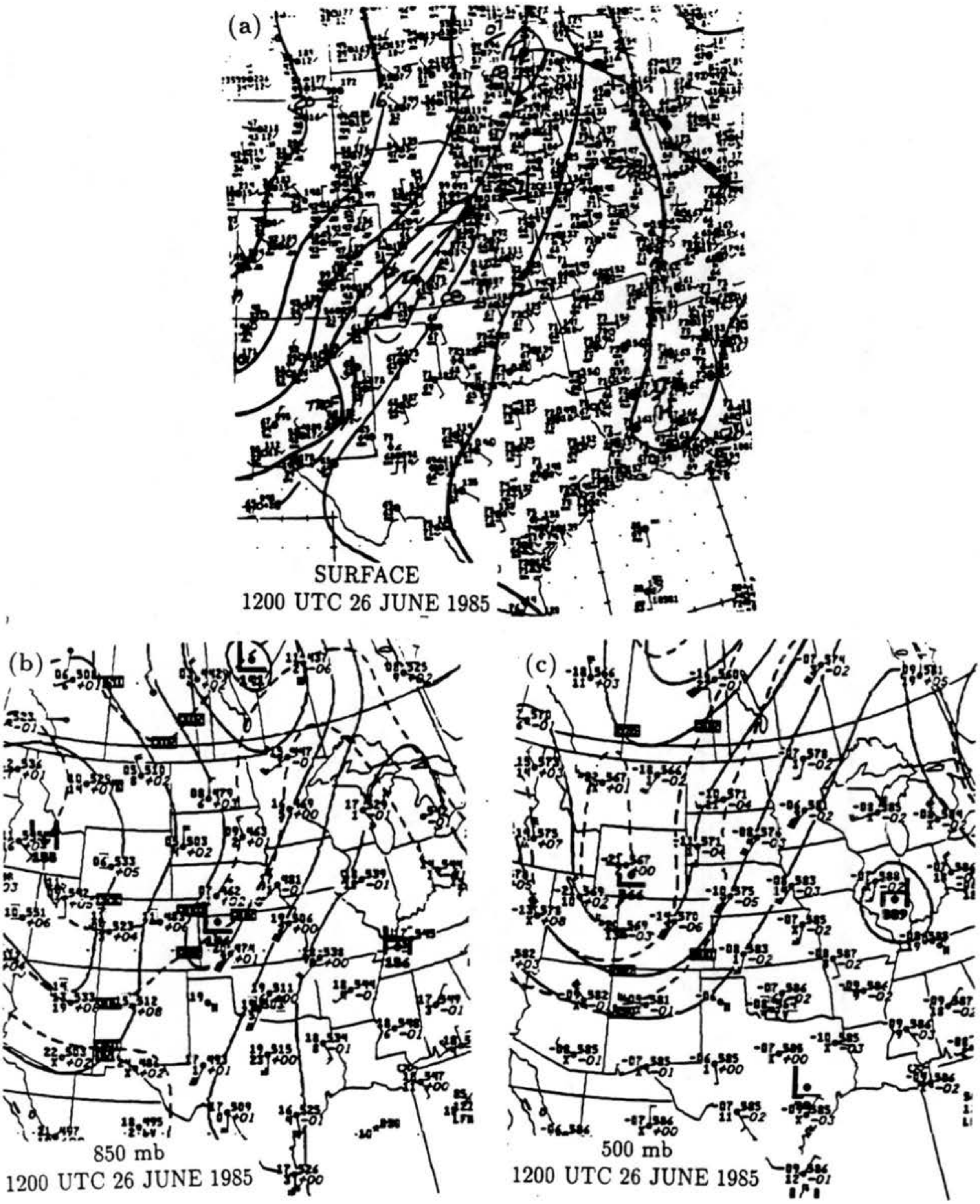

Figure 5.77: Same as Fig. 5.1 except for 1200 UTC 26 June.

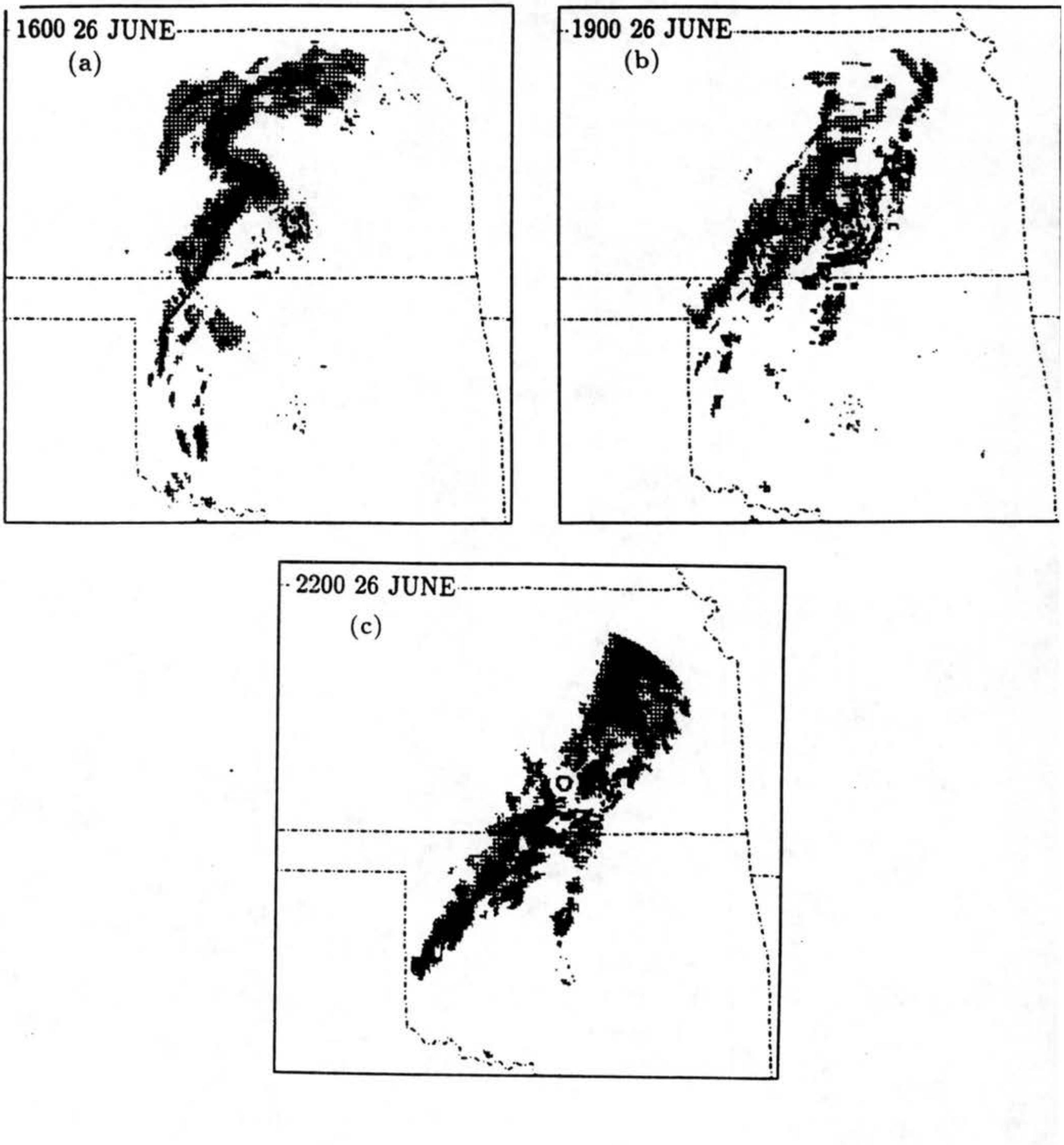

Figure 5.78: Same as Fig. 5.2 except for: a) 1600 UTC 26 June; b) 1900 UTC 26 June; c) 2200 UTC 26 June; d) 0130 UTC 27 June; e) 0430 UTC 27 June; f) 0700 UTC 27 June. All using Oklahoma City OK and Wichita KS.

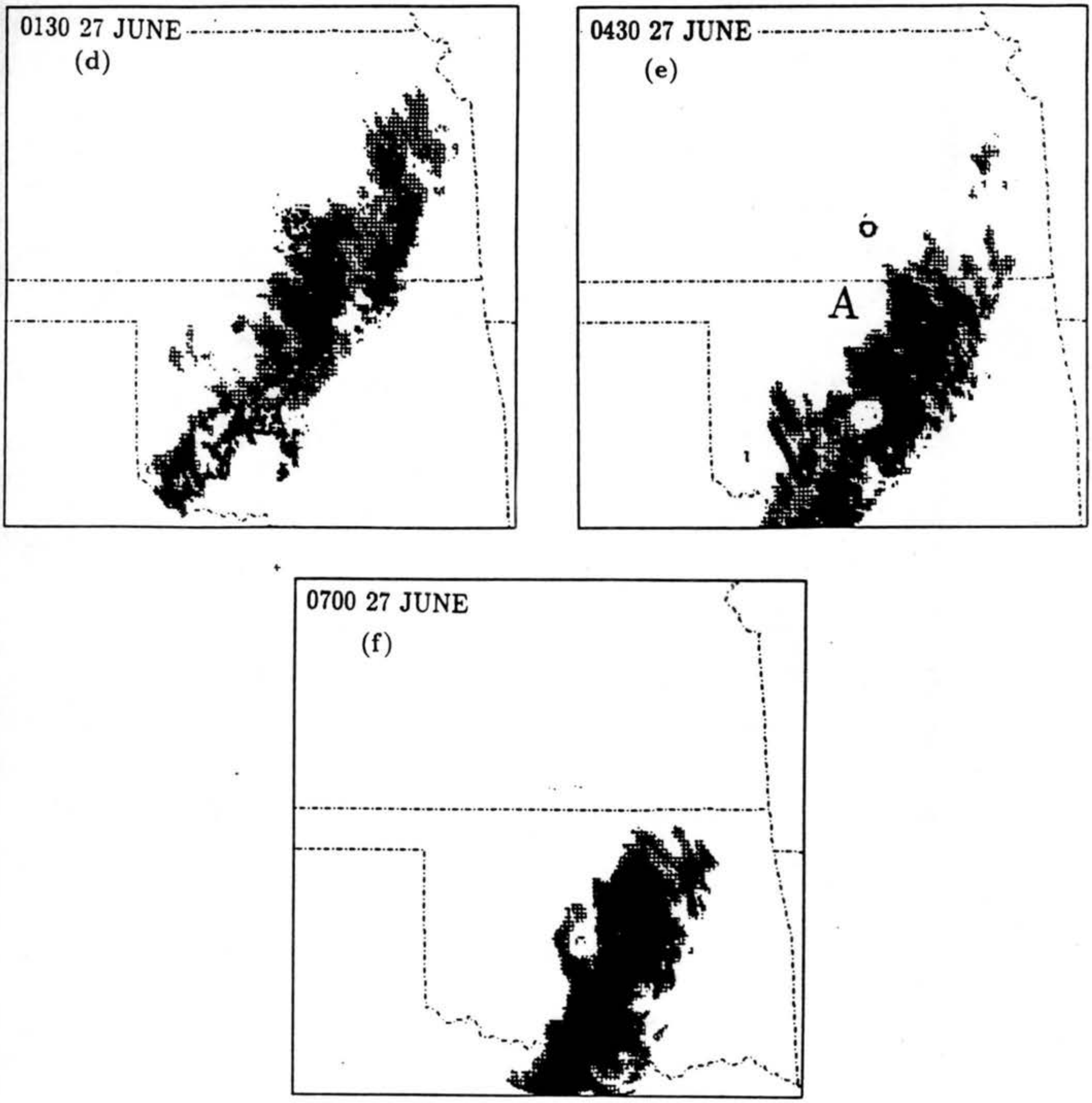

Figure 5.78: Continued.

convection associated with the system. The northeastern portion of the system became largely stratiform in nature. By 0130 (Fig. 5.78d) the trend was continuing for the northern portions of the MCS to become more stratiform in nature as the convection which was in Kansas had dissipated. In Oklahoma, there were scattered intense convective cells along the line. The stratiform precipitation region was just beginning to expand into Oklahoma. By 0430 (Fig. 5.78e) the precipitation in Kansas dissipated and in northern Oklahoma the convection also dissipated, leaving a large area of heavy stratiform precipitation. On the back edge of this heavy stratiform precipitation on the northern end of the MCS a rear echo notch developed (point A in Fig. 5.78e). The southern end of the MCS was characterized by a fairly weak leading convective line and a just developing enhanced stratiform region. Then by 0700 (Fig. 5.78f) the convection dissipated over all of Oklahoma, and all that was left was a large area of heavy stratiform precipitation.

5.10.3 System overview

Early development of convective line (1600)

This time is viewed to simply view the pressure field before the system really affected it. It can be seen (Fig. 5.79) that the pressure falls quite evenly from the southeast corner to the central regions of the mesonet. Then there was a low pressure area which was associated with the cold front and then the pressure began to rapidly rise to the northwest. The flow ahead of the cold front was moderate-to-strong (5-10 m s^{-1}) out of the southwest. To the rear of the front the flow was moderate-to-strong (5-10 m s^{-1}) out of the northeast. This set up a confluent zone along the front. The low, interestingly, was at the apex of the two convective lines. The northeast-southwest oriented convective line was pre-frontal in nature.

Development of multiple convective lines (1900-2100)

By 1900 (Fig. 5.80) the secondary convective line which was mentioned earlier can be seen to be developing right along the cold front, and as this became the dominant convection, it gave this system its frontal convective nature. The pressure and flow fields

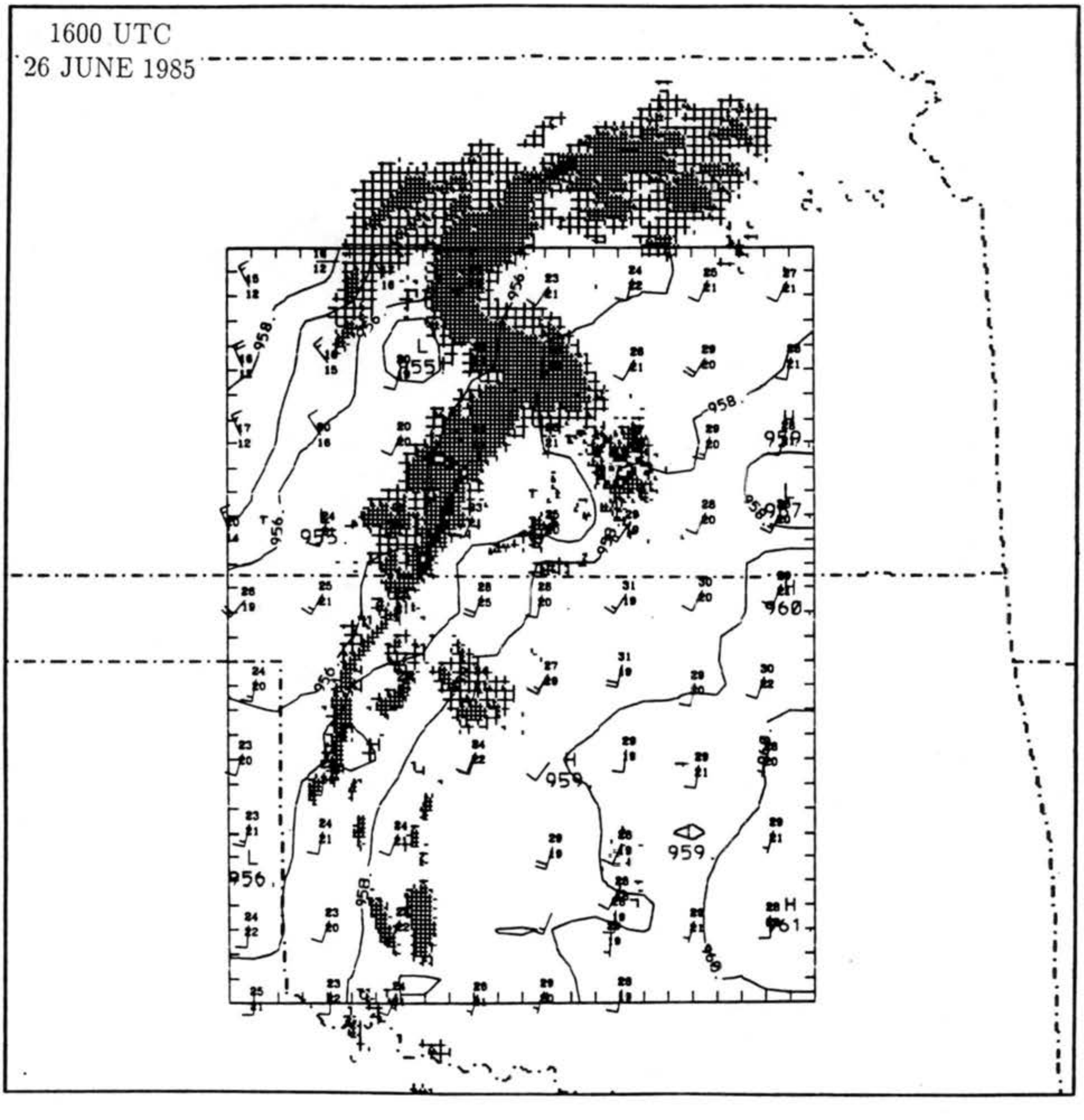

Figure 5.79: Same as Fig. 5.3 except for 1600 UTC 26 June.

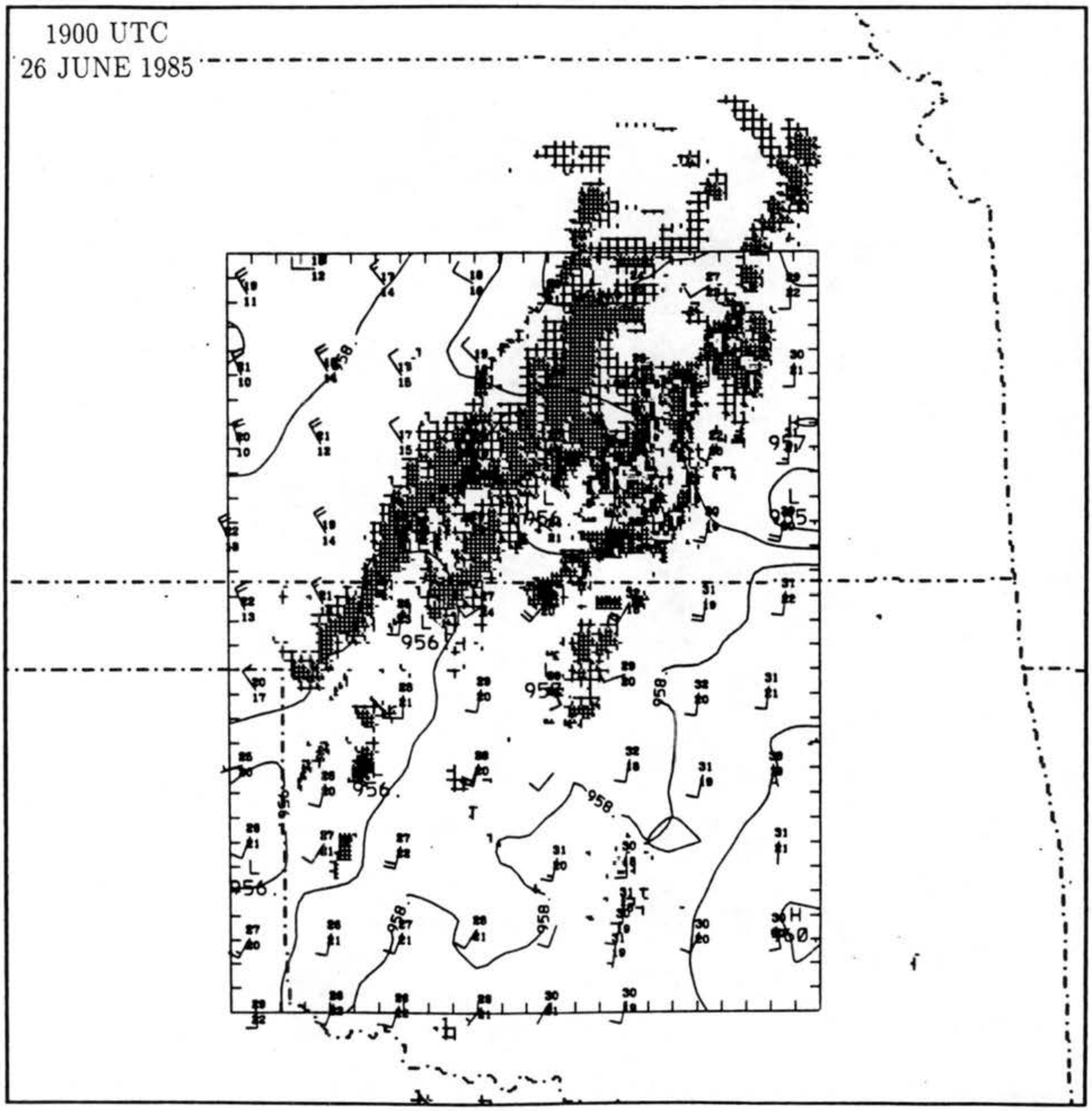

Figure 5.80: Same as Fig. 5.3 except for 1900 UTC 26 June.

were still largely unaffected by the system. This was partly due to the very moist, tropical-like environment which prevented strong, evaporatively driven downdrafts and strong mesohighs and wake lows.

By 2100 (Fig. 5.81) the first changes in the pressure field occurred. A mesohigh covered virtually the entire northern portion of the system, which was largely stratiform in nature. But the flow field was still not significantly affected.

As an example of the typical flow structure to the rear of the entire system at this time there was the WWR sounding (Fig. 5.82). WWR was along the back edge of the convective line (point A in Fig. 5.81) and it shows two layers of very weak rear inflow. The lower layer was associated with the northwesterly flow to the rear of the cold front. The upper layer was a weak rear inflow jet. Aloft there was very strong (20 m s^{-1}) FTR flow. There was little change in the relative positions of these flows. This sounding was typical of all soundings until very late in the lifetime of the system.

Wake low development (0300-0600)

At 0300 (Fig. 5.83), despite the fact that in northern Oklahoma there was a very well developed enhanced region of stratiform precipitation as well as a well developed rear echo notch, there was not a wake low in this region, nor was there even a significantly enhanced gradient. In southern Oklahoma, where there was newly developed enhanced stratiform precipitation, there was the beginning of the appearance of a wake low. Winds there became more east-northeasterly along the back edge of the system in response to the lowering of the pressure.

At 0400 (Fig. 5.84) the rear echo notch was still present and there was a mesohigh there. The southern area developed a wake low along the western edge of a region of enhanced stratiform precipitation. The flow responded with a 5-10 m s^{-1} northeasterly flow versus a more northerly flow elsewhere.

At 0530 (Fig. 5.85) the wake lows reached their peak intensity and developed a moderate gradient along thier back side. The flow continued to be the same in this region.

To examine why a wake low did not develop in an area that seems a common position for one (on the back side of an enhanced stratiform region and in a rear echo notch) and

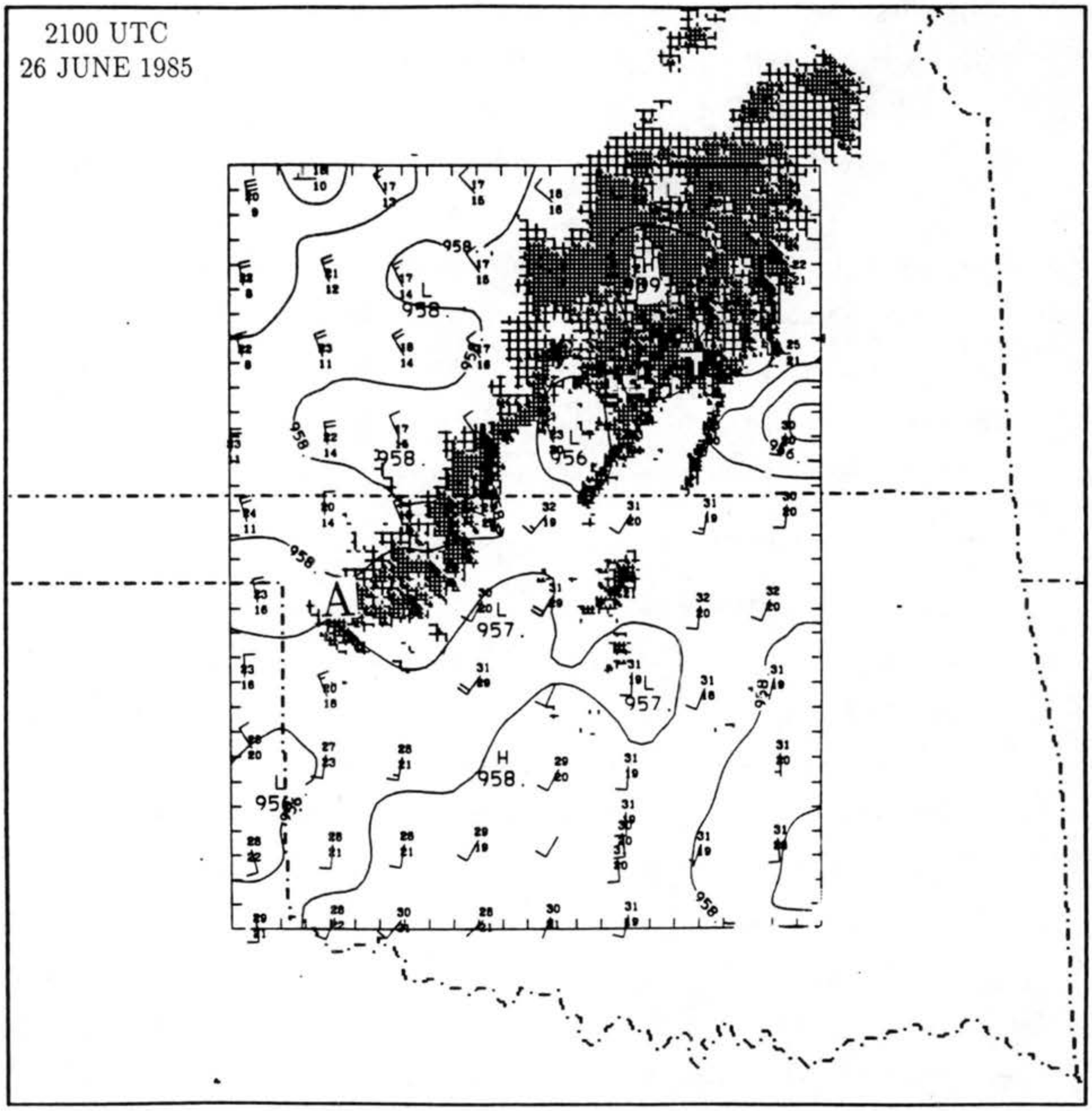

Figure 5.81: Same as Fig. 5.3 except for 2100 UTC 26 June.

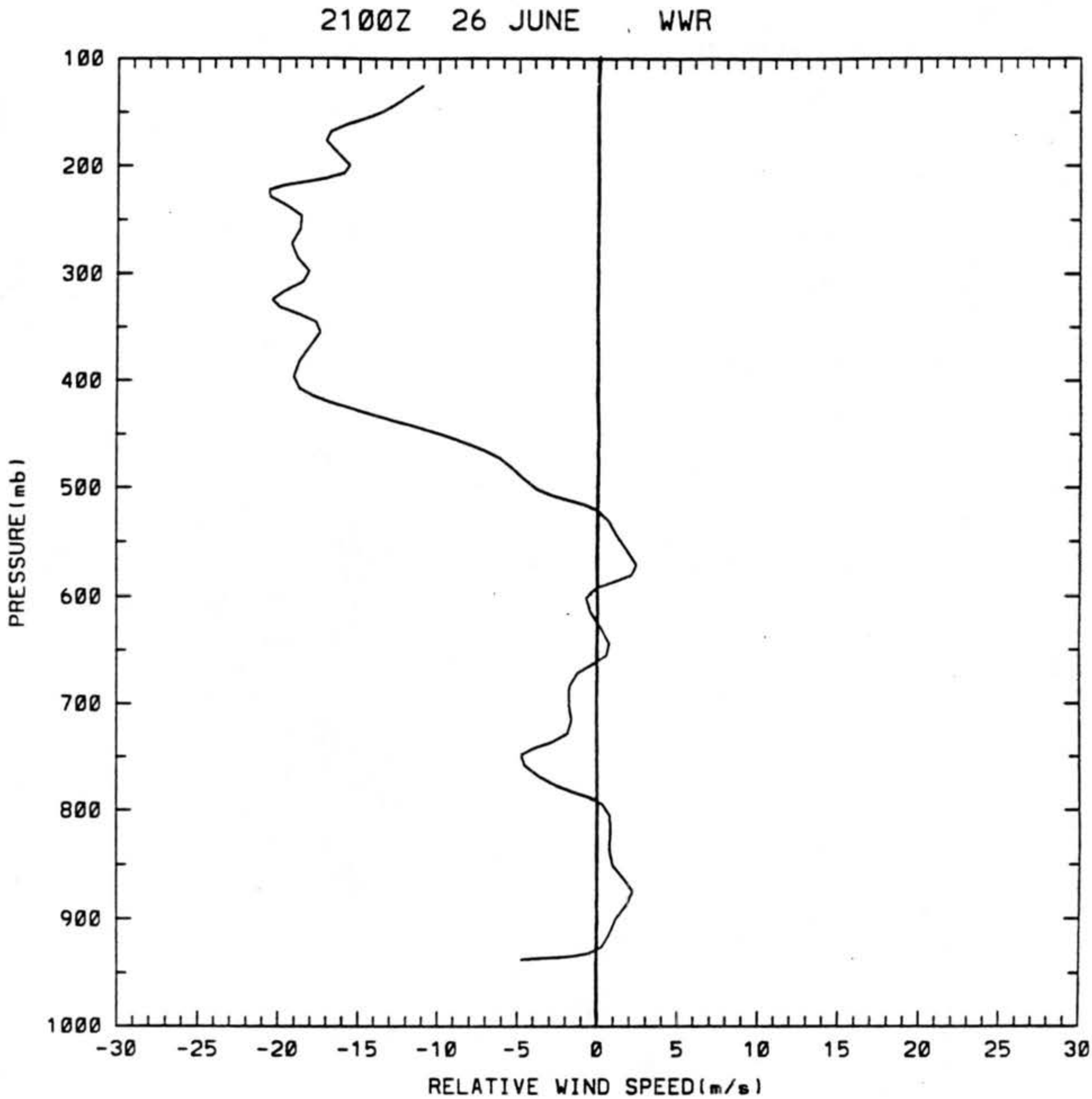

Figure 5.82: Same as Fig. 5.8 except for 2100 UTC 26 June at WWR.

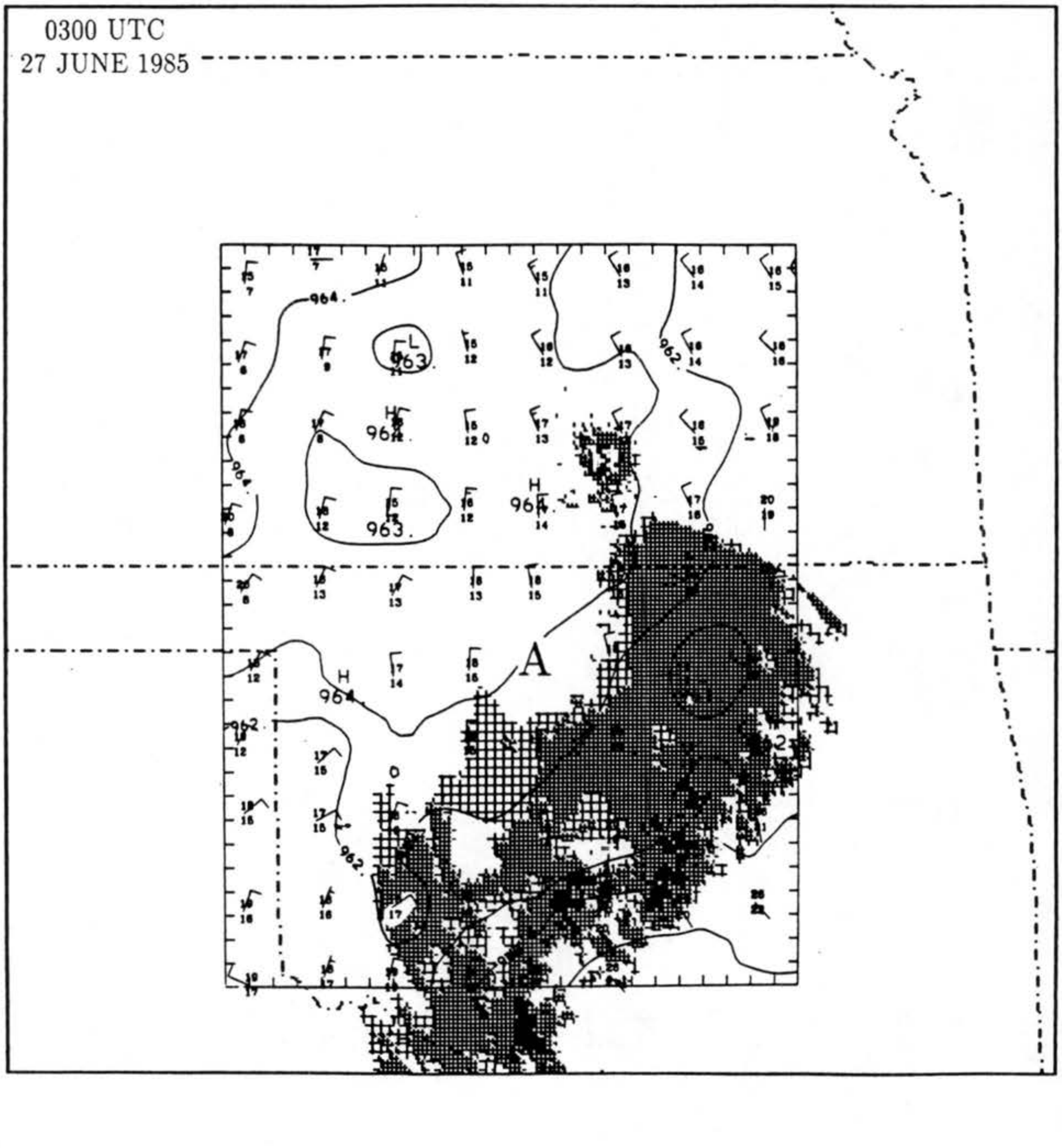

Figure 5.83: Same as Fig. 5.3 except for 0300 UTC 27 June.

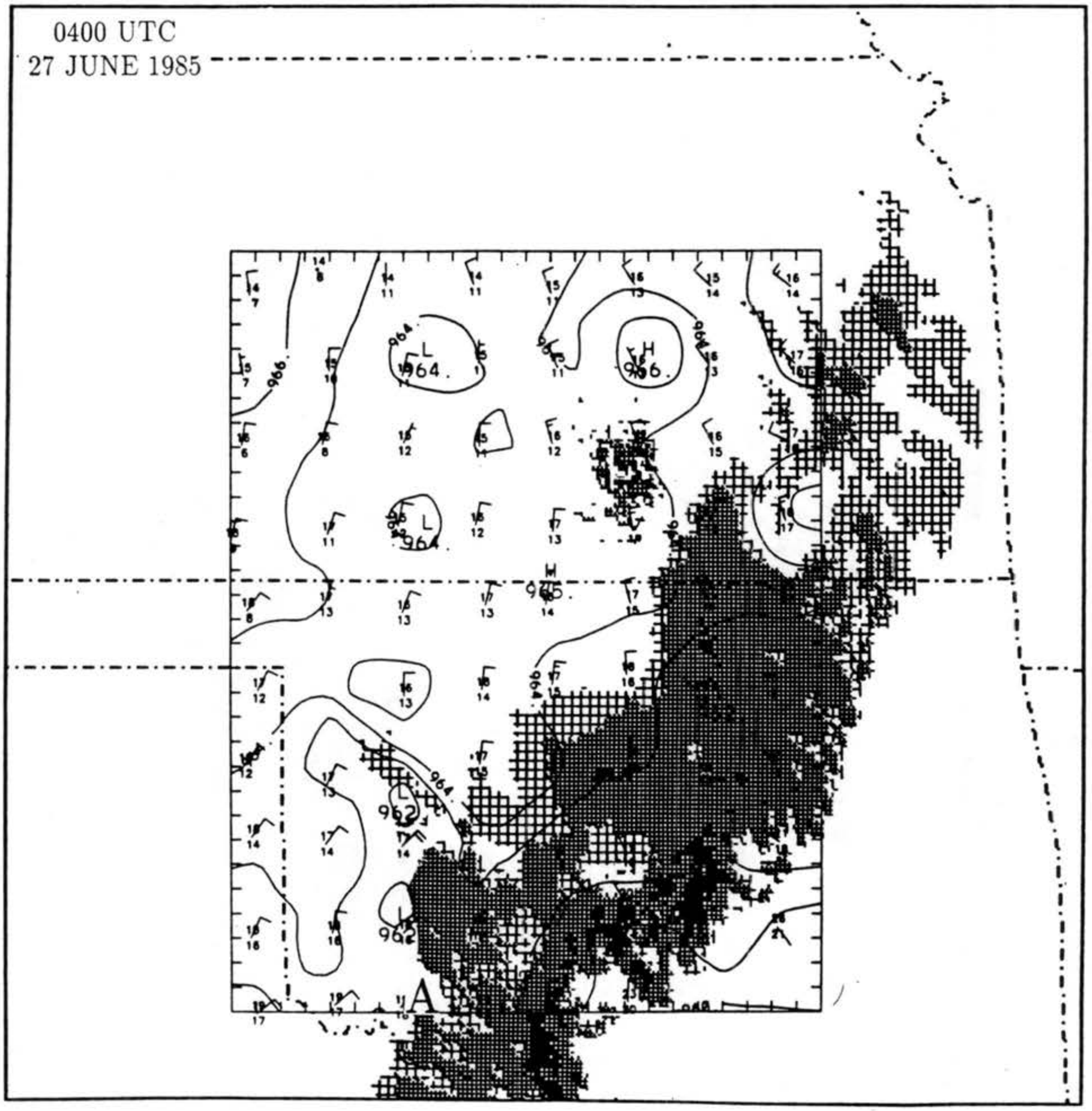

Figure 5.84: Same as Fig. 5.3 except for 0400 UTC 27 June.

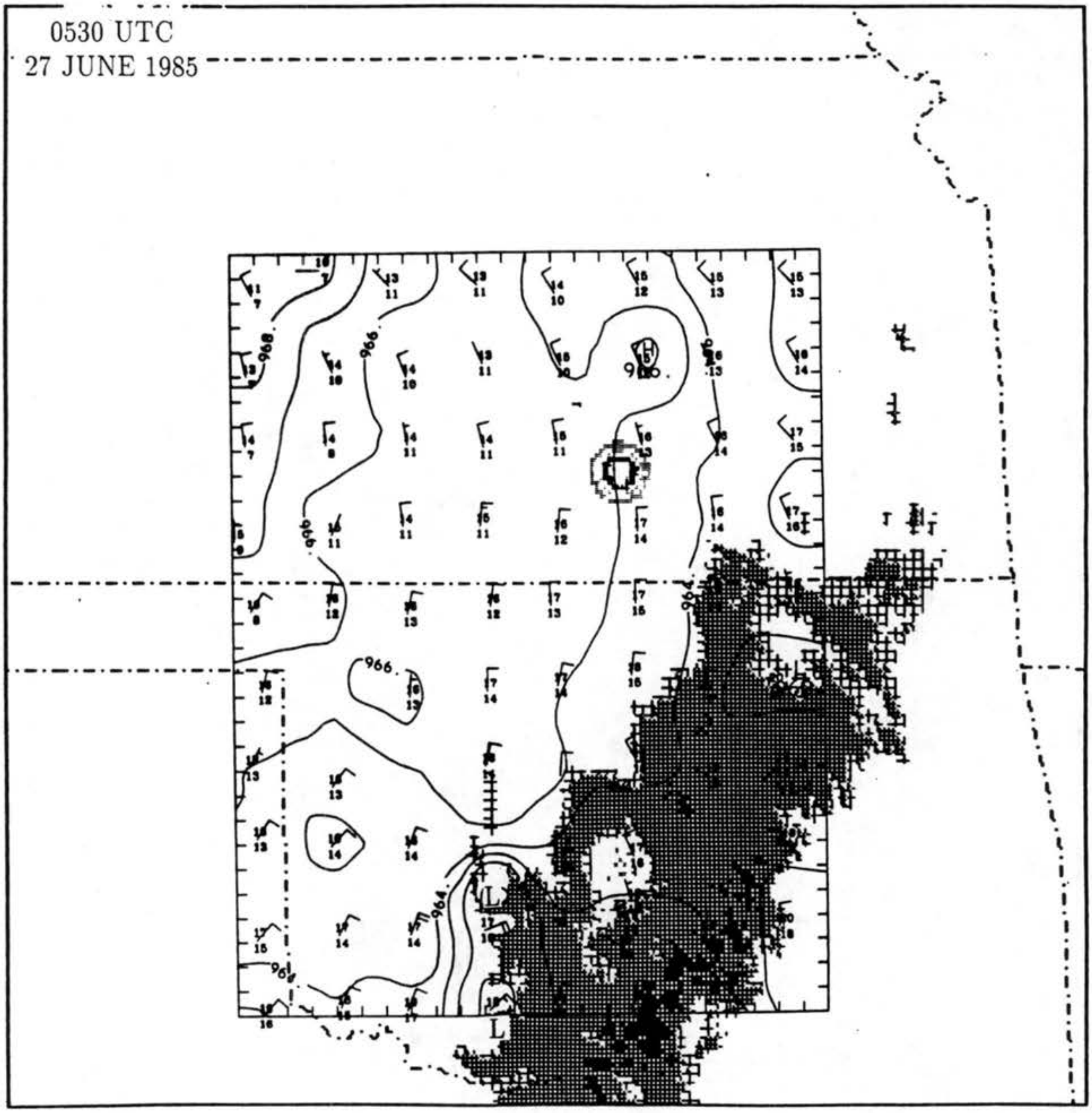

Figure 5.85: Same as Fig. 5.3 except for 0530 UTC 27 June.

why one did develop to the south, several soundings are examined. Soundings from END at 0242 and 0420 are shown in Figs. 5.86a and b. At 0242 END was within the echo notch along the back edge of the stratiform precipitation (point A in Fig. 5.83). It shows that there was a layer of weak rear inflow which peaked at 600 mb (5 m s^{-1}). While at 0420, when END was just about 25 km to the rear of the back edge of the system (point A in Fig. 5.84), there was a shallow layer of rear inflow peaking at 600 mb (5 m s^{-1}). So in this region, despite the presence of many features commonly associated with wake lows, one did not develop due to the rear inflow being weak and it also did not descend as it approached the convective line.

In the southern areas where a wake low did form, the flow structure is examined with the 0430 (Fig. 5.86c) and 0600 (Fig. 5.86d) FSB soundings. At 0430 FSB was within the stratiform precipitation region about 10-25 km to the east of the wake low (point B in Fig. 5.84) and it shows a 300 mb deep layer of strong rear inflow with its peak between 700 mb and 800 mb (12 m s^{-1}). However, at 0600 when FSB was just to the rear of the stratiform precipitation region and the wake low (point A in Fig. 5.85), there was a 200 mb deep layer of strong rear inflow with its peak at 500 mb (12 m s^{-1}). So in this region there was a strong rear inflow which showed a rapid descent in the region of the wake low.

5.10.4 Mesonet time series

The wake low conditions are summarized by station S13 (Fig. 5.87, see Fig. 3.1). As the system passed, combined with the cold front, there was just a general pressure rise (000-0400), not a mesohigh. There was a sharp cooling of 11°C and a 16 m s^{-1} wind gust and a shift to northerly flow. Around 0530 the wake low passed over with a 3 mb decrease in 10 min and a 17 m s^{-1} wind gust as well as a shift to northeast flow. This was in contrast to areas away from the wake low where the pressure just underwent a general increase and the flow remained out of the north.

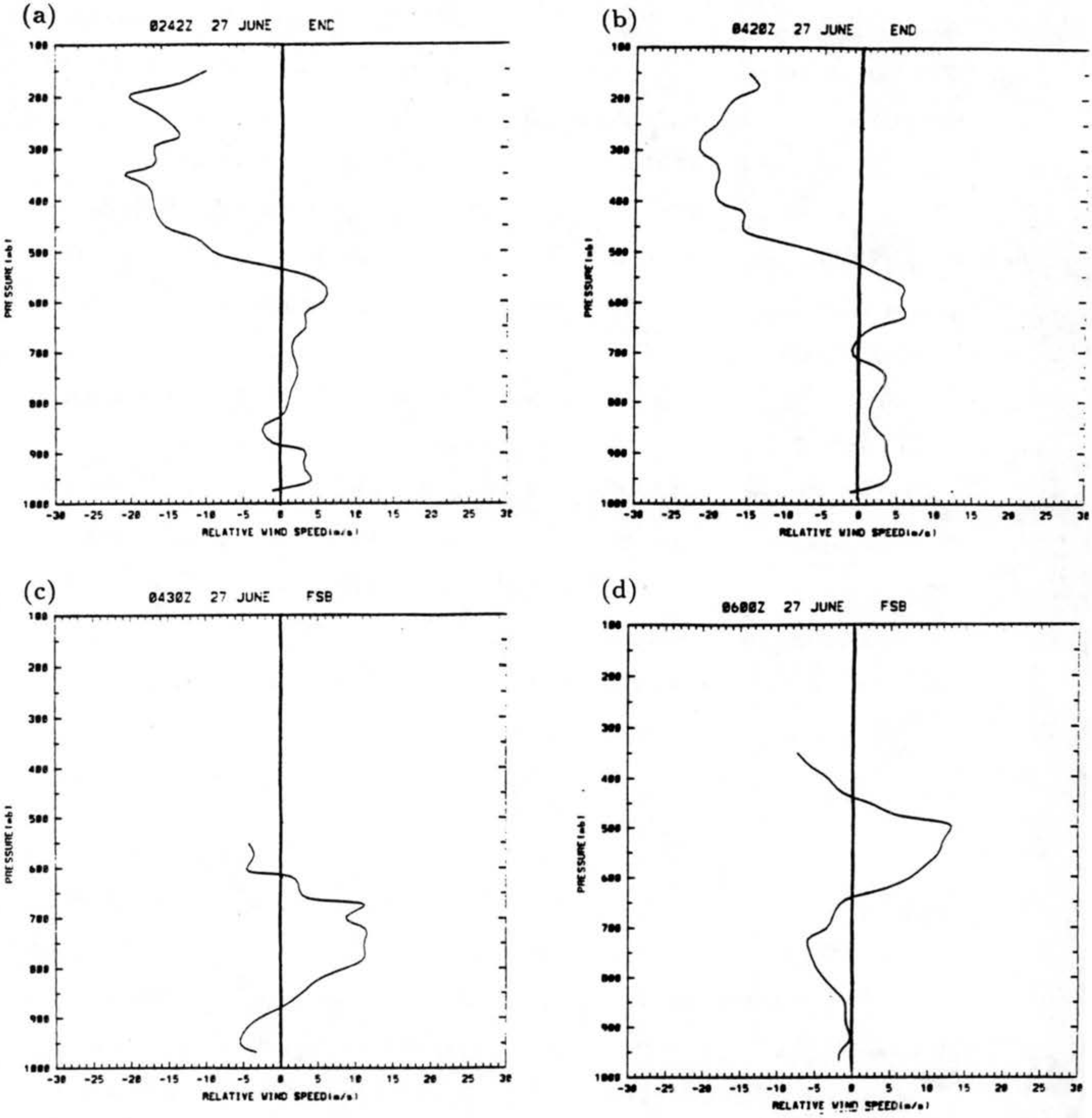

Figure 5.86: Same as Fig. 5.8 except for 27 June at: a) 0242 UTC at END; b) 0420 UTC at END; c) 0430 UTC at FSB; d) 0600 UTC at FSB.

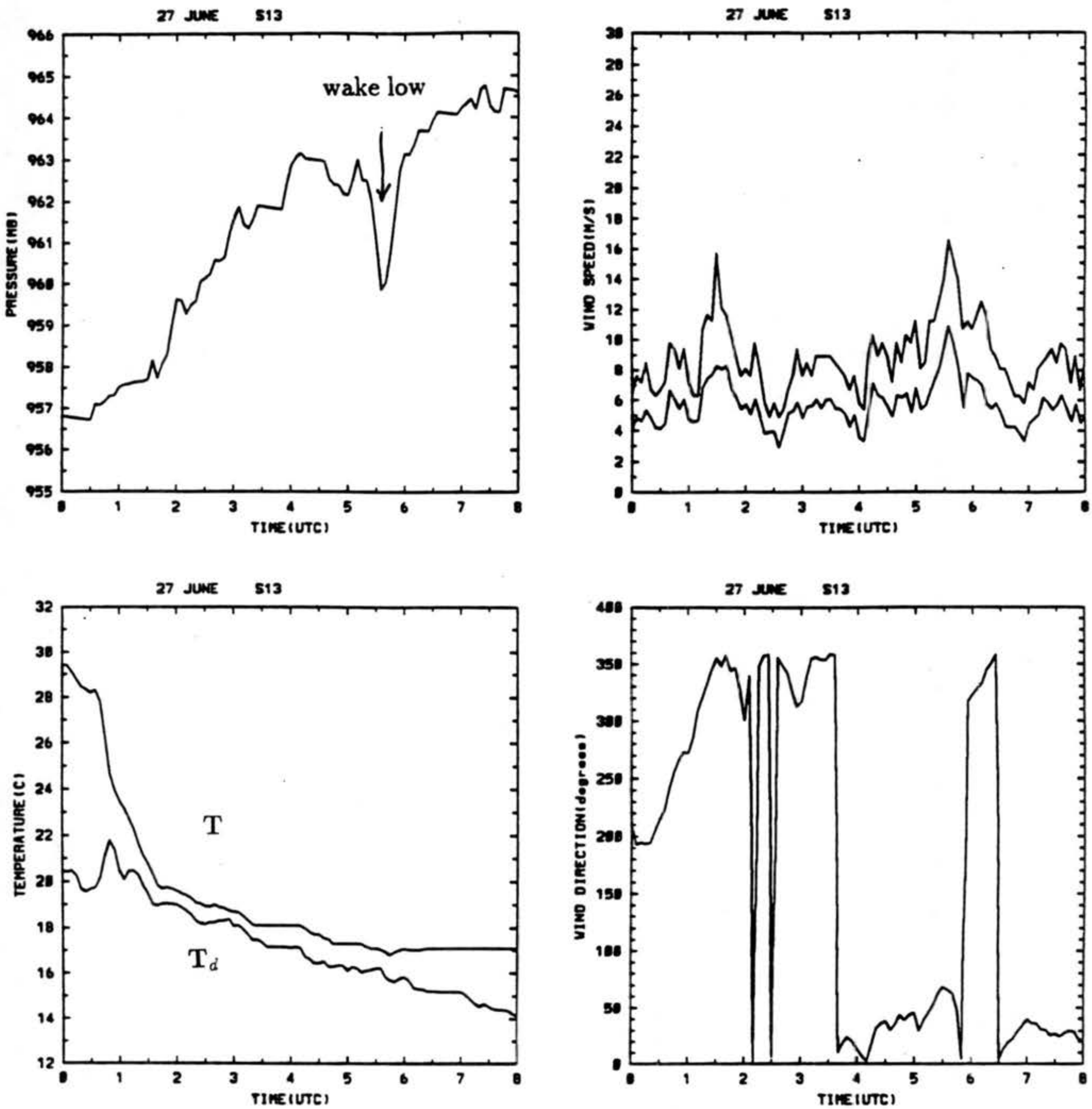

Figure 5.87: Same as Fig. 5.9 except for 27 June at station S13. Note different time scale as each tick mark represents 30 minutes.

Chapter 6

MCS SCHEMATICS

6.1 Introduction

The previous two chapters contain comprehensive summaries of the 16 MCS cases which occurred during the months of May and June 1985. This chapter is used to synthesize these findings into several models representing the similar patterns that appeared in many aspects of these MCSs. Section 6.2 lays out a schematic of the general synoptic-scale environment found in the PRE-STORM and surrounding areas prior to the development of these MCSs. This section is comparable to the work of Maddox (1983) and his description of the "Genesis Region" of Mesoscale Convective Complex (MCC) development. Section 6.3 summarizes all aspects of the "typical" MCS during its mature-to-dissipating stage. Included are schematics of the low-level radar reflectivity field, the 480 m pressure and surface flow, as well as the system-relative upper-air flow.

It is proposed that these models of the cloud and precipitation structure and surface pressure features of MCSs will have somewhat greater generality than those based on a smaller number of cases (Fujita 1955, Pedgley 1962, Johnson and Hamilton 1988) However, it is recognized that our results are based on a single year and the extent to which they can be generalized further requires additional study.

6.2 Schematic of pre-MCS synoptic-scale conditions

In this section the general pre-MCS synoptic-scale conditions are summarized based on the 16 examined cases. For the purposes of this thesis only the most general features are summarized. Fig. 6.1 is the schematic of the synoptic-scale features and their positions relative to the PRE-STORM region. These features very much resemble those of Maddox (1983) for the genesis region of MCCs.

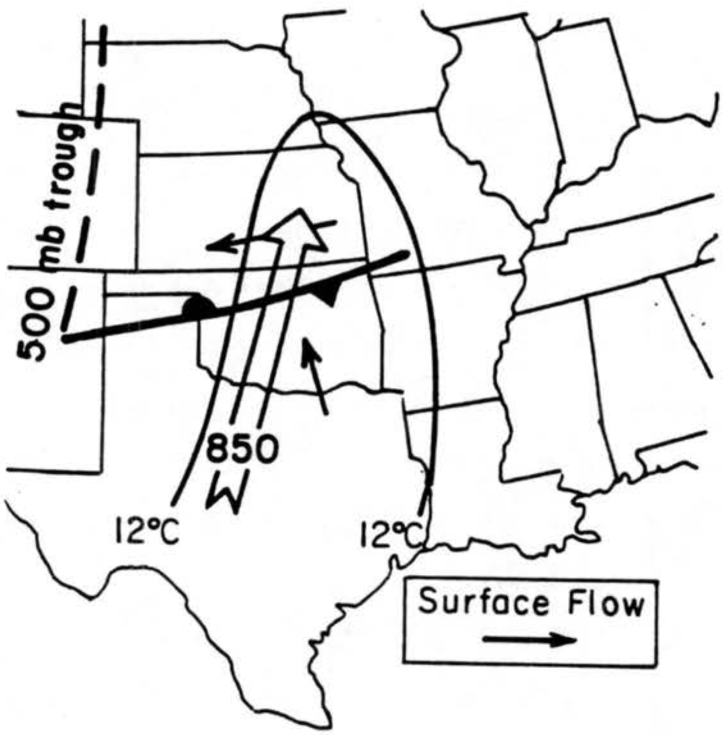

Figure 6.1: Schematic of synoptic-scale conditions in the region of MCS development. Dashed line represents the 500 mb short wave. Solid curve is the 12°C 850 mb dewpoint contour. Small arrows are the surface flow, large arrow is the 850 mb jet.

The surface front typically was just to the south of the Kansas-Oklahoma border and was oriented nearly along a straight east-west line. The front was most often quasi-stationary in nature, but in several cases it was a cold front. The cases from mid-to-late June (9, 15, 22 and 26-27 June) began to diverge from this pattern as they developed more in connection with northeast-southwest oriented cold fronts extending across northwestern Kansas and moving to the southeast. It is not known if this feature represents a normal shift in the frontal conditions associated with MCSs in this region during this time of year or if it was a chance occurrence. The ground-relative surface wind flow was nearly the same for all cases, at least in relation to the surface front position. Ahead of the front, to its south and east, there was a south-southeast flow while to its rear, north and west, the flow was more northeasterly. This flow structure led to convergence along the region of the front. In all cases the flow to the rear of the front had an easterly component except 26-27 June which had a northwesterly flow due to its association with a very strong cold front.

In all cases at 850 mb there was a 10-20 m s^{-1} jet out of the south to southwest. This jet helped lead to the development of an axis of moisture-laden air (dewpoints in excess of 12°C at 850 mb) extending from the Texas Gulf Coast north through central and eastern Oklahoma and Kansas. The only variation in this feature was its westward extent, varying from central Kansas and Oklahoma (27 May and 9 June) to far western Kansas and/or the western Texas panhandle (28 May and 3 June).

At 500 mb there was generally a weak short-wave trough extending from extreme western South Dakota south through eastern Colorado and eastern New Mexico. The position and strength of the trough were the most variable of any of the features. Very deep troughs were found in conjunction with several cases (13 May, 3, 3-4, 4, and 26-27 June) and the 3-4 June trough was located in the extreme southwestern U.S.

The cases in which a midlevel mesovortex was known to have developed included: 7, 21, and 28 May; 9, 22, and 24 June. The conditions at 500 mb prior to the development of these MCSs differed in a couple of respects from those of the other systems. First, the short-wave troughs found in connection with mesovortex-producing systems were typically very weak and relatively small features. They also had generally weaker ground-relative flow associated with them. They had 0-15 m s^{-1} flow versus a 10-20 m s^{-1} flow in the other systems. The June mesovortex cases had especially weak flow (0-5 m s^{-1}). These features of a weak short-wave trough (weak background relative vorticity) and weak upper-air flow were also shown by Bartels and Maddox (1991) to be associated with mesovortex-producing MCSs.

6.3 Schematics of a mature-to-dissipating MCS

The purpose of this section is to give an overall view of the precipitation structure of these systems through the use of schematics. First, the low-level radar reflectivity features are discussed including the organizing characteristics of these MCSs. Second, the surface fields are disscussed, especially the positioning of pressure features relative to the various precipitation areas. Lastly, the system-relative rear inflow is examined particularly relative to the wake low region. It is hoped that through this procedure an overall impression of the structure of MCSs is given.

6.3.1 Radar reflectivity structure

At first look, there appear to be large variations in the radar reflectivity structure of MCSs. While true, there are also several very important similarities amongst these systems and this section is used to give an impression of these similarities.

The time and length of development of MCCs (a subset of MCSs) have long been studied (Maddox 1980, McAnelly and Cotton 1986, Cotton et al. 1989). Table 6.1 summarizes the times of occurrence of several important stages of the 12 cases used in the construction of the actual schematics (Table 6.2 provides the same data for the remainder (4) of the cases). First, there is the time (here Local Standard Time (LST) is used; LST = UTC - 6 h) of initiation, i.e. first cell development. In many cases this determination is difficult due to the need to use the poor resolution NMC radar summaries, where it is often difficult to separate areas of convection associated with the development of a particular MCS from other areas of precipitation. Second, there is the time the convection first develops into an MCS. Determining this time is very subjective (again sometimes based

Table 6.1: Data for the 12 mesoscale convective systems used to construct schematics

No.	Date	Time (LST) of Initiation	Time (LST) of First MCS	Time (LST) of Mature Stage
1	7 May	1600	2300	0930
2	13 May	0600	0825	1100
4	21 May	1430	1930	2130
5	27 May	1400	2300	0100
6	28 May	1700	0000	0500
7	29 May	1930	2230	2330
8	3 June	0630	1030	1330
9	3–4 June	1100	1630	1800
10	4 June	2300	0200	0300
12	11 June	1500	1800	2000
14	22 June	1500	2000	2230
15	24 June	1300	1900	2100

on NMC radar maps) and is based on when there is more organization to the convection and also when the stratiform precipitation region initially develops. Finally, there is the time the system initially reaches its mature stage. This determination is again subjective but is defined as when the system has achieved its greatest amount of organization with an enhanced stratiform region and still has an intense line of convection.

To help visualize these times, Fig. 6.2 was constructed. Only those systems used to construct the schematics to follow are plotted (see Table 6.1). It is apparent from this

Table 6.2: Data for the 4 mesoscale convective systems not used to construct schematics.

No.	Date	Time (LST) of Initiation	Time (LST) of First MCS	Time (LST) of Mature Stage
3	13 May	0600	1030	1130
11	9 June	1600	0030	0430
13	15 June	1500	2200	0100
16	26–27 June	0600	1100	1600

figure that these systems underwent remarkably similar development patterns in terms of time. The initial cell development patterns typically occurred during the afternoon hours

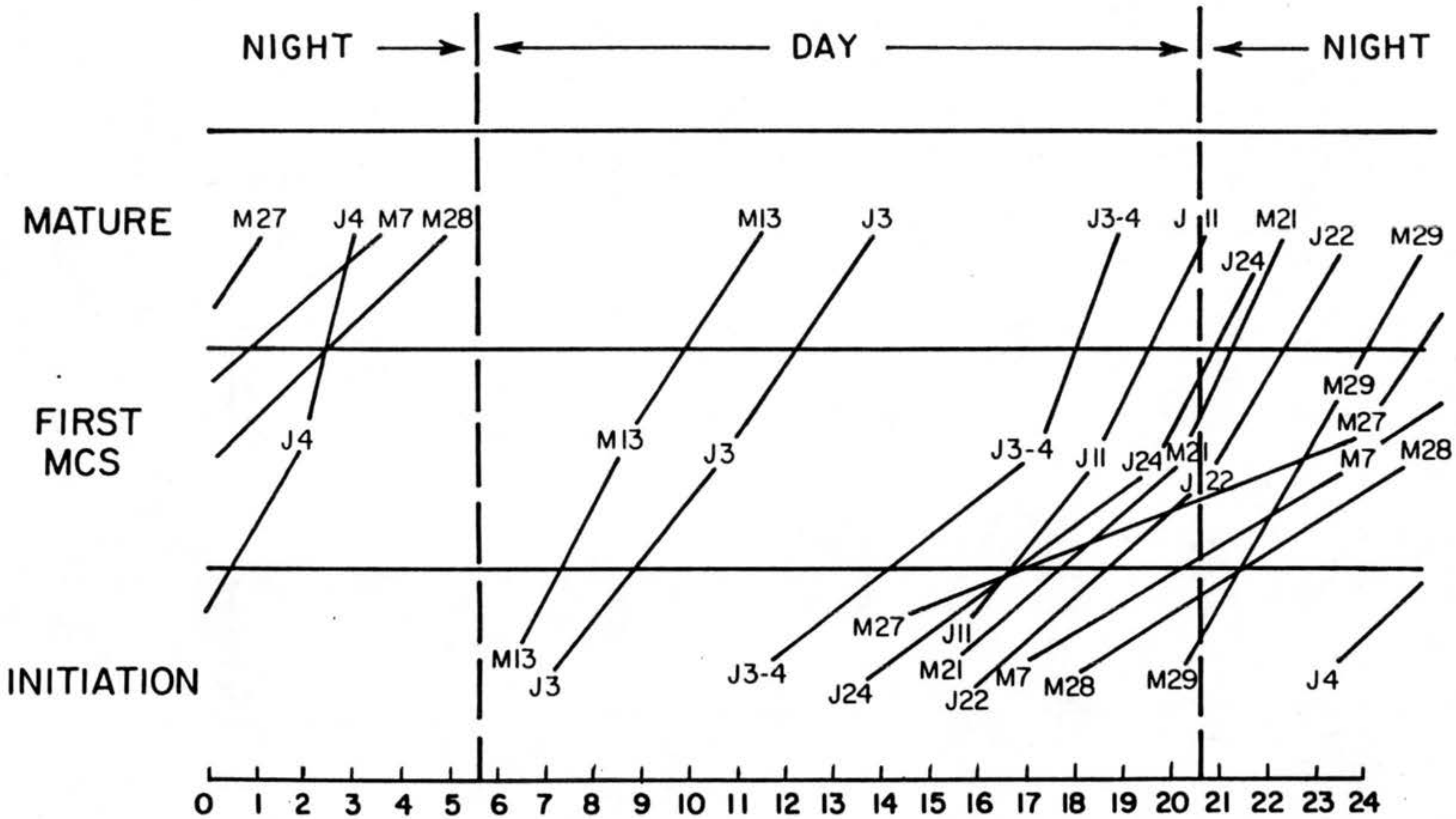

Figure 6.2: Times (LST) of important developments with the MCSs.

(1100-2000 LST). The systems then reached MCS status during the evening to early night hours (1700-0000 LST) and finally reached their mature stage during the night (2000-0500 LST). This pattern has been found to be typical of MCCs (Maddox, 1980). The only exceptions to this pattern were the 13 May, 3 and 4 June cases. The 3 and 4 June cases occurred in response to a rather remarkable amount of low-level warm advection and considerable frontal lifting (Trier and Parsons 1992) which helped to continually destabilize the region leading to less importance placed on solar heating and hence the morning and night development. In particular, Trier and Parsons (1992) argue that frontal lifting in these cases removes the need for solar heating to force the convection. The 13 May case was also exceptional due to the intensity of the convective forcing both at the surface (strong frontal system) and aloft (low-level warm advection, a deep 500 mb trough, and a strong 35 m s^{-1} 300 mb jet core to its northwest) such that solar heating was again not a necessary feature for triggering the convection.

In order to develop a schematic of the radar reflectivity structure of a mature-to-dissipating MCS, a time was selected during the stage of each MCS when the most intense wake low pressure gradient was established. The results are shown in Fig. 6.3 with the convective line (in excess of 40 dBZ) and enhanced stratiform region (in excess of 30 dBZ) highlighted. The outer contour is the lowest available reflectivity, 15 dBZ. The 21 May case is not included in these figures, even though it does fit into the schematic, because it is mostly outside of the network and the only radar data are the low resolution NMC radar summary charts. Also the surface pressure field was inadequately observed to relate to the other cases. What is obvious from Fig. 6.3 is that at the stage selected these MCSs (again this comprises only 12 of the 16 cases) had remarkably similar reflectivity structures as well as sizes (except for 21 May, and 11 June). This structure can be defined as a northeast-southwest oriented convective line at the leading edge with a general area of stratiform precipitation mostly at its northern end to the rear of the convective line. Also a region of enhanced stratiform precipitation was found to the north and west of the convective line. Notice that the 24 June case also fits this general structure (if it is rotated 90°) due to its movement to the south rather than the more eastward (both

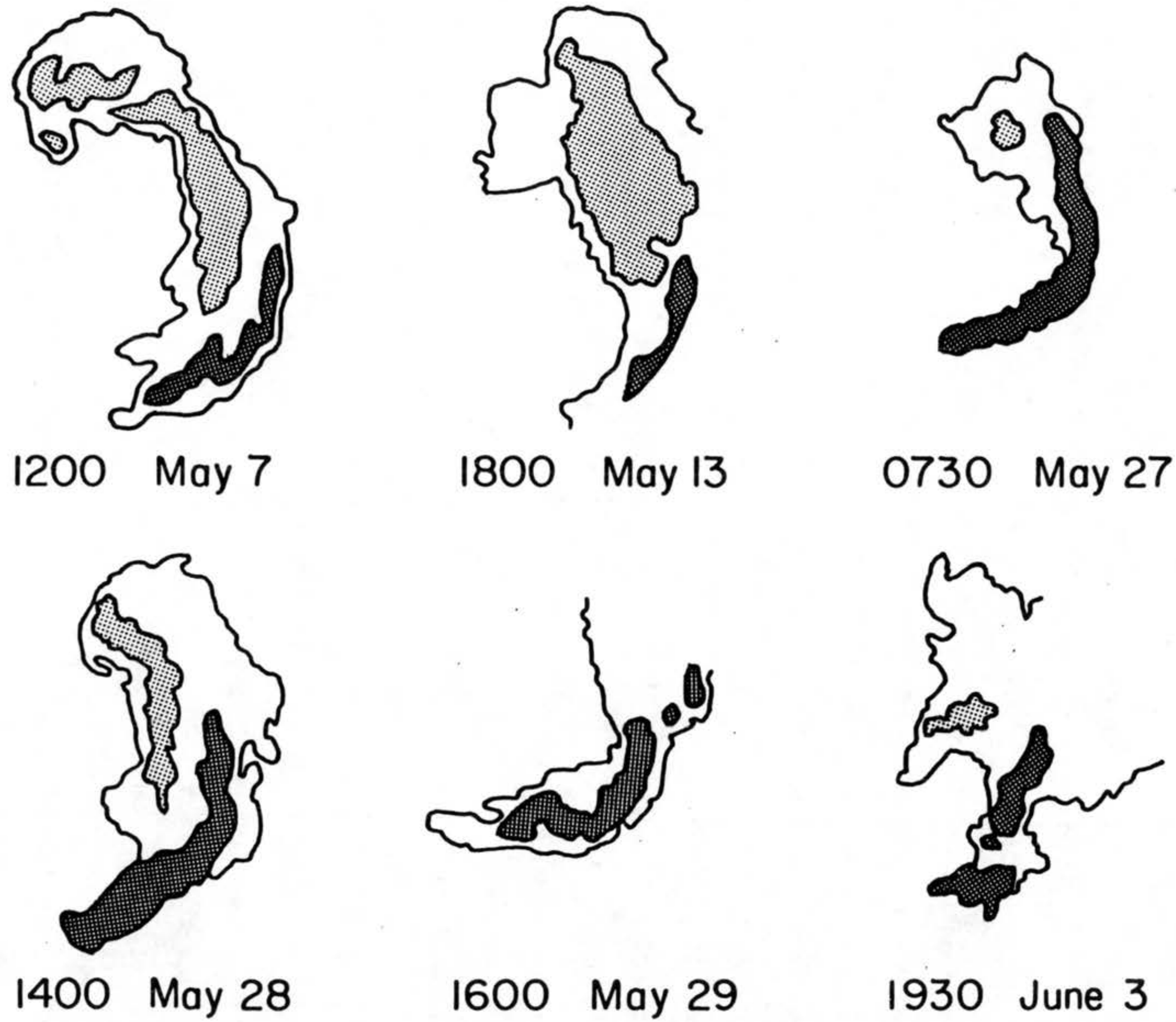

Figure 6.3: Mature-to-dissipating stage reflectivity plots including the systems used to construct schematics. Light shading indicates reflectivities over 30 dBZ (enhanced stratform precipitation region). Dark shading represents reflectivities over 40 dBZ (convective line).

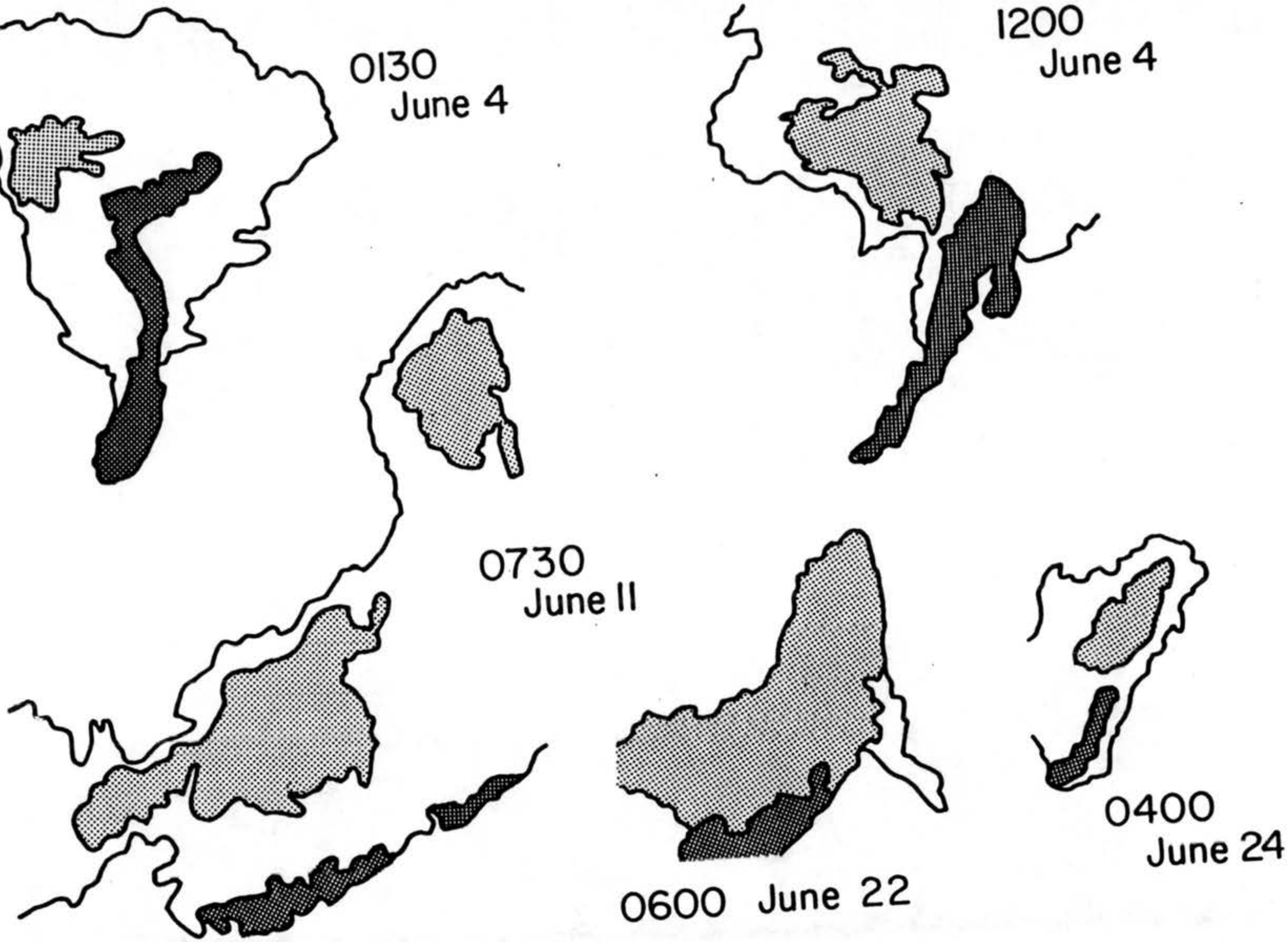

Figure 6.3: Continued.

north and south) movement of the other systems. Therefore, this structure seems to be a mode of precipitation structure that most (12 of 16 here) MCSs pass through in their mature-to-dissipating stage.

Several cases did not acheive this structure and one of the important factors seems to be whether or not the system was cold-frontal in nature. In other words, was it positioned right along a cold front throughout its existence or not? Two cases (15 and 26-27 June) were cold-frontal systems and neither case developed this structure. The lack of asymmetric development may be partially due to the very different upper-air structures that were associated with the cold front in these cases. The 15 June case developed in a very strong northwest flow at midlevels which led to the development of leading rather than trailing stratiform precipitation during most of its existence. Whether this system, when it later developed trailing stratiform precipitation, developed a structure like that of the systems in Fig. 6.3 is not clear). The 26-27 June case was associated with a very deep trough as well as the most intense cold front observed in any of these cases. The 13 May Kansas system was a small and short-lived system that had a symmetric structure during its mature stage and then it quickly dissipated. This system may not have had the available time to develop this structure. Lastly, the 9 June case was a very complex case with a not very well-defined reflectivity structure at any point of its existence.

Based on the similarities in 12 of the 16 MCS cases, a schematic of the radar reflectivity structure was constructed (Fig. 6.4). In Fig. 6.4a the symmetric structure is shown for comparison. Also many of the systems had such a structure at earlier points in their life cycles. It conforms closely to the structure presented in Johnson and Hamilton (1988) and is similar to the early schematics of Fujita (1955). Fig. 6.4b is based on the examples shown in Fig. 6.3 and resembles the asymmetric structure given in the studies by Houze et al. (1989) and Houze et al. (1990). Included in this schematic is a northeast-southwest oriented convective line with a curved "bow"-type structure. Then extending to the rear (north and west) of the convective line there is a general area of stratiform precipitation with an embedded region of enhanced stratiform precipitation. This asymmetric structure does not represent a type of MCS, rather it is a part of the life cycle of many MCSs. In

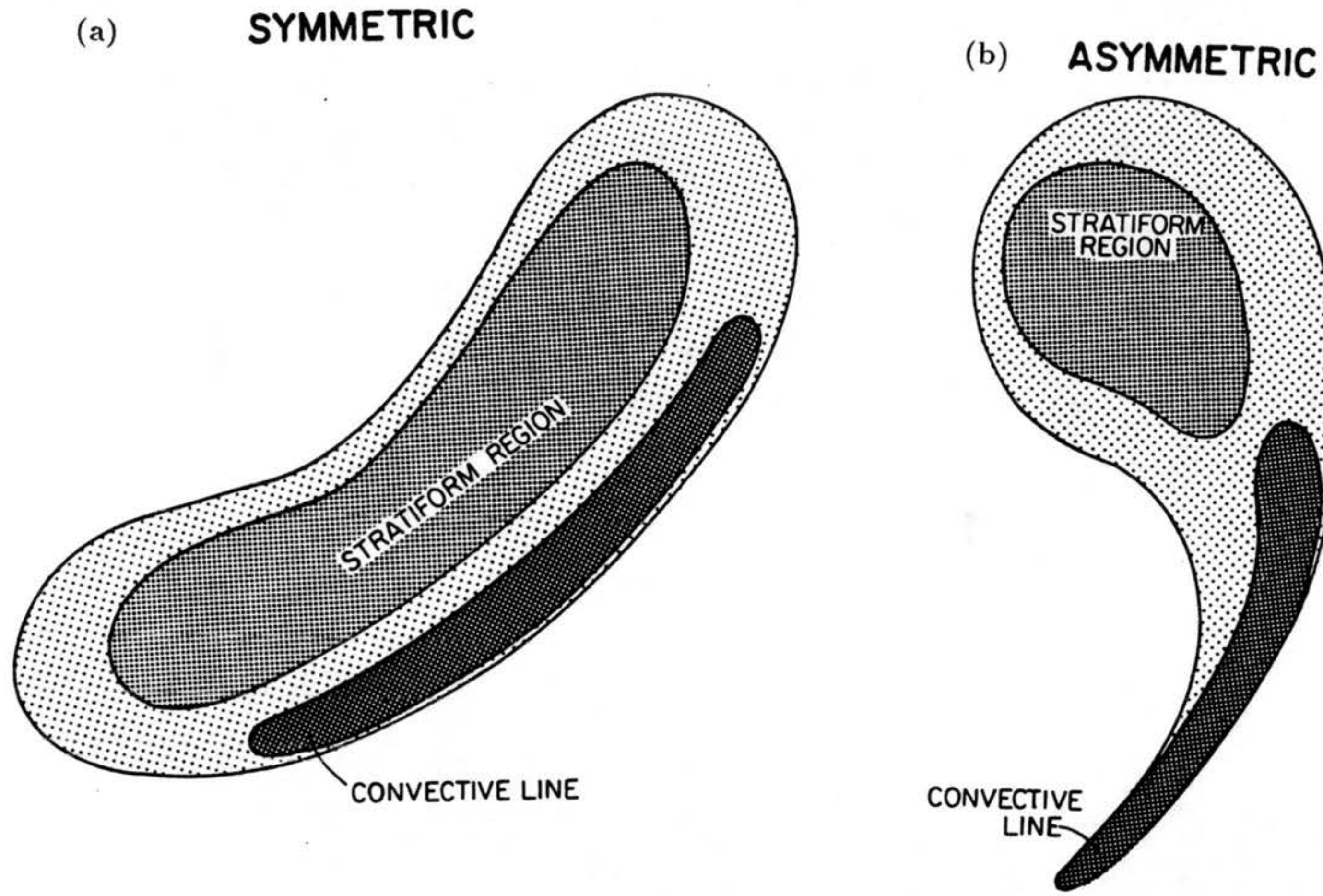

Figure 6.4: Schematic of the radar reflectivity field, for: a) symmetric and b) asymmetric (based on Fig. 6.3) structures. Light shading represents reflectivities less than 30 dBZ. Moderate shading indicates the enhanced stratiform precipitation region (over 30 dBZ). Heavy shading indicates the convective line (over 40 dBZ).

fact, many of the systems pass through a more symmetric stage at earlier points of their life cycles. This examination of the changeable nature of the systems is where this study differs from previous studies on this topic. The Houze et al. (1990) study was based on data from a single radar and, hence, the changeable nature of the systems over their life cycles was not able to be determined. Blanchard (1990) placed systems into specific categories even though many of the systems changed their structure over time. In particular, the 28 May case which he labels as being "linear", in its later stages, actually became "occluded". The system was, in fact, linear during its early stages so his analysis is correct, but with the changeable nature of the system, it is difficult to place it into a strict category.

An important point is that despite the similarity of the reflectivity structure at this stage, each system underwent its own path of development. There appear to be four major paths that the systems follow. The first major path is a system that initially had a disorganized structure. Towards the end of its existence, it develops a fairly small convective line on its southern end, often in response to enhanced convergence due to the outflow from the southern end of the system. Also, any convection which was on the system's northern end becomes more stratiform in nature, leading to the asymmetric structure. This path was followed by the 3 and 4 June cases. This structure, at its early stages, resembles the "chaotic" MCS structure proposed by Blanchard (1990). Second, there were convective lines which slowly developed a region of enhanced stratiform precipitation at their northern ends (the 13 May, 11, 22, and 24 June cases). These cases, in their early stages, resembled the "linear" MCSs of Blanchard (1990) and the "symmetric" MCSs of Houze et al. (1990). Third, there were cases where the convective line built back to the southwest again often in response to enhanced convergence along a gust front emanating from the southern end of the system. This development led to an area on the southern end of the line where there was no stratiform precipitation due to the short time the convection had been present here, thus leading to this asymmetric structure (27, 28 and 29 May cases). This pattern is much like the back-building classification of squall line development proposed by Bluestein and Jain (1985); however, the applicability of their research to this study is in doubt since they examine the formation of the squall line itself. Here the feature studied is the formation of the asymmetric structure, which can occur several hours after the initial squall line development. Finally, there were cases where a pattern of intersecting convective lines developed with one being oriented nearly east-west and the other extending to its south oriented northeast-southwest. An area of enhanced stratiform precipitation developed to the northwest of the apex of these two lines and then the east-west oriented line dissipated, leaving an asymmetric structure (the 7, 21 May and 3-4 June cases). This pattern resembles the "occluded" pattern proposed in the classification scheme of Blanchard (1990).

6.3.2 Surface pressure and flow structure

This section is used to develop a model of the surface pressure and flow structure of a mature-to-dissipating MCS, in particular, the positioning of these features relative to the precipitation areas detailed in the previous section. In Fig. 6.5, the pressure features are overlayed on the radar reflectivity maps for 11 of the 12 systems (May 21 is not included as explained earlier). These pressure features are from the same times as the radar maps. This figure again shows that there were very repeatable features in the pressure fields as well as in the radar reflectivity. There are mesohighs positioned over the convective regions as well as over much of the stratiform regions of these MCSs. The wake low was found to the rear of a region of enhanced stratiform precipitation and at the back edge of the precipitation. The intense pressure gradient was typically along the back edge of the enhanced pressure gradient feature.

Fig. 6.6 is a schematic of the surface pressure and flow field along with the radar schematics from the previous section. In Fig. 6.6a there is the symmetric pattern from Johnson and Hamilton (1988), which is shown for comparison purposes. Also many of these systems went through this symmetric stage earlier in their life cycles. In Fig. 6.6b is the asymmetric pattern, which will has been found to be common amongst 12 cases during their mature-to-dissipating stages and is detailed here. The pre-squall low is a generally weak feature and is found ahead of the central and southern portions of the systems. The mesohigh by this stage of development is an expansive feature covering

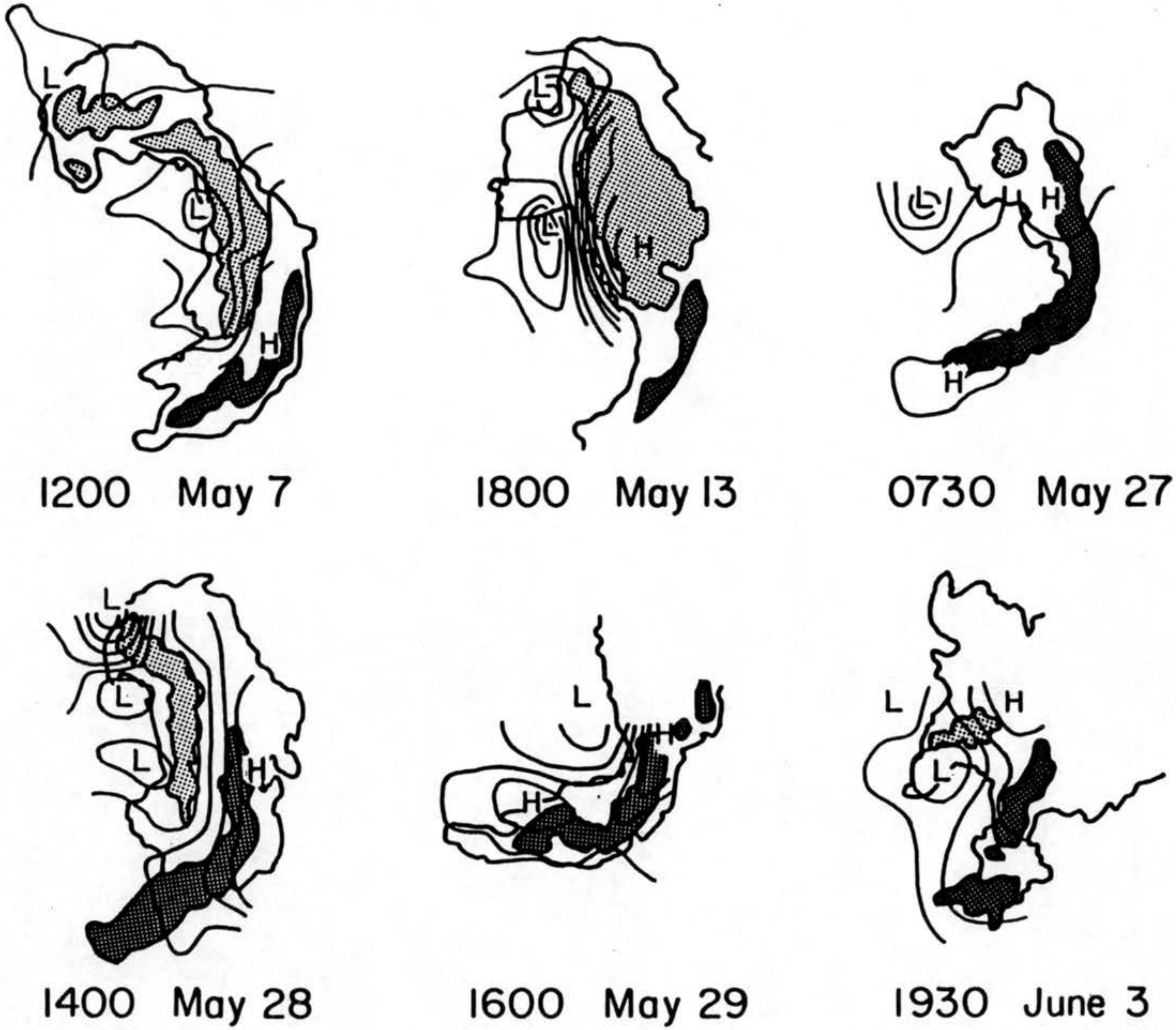

Figure 6.5: Same as Fig. 6.3 except with 480 m pressure contours overlaid.

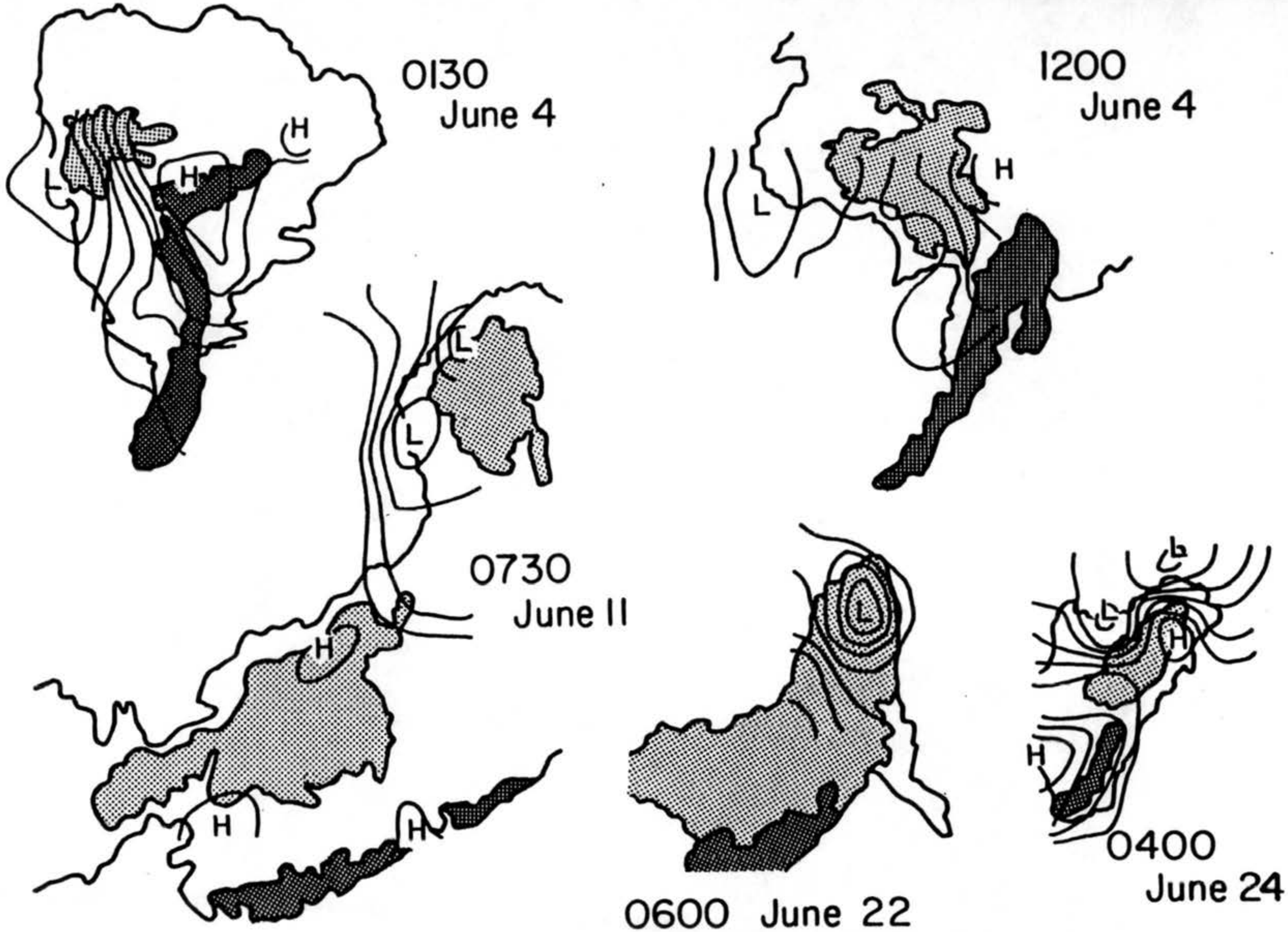

Figure 6.5: Continued.

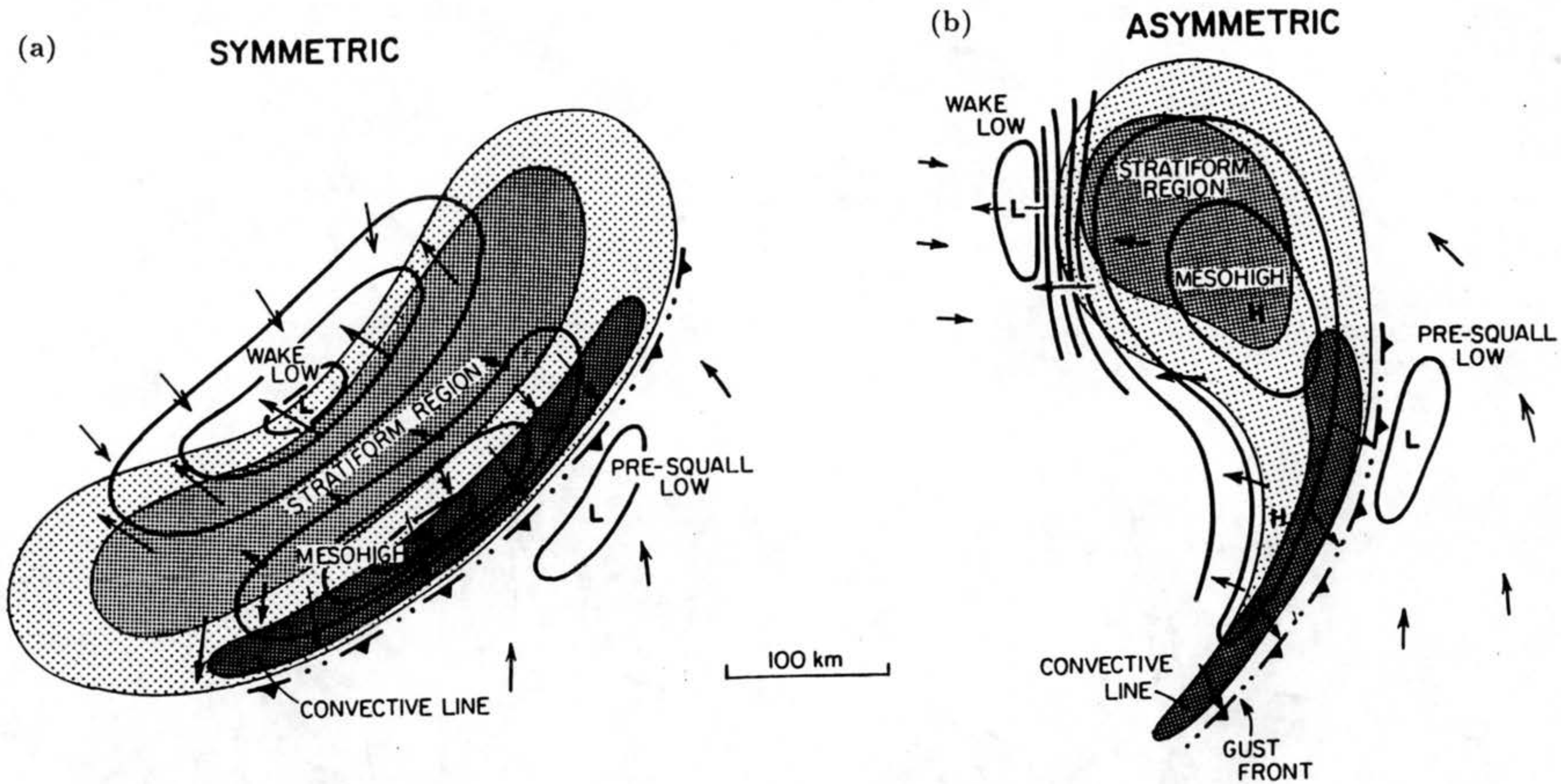

Figure 6.6: Schematic of the surface pressure and flow fields associated with: a) symmetric and b) asymmetric MCS structures. Radar reflectivity field is that of Fig. 6.4. Arrows represent the surface flow.

much of the precipitation structure of these systems, particularly the convective regions as well as much of the stratiform region. It is typical of the mesohigh to become a much enlarged feature by this time and not just associated with the convective regions as it is at earlier times (Fujita 1955). Then to the rear of the mesohigh there is a very intense pressure gradient typically found along the axis of or just to the rear of the enhanced stratiform precipitation region. Its position is nearly the same as that depicted in the previous schematics (Fujita 1955, Pedgley 1962, Johnson and Hamilton 1988). Then to the rear of the intense pressure gradient there is the wake low which is typically found along the back edge of a region of enhanced stratiform precipitation. It is typically positioned to the northwest of the northern end of the convective line. This asymmetric schematic (Fig. 6.6b) contrasts with those of Fujita (1955) and Johnson and Hamilton (1988) which depict the wake low to the rear of the central portion of the convective line. Again, this is a proper schematic for their particular cases at the particular stages they examined, but they may not be generally applicable to the later stages of MCSs.

The surface flow found in conjunction with these MCSs generally followed the findings of Garratt and Physick (1983) and Vescio and Johnson (1992). Ahead of the system the flow was generally fairly weak (0-5 m s^{-1}) and out of the south-southeast in the southern regions, gradually shifting to the southeast to east-southeast farther to the north. The positioning of the changes in this flow structure depended on the location of the surface front in each case. For example, the 3-4 June cases consisted entirely of easterly flow ahead of the system due to the system being to the north of the surface front. Alternately, the 13 May case (Oklahoma system) developed in the warm sector of an intense frontal system and was under only southerly flow.

The next flow regime is the westerly flow behind the gust front ahead of the mesohigh. It is typically a very strong flow of 10-15 m s^{-1} with the strongest outflow usually emanating from the southern end of the convection, since the strongest convection was typically in this region. Next, to the rear of the axis of the mesohigh there is a shift to a strong flow out of the east. This leads to strong divergence to the rear of the mesohigh axis. This flow is usually weak-to-moderate (0-10 m s^{-1}) at the southern end of the system where the pressure gradient is relatively weak. In the northern portion of the system where the intense pressure gradient is evident, the flow is very strong with 10-15 m s^{-1} winds and gusts very often reach in excess of 20 m s^{-1}. Then to the rear of this there is generally very weak and variable flow, which leads to some convergence to the rear of the system, particularly to the rear of the wake low.

This schematic again agrees quite well with that developed by Pedgley (1962). There are several differences, however. First, the Pedgley schematic does not depict a region of enhanced stratiform precipitation. Second, he depicts the strongest outflow ahead of the convective line being from the opposite end of the line (northern versus southern in the schematic presented here). Also, he depicts the maximum convergence to be along the wake low axis, but it actually appears to be to its rear as the flow actually passes through the low, as has been discussed by Garratt and Physick (1983), Johnson and Hamilton (1988) and Vescio and Johnson (1992).

6.3.3 Rear inflow structure

In this section the rear inflow structure in the region of the wake low is summarized. In order to get a view of the rear inflow structure in all areas of the system, the soundings were subjectively separated into four categories: soundings ahead of the system, soundings just to the rear of the convective line, soundings along the back edge of the stratiform region, and soundings from well to the rear of the system. The soundings chosen were along the axis of the wake low or as close as possible to view the flow structure in that location. As previously mentioned, soundings were available for most, but not all, of the cases. Those where soundings were taken included 7 and 27 May and 3, 3-4, 11, 22, and 24 June. Also Doppler radar data were available from previous studies of the 28 May (Houze et al. 1989) and the 3 June case (Nachamkin 1992). The soundings used in all four categories were well divided amongst the cases so that the findings are felt to be generally applicable to all MCSs with a wake low.

Fig. 6.7 shows the system-relative upper-air flow structure at the preselected positions, along with the radar reflectivity schematic. The soundings were also remarkably

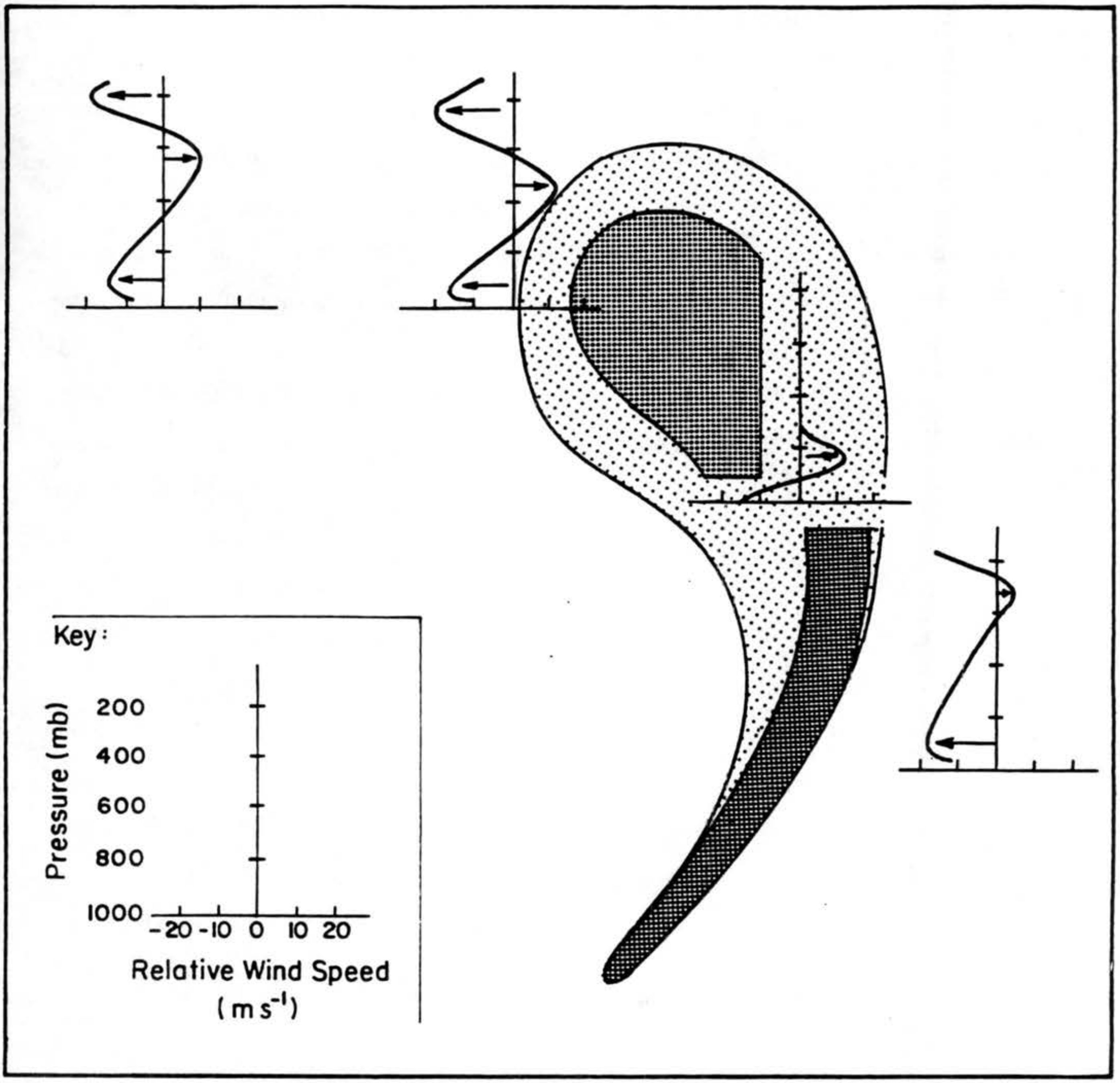

Figure 6.7: Schematic of the system-relative rear inflow jet in the region of the wake low during the mature-to-dissipating stage of MCSs. Positive (negative) represents RTF (FTR) flow. Radar reflectivity plot is that of Fig. 6.4.

similar amongst all of the cases. Ahead of the MCS the flow is mostly FTR with a low-level maximum, which is the low-level southerly jet. In upper levels there is a small area of RTF flow which is apparently due to the outflow from the system near cloud top. In the region just to the rear of the convective line most of the soundings did not reach much above 700 mb but valuable information is still to be found. There is a surface maximum of FTR flow (12 m s^{-1}) which is due to the outflow from the convective line. Then there is a layer of RTF flow (the rear inflow jet) with a maximum at 830 mb (11 m s^{-1}). At the back edge of the stratiform region the rear inflow has elevated dramatically to 530 mb and is still in the strong category (12 m s^{-1}). Below and above this are regions of very strong FTR flow. The low-level flow is still the system outflow and is stronger than behind the convective line as well as farther to the rear of the system (16 m s^{-1}) and its strength is probably partially due to the intense pressure gradient found in this region at low-levels. In the upper levels the FTR flow is also quite strong (19 m s^{-1}) and is the ascending flow which carries the hydrometeors back from the convective line leading to the development of the stratiform region. This system-relative flow structure at the back edge of the system agrees very well with that found by Smull and Houze (1987b) for the "Strong Rear Inflow" cases that they found in their own work and in their summary of previous studies. Every case examined here reached the strong category in at least a portion of its existence.

Well to the rear of the system the rear inflow has elevated further to 430 mb and remains strong (10 m s^{-1}). The other flow maxima are nearly the same as at the rear of the system, but just slightly weaker. This gives the impression that in these MCSs there is a rapidly descending strong rear inflow leading to the development of the wake low, as has been suggested by Johnson and Hamilton (1988) and modeled by Zhang and Gao (1989). In a couple of cases (27 May and 3-4 June) the rear inflow was examined in a region without a stratiform region or a wake low and it was found that the rear inflow in these regions was in the weak-to-moderate category (0-9 m s^{-1}) and remained level or ascended as it approached the convective line (also discussed for the 3-4 June case by Stumpf et al. 1990). Also, cases were examined at an early stage where there was only a very weak, or no, wake low (27 May and 3 June) and these also showed a weaker rear inflow (0-10 m

s^{-1}) and only very weak or no descent. These findings support the observational studies of Johnson and Hamilton (1988), Johnson et al. (1989) and Johnson and Bartels (1992) as well as the modeling studies of Zhang and Gao (1989) for the descending, strong rear inflow as a cause of the wake low feature.

Chapter 7

SUMMARY AND FUTURE RESEARCH

The motivation behind this study was to conduct a comprehensive investigation of the precipitation structure, surface pressure and flow, and the system-relative upper-air flow found in association with MCSs. The procedure has been to conduct a detailed analysis of 16 MCS cases that occurred during the PRE-STORM experiment. The analysis showed that 12 of the 16 MCSs developed into remarkably similar structures during the mature-to-dissipating stages of their life cycles.

Based on radar reflectivity patterns, each of the 12 systems eventually developed into an asymmetric system with a northeast-southwest oriented convective line with a region of enhanced stratiform precipitation to its northwest. The paths taken to get to this structure fell into four general categories. First, there were systems that initially had a disorganized convective structure. Towards the end of their existence, they developed a fairly small convective line on their southern end, often in response to enhanced convergence due to the outflow from the southern end of the system. Also, any convection which was present on the systems' northern end became more stratiform in nature, leading to an asymmetric structure (2 cases). Second, there were convective lines which slowly developed a region of enhanced stratiform precipitation at their northern ends (4 cases). Third, there were cases where the convective line built back to the southwest, often in response to enhanced convergence along a gust front emanating from the southern end of the system. This process leads to a region at the southern end of the system where there is a lack of stratiform precipitation due to the short time of existence of the convection in this region, thus leading to an asymmetric structure (3 cases). Finally, there were cases where there were intersecting convective lines, one being oriented nearly east-west and the other extending to its south oriented northeast-southwest. An area of enhanced stratiform precipitation developed to the northwest of the apex of these two lines and then the east-west oriented line dissipates, leaving an asymmetric structure (3 cases).

The surface patterns were also quite similar among these 12 systems. The general flow features supported the results of Garratt and Physick (1983) and Vescio and Johnson (1992) with flow forward through the mesohigh, divergence to the rear of the mesohigh axis, flow back through the wake low and convergence to the rear of the wake low. The flow at the back edge of the system was also stronger in the wake low region than farther to the south. The pressure structure showed a weak pre-squall low ahead of the central or southern portion of the MCS, a mesohigh within the convective and much of the stratiform region, an intense pressure gradient along the back edge of the enhanced stratiform region and a wake low just to its rear. Finally, the rear inflow structure of these systems verifies the earlier study of Johnson and Hamilton (1988) showing that a descending, strong rear inflow is a primary factor in the generation of the wake low. In the wake low region of these systems the rear inflow was strong (at least 10 m s^{-1}) and rapidly descending in the region where the strong pressure gradient was present.

A major need in future research on this topic is to discover the applicability of these findings for MCSs occurring during other years, times of the year or in other regions or areas around the world. Also further detailed dual-Doppler radar studies need to be conducted systematically on a large number of cases to examine in more detail the rear inflow of these systems. An important question is whether there is a systematic time in the development cycle when the rear inflow develops and if this is variable depending on the path each system takes to this asymmetric structure. Also of importance is how the rear inflow structure varies with the strength of the surface pressure gradient and precipitation structure. Based on soundings, one is left to chance as to where in the storm the samples are being taken. The recently operational NWS Wind Profiler Demonstration Network over the central United States may help in this regard. Also, it may be possible to better plan airborne Doppler radar missions in a field project so as to get the best view of the rear inflow structure in the wake low region since from this study it is apparent that the wake low tends to develop on the system's northern end. Also more work needs to be done to see if there are particular reasons that a system takes one path to asymmetry over another and why initially disorganized convective cells organize into a coherent pattern at all. In particular further mesoscale modeling of these features is needed to lead to a greater understanding of their developmental characteristics. Finally, a detailed study such as this one should be done in reference to the thermodynamic structure of these systems so as to obtain an even better understanding of these complex systems.

REFERENCES

Augustine, J. A., and K. W. Howard, 1988: Mesoscale convective complexes over the United States during 1985. *Mon. Wea. Rev.*, **116**, 685-701.

Barnes, S. L., 1964: A technique for maximizing details in numerical weather map analysis. *J. Appl. Meteor.*, **3**, 396-409.

Barnes, S. L., 1973: Mesoscale objective map analysis using weighted time-series observations. NOAA Tech. Memo. ERL NSSL-62, Norman, Oklahoma, 60pp.

Bartels, D. L., and R. A. Maddox, 1991: Midlevel cyclonic vorticies generated by mesoscale convective systems. *Mon. Wea. Rev.*, **119**, 104-118.

Blanchard, D. O., 1990: Mesoscale convective patterns of the southern high plains. *Bull. Amer. Meteor. Soc.*, **71**, 994-1005.

Bluestein, H. B., and M. H. Jain, 1985: Formation of mesoscale lines of precipitation: Severe squall lines in Oklahoma during the spring. *J. Atmos. Sci.*, **42**, 1711-1732.

Brandes, E. A., 1990: Evolution and structure of the 6-7 May 1985 mesoscale convective system and associated vortex. *Mon. Wea. Rev.*, **118**, 109-127.

Brandes, E. A., and C. L. Ziegler, 1992: Mesoscale downdraft influences on vertical vorticity in a mature mesoscale convective system. *Mon. Wea. Rev.*, (submitted).

Byers, H. R., and R. R. Braham, 1949: The thunderstorm. U. S. Weather Bureau, Washington, D. C., 287pp.

Carbone, R. E., J. W. Conway, N. A. Crook, and M. W. Moncrieff, 1990: The generation and propagation of a nocturnal squall line. Part I: Observations and implications for mesoscale predictability. *Mon. Wea. Rev.*, **118**, 26-49.

Cotton, W. R., M. S. Lin, R. L. McAnelly, and C. J. Tremback, 1989: A composite model of mesoscale convective complexes. *Mon. Wea. Rev.*, **117**, 765-783.

Crook, N. A., R. E. Carbone, M. W. Moncrieff, and J. W. Conway, 1990: The generation and propagation of a nocturnal squall line. Part II: Numerical simulations. *Mon. Wea. Rev.*, **118**, 50-65.

Cunning, J. B., 1986: The Oklahoma-Kansas Preliminary Regional Experiment for STORM-Central. *Bull. Amer. Meteor. Soc.*, **67**, 1478-1486.

Doswell, C. A. III, 1991: Comments on mesoscale convective patterns of the southern high plains. *Bull. Amer. Meteor. Soc.*, **72**, 389-390.

Fritsch, J. M., 1975: Cumulus dynamics: Local compensating subsidence and its implications for cumulus parameterization. *Pure Appl. Geophys.*, **113**, 851-867.

Fritsch, J. M., and C. G. Chappell, 1980: Numerical prediction of convectively driven mesoscale pressure systems. Part II: Mesoscale model. *J. Atmos. Sci.*, **37**, 1734-1762.

Fujita, T. T., 1955: Results of detailed synoptic studies of squall lines. *Tellus*, **7**, 405-436.

Fujita, T. T., 1959: Precipitation and cold air production in mesoscale thunderstorm systems. *J. Meteor.*, **16**, 454-466.

Fujita, T. T., 1963: Analytical mesometeorology. A review. *Met. Monogr.*, **5**, 77-125.

Fujita, T. T., 1985: The Downburst. SMRP Research Paper Number 210, Dept. of Geophysical Sciences, University of Chicago, 122pp. [NTIS PB-148880.]

Garratt, J. R., and W. L. Physick, 1983: Low-level wind response to mesoscale pressure systems. *Bound. Layer Meteor.*, **27**, 69-87.

Green, J. L., 1989: Analysis of surface pressure features during an episode of mesoscale convective systems. M.S. Thesis, Texas Tech University, 75pp.

Houze, R. A., B. F. Smull, and P. Dodge, 1990: Mesoscale organization of springtime rainstorms in Oklahoma. *Mon. Wea. Rev.*, **118**, 613-654.

Houze, R. A., S. A. Rutledge, M. I. Biggerstaff, and B. F. Smull, 1989: Interpretation of Doppler weather radar displays of midlatitude mesoscale convective systems. *Bull. Amer. Meteor. Soc.*, **70**, 608-619.

Hoxit, L. R., C. F. Chappell, and J. M. Fritsch, 1976: Formation of mesolows or pressure troughs in advance of cumulonimbus clouds. *Mon. Wea. Rev.*, **104**, 1419-1428.

Johnson, B. C., 1983: The heat burst of 29 May 1976. *Mon. Wea. Rev.*, **111**, 1776-1792.

Johnson, R. H., and D. L. Bartels, 1992: Circulations associated with a mature-to-decaying midlatitude mesoscale convective system. Part II: Upper-level features. *Mon. Wea. Rev.*, **120**, 1301-1320.

Johnson, R. H., and P. J. Hamilton, 1988: The relationship of surface pressure features to the precipitation and airflow structure of an intense midlatitude squall line. *Mon. Wea. Rev.*, **116**, 1444-1472.

Johnson, R. H., and J. J. Toth, 1986: Preliminary data quality analysis for May-June 1985 Oklahoma-Kansas PRE-STORM PAM-II mesonetwork. Atmospheric Science Paper No. 407, Colorado State University, Dept. of Atmos. Sci., Fort Collins, Colorado, 41pp.

Johnson, R. H., S. Chen, and J. J. Toth, 1989: Circulations associated with a mature-to-decaying midlatitude mesoscale convective system. Part I: Surface features–Heat bursts and mesolow development. *Mon. Wea. Rev.*, **117**, 942-959.

Johnston, E. C., 1982: Mesoscale vorticity centers induced by mesoscale convective complexes. Preprints, *Ninth Conference on Weather Forecasting and Analysis*, Seattle, Amer. Meteor. Soc., 196-200.

Leary, C. A., and E. N. Rappaport, 1987: The life cycle and internal structure of a mesoscale convective complex. *Mon. Wea. Rev.*, **115**, 1503-1527.

Maddox, R. A., 1980: Mesoscale convective complexes. *Bull. Amer. Meteor. Soc.*, **61**, 1374-1400.

Maddox, R. A., 1983: Large-scale meteorological conditions associated with midlatitude, mesoscale convective complexes. *Mon. Wea. Rev.*, **111**, 1475-1493.

McAnelly, R. L., and W. R. Cotton, 1986: Meso-β-scale characteristics of an episode of meso-α-scale convective complexes. *Mon. Wea. Rev.*, **114**, 1740-1770.

Meitín, J. G., 1987: The Oklahoma-Kansas preliminary regional experiment for STORM-Central (OK PRE-STORM), Volume II. Radar data summary. NOAA Tech. Memo. ERL ESG-26, Dept. of Commerce, Weather Research Program, Boulder, Colorado, 84pp.

Meitín, J. G., and J. B. Cunning, 1985: The Oklahoma-Kansas preliminary regional experiment for STORM-Central (OK PRE-STORM), Volume I. Daily operations summary. NOAA Tech. Memo. ERL ESG-20, Dept. of Commerce, Weather Research Program, Boulder, Colorado, 313pp.

Nachamkin, J. E., 1992: The upscale evolution of a midlatitude mesoscale convective complex. M.S. Thesis, Colorado State University, Dept. of Atmos. Sci., 122pp.

Newton, C. W., 1950: Structure and mechanism of the prefrontal squall line. *J. Meteor.*, **7**, 210-222.

Pedgley, D. E., 1962: A meso-synoptic analysis of the thunderstorms on 28 August 1958. Brit. Meteor. Off., Geophys. Mem., No. 106, 74pp.

Rutledge, S. A., and R. A. Houze, 1987: A diagnostic modeling study of the trailing stratiform region of a midlatitude squall line. *J. Atmos. Sci.*, **44**, 2640-2656.

Smull, B. F., and J. A. Augustine, 1991: Multi-scale analysis of a mature mesoscale convective complex. *Mon. Wea. Rev.*, (submitted).

Smull, B. F., and R. A. Houze, 1985: A midlatitude squall line with a trailing region of stratiform rain: Radar and satellite observations. *Mon. Wea. Rev.*, **113**, 117-133.

Smull, B. F., and R. A. Houze, 1987: Dual-Doppler radar analysis of a midlatitude squall line with a trailing region of stratiform rain. *J. Atmos. Sci.*, **44**, 2128-2148.

Smull, B. F., and R. A. Houze, 1987: Rear inflow in squall lines with trailing stratiform precipitation. *Mon. Wea. Rev.*, **115**, 2869-2889.

Stumpf, G. J., 1988: Surface pressure features associated with a mesoscale convective system in OK PRE-STORM. M.S. Thesis, Colorado State University, Dept. of Atmos. Sci., 148pp.

Stumpf, G. J., R. H. Johnson, and B. F. Smull, 1991: The wake low in a midlatitude mesoscale convective system having complex convective organization. *Mon. Wea. Rev.*, **119**, 134-158.

Tepper, M., 1950: A proposed mechanism of squall lines: The pressure jump line. *J. Meteor.*, **7**, 21-29.

Trier, S. B., and D. B. Parsons, 1992: Evolution of environmental conditions preceeding the development of a nocturnal mesoscale convective complex. *Mon. Wea. Rev.* (submitted).

Vescio, M. D., 1990: The wind's response to transient mesoscale pressure fields associated with squall lines. M.S. Thesis, Colorado State University, Dept. of Atmos. Sci., 86pp.

Vescio, M. D., and R. H. Johnson, 1992: The surface-wind response to transient mesoscale pressure fields associated with squall lines. *Mon. Wea. Rev.*, **120**, 1837-1850.

Williams, D. T., 1948: A surface micro-study of squall-line thunderstorms. *Mon. Wea. Rev.*, **76**, 239-246.

Williams, D. T., 1953: Pressure wave observations in the central Midwest, 1952. *Mon. Wea. Rev.*, **81**, 278-298.

Williams, D. T., 1954: A surface study of a depression-type pressure wave. *Mon. Wea. Rev.*, **82**, 289-295.

Williams, D. T., 1963: The thunderstorm wake of May 4, 1961. Nat. Severe Storms Project Rep. No. 18, U. S. Dept. of Commerce, Washington D. C., 23pp. [NTIS PB 168223].

Zhang, D.-L., and J. M. Fritsch, 1987: Numerical simulation of the mesoβ-scale structure and evolution of the 1977 Johnstown flood. Part II: Inertially stable warm-core vortex and the mesoscale convective complex. *J. Atmos. Sci.*, **44**, 2593-2612.

Zhang, D.-L., and J. M. Fritsch, 1988: Numerical sensitivity experiments of varying model physics on the structure, evolution and dynamics of two mesoscale convective systems. *J. Atmos. Sci.*, **45**, 261-293.

Zhang, D.-L., and J. M. Fritsch, 1988: A numerical investigation of a convectively generated inertially stable, extratropical warm-core mesovortex over land. Part I: Structure and evolution. *Mon. Wea. Rev.*, **116**, 2660-2687.

Zhang, D.-L., and K. Gao, 1989: Numerical simulation of an intense squall line during 10-11 June 1985 PRE-STORM. Part II: Rear inflow, surface pressure perturbations and stratiform precipitation. *Mon. Wea. Rev.*, **117**, 2067-2094.

Zipser, E. J., 1977: Mesoscale and convective-scale downdrafts as distinct components of squall-line structure. *Mon. Wea. Rev.*, **105**, 1568-1589.

APPENDIX A

Instrument Bias Corrections

To arrive at an accurate mesoscale analysis of the surface pressure data, the data must have an accuracy of about 0.5 mb. Fujita (1963) suggested the use of data from surrounding, well-calibrated stations, such as the NWS stations, to compare with the mesonet stations. Johnson and Toth (1986) used the comparison of PAM station data with NWS stations in addition to examination of field calibration logs and monthly mean fields to arrive at corrections for the PAM stations during PRE-STORM. They did not examine the SAM station corrections. Johnson and Hamilton (1988) did have a complete set of corrections (PAM and SAM) for the 10-11 June case. Stumpf (1988) did the same for the 3-4 June case. For this thesis, corrections were derived for every case examined.

The method used here is generally the same used in Stumpf (1988) but over the entire PRE-STORM period. A three-hour period with relatively undisturbed conditions within, at most, a few days of the particular case is used for the intercomparisons of the PAM and SAM data with the NWS data. Undisturbed is defined as a period with a weak pressure gradient and no major convective systems across the PRE-STORM region. The time (all times UTC) periods chosen were: 2100-2300 May 3; 2100-2300 May 9; 2100-2300 May 19; 1800-2000 May 25; 2100 May 31, 0000-0100 June 1; 2100-2300 June 10; 2100-2300 June 13; 2100-2300 June 19 and; 2100-2300 June 24. The hydrostatically adjusted NWS pressure data (to 480 m; see section 3.1) were objectively analyzed using a Barnes-type scheme (Barnes 1964) for every time. Then, based on these analyses an "expected" pressure value was determined objectively for each PAM and SAM station at every time. Then these values were compared to the actual values recorded at each station and the differences were calculated. Then for each three-hour time period, the correction values were averaged for each station, giving the actual applied correction for that station. The applied corrections are listed in Tables A.1-11.

Table A.1: PAM and SAM pressure corrections for 7 May case.

Station	Applied pressure correction (mb)	Station	Applied pressure correction (mb)
P01	0.40	S01	0.58
P02	0.49	S02	-0.44
P03	-0.83	S03	0.92
P04	-0.80	S04	M
P05	-0.62	S05	0.24
P06	-0.95	S06	1.18
P07	-0.28	S07	0.09
P08	-0.55	S08	0.94
P09	-0.67	S09	0.07
P10	-0.88	S10	0.60
P11	-0.82	S11	-0.43
P12	0.37	S12	0.88
P13	0.10	S13	0.97
P14	-1.70	S14	0.54
P15	0.03	S15	0.27
P16	-0.01	S16	0.25
P17	-0.24	S17	0.29
P18	-0.69	S18	-0.26
P19	-0.60	S19	0.44
P20	-0.91	S20	0.47
P21	0.12	S21	-1.07
P22	-1.21	S22	0.62
P23	-0.12	S23	0.78
P24	-0.50	S24	M
P25	0.61	S25	M
P26	-0.93	S26	0.92
P27	-0.45	S27	0.41
P28	-1.48	S28	0.53
P29	0.93	S29	0.59
P30	0.25	S30	-0.12
P31	0.76	S31	1.16
P32	-0.66	S32	1.25
P33	0.46	S33	0.14
P34	0.00	S34	1.20
P35	-0.09	S35	0.51
P36	-1.61	S36	0.70
P37	-0.13	S37	M
P38	0.18	S38	M
P39	1.40	S39	0.77
P40	-0.24	S40	M
P41	M	S41	1.32
P42	M	S42	0.38

Table A.2: PAM and SAM pressure corrections for 13 May case.

Station	Applied pressure correction (mb)	Station	Applied pressure correction (mb)
P01	1.70	S01	0.57
P02	1.82	S02	-0.15
P03	M	S03	1.51
P04	-0.06	S04	0.45
P05	-0.16	S05	0.16
P06	-0.59	S06	1.20
P07	0.04	S07	0.00
P08	-0.75	S08	0.42
P09	0.25	S09	-0.44
P10	-0.70	S10	M
P11	-0.10	S11	0.29
P12	1.33	S12	1.36
P13	0.51	S13	0.76
P14	-1.28	S14	0.43
P15	0.68	S15	0.15
P16	-0.14	S16	0.09
P17	-0.04	S17	-0.08
P18	-0.21	S18	0.03
P19	0.44	S19	1.01
P20	-0.49	S20	0.81
P21	0.48	S21	-1.16
P22	-1.05	S22	0.69
P23	-0.05	S23	0.58
P24	-0.66	S24	1.00
P25	0.56	S25	0.70
P26	-0.73	S26	1.29
P27	-0.45	S27	0.82
P28	-1.23	S28	0.91
P29	1.22	S29	0.96
P30	0.35	S30	0.24
P31	1.10	S31	1.25
P32	-0.69	S32	0.99
P33	0.70	S33	-0.32
P34	0.24	S34	1.35
P35	0.27	S35	0.69
P36	-1.65	S36	0.83
P37	0.18	S37	M
P38	0.11	S38	0.77
P39	1.61	S39	0.89
P40	-0.20	S40	M
P41	M	S41	2.19
P42	-0.25	S42	0.25

Table A.3: PAM and SAM pressure corrections for 21 May case.

Station	Applied pressure correction (mb)	Station	Applied pressure correction (mb)
P01	1.40	S01	0.44
P02	1.68	S02	1.03
P03	-0.06	S03	1.90
P04	-0.42	S04	1.67
P05	-0.12	S05	0.41
P06	-0.53	S06	1.21
P07	0.17	S07	-0.30
P08	-0.76	S08	0.41
P09	-0.34	S09	M
P10	-0.17	S10	1.25
P11	-0.18	S11	0.50
P12	1.35	S12	1.65
P13	0.65	S13	1.50
P14	-1.30	S14	0.63
P15	0.66	S15	0.37
P16	0.09	S16	0.29
P17	-0.58	S17	M
P18	0.15	S18	0.51
P19	0.53	S19	1.07
P20	-0.56	S20	1.26
P21	0.49	S21	-0.36
P22	-0.97	S22	0.79
P23	-0.12	S23	0.74
P24	-0.74	S24	1.07
P25	-0.27	S25	0.90
P26	-0.40	S26	1.28
P27	-0.23	S27	1.21
P28	-1.63	S28	0.97
P29	1.56	S29	0.83
P30	0.54	S30	0.07
P31	1.22	S31	0.94
P32	-0.89	S32	0.13
P33	-0.03	S33	-0.34
P34	0.36	S34	1.11
P35	-0.27	S35	0.41
P36	-2.30	S36	0.69
P37	0.22	S37	0.75
P38	0.29	S38	1.10
P39	1.74	S39	0.78
P40	-0.31	S40	M
P41	-0.98	S41	1.99
P42	-0.48	S42	0.14

Table A.4: PAM and SAM pressure corrections for 27, 28, and 29 May cases.

Station	Applied pressure correction (mb)	Station	Applied pressure correction (mb)
P01	1.56	S01	0.35
P02	1.86	S02	0.34
P03	0.00	S03	1.55
P04	-0.57	S04	1.28
P05	-0.32	S05	0.05
P06	-0.80	S06	0.50
P07	0.08	S07	-0.42
P08	-0.94	S08	0.03
P09	0.31	S09	-1.95
P10	-0.10	S10	1.19
P11	0.25	S11	0.11
P12	1.55	S12	1.25
P13	0.56	S13	1.10
P14	-1.53	S14	M
P15	0.46	S15	0.18
P16	0.04	S16	0.02
P17	-0.48	S17	-0.12
P18	0.18	S18	0.63
P19	0.44	S19	M
P20	-0.34	S20	0.54
P21	0.36	S21	-1.39
P22	-0.81	S22	0.56
P23	-0.01	S23	0.46
P24	-0.70	S24	M
P25	0.42	S25	0.58
P26	-0.38	S26	1.20
P27	-0.97	S27	0.23
P28	-1.61	S28	0.58
P29	1.87	S29	0.70
P30	0.70	S30	0.13
P31	1.27	S31	1.30
P32	-1.73	S32	0.20
P33	0.06	S33	-0.25
P34	0.34	S34	0.99
P35	-0.11	S35	0.54
P36	-0.08	S36	0.61
P37	0.40	S37	0.76
P38	0.03	S38	1.25
P39	1.75	S39	0.63
P40	0.02	S40	M
P41	-0.81	S41	2.06
P42	0.18	S42	-0.24

Table A.5: PAM and SAM pressure corrections for 3, 3–4 and 4 June cases.

Station	Applied pressure correction (mb)	Station	Applied pressure correction (mb)
P01	1.17	S01	-0.23
P02	1.06	S02	0.71
P03	-0.38	S03	2.02
P04	-1.14	S04	1.87
P05	-0.35	S05	0.70
P06	-0.55	S06	1.14
P07	0.43	S07	0.11
P08	-0.59	S08	0.24
P09	0.09	S09	-0.19
P10	-0.26	S10	M
P11	0.03	S11	M
P12	1.31	S12	1.92
P13	0.64	S13	1.26
P14	-2.53	S14	M
P15	1.03	S15	0.03
P16	0.05	S16	-0.60
P17	-0.16	S17	-0.57
P18	0.03	S18	0.33
P19	0.41	S19	M
P20	-0.16	S20	0.97
P21	0.53	S21	-1.08
P22	-0.71	S22	0.41
P23	0.08	S23	0.06
P24	-1.09	S24	M
P25	0.75	S25	0.17
P26	0.14	S26	0.99
P27	-0.17	S27	0.18
P28	-1.09	S28	0.50
P29	1.80	S29	0.87
P30	0.80	S30	-0.29
P31	1.27	S31	0.84
P32	-1.94	S32	0.08
P33	0.30	S33	-0.18
P34	0.49	S34	0.80
P35	0.05	S35	0.58
P36	0.29	S36	0.57
P37	0.80	S37	0.76
P38	0.23	S38	1.57
P39	2.11	S39	0.81
P40	0.54	S40	1.02
P41	-0.70	S41	2.30
P42	-0.09	S42	-0.37

Table A.6: PAM and SAM pressure corrections for 9 June case.

Station	Applied pressure correction (mb)	Station	Applied pressure correction (mb)
P01	1.64	S01	0.66
P02	1.90	S02	0.54
P03	0.02	S03	2.08
P04	-1.63	S04	1.65
P05	-0.50	S05	0.64
P06	-0.47	S06	0.74
P07	0.28	S07	0.22
P08	-1.02	S08	0.30
P09	0.67	S09	0.54
P10	-0.33	S10	M
P11	-0.51	S11	M
P12	0.96	S12	1.45
P13	0.41	S13	0.94
P14	-1.78	S14	M
P15	0.70	S15	-0.58
P16	-0.44	S16	0.22
P17	-0.49	S17	0.26
P18	-0.62	S18	0.43
P19	-1.71	S19	M
P20	-0.38	S20	0.79
P21	-0.06	S21	-0.80
P22	-0.20	S22	0.57
P23	0.39	S23	0.36
P24	-1.07	S24	M
P25	-0.09	S25	0.46
P26	-0.73	S26	1.29
P27	-1.48	S27	0.44
P28	-2.20	S28	M
P29	2.21	S29	1.00
P30	1.34	S30	0.76
P31	1.09	S31	1.45
P32	-1.29	S32	M
P33	-0.04	S33	-0.44
P34	0.34	S34	0.69
P35	-0.36	S35	M
P36	0.06	S36	1.50
P37	1.36	S37	0.88
P38	0.65	S38	1.88
P39	1.09	S39	1.06
P40	0.66	S40	M
P41	-0.59	S41	1.60
P42	0.61	S42	-0.08

Table A.7: PAM and SAM pressure corrections for 11 June case.

Station	Applied pressure correction (mb)	Station	Applied pressure correction (mb)
P01	1.30	S01	0.60
P02	0.90	S02	0.80
P03	-0.50	S03	2.20
P04	-1.20	S04	1.80
P05	0.00	S05	0.80
P06	-0.10	S06	1.00
P07	0.80	S07	0.10
P08	-0.60	S08	0.10
P09	-0.20	S09	0.60
P10	-0.30	S10	M
P11	-0.20	S11	M
P12	1.10	S12	1.90
P13	0.70	S13	1.40
P14	-2.20	S14	M
P15	1.00	S15	-0.30
P16	0.20	S16	0.20
P17	-0.10	S17	0.60
P18	-0.10	S18	-0.30
P19	0.40	S19	M
P20	-0.20	S20	1.30
P21	0.40	S21	M
P22	-0.70	S22	1.10
P23	0.30	S23	0.50
P24	-0.40	S24	M
P25	0.10	S25	0.50
P26	0.00	S26	0.00
P27	-0.10	S27	0.40
P28	-1.80	S28	M
P29	1.40	S29	1.20
P30	0.80	S30	0.40
P31	1.40	S31	1.50
P32	M	S32	M
P33	-0.10	S33	-0.30
P34	0.30	S34	0.40
P35	0.00	S35	M
P36	0.20	S36	0.90
P37	0.50	S37	0.60
P38	0.20	S38	1.80
P39	2.00	S39	0.80
P40	1.10	S40	M
P41	-0.70	S41	1.90
P42	0.20	S42	0.20

Table A.8: PAM and SAM pressure corrections for 15 June case.

Station	Applied pressure correction (mb)	Station	Applied pressure correction (mb)
P01	1.47	S01	0.43
P02	1.89	S02	0.39
P03	-0.03	S03	1.62
P04	-1.18	S04	1.54
P05	-0.35	S05	0.18
P06	-0.67	S06	M
P07	0.00	S07	-0.03
P08	-1.28	S08	0.23
P09	0.13	S09	M
P10	-0.83	S10	M
P11	-0.66	S11	M
P12	1.24	S12	1.79
P13	0.70	S13	1.10
P14	-1.69	S14	0.38
P15	0.05	S15	-0.13
P16	-0.82	S16	0.15
P17	-0.29	S17	0.57
P18	-0.84	S18	0.52
P19	0.77	S19	0.95
P20	-0.48	S20	1.04
P21	0.18	S21	M
P22	-0.88	S22	0.65
P23	-0.12	S23	0.64
P24	-1.23	S24	0.45
P25	0.58	S25	0.65
P26	-0.58	S26	1.38
P27	-1.12	S27	0.60
P28	-2.06	S28	0.70
P29	1.60	S29	1.29
P30	0.53	S30	-0.01
P31	1.10	S31	1.12
P32	-0.38	S32	0.44
P33	0.04	S33	-0.17
P34	0.42	S34	1.17
P35	-0.09	S35	M
P36	-0.17	S36	0.53
P37	0.61	S37	0.81
P38	0.15	S38	1.42
P39	1.70	S39	1.04
P40	0.71	S40	0.66
P41	-0.71	S41	1.90
P42	0.21	S42	0.18

Table A.9: PAM and SAM pressure corrections for 22 June case.

Station	Applied pressure correction (mb)	Station	Applied pressure correction (mb)
P01	0.95	S01	0.55
P02	1.20	S02	-0.02
P03	0.08	S03	1.03
P04	-1.44	S04	M
P05	-0.52	S05	M
P06	-0.41	S06	1.03
P07	0.44	S07	0.21
P08	-1.05	S08	M
P09	0.45	S09	M
P10	-0.25	S10	-0.33
P11	-0.28	S11	0.76
P12	1.26	S12	1.53
P13	0.56	S13	1.01
P14	-1.56	S14	M
P15	0.42	S15	-0.10
P16	-0.33	S16	0.32
P17	-0.11	S17	0.58
P18	-0.61	S18	-0.02
P19	1.66	S19	0.25
P20	-0.33	S20	0.56
P21	0.29	S21	-0.78
P22	-0.69	S22	0.65
P23	0.09	S23	0.25
P24	-0.96	S24	M
P25	0.90	S25	0.51
P26	-0.50	S26	0.46
P27	-1.31	S27	M
P28	-2.20	S28	0.43
P29	1.78	S29	0.97
P30	0.82	S30	0.90
P31	1.23	S31	1.25
P32	3.43	S32	0.38
P33	0.61	S33	-0.32
P34	0.51	S34	0.90
P35	-0.48	S35	-0.04
P36	-0.06	S36	0.23
P37	0.46	S37	0.51
P38	-0.07	S38	1.68
P39	M	S39	M
P40	0.75	S40	0.50
P41	-0.73	S41	M
P42	0.08	S42	0.26

Table A.10: PAM and SAM pressure corrections for 24 June case.

Station	Applied pressure correction (mb)	Station	Applied pressure correction (mb)
P01	1.34	S01	0.39
P02	1.63	S02	0.25
P03	-0.46	S03	1.55
P04	-1.89	S04	M
P05	-0.39	S05	-2.34
P06	-0.21	S06	0.63
P07	0.54	S07	-0.03
P08	-1.23	S08	M
P09	0.24	S09	M
P10	-0.74	S10	0.17
P11	-1.34	S11	0.92
P12	0.70	S12	1.78
P13	0.50	S13	0.77
P14	-1.75	S14	M
P15	0.38	S15	-0.25
P16	-0.55	S16	0.04
P17	-0.47	S17	0.49
P18	-1.05	S18	0.47
P19	-0.10	S19	0.51
P20	-0.43	S20	0.74
P21	0.26	S21	-1.46
P22	-0.56	S22	0.85
P23	0.14	S23	0.18
P24	-1.42	S24	M
P25	0.15	S25	0.50
P26	-0.69	S26	0.87
P27	-1.09	S27	M
P28	-1.75	S28	0.87
P29	1.58	S29	1.07
P30	0.86	S30	M
P31	1.03	S31	1.21
P32	2.58	S32	0.10
P33	0.06	S33	-0.25
P34	0.20	S34	1.10
P35	-0.16	S35	M
P36	0.31	S36	0.94
P37	0.91	S37	1.02
P38	0.23	S38	1.69
P39	M	S39	0.93
P40	0.84	S40	0.28
P41	-0.24	S41	1.83
P42	0.48	S42	0.11

Table A.11: PAM and SAM pressure corrections for 26–27 June cases.

Station	Applied pressure correction (mb)	Station	Applied pressure correction (mb)
P01	1.34	S01	0.39
P02	1.63	S02	0.25
P03	-0.46	S03	1.55
P04	-1.89	S04	1.54
P05	-0.39	S05	0.40
P06	-0.21	S06	0.63
P07	0.54	S07	-0.03
P08	-1.23	S08	M
P09	0.24	S09	M
P10	-0.74	S10	0.17
P11	-1.34	S11	0.92
P12	0.70	S12	1.78
P13	0.50	S13	0.77
P14	-1.75	S14	M
P15	0.38	S15	-0.25
P16	-0.55	S16	0.04
P17	-0.47	S17	0.49
P18	-1.05	S18	0.47
P19	-0.10	S19	0.51
P20	-0.43	S20	0.74
P21	0.26	S21	M
P22	-0.56	S22	0.85
P23	0.14	S23	0.18
P24	-1.42	S24	M
P25	0.15	S25	0.50
P26	-0.69	S26	0.87
P27	-1.09	S27	0.57
P28	-1.75	S28	M
P29	1.58	S29	1.07
P30	0.86	S30	M
P31	1.03	S31	1.21
P32	-0.80	S32	0.10
P33	0.06	S33	-0.25
P34	0.20	S34	1.10
P35	-0.16	S35	M
P36	0.31	S36	0.94
P37	0.91	S37	1.02
P38	0.23	S38	1.69
P39	1.59	S39	0.93
P40	0.84	S40	0.28
P41	-0.24	S41	1.83
P42	0.48	S42	0.11